Lithostratigraphy, depositional environments, and sequence ...
Abegg, Frederick Edmund
ProQuest Dissertations and Theses; 1992; Dissertations & Theses @ University of Kansas
pg. n/a

INFORMATION TO USERS

This manuscript has been reproduced from the microfilm master. UMI films the text directly from the original or copy submitted. Thus, some thesis and dissertation copies are in typewriter face, while others may be from any type of computer printer.

The quality of this reproduction is dependent upon the quality of the copy submitted. Broken or indistinct print, colored or poor quality illustrations and photographs, print bleedthrough, substandard margins, and improper alignment can adversely affect reproduction.

In the unlikely event that the author did not send UMI a complete manuscript and there are missing pages, these will be noted. Also, if unauthorized copyright material had to be removed, a note will indicate the deletion.

Oversize materials (e.g., maps, drawings, charts) are reproduced by sectioning the original, beginning at the upper left-hand corner and continuing from left to right in equal sections with small overlaps. Each original is also photographed in one exposure and is included in reduced form at the back of the book.

Photographs included in the original manuscript have been reproduced xerographically in this copy. Higher quality 6" x 9" black and white photographic prints are available for any photographs or illustrations appearing in this copy for an additional charge. Contact UMI directly to order.

U·M·I

University Microfilms International
A Bell & Howell Information Company
300 North Zeeb Road, Ann Arbor, MI 48106-1346 USA
313 761-4700 800 521-0600

Reproduced with permission of the copyright owner. Further reproduction prohibited without permission.

Order Number 9313080

Lithostratigraphy, depositional environments, and sequence stratigraphy of the St. Louis and Ste. Genevieve limestones (Upper Mississippian), southwestern Kansas

Abegg, Frederick Edmund, Ph.D.

University of Kansas, 1992

U·M·I
300 N. Zeeb Rd.
Ann Arbor, MI 48106

Reproduced with permission of the copyright owner. Further reproduction prohibited without permission.

LITHOSTRATIGRAPHY, DEPOSITIONAL ENVIRONMENTS, AND SEQUENCE STRATIGRAPHY OF THE ST. LOUIS AND STE. GENEVIEVE LIMESTONES (UPPER MISSISSIPPIAN), SOUTHWESTERN KANSAS

by

Frederick E. Abegg

B.S., Pennsylvania State University, 1983
M.S., Southern Illinois University at Carbondale, 1987

Submitted to the Department of Geology and
the Faculty of the Graduate School of the
University of Kansas in partial fulfillment
of the requirements for the degree of
Doctor of Philosophy

D.Geo
1992
A244

Archives

Chairman

Committee Members

For the Department

MAY 17 1992

R00227 39861

Reproduced with permission of the copyright owner. Further reproduction prohibited without permission.

TABLE OF CONTENTS

ABSTRACT 1

ACKNOWLEDGMENTS 3

CHAPTER 1. INTRODUCTION

REGIONAL SETTING 4

PREVIOUS INVESTIGATIONS 8

METHODS 9

CHAPTER 2. LITHOFACIES

INTRODUCTION 14

LITHOFACIES 14
- Dolomitic Peloid Grainstone/Packstone 14
- Anhydrite 15
- Breccia 25
- Dolomite 30
- Dolomitic Lime Mudstone 33
- Algal Boundstone 34
- Skeletal Packstone/Wackestone 40
- Oolitic Grainstone/Packstone 43
- Fenestral Packstone/Wackestone 45
- Quartzose Grainstone 45

SUMMARY 56

CHAPTER 3. DEPOSITIONAL ENVIRONMENTS

INTRODUCTION 59

DEPOSITIONAL ENVIRONMENTS 59
- Dolomitic Peloid Grainstone/Packstone - Restricted Shelf 60
- Anhydrite - Saltern (Shallow-subaqueous Evaporite) 60

Reproduced with permission of the copyright owner. Further reproduction prohibited without permission.

Breccia -Evaporite Solution-Collapse 65
Dolomite - Dolomitized Limestone 67
Dolomitic Lime Mudstone - Restricted Shelf 67
Dolomitic Algal Boundstone - Subtidal to Lower Intertidal Restricted Shelf 68
Skeletal Packstone/Wackestone - Marine Shelf 71
Ooid Grainstone/Packstone - Oolite Shoal 71
Fenestral Packstone/Wackestone - Tidal Flat 72
Quartzose Grainstone - Eolian 73

SUMMARY 85

CHAPTER 3. LITHOSTRATIGRAPHY

INTRODUCTION 86

LITHOSTRATIGRAPHIC UNITS 87

LATERAL VARIABILITY 91

LITHOSTRATIGRAPHIC BOUNDARIES 93

CONODONT BIOSTRATIGRAPHY 97

SUMMARY 100

CHAPTER 5. SEQUENCE STRATIGRAPHY

INTRODUCTION 101

EVIDENCE FOR SEQUENCE BOUNDARIES 103

ST. LOUIS SEQUENCES 104
Sequence 1 104
Sequence 2 108
Sequence 3 109
STE. GENEVIEVE SEQUENCES 110
Sequences 4-7 110
SHORE AIRPORT FORMATION 114
SUB-PENNSYLVANIAN UNCONFORMITY 114

Reproduced with permission of the copyright owner. Further reproduction prohibited without permission.

CORRELATION OF SEQUENCE BOUNDARIES 115

SEQUENCE DURATION 116
Fourth-order Cycles 117
Second-order Cycles 117

UPPER MISSISSIPPIAN SEQUENCE SET 117

MECHANISMS FOR SEA-LEVEL CHANGE 118
Changes in Ice Volume 118
Changes in Volume of Mid-Oceanic Ridge 122
Tectonism 122
Autocyclicity 123
Climate 124

SUMMARY 125

CHAPTER 6. WHOLE-ROCK ISOTOPE PROFILES

INTRODUCTION 127
Methods 130

LITHOFACIES AND DEPOSITIONAL ENVIRONMENTS 132

DIAGENESIS 135
Eogenesis 135
Mesogenesis 140

DISCUSSION OF WHOLE-ROCK ISOTOPIC DATA 140
Carbon Isotopic Profiles 140
Oxygen Isotopic Profiles 145
Carbon-Oxygen Isotopic Crossplots 149

SUMMARY 152

Reproduced with permission of the copyright owner. Further reproduction prohibited without permission.

CHAPTER 7. CONCLUSIONS AND SUGGESTIONS FOR FURTHER RESEARCH

CONCLUSIONS 155

SUGGESTIONS FOR FURTHER RESEARCH 157

REFERENCES CITED 160

LIST OF FIGURES

Figure 1.1 Subcrop map of Mississippian strata beneath the sub-Pennsylvanian unconformity in southwest Kansas (modified from Thompson and Goebel, 1968). 6

Figure 1.2 Late Mississippian-Early Pennsylvanian tectonic features in Kansas (modified from Merriam, 1963; Ebanks et al., 1979). Shaded areas represent regions where Mississippian strata are absent due to Late Mississippian-Early Pennsylvanian erosion. 7

Figure 1.3 Upper Mississippian lithostratigraphic units in the Hugoton embayment of the Anadarko basin in southwestern Kansas. Hugoton and Stevens Members of the St. Louis Limestone (Abegg, 1992b), Shore Airport Formation (Abegg, 1992a), and the informal "Gray group" (Youle, 1991) are new names. The sub-Pennsylvanian unconformity erodes the entire Mississippian section over structural highs (cf. Fig. 1.2). Scale is approximate as thicknesses are variable. 10

Figure 1.4 Location of cores used in study of Upper Mississippian strata in southwestern Kansas. Township and range locations are given in Table 1.1. Core descriptions are in Appendix 1. 12

Figure 2.1 Location of preserved anhydrite in southwestern Kansas. To the north and east, evaporites were dissolved forming solution-collapse breccia. Anhydrite is thin to absent to the south in southern Morton and Stevens Counties, suggesting increasing marine influence

Reproduced with permission of the copyright owner. Further reproduction prohibited without permission.

toward the Anadarko basin. Dashed lines indicate areas where well control is sparse or absent. Updip limit of St. Louis from Thompson and Goebel (1968, their Fig. 3). 16

Figure 2.2 Typical gamma-ray and neutron-density log for Upper Mississippian strata from the Amoco #1 Puyear (sec. 23, T28S, R40W). Note the extremely low gamma ray values and negative density readings for anhydrite beds (E1 and E2). See text for explanation. Compare with Fig. 2.14. 17

Figure 2.3 Anhydrite textures from the Hugoton Member of the St. Louis Limestone. Massive (M) and mosaic (Mo) (cf. Maiklem et al., 1969) are the most abundant structures. Mobil #1 Foster, 6842-6844 ft core depth. 19

Figure 2.4 Mosaic anhydrite overlain by dark-brown intraclast packstone, laminar stromatolites, and skeletal packstone and wackestone. Paucity of carbonate matrix and thickness (individual beds up to 8.2 m thick) suggest the evaporites are subtidal in origin. Amoco #1 Nordling, 5864-5872 ft core depth. 20

Figure 2.5 Possible vertically-elongate anhydrite nodules (arrows) interpreted as possible relict subaqueous gypsum crystals in the Hugoton Member. Upward-oriented anhydrite nodules are very rare, but are best developed where significant matrix is present. Amoco #1 Nordling, 5826 ft core depth. 21

Figure 2.6 East-west stratigraphic cross section of Hugoton Member anhydrite. Many anhydrite beds are laterally correlative. See Fig. 2.8 for location. 22

Figure 2.7 North-south stratigraphic cross section of Hugoton Member anhydrite. Most E2 anhydrite beds do not extend as far south as E1 anhydrite. See Fig. 2.8 for location. 23

Figure 2.8 Location map for anhydrite cross sections in Figures 2.6 and 2.7. 24

Figure 2.9 Breccia horizons in the Hugoton Member of the

Reproduced with permission of the copyright owner. Further reproduction prohibited without permission.

St. Louis are interpreted as evaporite solution-coliapse breccias. Thin breccias typically only contain monomictic horizons. 26

Figure 2.10 Polymictic breccia with varied clast types. Pan American #1 Moser, 5401-5399 ft core depth. 27

Figure 2.11 Photomicrograph of calcite pseudomorphs after gypsum in a lime mudstone clast in a polymictic breccia. Amoco #1 Wilson, 5611.6 ft core depth. Plane-polarized light. Scale bar is 0.5 mm. 28

Figure 2.12 Photomicrograph of length-slow spherulitic chalcedony (c) and megaquartz (m) in a polymictic breccia. Amoco #1 Wilson, 5611.6 ft core depth. Plane-polarized light. Scale bar is 0.5 mm. 29

Figure 2.13 Monomictic breccia with rotated to nearly *in situ* clasts. Amoco #3 Cohen C, 5386-5387 ft core depth. 31

Figure 2.14 Gamma-ray and neutron-density logs from the Flynn #31-1 Shaw (sec. 31, T31S, R34W). Note the fairly low gamma-ray values and numerous minor shale kicks of the breccia and the corresponding lower density readings relative to neutron readings. These log signatures are calibrated to the cored breccias in the Amoco #3 Wilson A (sec. 30, T30S, R33W) approximately 9 miles (14.4 km) to the northeast. 32

Figure 2.15 Photomicrograph of laminar algal boundstone from a 0.2 ft (0.06 m) thick bed interstratified with anhydrite. The stromatolite is composed of micritic and peloidal laminae that are partially replaced by blocky anhydrite. Amoco #1 Nordling, 5949.9 ft core depth. Plane-polarized light. Scale bar is 1 mm. 35

Figure 2.16 Photomicrograph of digitate algal boundstone surrounded by oolitic-skeletal mud-poor packstone. Amoco #1 Nordling, 5800.8 ft core depth. Plane-polarized light. Scale bar is 1 mm. 37

Figure 2.17 Photomicrograph of spirorbid-encrusted colloform algal boundstone. Fibrous calcite cement locally hangs from the

Reproduced with permission of the copyright owner. Further reproduction prohibited without permission.

tops of pores (arrows) suggesting it may be a pendant cement. Amoco #3 Cohen C, 5402.1 ft core depth. Plane-polarized light. Scale bar is 1 mm. 38

Figure 2.18 Spirorbid-encrusted colloform algal boundstone (C) overlain by laminar algal boundstone (L) and anhydrite (A). Amoco #1 Puyear, 5700 ft core depth. 39

Figure 2.19 Skeletal packstone/wackestone from the Stevens Member of the St. Louis Limestone. Microstylolites (M), burrows (Bu), bryozoans (Br), solitary rugose coral (RC), and crinoids (C) are indicated by arrows. Mobil #1 Foster, 6747-6748 ft core depth. 41

Figure 2.20 Two hardgrounds in skeletal and oolitic, mud-poor packstones from the Stevens Member of the St. Louis Limestone. Note the relief on the upper hardground surface. The upper hardground is overlain by a vaguely laminated peloidal crust (arrow) that is possibly algal in origin. Mobil #1 Foster, 6715 ft core depth. 42

Figure 2.21 Ooid grainstone from the Stevens Member of the St. Louis Limestone. Note scattered lithoclasts (arrow). Crinoids and, to a lesser degree, brachiopods nucleate cements more readily than ooids. Rare uncoated crinoids nucleate syntaxial cements that occlude much of the interparticle porosity. Mobil #1 Foster, 6693 ft core depth. 44

Figure 2.22 Quartzose grainstone in the Stevens Member of the St. Louis Limestone. Climbing translatent stratification, interpreted as eolian, dip at approximately 6°. The strata are unusually thick (up to 9 millimeters), coarsen upward, and contain well-developed ripple-foreset lamination. Direction of ripple migration is down the slope or to the right. Note the vertical rhizolith (arrow). Mobil #1 Foster, 6707 ft core depth. 47

Figure 2.23 Photomicrograph of climbing translatent stratification interpreted as eolian in origin. Mobil #1 Foster, 6707.3 ft core depth. Plane-polarized light. Scale bar is 1 mm. 48

Figure 2.24 Ste. Genevieve quartzose grainstone displaying three

Reproduced with permission of the copyright owner. Further reproduction prohibited without permission.

types of fine structure. Climbing translatent strata (1) are 2-5 millimeter thick and distinctly coarsen upward. Ripple-foreset lamination is developed only in the thicker strata. Grainfall units (2) consist of very fine to fine sand that is only vaguely stratified due to the excellent sorting. Grainflow (3) toes are fining upward to structureless, not as well sorted, and thin downward. The lower surface of the grainflows is concave-upward, possibly reflecting the preflow depositional surface. Dip of the grainflows is an apparent dip; true dip is slightly greater than 20°. Mobil #1 Foster, 6657-6658 ft core depth. 50

Figure 2.25 Quartzose grainstone from the Stevens Member was deposited as a vegetated eolian sand sheet. Note the dark brown rhizoliths in the two separate calcretes (C). Calcretes are overlain by lithoclast conglomerates containing reworked calcrete clasts (arrows). The strata are almost exclusively climbing translatent strata dipping at angles of less than 7°. Mobil #1 Foster , 6706-6710 ft core depth. 52

Figure 2.26 Thin micritic walls (arrows) that divide pores are interpreted as alveolar texture in a calcrete in the thin St. Louis eolianite. Mobil #1 Foster, 6709.0 ft core depth. Plane-polarized light. Scale bar is 0.25 mm. 53

Figure 2.27 Upward-oriented brownish calcite cement formed along sheet cracks beneath a calcrete in the St. Louis eolianite. Possible rounded terminations, upward-orientation, and proximity to a calcrete suggest these cements may have formed in the capillary fringe. Mobil #1 Foster, 6709.0 ft core depth. Plane-polarized light. Scale bar is 0.5 mm. 54

Figure 2.28 Photomicrograph of pendant sparry-calcite and micritic cements with rounded terminations. These cements are commonly associated with rhizoliths, a further indication of origin in the meteoric vadose zone. Amoco #3 Cohen C, 5285.9 ft core depth. Plane-polarized light. Scale bar is 0.25 mm. 55

Figure 2.29 Quartzose grainstone from the base of the Ste. Genevieve Limestone. The base of the lithoclast conglomerate

Reproduced with permission of the copyright owner. Further reproduction prohibited without permission.

(arrow) at 6661 ft core depth is the St. Louis-Ste. Genevieve boundary. Abundance of cross-stratification sets and absence of rhizoliths indicates deposition took place in an active dune field. The majority of stratification is climbing translatent (1), but grainfall (2) and rare grainflow strata (3) also occur. Mobil #1 Foster, 6657-6661 ft core depth. 57

Figure 2.30 Brownish micritic and sparry-calcite cement (arrow) in a lithoclast at the base of the Ste. Genevieve. Rounded crystal terminations and geopetal sediment inside the brachiopod indicates the cement is a pendant cement (i.e. not upward oriented). Mobil #1 Foster, 6660.25 ft core depth. Plane-polarized light. Scale bar is 0.5 mm. 58

Figure 3.1 Features typical of interbedded algal boundstone and anhydrite from the Hugoton Member of the St. Louis Limestone. 70

Figure 3.2 Features of eolian and subaqueous climbing ripples. Wind ripples have low amplitudes and relatively long wavelengths with the coarser grains concentrated at the ripple crest. Low-angle foresets retard avalanching on lee sides of ripples. These features produce climbing translatent strata that are characteristically thin, uniform thickness, commonly inversely graded, and contain few visible ripple-foreset laminae. In contrast, subaqueous ripples have higher amplitudes with the coarser grains relegated to the ripple troughs. Avalanching is common on the steep lee sides of the ripples. These features produce climbing translatent strata that are typically thicker, normally graded, and contain well-developed ripple-foreset laminae (Modified from Kocurek and Dott, 1981, their Fig. 3). 75

Figure 3.3 Features of eolian sand-sheets deposits. Stratification is almost exclusively climbing translatent with dips commonly less than 15°. Tangential cross-strata sets with grainfall (and grainflow?) deposits are rare. Rhizoliths are scattered throughout the unit and locally disrupt stratification. An entire eolian interval may form from sand sheets or contain interbedded cross-stratified units deposited by migrating dunes. Most Upper Mississippian eolianites in southwestern Kansas contain sand-sheet deposits, but not all (e.g., Abegg, 1991). 80

Figure 3.4 Distribution of stratification types in deposits of

Reproduced with permission of the copyright owner. Further reproduction prohibited without permission.

active dune fields in Upper Mississippian eolianites of southwestern Kansas. Preserved strata are composed of abundant climbing translatent strata, common grainfall deposits, and rare grainflow units. Rhizoliths are rare to absent. Dips typically increase upward, reflecting preferential preservation of dune aprons and lower slipfaces and tangential foresets. Cross-strata sets are up to 2.5 ft (0.8 m) thick. 82

Figure 4.1 Gamma ray-sonic log from the Mobil #1 Foster (sec. 5, T34S, R36W), Stevens County, Kansas. Lithostratigraphic boundaries are picked from a combination of core studies and cross-section correlations (SG, Ste. Genevieve; STV, Stevens Member of the St. Louis Limestone; HUG, Hugoton Member of the St. Louis Limestone). Shore Airport (Chesterian) overlies the Ste. Genevieve. Note the extremely clean gamma ray response of the E1 anhydrite (6854-6842 ft). Cored interval is indicated in depth track. Core and log depths are approximately equal. Depths in feet. 88

Figure 5.1 Block diagram of depositional environments of the upper Salem and Hugoton Member of the St. Louis. Oolitic shoals combined with a fall in relative sea level restricted marine circulation enough to precipitate gypsum but not halite. Most evaporites are interpreted as extensive deposits of shallow lagoons (salterns). Diagnostic intertidal and supratidal features are rare. Stromatolites, interpreted to be largely subtidal in origin, occur in many Upper Mississippian cores and are interbedded with both anhydrite and subtidal strata. GR-grainstone; PK-packstone; WK-wackestone. 105

Figure 5.2 North-south schematic cross section of upper Hugoton and lower Stevens strata from Stanton to Stevens Counties showing the inferred location of SB1. 107

Figure 5.3 Block diagram showing the lateral distribution of facies that deposited strata of the Stevens Member of the St. Louis and Ste. Genevieve. Angle of dune climb is exaggerated for illustrative purposes. Dunes are shown as crescentic, but their morphology is uncertain. Because most subtidal strata lack detrital quartz, such grains in eolianites may have been transported by wadis. Detrital carbonate grains are interpreted to have been derived

Reproduced with permission of the copyright owner. Further reproduction prohibited without permission.

from beach sediments or, based on lithoclasts and reworked crinoids with rounded overgrowths, erosion of previously lithified limestones. The shoreline is interpreted to be a low-energy beach, energy having been dissipated on oolitic shoals. Beach strata have not been recognized, perhaps owing to subsequent erosion. Modified from Handford and Francka (1991, their Fig. 15). 111

Figure 5.4 S1 and S2 in the St. Louis Limestone are marine-dominated sequences. S2 is a thick type-2 sequence that contains little evidence of subaerial exposure. Wavy line indicates a sequence boundary marked by subaerial exposure, whereas a bold, straight line indicates a relatively conformable sequence boundary. 119

Figure 5.5 Eolian-dominated sequences are characteristic of S3 through S7 in the uppermost St. Louis and Ste. Genevieve Limestones. These are type-1 or type-2 sequences that are typically thinner than marine-dominated sequences and contain abundant evidence of subaerial exposure. Wavy line indicates a sequence boundary marked by subaerial exposure. 120

Figure 6.1 Potentially useful patterns in $\delta^{13}C$ and $\delta^{18}O$ in the recognition of ancient subaerial exposure surfaces. Modified from Allan and Matthews (1982, their Fig. 11) and from Goldstein (1991, his Fig. 2). 129

Figure 6.2 Carbon-oxygen crossplot patterns that are associated with subaerial exposure. Modified from Allan and Matthews (1982, their Fig. 11). The large variation in $\delta^{13}C$ and the small variation in $\delta^{18}O$ (dark stipple) results from meteoric diagenesis. Covariance of $\delta^{13}C$ and $\delta^{18}O$ (light stipple) may result from mixing-zone diagenesis or from marine sediments with cementation in several diagenetic environments (Allan and Matthews, 1982; Givens and Lohmann, 1985). 131

Figure 6.3 Paragenesis of most extensive diagenetic features (excluding evaporite diagenesis and dolomitization) from the Amoco #1 Nordling and Amoco #3 Cohen C. Width of features indicates relative abundance. Eogenetic refers to early diagenesis that took place in waters that are affected by near-surface conditions.

Reproduced with permission of the copyright owner. Further reproduction prohibited without permission.

Mesogenetic refers to later diagenesis in waters that are buried deeply enough to be unaffected by near-surface processes. No overlap of diagenetic features was observed in any individual sample. These diagenetic features are common in many St. Louis and Ste. Genevieve cores in southwestern Kansas. 136

Figure 6.4 Photomicrograph of bladed isopachous calcite cement (arrows) below a truncation surface, most likely a hardground. FeIV cement (E) patchily occludes primary intergranular porosity (BP). The isopachous cement is absent above the truncation surface, suggesting it is a marine cement. Amoco #1 Nordling, 5742.3 ft core depth. Plane-polarized light. Scale bar is 0.25 mm. 137

Figure 6.5 Photomicrograph of a syntaxial overgrowth of calcite cement on an echinoderm. Zoned eogenetic NFeI, FeII, and NFeIII calcite cements (arrow) penetrate into a trilobite, indicating these cements are precompactional. NFeIV, unzoned ferroan calcite cement (F), does not penetrate into the trilobite and locally this cement heals fractured allochems, indicating it is a postcompactional burial cement. Amoco #1 Nordling, 5665.1 ft core depth. Plane-polarized light. Scale bar is 0.5 mm. 139

Figure 6.6 Key to grains and lithic symbols for Figures 6.7 to 6.10. 141

Figure 6.7 Carbon isotopic profile of the Hugoton Member of the St. Louis and Ste. Genevieve in the Amoco #1 Nordling. Note minor light carbon shift in subtidal strata below lower eolianite. Light carbon values at 5665.1 may correspond to a subaerial-exposure surface at the base of an eolianite at 5655.5 See Table 6.1 for $\delta^{13}C$ values. See Fig. 6.6 for key to grains and lithic symbols. 142

Figure 6.8 Carbon isotopic profile of the Hugoton Member of the St. Louis and Ste. Genevieve in the Amoco #3 Cohen C. A light carbon shift corresponds to an exposure surface (5322) marked by a calcrete. Eolian interpretation of sample at 5321.6 is questionable. See Table 6.2 for $\delta^{13}C$ values. See Fig. 6.6 for key to grains and lithic symbols. 143

Figure 6.9 Oxygen isotopic profile of the Hugoton Member of

Reproduced with permission of the copyright owner. Further reproduction prohibited without permission.

the St. Louis and Ste. Genevieve in the Amoco #1 Nordling. See Table 6.1 for $\delta^{18}O$ values. See Fig. 6.6 for key to grains and lithic symbols. 146

Figure 6.10 Oxygen isotopic profile of the Hugoton Member of the St. Louis and Ste. Genevieve in the Amoco #3 Cohen C. Eolian interpretation of sample at 5321.6 is questionable. See Table 6.2 for $\delta^{18}O$ values. See Fig. 6.6 for key to grains and lithic symbols. 147

Figure 6.11 Carbon-oxygen crossplot from the Amoco #1 Nordling. Eolian and subtidal samples plot separately mainly due to lighter $\delta^{13}C$ values in eolian strata. 150

Figure 6.12 Carbon-oxygen crossplot from the Amoco #3 Cohen C. Eolian and subtidal samples plot separately except for the thin eolian? (5321.6 ft) unit in the Stevens Member. 151

Figure 6.13 Carbon-oxygen crossplot from both the Amoco #1 Nordling and Amoco #3 Cohen C. Eolian and subtidal samples overlap slightly. 153

LIST OF TABLES

Table 1.1 Location and depths of cores logged in this study (see Fig. 1.4 and Appendix 1). 11

Table 3.1 Distinguishing features of sabkha and saltern (extensive shallow-subaqueous) evaporites (modified from Warren, 1989, his Table 3.1). 61

Table 3.2 Contrasting features of eolian and subaqueous grainstones (based largely on Hunter, 1981 and 1989). Boldface indicates features present in quartzose grainstones in the Upper Mississippian of southwestern Kansas. Also refer to Figures 2.22, 2.23, 2.24, 2.25, 2.26, 2.27, 2.28, 2.29, 2.30, and 3.2. 74

Table 4.1 Conodonts recovered at various intervals from the Mobil #1 Foster. Formation and member boundaries determined

Reproduced with permission of the copyright owner. Further reproduction prohibited without permission.

independently of conodont biostratigraphy. Conodont identification by Richard Lane of Amoco. 99

Table 5.1 Definitions of sequence stratigraphic terms used in this report. 102

Table 6.1 Summary of stable isotope data and description of samples from Amoco #1 Nordling. 133

Table 6.2 Summary of stable isotope data and description of samples from Amoco #3 Cohen C. 134

LIST OF APPENDICES

Appendix 1. Core Descriptions from the 13 core logged from southwestern Kansas. Locations are given in Table 1.1 and Figure 1.4. 173

Appendix 2. List of 125 wells used in stratigraphic cross sections in southwestern Kansas. Cross sections A-A', C-C', I-I', and J-J' are included as pocket enclosures. 197

Appendix 3. T-test of $\delta^{13}C$ values from eolian and subtidal strata. 205

LIST OF POCKET ENCLOSURES

Cross sections A-A', C-C', I-I', and J-J' are included as pocket enclosures. Nine stratigraphic cross sections were hung on the top of the Ste. Genevieve or the top of the Mississippian where the St. Genevieve is missing. Those not included here are available at the Kansas Geological Survey. A-A', B-B', C-C', and D-D' are east-west cross sections and E-E', F-F', G-G', H-H', and I-I' are north-south cross sections. Cross section J-J' is a sequence stratigraphic interpretation of cores located along I-I'.

Reproduced with permission of the copyright owner. Further reproduction prohibited without permission.

ABSTRACT

The St. Louis (Meramecian) and Ste. Genevieve (Chesterian) Limestones in southwestern Kansas were the last dominantly carbonate Mississippian units deposited on a shelf that extended southward from the Transcontinental arch. The Hugoton Member of the St. Louis Limestone primarily consists of peloid grainstone/packstone, subtidal anhydrite, evaporite solution-collapse breccia, and dolomite that were deposited on a restricted shelf. The overlying Stevens Member of the St. Louis Limestone contains abundant normal-marine skeletal packstone/wackestone. The upper part of the Stevens contains parasequences capped by ooid grainstone/packstone and a thin eolian quartzose grainstone. Ste. Genevieve consists of interbedded eolian quartzose grainstone and subtidal oolitic and peloidal grainstone/packstone along with minor normal-marine skeletal packstone/wackestone.

The St. Louis and Ste. Genevieve Limestones contain seven fourth-order depositional sequences (S1 to S7). S1 and S2 are relatively thick, subtidally-dominated sequences. The top of the Hugoton Member is the tentative location of the S1-S2 sequence boundary and is interpreted as a type 2 sequence boundary that contains no evidence of significant subaerial exposure on this part of the shelf. S3 through S7 are relatively thin eolian-dominated sequences. The lower sequence boundaries of S3 through S7 are marked by calcretes with rhizoliths, lithoclast conglomerates with reworked calcrete clasts, vadose cement, negative whole-rock $\delta^{13}C$ shifts, and are overlain by eolian units. Eolian units directly overlie subtidal strata indicating they formed as a result of a fall in relative sea level. An upward decrease in thickness of sequences as well as an increase in the number of eolianites and exposure surfaces suggest St. Louis and Ste. Genevieve strata comprise an aggradational or progradational sequence set, the result of a second-order fall of relative sea level that reduced the rate of increase in accomodation on the shelf.

Reproduced with permission of the copyright owner. Further reproduction prohibited without permission.

Mean whole-rock $\delta^{13}C$ values of eolian strata, excluding detailed samples of rhizoliths and pendant cements, are 0.43 to 0.56 ‰ less positive and statistically different from subtidal strata. Sources of isotopically depleted carbon in eolianites include rhizoliths, pendant cements, and possibly zoned cements precipitated in the meteoric phreatic zone.

Reproduced with permission of the copyright owner. Further reproduction prohibited without permission.

ACKNOWLEDGMENTS

The author gratefully acknowledges the guidance and input of dissertation advisor Dr. Paul Enos. His careful editorial comments and insights significantly improved this dissertation. Editorial comments and suggestions of Drs. Lynn Watney and Robert Goldstein are also greatly appreciated. I also wish to thank Drs. W. R. Van Schmus and N. A. Slade for their reading and helpful suggestions. Dr. Jack Allan of Chevron Oil Field Research Company provided editorial comments and suggestions for the whole-rock isotope section (Chapter 6).

This research has been supported by the Geology Associates Program of the University of Kansas Endowment Association, the Kansas Geological Survey, Amoco Production Company, and Phillips Petroleum Company. I would like to thank Amoco Production Company and the Kansas Geological Survey for providing access to numerous Upper Mississippian cores. Special thanks are extended to Amoco's Van Leighton for his assistance and consideration. Drs. Chris Maples and Evan Franseen of the Kansas Geological Survey also contributed to discussions on Upper Mississippian lithostratigraphy and sequence stratigraphy. Dr. Richard Lane of Amoco graciously provided conodont identifications for the Mobil #1 Foster. Dr. Tom Thompson of the Missouri Geology and Land Survey assisted with the interpretation of conodont data.

Numerous graduate students assisted in various stages of completion of this dissertation. Kevin Evans, John Youle, and Jeff Johnson contributed to discussions that improved ideas used in this report. Drs. Ken Hood, Loren Babcock, and Matt Beebe provided helpful guidance during the early stages of this research.

My wife Michelle assisted in word processing and computer drafting for this report. Her endless encouragement, patience, and companionship have been invaluable. I would also like to thank my daughter Kylie for putting it all in perspective. In addition, the tremendous support and concern of my parents are greatly appreciated.

Reproduced with permission of the copyright owner. Further reproduction prohibited without permission.

CHAPTER 1
Introduction

Mississippian strata in Kansas are confined to the subsurface, except for outcrops of Burlington-Keokuk and Warsaw Limestones (Osagean to Meramecian) in two townships of Cherokee County, in the extreme southeastern corner of the state (Thompson and Goebel, 1968; Kammer et al., 1990; Maples, 1992). Upper Mississippian lithostratigraphic nomenclature of the Mississippi Valley region was originally extended to the subsurface of Kansas by Lee (1940) and Clair (1948, 1949), and most recently updated by Goebel (1968), Thompson and Goebel (1963, 1968), and Maples (1992).

Most previous studies of Upper Mississippian strata in Kansas used insoluble residues and biostratigraphy extensively to define lithostratigraphic units. It is more practical to base definitions on the more abundant carbonate fraction that is observable in cores and cuttings, or indicated with certain wireline logs. Formations are rock-stratigraphic units (i.e. lithofacies); accordingly biostratigraphic data should serve to constrain lithostratigraphic correlations, but not to delineate formations. Recent advances in carbonate petrology, sequence stratigraphy, and subsurface data warrant an update of existing lithostratigraphic definitions and interpretations of depositional history of the Upper Mississippian in southwestern Kansas. Increased understanding of facies, lithostratigraphy, and depositional history should enhance hydrocarbon exploration and production from these strata.

REGIONAL SETTING

In the Mississippi Valley type area, the St. Louis Limestone is primarily a mud-rich carbonate, generally interpreted to have been deposited in restricted lagoonal to tidal flat or sabkha settings (Jorgensen and Carr, 1973; Martorana, 1987). The overlying Ste.

Reproduced with permission of the copyright owner. Further reproduction prohibited without permission.

Genevieve is oolitic. Ste. Genevieve oolitic carbonates of the Illinois basin are a primary hydrocarbon target, whereas the St. Louis is generally unproductive. In the Hugoton embayment of southwestern Kansas, however, the upper St. Louis oolites are a major hydrocarbon reservoir, whereas Ste. Genevieve carbonates are less productive.

Ste. Genevieve and St. Louis strata in southwestern Kansas were deposited on a carbonate shelf that extended southward from the Transcontinental arch. Ste. Genevieve and St. Louis strata overlie carbonates of the Salem Limestone. The top of the Ste. Genevieve is marked by a shift to argillaceous carbonates and siliciclastics of the overlying Shore Airport Formation (Abegg, in press (a)). This siliciclastic influx marks the termination of dominantly carbonate shelf deposition that continued throughout much of Mississippian time (Lane and De Keyser, 1980). Mississippian strata in Kansas were subaerially exposed and extensively eroded prior to deposition of Lower Pennsylvanian strata.

St. Louis and Ste. Genevieve strata in Kansas are most completely preserved in the Hugoton embayment of the Anadarko basin (Figs. 1.1 and 1.2). Ste. Genevieve is also preserved in the Forest City basin. The St. Louis is more widespread than the Ste. Genevieve and is preserved in the Forest City, Cherokee, Salina, and Sedgwick basins (Thompson and Goebel, 1968). The St. Louis outcrops nearest to Kansas are in a downfaulted block along the Chesapeake Fault in southwestern Dade and eastern Barton Counties, southwestern Missouri (Clark, 1937; Thompson, 1986; personal observation). The outcrops of Ste. Genevieve strata nearest to Kansas are in the Mississippi Valley, the type area in eastern Missouri (e.g., Thompson, 1986).

The Hugoton embayment is a south-plunging structure located in western Kansas and eastern Colorado that was preceded by the pre-Mississippian Southwest Kansas basin (Merriam, 1963). The Hugoton embayment subsided throughout the Late Paleozoic, but by the Mesozoic it was inactive (Merriam, 1963). The Hugoton

Reproduced with permission of the copyright owner. Further reproduction prohibited without permission.

Reproduced with permission of the copyright owner. Further reproduction prohibited without permission.

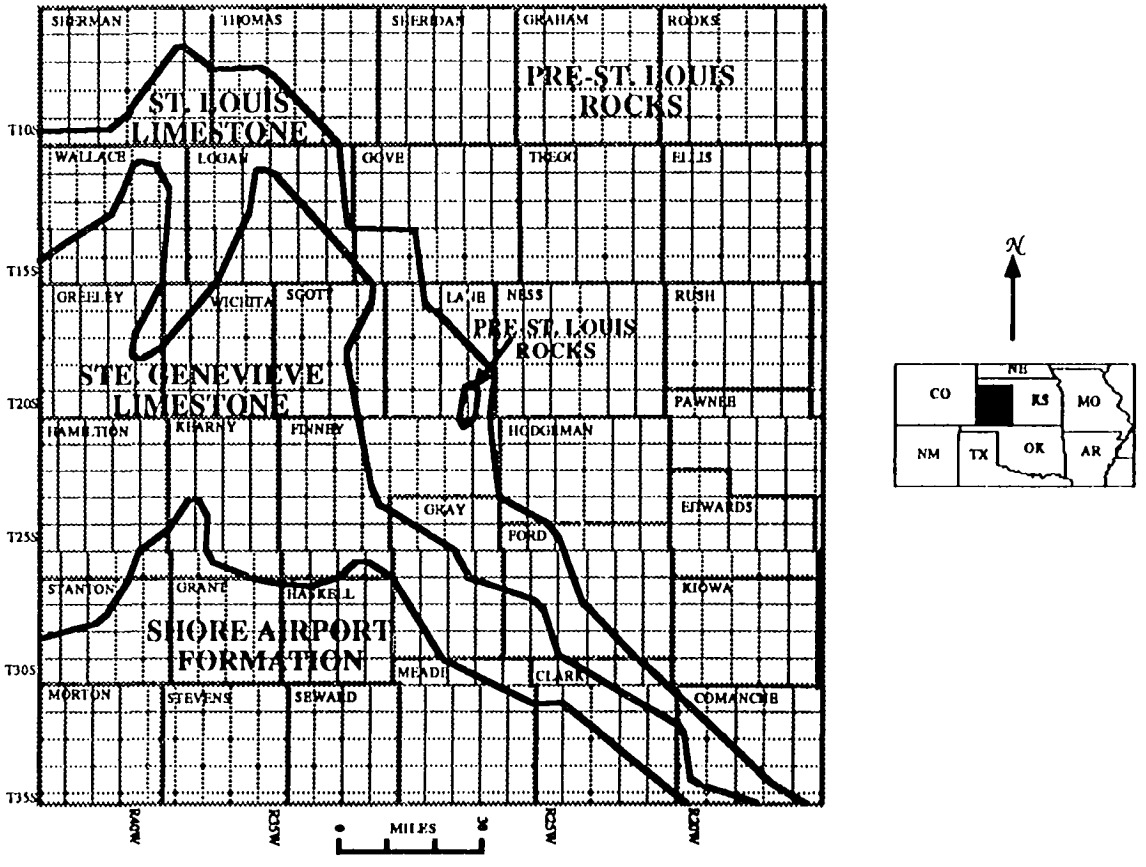


Figure 1.1 Subcrop map of Mississippian strata beneath the sub-Pennsylvanian unconformity in southwest Kansas (modified from Thompson and Goebel, 1968).

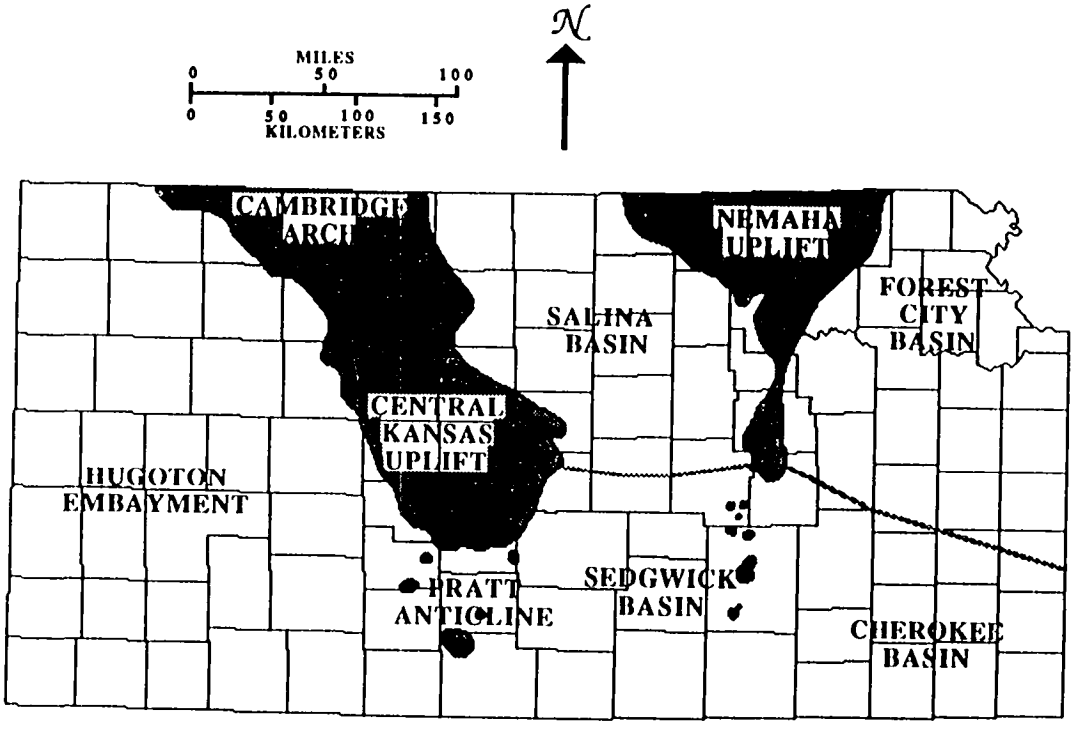


Figure 1.2 Late Mississippian-Early Pennsylvanian tectonic features in Kansas (modified from Merriam, 1963; Ebanks et al., 1979). Shaded areas represent regions where Mississippian strata are absent due to Late Mississippian-Early Pennsylvanian erosion.

Reproduced with permission of the copyright owner. Further reproduction prohibited without permission.

embayment is bounded by the Pratt anticline, Central Kansas uplift, and Cambridge arch to the east and north (Fig. 1.2), and by the Las Animas arch, Apishapa-Sierra Grande uplift, and Front Range to the west, and by the Anadarko basin to the south. Many of these are considered to be Late Mississippian-Early Pennsylvanian tectonic features (Merriam, 1963; Goebel and Stewart, 1979; Kluth and Coney, 1981). In the vicinity of the Sierra Grande uplift in Colorado, DeVoto (1980) interpreted the onlap of St. Louis strata and the change from subtidal to intertidal and nearshore facies to indicate that this structure was tectonically active as early as the Meramecian. In southwestern Kansas, local thinning of Shore Airport (Chesterian) strata from structurally positive areas suggests uplift began prior to deposition of the Morrowan Kearny Formation (Abegg, 1991).

PREVIOUS INVESTIGATIONS

According to Lee (1940), upper Meramecian and Chesterian strata of southwestern Kansas were first penetrated by the Watchorn Oil and Gas Company #2 Morrison in Clark County in 1931. Strata of "late Meramecian age" in southwestern Kansas were initially grouped into the Watchorn Formation "where subdivision of...the Spergen [Salem], St. Louis, and possibly Ste. Genevieve limestones is impracticable" (Lee, 1940, p. 84-85). Lee relied heavily on insoluble residues to assist in recognition of Mississippian units. In the same report, Girty (1940) reported on the megafossils of the Watchorn and unnamed Chesterian strata.

Clair (1948, 1949) subsequently divided the Watchorn into three formations using Mississippi Valley nomenclature. Recognition of the Ste. Genevieve, St. Louis, and Spergen (Salem) Limestones was based primarily on lithologic criteria. Chesterian strata (above the Ste. Genevieve) were not named due to lithologic heterogeneity (Clair, 1948, 1949; Beebe, 1959a, 1959b). Thompson and Goebel (1963, 1968) and Goebel

Reproduced with permission of the copyright owner. Further reproduction prohibited without permission.

(1968) redefined Mississippian strata using a combination of lithologic criteria, insoluble residues, and conodont biostratigraphy.

The Ste. Genevieve Limestone has traditionally been placed within the Meramecian Stage (e.g., Thompson and Goebel, 1963, 1968; Zeller, 1968). Maples and Waters (1987) redefined the Meramecian-Chesterian boundary, however, placing the Ste. Genevieve in the type area at the base of the Chesterian Stage, a usage followed in this report (Fig. 1.3).

The first details of the depositional environments of the upper St. Louis Limestone were provided by Ball (1969). Ball suggested Walther's Law as a technique for locating oolitic reservoir beds. More recently, Handford (1988, 1990) and Handford and Francka (1991) provided some details on the sedimentology of the St. Louis and Ste. Genevieve from the Damme Field (Finney County, Kansas) and the Big Bow Field (Stanton and Grant Counties, Kansas).

The St. Louis Limestone is subdivided into two members (Abegg, in press (b)). Hugoton Member strata consist of restricted-shelf dolomitic carbonate and anhydrite. The overlying Stevens Member is dominated by normal-marine limestones.

METHODS

Thirteen cores totalling 2,904 ft (885 m) were described in detail (Table 1.1, Fig. 1.4, Appendix 1). Cores were selected primarily for maximum stratigraphic coverage (>30 m, 100 ft, each) and areal distribution. Several shorter cores were examined in less detail to evaluate lateral variability. Cores were originally logged at a scale of 1:12 or 1:24. Carbonate textures were described following Dunham (1962). Anhydrite textures were described following Maiklem et al. (1969). Choquette and Pray's (1970) classification was applied to carbonate porosity. A total of 491 thin sections were examined from these cores. To facilitate recognition of detrital siliciclastic grains,

Reproduced with permission of the copyright owner. Further reproduction prohibited without permission.

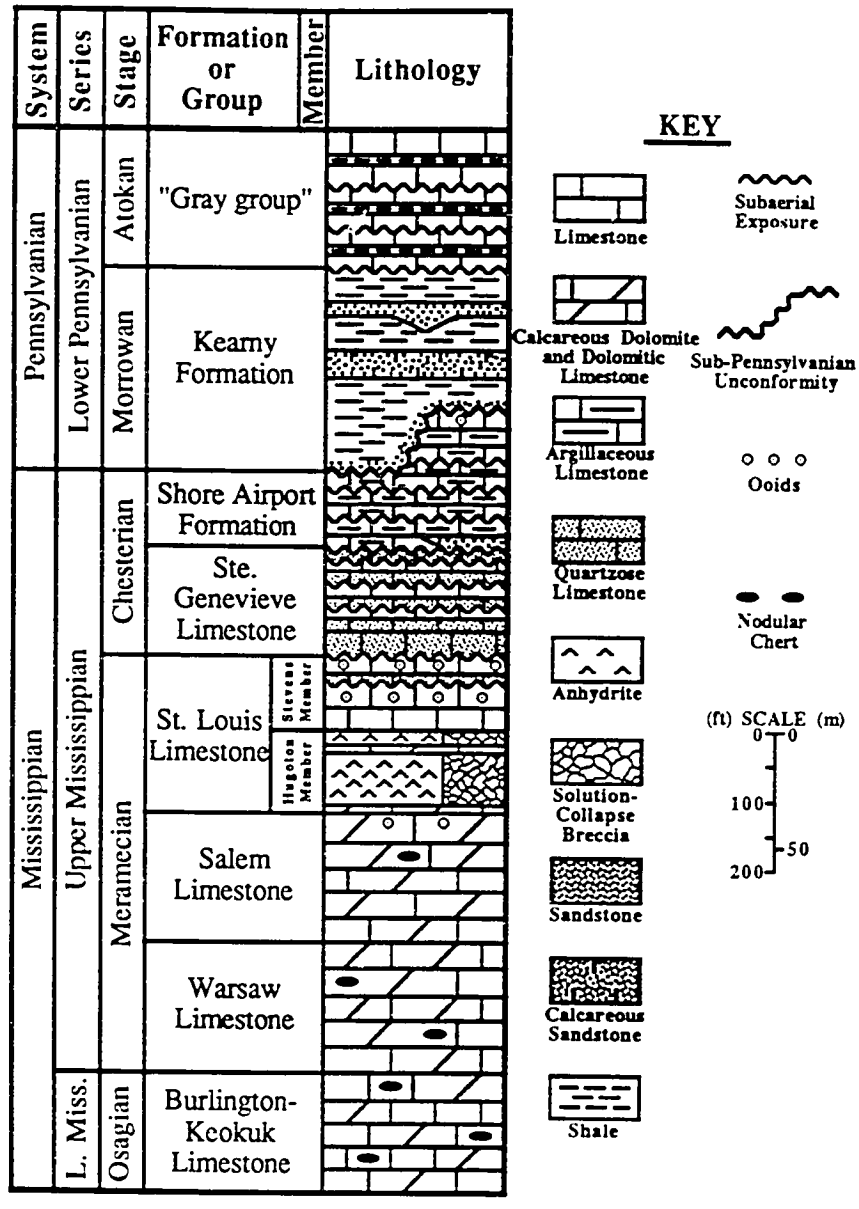


Figure 1.3 Upper Mississippian lithostratigraphic units in the Hugoton embayment of the Anadarko basin in southwestern Kansas. Hugoton and Stevens Members of the St. Louis Limestone (Abegg, 1992b), Shore Airport Formation (Abegg, 1992a), and the informal "Gray group" (Youle, 1991) are new names. The sub-Pennsylvanian unconformity erodes the entire Mississippian section over structural highs (cf. Fig. 1.2). Scale is approximate as thicknesses are variable.

Reproduced with permission of the copyright owner. Further reproduction prohibited without permission.

Table 1.1. Location and depths of core logged in this study.

WELL	LOCATION	COUNTY	INTERVAL
Alma #1 Watchorn	C SW NE, 13-15S-33W	Logan	4445'-4646'
Shallow Water #4 Maune	C NE NW, 31-21S-33W	Finney	4628'-4775'
Pan American #1 Moser	C NW NW, 31-24S-36W	Kearny	4960'-5235'
Amoco #3 Cohen C	C SE NE, 27-25S-38W	Kearny	5226'-5459'
Pendleton #1 Schauf	SW SW NE, 16-27S-29W	Gray	4956'-5080'
Cities Service #1 Kells B	C NW NW, 05-28S-34W	Haskell	5590'-5710'
Amoco #1 Puyear	660' FWL 1980' FSL, 23-28S-40W	Stanton	5454'-5716'
Amoco #1 Nordling	SW SE NE, 30-29S-39W	Stanton	5650'-6030'
Amoco #3 Wilson A	SE SE NW, 30-30S-33W	Haskell	5310'-5818'
Amoco #1 Breeding F	SW, 34-31S-40W	Morton	5040'-5416'
Mobil #1 A. W. Foster	C NE SW, 05-34S-36W	Stevens	6625'-6910'
Colorado #2 Fox A	C NE SE, 03-35S-30W	Meade	6240'-6299'
Mobil #1 Headrick	SW NW, 03-35S-37W	Stevens	6733'-6911'

Reproduced with permission of the copyright owner. Further reproduction prohibited without permission.

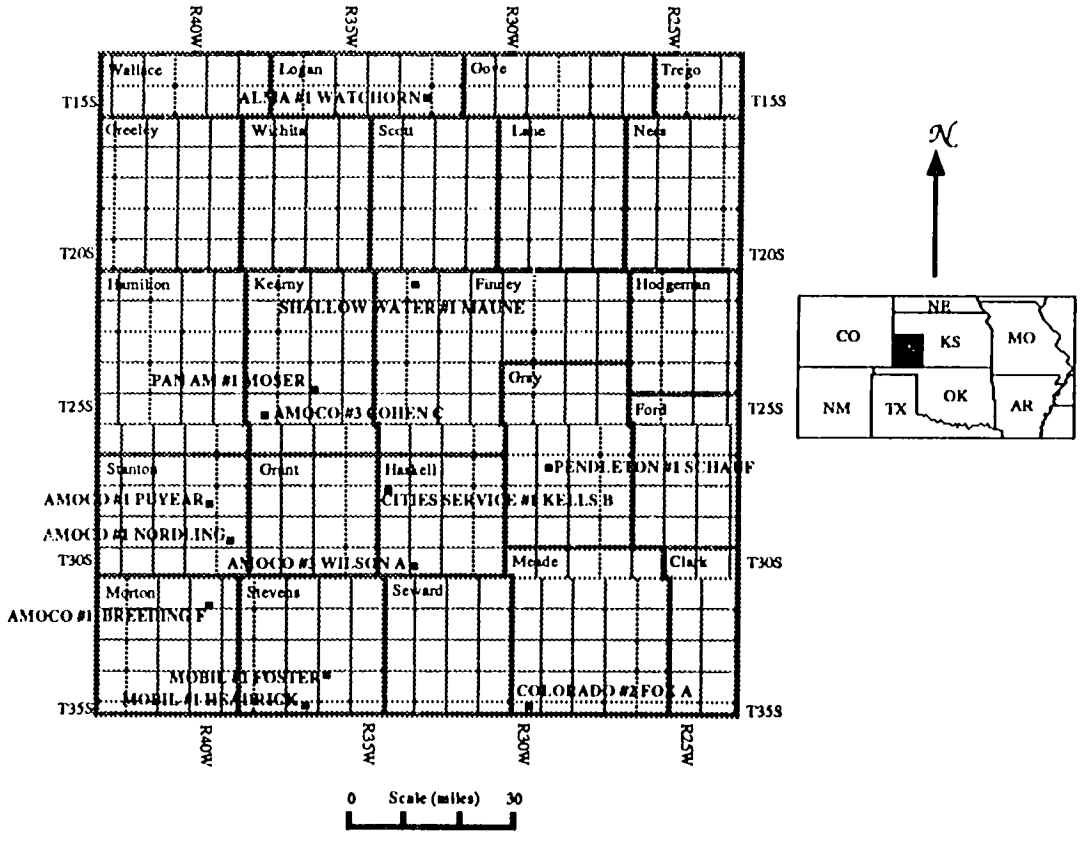


Figure 1.4 Location of cores used in study of Upper Mississippian strata in southwestern Kansas. Township and range locations are given in Table 1.1. Core descriptions are in Appendix 1.

Reproduced with permission of the copyright owner. Further reproduction prohibited without permission.

dolomite crystals, and ferroan cements, many thin sections were stained with Alizarin Red-S and potassium ferricyanide (Dickson, 1966). Cross-strata dip angles were measured where true dip could be determined on cores. Structural dip and borehole deviation were assumed to be negligible.

Ste. Genevieve, St. Louis, and Salem Limestones and the Warsaw Formation were examined in the type sections and type areas in the Illinois basin to compare and contrast with the St. Louis and Ste. Genevieve Limestones in southwestern Kansas. Outcrops of Warsaw, Salem (?), and St. Louis Limestones from southwestern Missouri were also described. St. Louis and Salem (?) strata are locally preserved on the downthrown side of the Cheasepeake Fault in southwestern Dade and eastern Barton Counties, southwestern Missouri (Clark, 1937; Thompson, 1986; personal observation).

Four east-west and five north-south stratigraphic cross sections involving 125 wells were constructed to evaluate lateral variability of the Upper Mississippian units (Appendix 2, Pocket Enclosures). Wells that penetrate the maximum thickness of Mississippian strata were selected for the cross sections. Gamma ray and neutron-density are the most informative logs, as they most accurately reveal lithologic variations. Cores allow calibration of log signatures to lithologies. Cross sections were hung on the top of the Ste. Genevieve as this is the most consistent Mississippian log pick. In a few wells where the Shore Airport and Ste. Genevieve were eroded beneath the sub-Pennsylvanian unconformity, the logs were hung on the top of the Mississippian.

Reproduced with permission of the copyright owner. Further reproduction prohibited without permission.

CHAPTER 2
Lithofacies

INTRODUCTION

Previous descriptions of lithofacies in the St. Louis and Ste.Genevieve Limestones in the Hugoton embayment of the Anadarko basin in southwestern Kansas are outdated (e.g., Clair, 1948, 1949; Goebel, 1968) or are spatially limited (Handford, 1988, 1990; Handford and Francka, 1991). A detailed regional description of lengthy cores using updated petrographic terminology is needed to facilitate recognition of lithofacies and lithostratigraphic units, as well as provide the data for sedimentological interpretations.

LITHOFACIES

Ten lithofacies are recognized in the St. Louis and Ste. Genevieve cores examined in this study (Appendix 1): 1) dolomitic peloid grainstone/packstone, 2) anhydrite, 3) breccia, 4) dolomite, 5) dolomitic lime mudstone, 6) algal boundstone, 7) skeletal packstone/wackestone, 8) ooid grainstone/packstone, 9) fenestral packstone/wackestone, and 10) quartzose grainstone. Lithofacies descriptions are listed in roughly ascending stratigraphic order, although some facies occur in both the St. Louis and Ste. Genevieve Limestones.

Dolomitic Peloid Grainstone/Packstone

Peloids are abundant to common. Partially micritized allochems suggest that some peloids are micritized grains. Ellipsoidal shape of others suggest they are fecal pellets. Echinoderms are rare to common. Other allochems are rare and include brachiopods, bryozoans, ostracodes, calcispheres, sponge spicules, and intraclasts. Detrital quartz

Reproduced with permission of the copyright owner. Further reproduction prohibited without permission.

of very fine sand size typically comprises 5 to 10 percent of this facies; feldspar, muscovite, glauconite, amphibole, and organic fragments are rare. Relative to the St. Louis, peloid packstone in the Ste. Genevieve commonly has more detrital quartz, up to 60 percent locally. Dolomite replaces up to 70 (most commonly 5-30) of the peloidal grainstones and packstones. Dolomitization is typically fabric selective, preferentially replacing the micritic fraction. Bluish-gray chert is present in some horizons and is commonly associated with casts of sponge spicules. This suggests a local biogenic source for much of the silica. Cubic pyrite, typically 10-50 μm, is scattered throughout much of the facies.

Many intervals are marked by parallel laminae. Some strata are ripple cross-laminated (cf. Abegg, 1991, his Fig. 5A). In the Ste. Genevieve in Mobil #1 Foster, mm-scale laminae rhythmically thicken and thin (cf. Abegg, 1991, his Fig. 5B). Horizontal feeding traces are present in some horizons.

Interparticle porosity is totally occluded by equant calcite cement. Much of the original interparticle porosity has been destroyed by compaction. Sutured stylolites are common, but wispy microstylolite swarms are more abundant (cf. Wanless, 1979).

Peloid dolomitic grainstone/packstone is most common in the Hugoton Member of the St. Louis Limestone and in the Ste. Genevieve Limestone, but is rare in the Stevens Member of the St. Louis Limestone. Interstratified facies include ooid grainstone/packst e, nodular anhydrite, skeletal packstone/wackestone, or quartzose grainstone (Appendix 1).

Anhydrite

In southwestern Kansas, preserved anhydrite is restricted to portions of Morton, Stanton, Hamilton, Stevens, Grant, Seward, Haskell, and possibly Meade Counties (Fig. 2.1). Thirteen separate anhydrite beds have been recognized from the density log of Amoco #1 Puyear (sec. 23, T28S, R40W) (Fig. 2.2). In cores, individual beds are

Reproduced with permission of the copyright owner. Further reproduction prohibited without permission.

Reproduced with permission of the copyright owner. Further reproduction prohibited without permission.

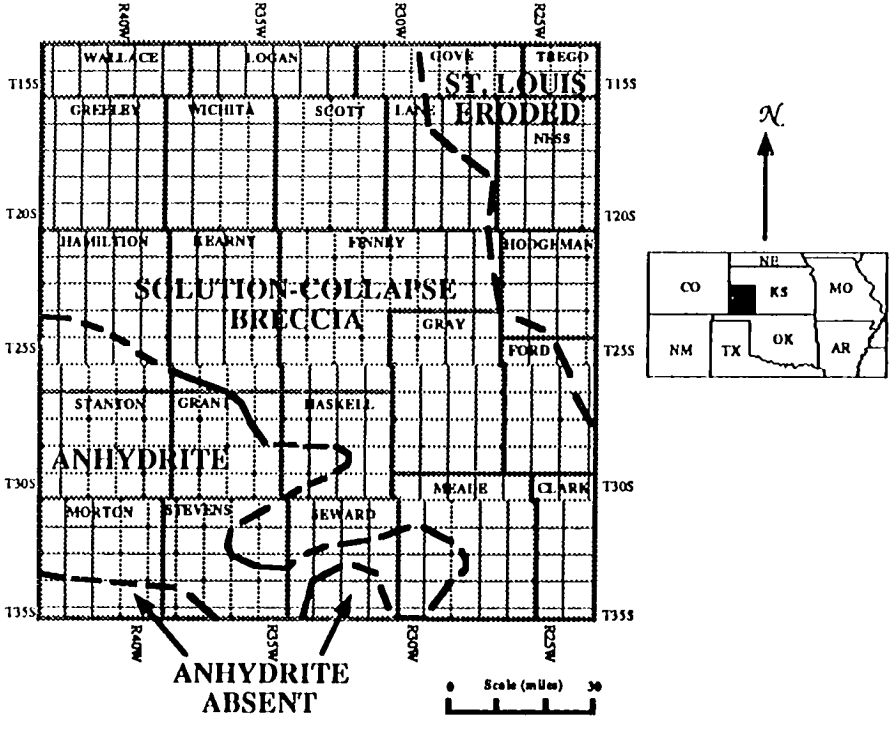


Figure 2.1 Location of preserved anhydrite in southwestern Kansas. To the north and east, evaporites were dissolved forming solution-collapse breccia. Anhydrite is thin to absent to the south in southern Morton and Stevens Counties, suggesting increasing marine influence toward the Anadarko basin. Dashed lines indicate areas where well control is sparse or absent. Updip limit of St. Louis from Thompson and Goebel (1968, their Fig. 3).

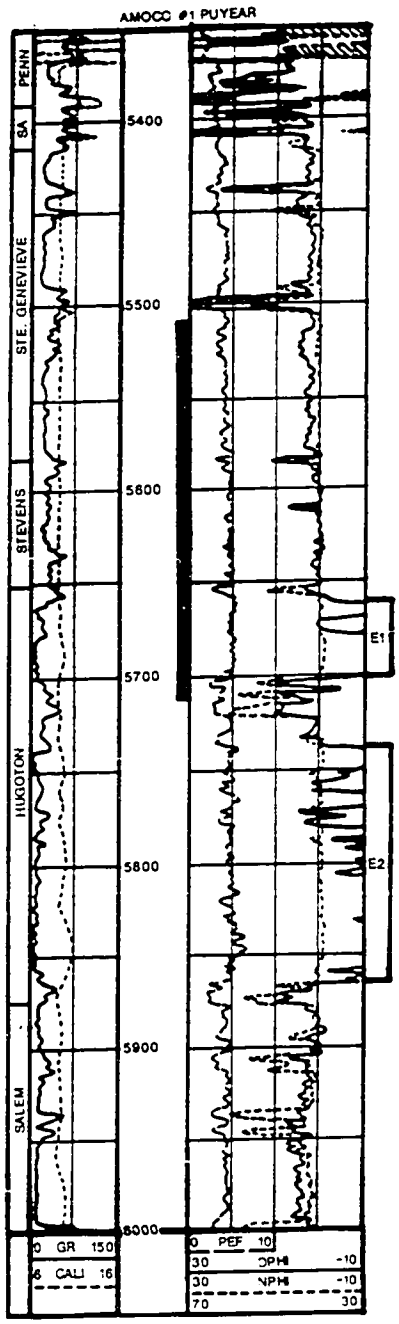


Figure 2.2 Typical gamma-ray and neutron-density log for Upper Mississippian strata from the Amoco #1 Puyear (sec. 23, T28S, R40W). Note the extremely low gamma ray values and negative density readings for anhydrite beds (E1 and E2). See text for explanation. Compare with Fig. 2.14.

Reproduced with permission of the copyright owner. Further reproduction prohibited without permission.

up to 27 ft (8.2 m) thick and are interstratified with peloid to ooid grainstone to packstone, dolomitic lime mudstone, dolomite, algal boundstone, and skeletal packstone to wackestone. Anhydrite is easily recognized by negative porosity readings on density logs (Fig. 2.2). Typically anhydrite has extremely low gamma ray intensity.

Anhydrite textures in the Hugoton Member are predominantly mosaic and massive (Figs. 2.3 and 2.4). Nodular-mosaic, nodular, bedded-nodular, bedded-mosaic, and crystallotopic textures also occur. In thin section, anhydrite crystals are mostly felted, with lath-shaped crystals occurring less frequently. Blocky crystals are observed in anhydrite-filled fractures. Many of the evaporite intervals contain little or no carbonate matrix. Anhydrite nodules are outlined by a matrix of thin, brown, dolomitic peloidal carbonates. Carbonates are typically interbedded between anhydrite intervals. Nodules are generally ellipsoidal and irregularly arranged without internal stratification or bedding. Vertically-elongate anhydrite nodules (cf. Loucks and Longman, 1982) are extremely rare (Figs. 2.3 and 2.5). Edges of anhydrite nodules are commonly partially replaced by light-blue, length-slow, spherulitic chalcedony (cf. Folk and Pittman, 1971) and rarely by euhedral, authigenic megaquartz. Highly birefringent crystals, interpreted as relict anhydrite, are sparsely distributed in the chalcedony and megaquartz.

Anhydrite is restricted to the Hugoton Member of the St. Louis Limestone. Two evaporite units, E1 and E2, consisting of interbedded anhydrite and carbonate, are recognized in the Hugoton Member (Fig. 1.4, 2.2, 2.6, 2.7, and 2.8). The upper anhydrite interval (E1) is typically 32-42 ft (9.8-12.8 m) thick. The E2 anhydrite is commonly 67-143 ft (20.4-43.6 m) thick and is typically thicker than the E1 anhydrite. E1 anhydrite extends further to the south than E2 anhydrite. The two evaporites are separated by 28-58 ft (8.5-17.7 m) of porous dolomitic carbonate that contains peloid and ooid grainstone/packstone, dolomite, skeletal packstone/wackestone, and, locally,

Reproduced with permission of the copyright owner. Further reproduction prohibited without permission.

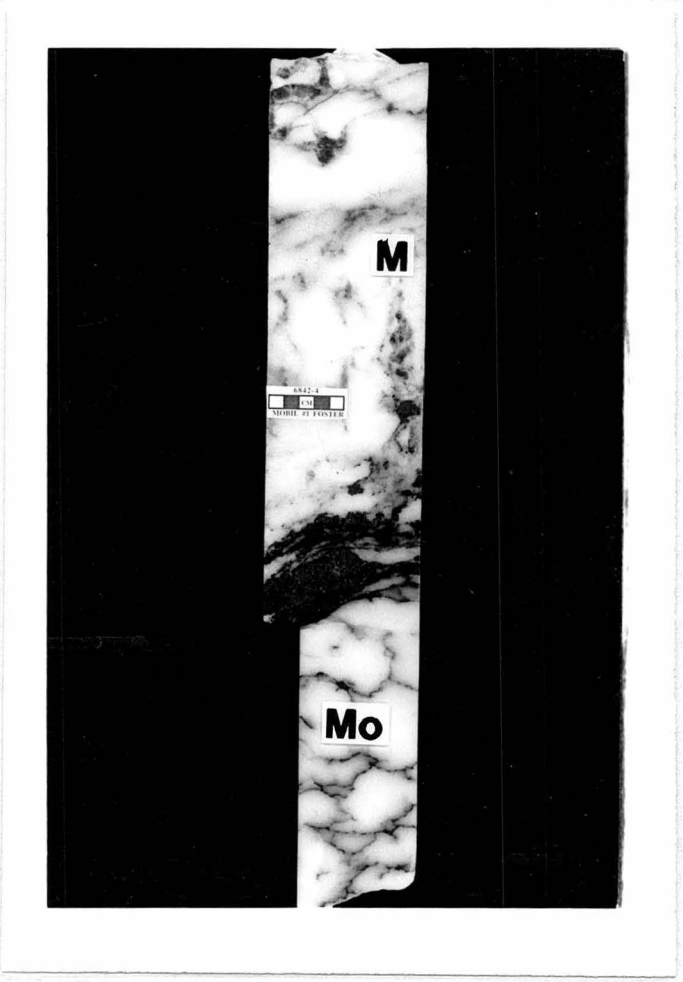


Figure 2.3 Anhydrite textures from the Hugoton Member of the St. Louis Limestone. Massive (M) and mosaic (Mo) (cf. Maiklem et al., 1969) are the most abundant structures. Mobil #1 Foster, 6842-6844 ft core depth.

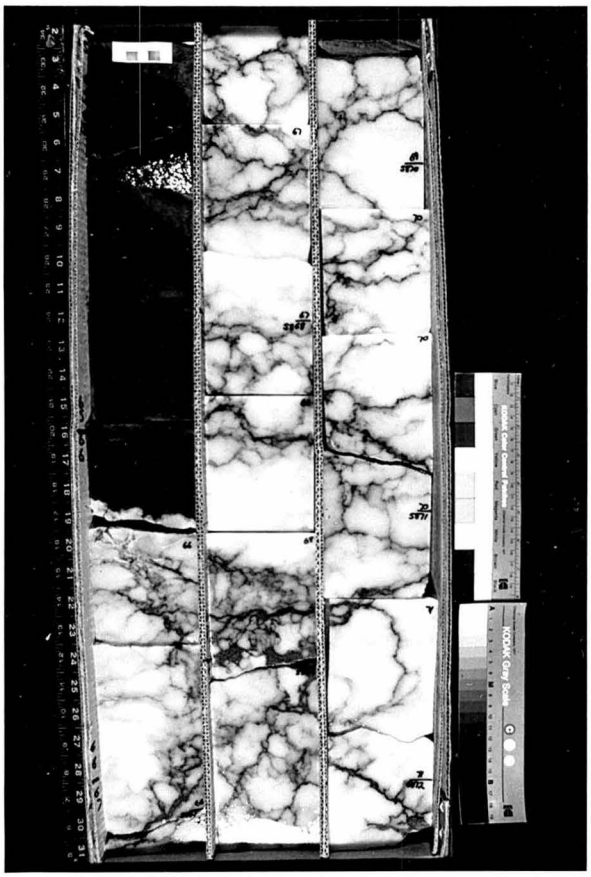


Figure 2.4 Mosaic anhydrite overlain by dark-brown intraclast packstone, laminar stromatolites, and skeletal packstone and wackestone. Paucity of carbonate matrix and thickness (individual beds up to 8.2 m thick) suggest the evaporites are subtidal in origin. Amoco #1 Nordling, 5864-5872 ft core depth.

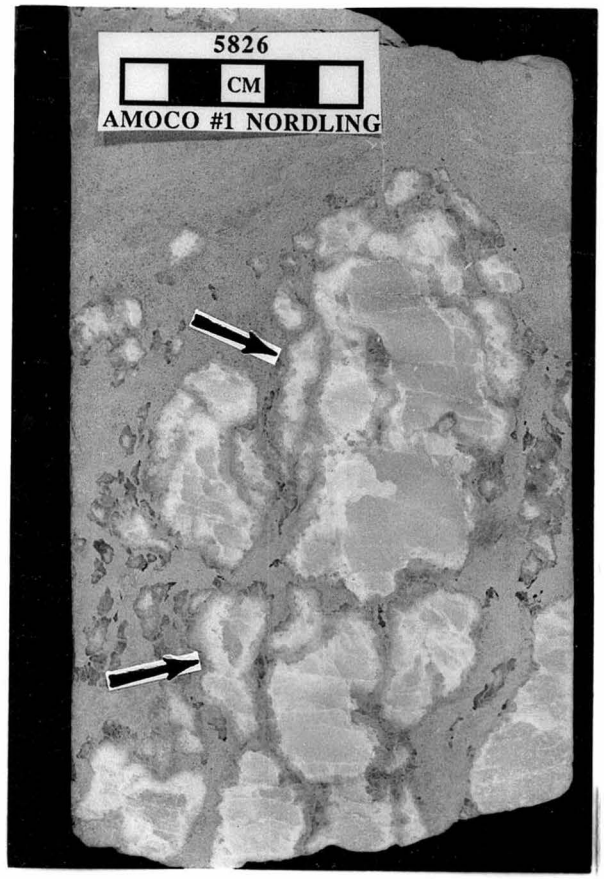


Figure 2.5 Possible vertically-elongate anhydrite nodules (arrows) interpreted as possible relict subaqueous gypsum crystals in the Hugoton Member. Upward-oriented anhydrite nodules are very rare, but are best developed where significant matrix is present. Amoco #1 Nordling, 5826 ft core depth.

Reproduced with permission of the copyright owner. Further reproduction prohibited without permission.

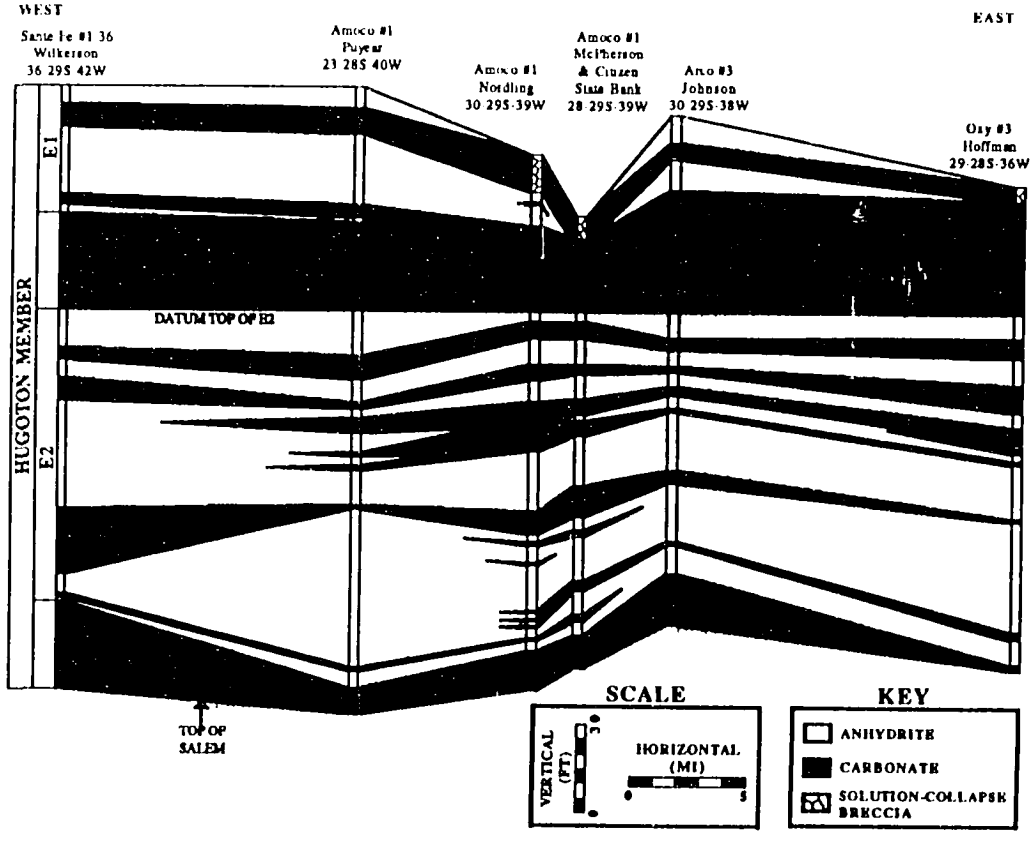


Figure 2.6 East-west stratigraphic cross section of Hugoton Member anhydrite. Many anhydrite beds are laterally correlative. See Fig. 2.8 for location.

Reproduced with permission of the copyright owner. Further reproduction prohibited without permission.

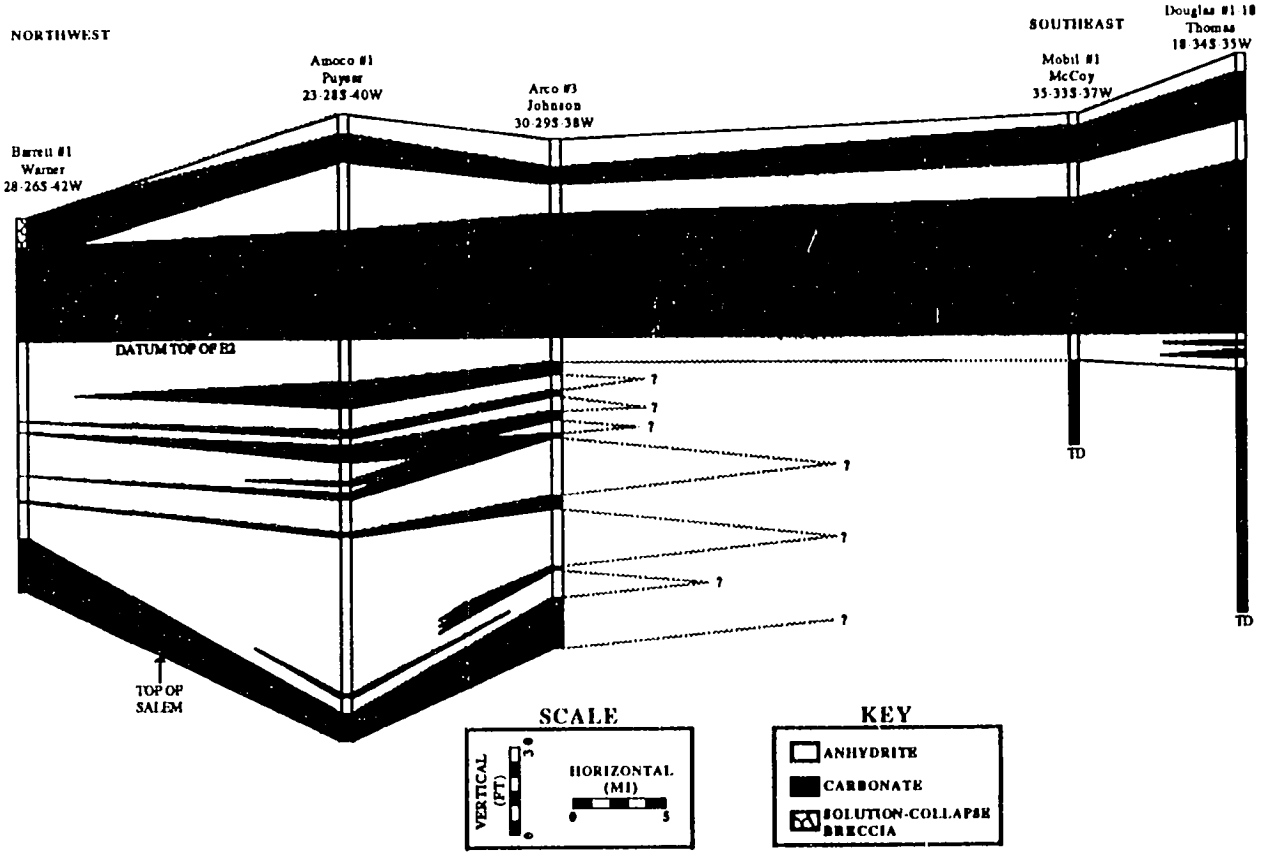


Figure 2.7 North-south stratigraphic cross section of Hugoton Member anhydrite. Most E2 anhydrite beds do not extend as far south as E1 anhydrite. See Fig. 2.8 for location.

Reproduced with permission of the copyright owner. Further reproduction prohibited without permission.

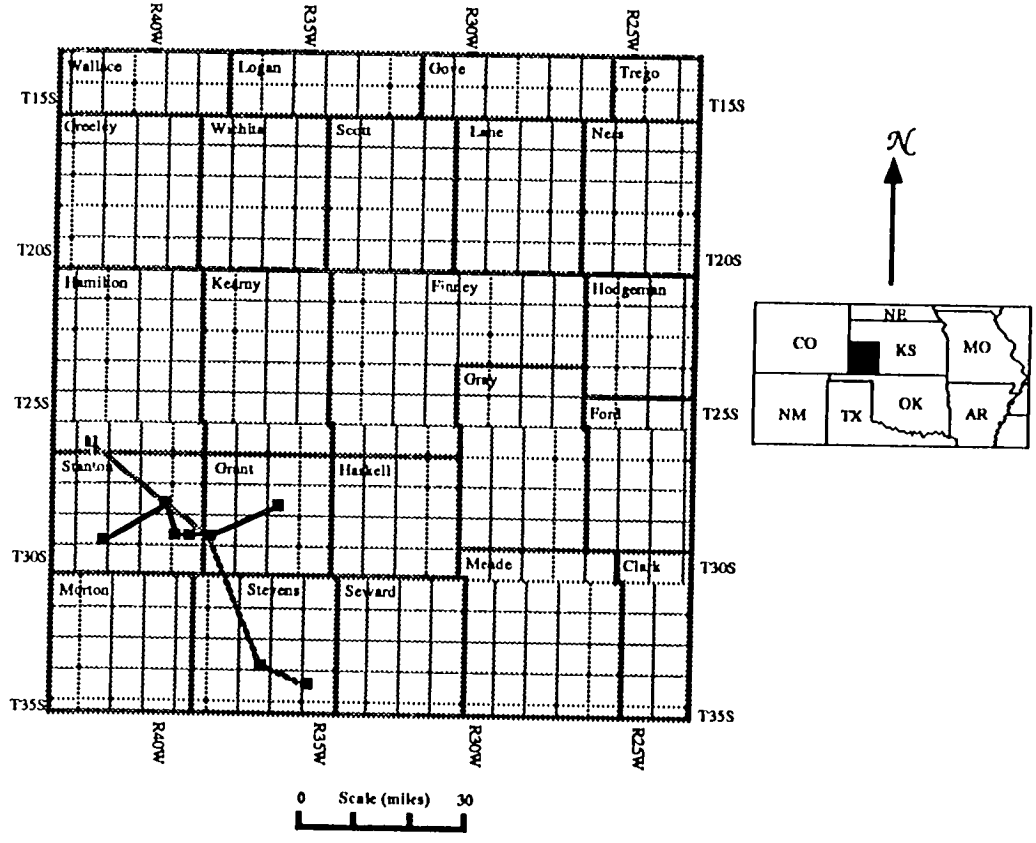


Figure 2.8 Location map for anhydrite cross sections in Figures 2.6 and 2.7.

algal boundstone.

Breccia

Breccias have been observed in five cores of the Hugoton Member of the St. Louis Limestone (Table 1.1, Appendix 1): Amoco #3 Wilson A, Amoco #1 Nordling, Amoco #3 Cohen C, Pan Am #1 Moser, and Alma #1 Watchorn. Thompson and Goebel (1968) and Goebel (1968) also report breccias from cores of the Hugoton Member in Scott and Gove Counties. Breccias have been recognized in the St. Louis in southwestern Missouri (Abegg, unpublished data) and in the Illinois basin (Atherton et al., 1975). The St. Louis in the subsurface of eastern Colorado also contains breccias (Ramirez, 1974). In southwestern Kansas, the thickest breccia observed from the Hugoton Member of the St. Louis Limestone is 36 ft (11 m) thick in an incomplete core from the Pan Am #1 Moser.

The majority of breccias can be divided into two horizons, in ascending order (Fig. 2.9): a polymictic breccia horizon and a monomictic breccia horizon. Breccias are typically overlain by fractured carbonate. These horizons are best developed in thicker brecciated units; thinner breccias are generally monomictic.

Polymictic Breccia.– The base of polymictic breccia beds is typically sharp. The basal portion of the breccia consists of angular clasts of various lithologies (Fig. 2.10). The most common clast types are skeletal packstone/wackestone and dolomitic lime mudstone. Peloid packstone and ooid grainstone/packstone clasts are rare. Stratification within clasts indicates the clasts are rotated at random angles, thus the brecciation is not *in situ*. The clasts show no rounding, imbrication, or sorting indicative of transport. Some dolomitic lime mudstone clasts contain calcite cement-filled casts of former gypsum crystals (Fig. 2.11). Abundant megaquartz with anhydrite inclusions and length-slow spherulitic chalcedony (Fig. 2.12) occur between

Reproduced with permission of the copyright owner. Further reproduction prohibited without permission.

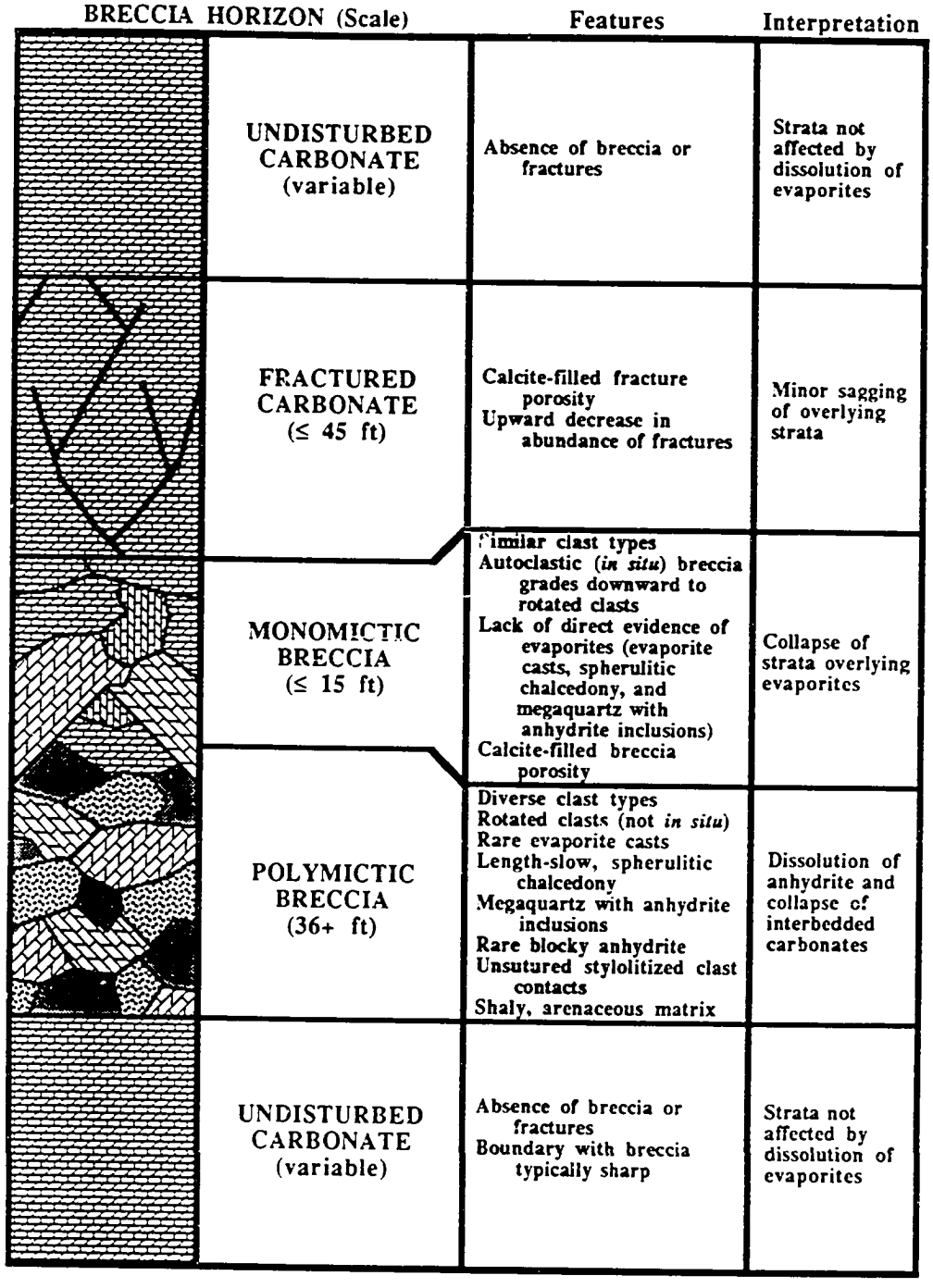


Figure 2.9 Breccia horizons in the Hugoton Member of the St. Louis are interpreted as evaporite solution-collapse breccias. Thin breccias typically only contain monomictic horizons.

Reproduced with permission of the copyright owner. Further reproduction prohibited without permission.

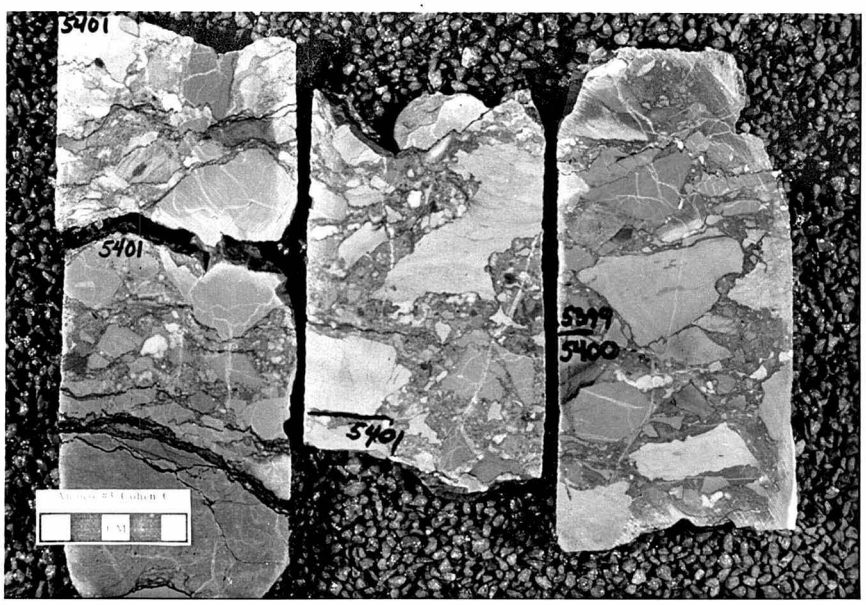


Figure 2.10 Polymictic breccia with varied clast types. Pan American #1 Moser, 5401-5399 ft core depth.

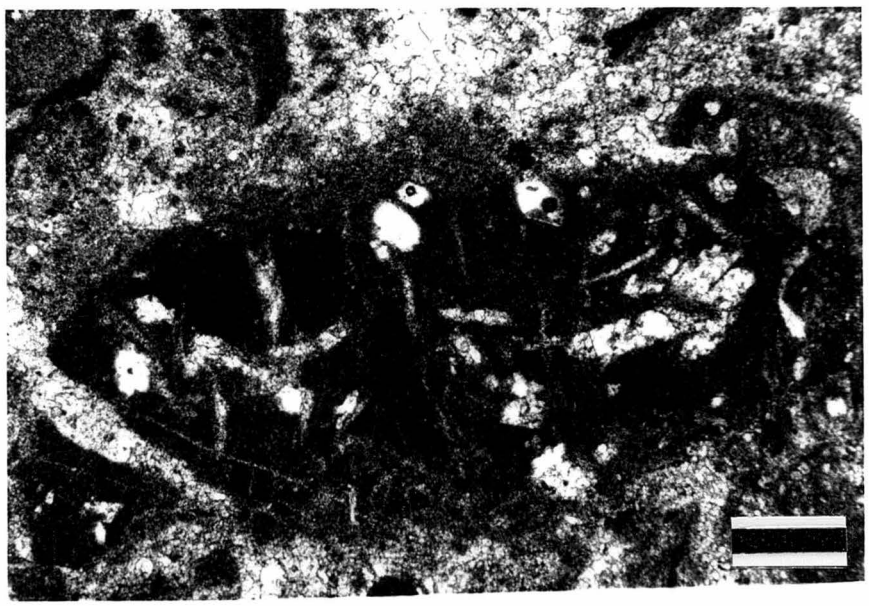


Figure 2.11 Photomicrograph of calcite pseudomorphs after gypsum in a lime mudstone clast in a polymictic breccia. Amoco #1 Wilson, 5611.6 ft core depth. Plane-polarized light. Scale bar is 0.5 mm.

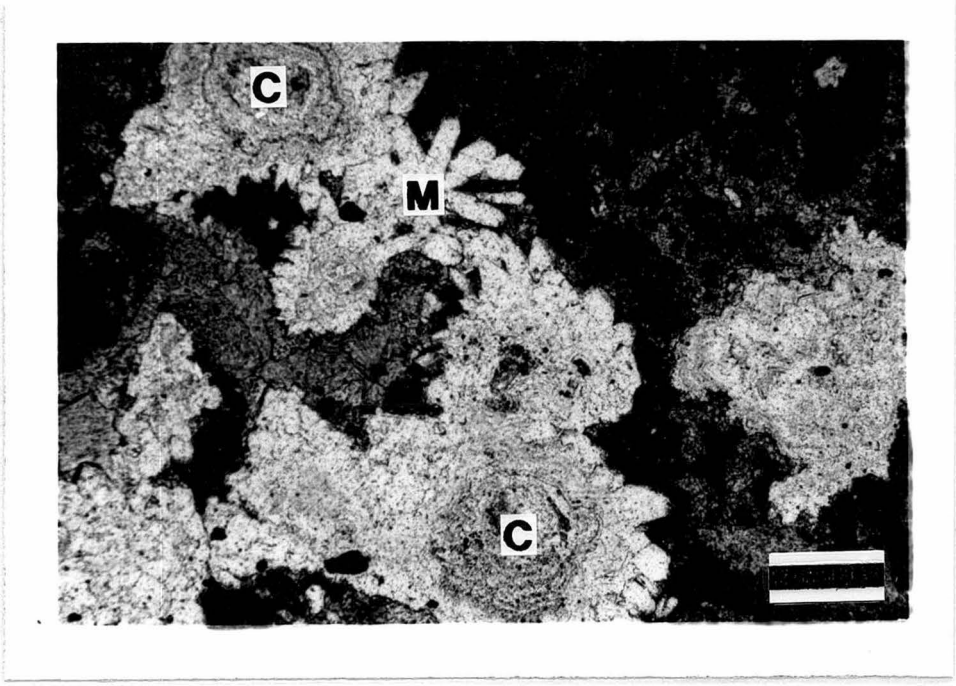


Figure 2.12 Photomicrograph of length-slow spherulitic chalcedony (c) and megaquartz (m) in a polymictic breccia. Amoco #1 Wilson, 5611.6 ft core depth. Plane-polarized light. Scale bar is 0.5 mm.

clasts, but are very rare within clasts. Blocky anhydrite is preserved locally in clasts. Breccias typically lack matrix and commonly have microstylolitized grain contacts.

Monomictic Breccia.– Polymictic breccias grade upward to monomictic breccias (Fig. 2.9). Texture of clasts at any horizon tend to be very similar (Fig. 2.13). Stratification within clasts indicates the clasts in the lower part of this breccia horizon are commonly rotated. The rotated clasts grade upward to autoclastic (*in situ*) breccias, where stratification within most clasts is nearly horizontal and clast boundaries can be fit back together. Evaporite casts, spherulitic chalcedony, megaquartz with evaporite relicts, and blocky anhydrite are commonly absent from this interval. Breccia porosity occurs locally and is filled by calcite cement.

Fractured Carbonates.– Monomictic breccias typically grade upward into fractured carbonates (Fig. 2.9). Fractures are commonly filled with nonferroan calcite cement followed by ferroan calcite. The fractures decrease in abundance gradationally upward into undisturbed rock. Most fractured carbonates are in the St. Louis, but locally they occur in the Ste. Genevieve (e.g., Pan American #1 Moser).

Breccias in core permit the calibration of this facies to log signatures (Fig. 2.14). Microstylolitzation at clast boundaries concentrates clay and arenaceous material, thus producing fairly low gamma ray readings with numerous minor shale kicks. Breccias can be traced and confirmed with core as far north as Logan County (Pocket Enclosures G-G', I-I').

Dolomite

Many carbonates in the Hugoton Member of the St. Louis are dolomitic (Appendix 1). However, only a few are extensively dolomitized. This facies is defined as rock containing greater than approximately 70 percent dolomite. The dolomite typically obscures the original depositional texture. Dolomitization is highly fabric selective,

Reproduced with permission of the copyright owner. Further reproduction prohibited without permission.

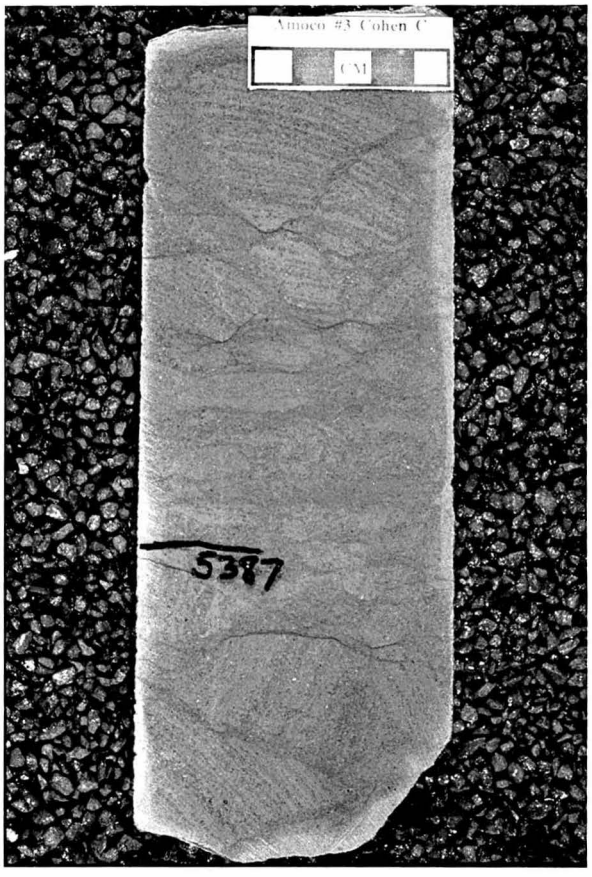


Figure 2.13 Monomictic breccia with rotated to nearly *in situ* clasts. Amoco #3 Cohen C, 5386-5387 ft core depth.

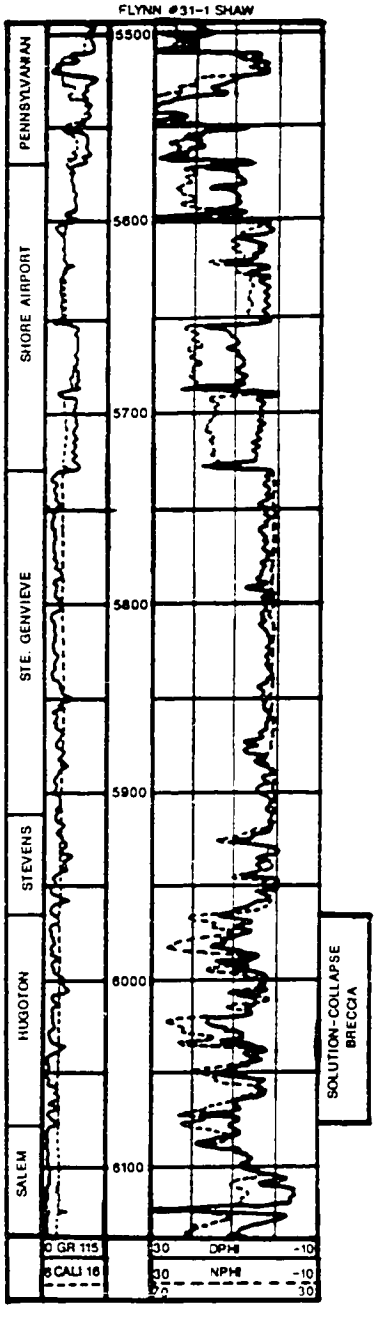


Figure 2.14 Gamma-ray and neutron-density logs from the Flynn #31-1 Shaw (sec. 31, T31S, R34W). Note the fairly low gamma-ray values and numerous minor shale kicks of the breccia and the corresponding lower density readings relative to neutron readings. These log signatures are calibrated to the cored breccias in the Amoco #3 Wilson A (sec. 30, T30S, R33W) approximately 9 miles (14.4 km) to the northeast.

Reproduced with permission of the copyright owner. Further reproduction prohibited without permission.

preferentially replacing the micritic fraction of the rock. The dolomite typically consists of finely-crystalline (10-15 μm), limpid crystals with euhedral to planar-s texture (cf. Sibley and Gregg, 1987). Floating within this finely crystalline dolomite are dolomite rhombs up to 350 μm with a planar-e texture. These coarse rhombs typically have cloudy cores and clear rims. Saddle-dolomite (nonplanar) cements with sweeping extinction are uncommon. Extensive dolomitization obliterates most grains, but peloids, crinoids, brachiopods, and fenestrate bryozoans are preserved in a few beds. Interbedded less dolomitized carbonates contain peloids, crinoids, brachiopods, bryozoans, foraminifera, and intraclasts.

Up to 10 percent detrital quartz sand and silt is present in some dolomite horizons. Rare chert nodules contain only planar-e dolomite crystals. Parallel lamination is common in many horizons, and are locally disrupted by horizontal burrows (cf. Abegg, 1991, his Fig. 8). Stylolites and fractures filled with calcite and anhydrite cement occur locally.

The dolomite facies is typically interbedded with the anhydrite, breccia, peloid dolomitic grainstone/packstone, and skeletal packstone/wackestone facies.

Dolomitic Lime Mudstone

Grains constitute less than 10 percent of dolomitic lime mudstone, by definition (Dunham, 1962). Ostracodes and peloids are the most typical. Calcite pseudomorphs after gypsum (Fig. 2.11), length-slow spherulitic chalcedony, and megaquartz with anhydrite inclusions occur in dolomitic lime mudstone clasts in solution-collapse breccias. Horizontal lamination occurs in some horizons.

Dolomitic lime mudstone is interstratified with anhydrite and solution-collapse breccia in the Hugoton Member of the St. Louis Limestone. It is extremely rare in the Ste. Genevieve Limestone.

Reproduced with permission of the copyright owner. Further reproduction prohibited without permission.

Algal Boundstone

Algal boundstone forms proximally to many evaporites and is observed as clasts in solution-collapse breccias. Algal boundstones are dominated by stromatolites that are characterized by alternating micritic and peloidal laminae. Calcareous algae are rare. Oolitic, skeletal, and peloidal packstones are commonly interstratified with stromatolites. Encrusting spirorbid worm tubes and ostracodes are typically associated with algal boundstone. Fenestrate bryozoans, bivalves, and ooids occur locally within algal boundstone where it is overlain by an oolitic skeletal packstone.

Laminar, domal, and spirorbid-encrusted colloform (cf. Hoffman, 1976) stromatolites are recognized in algal boundstone. The majority of algal boundstone occurs in the Hugoton Member of the St. Louis; some occurs in the Stevens Member of the St. Louis, especially near its base.

Laminar Stromatolites.– Laminar stromatolites are the most common type in the algal boundstone facies. These stromatolites consist of horizontal to slightly domal, smooth laminae (Fig. 2.15). Algal laminae are marked by <1 mm thick laminae composed of peloid packstone that fines upward to lime mudstone. Laminar stromatolites commonly occur immediately adjacent to anhydrite intervals, but are locally associated with other Hugoton Member facies. Anhydrite-filled fractures and replacive blocky anhydrite occur in algal boundstone adjacent to evaporites. Features indicative of subaerial exposure, such as mudcracks or fenestral porosity, were not observed.

Domal Stromatolites.– Domal stromatolites are typically interbedded with oolitic grainstone and packstone, but locally are interbedded with anhydrite. The smooth peloidal and micritic laminae are similar to those found in laminar algal boundstones. A large hemispheroid domal stromatolite, partially replaced by blocky anhydrite, occurs directly beneath anhydrite in the Hugoton Member of the St. Louis at 5889.8 ft in the

Reproduced with permission of the copyright owner. Further reproduction prohibited without permission.

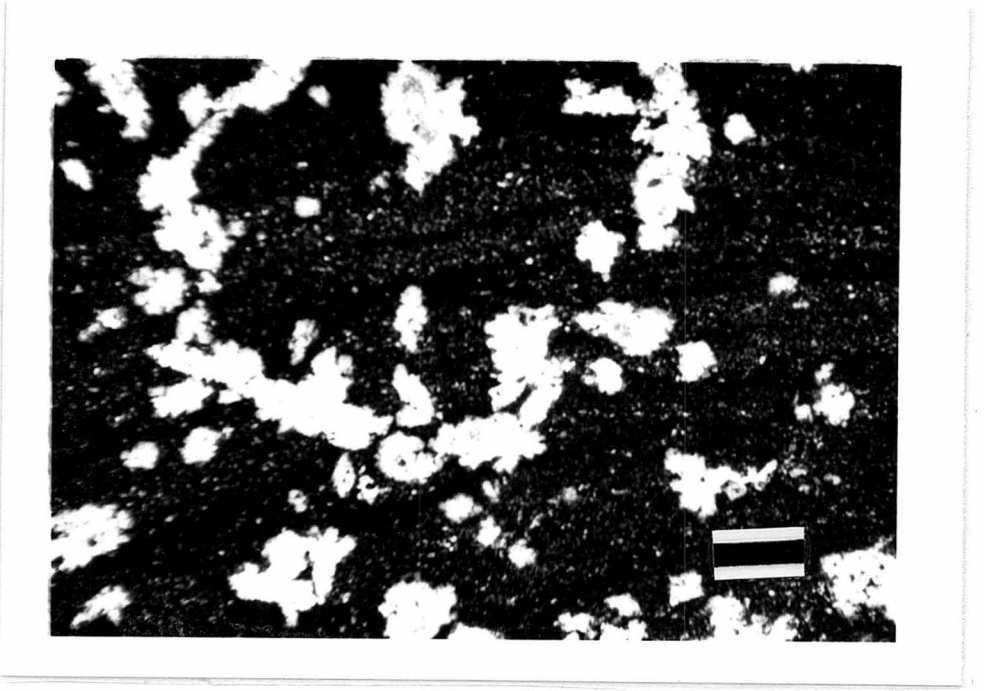


Figure 2.15 Photomicrograph of laminar algal boundstone from a 0.2 ft (0.06 m) thick bed interstratified with anhydrite. The stromatolite is composed of micritic and peloidal laminae that are partially replaced by blocky anhydrite. Amoco #1 Nordling, 5949.9 ft core depth. Plane-polarized light. Scale bar is 1 mm.

Amoco #1 Nordling. Digitate stromatolites occur near the base of the Stevens Member in the Nordling at 5800.8 ft (Fig. 2.16); the sides of these stromatolites are encrusted by micritic tubes, probably of worms. In the Hugoton Member in Amoco #1 Nordling at 5877.9 ft, hemispherical stromatolites cap minor topographic highs on a truncation surface of oolite.

Spirorbid-encrusted Colloform Stromatolites.– Colloform mat structures consist of multiconvex laminations with internal cavities (Hoffman, 1976) that are commonly heavily encrusted by spirorbid worm tubes. The absence of preserved molluscan wall structure or a protoconch, and rarity of septa indicate these tubes are not vermiform gastropods like those described from algal bioherms from the British Lower Carboniferous (Burchette and Riding, 1977). Encrusters typically decrease in abundance upward and are in some cases overlain by laminar stromatolites. Hemispherical masses of calcareous algae with radially arranged algal filaments occur locally. Regularly spaced partitions gives the algae a gridlike pattern. This alga, commonly partially to totally recrystallized, is similar to *Parachaetetes* described by Wray (1977). Internal pores are lined by crusts of brownish fibrous calcite cement (Fig. 2.17) that are irregularly distributed to locally isopachous. This cement also typically lines intraparticle pores of spirorbid worm tubes. Alveolar texture occurs locally. Ostracode-ooid-peloid packstone and peloid-ooid packstone occur in the internal cavities, locally covering fibrous cement crusts. This facies is very similar to the *Spirorbis*-foraminfer-alga boundstone from the Americus Limestone (Permian) in eastern Kansas described by Sporleder (1991, see his Fig. 15). Colloform algal boundstone is very rare and is confined to the Hugoton Member of the St. Louis. It is commonly overlain by laminar algal boundstones, anhydrite, or solution-collapse breccias (Fig. 2.18).

Reproduced with permission of the copyright owner. Further reproduction prohibited without permission.



Figure 2.16 Photomicrograph of digitate algal boundstone surrounded by oolitic-skeletal mud-poor packstone. Amoco #1 Nordling, 5800.8 ft core depth. Plane-polarized light. Scale bar is 1 mm.

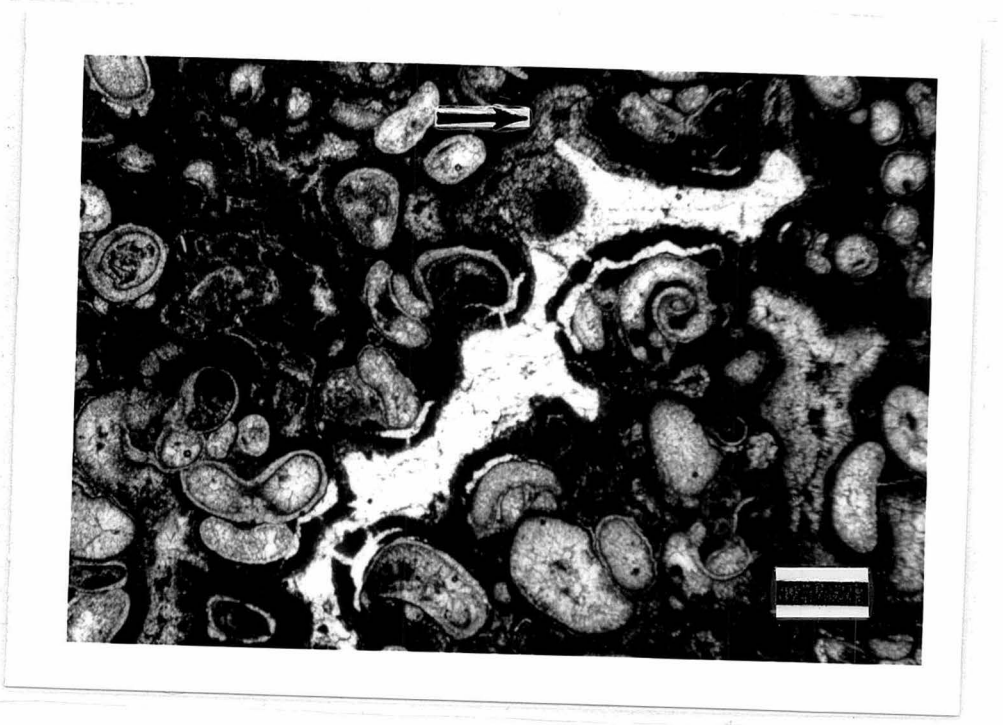


Figure 2.17 Photomicrograph of spirorbid-encrusted colloform algal boundstone. Fibrous calcite cement locally hangs from the tops of pores (arrows) suggesting it may be a pendant cement. Amoco #3 Cohen C, 5402.1 ft core depth. Plane-polarized light. Scale bar is 1 mm.

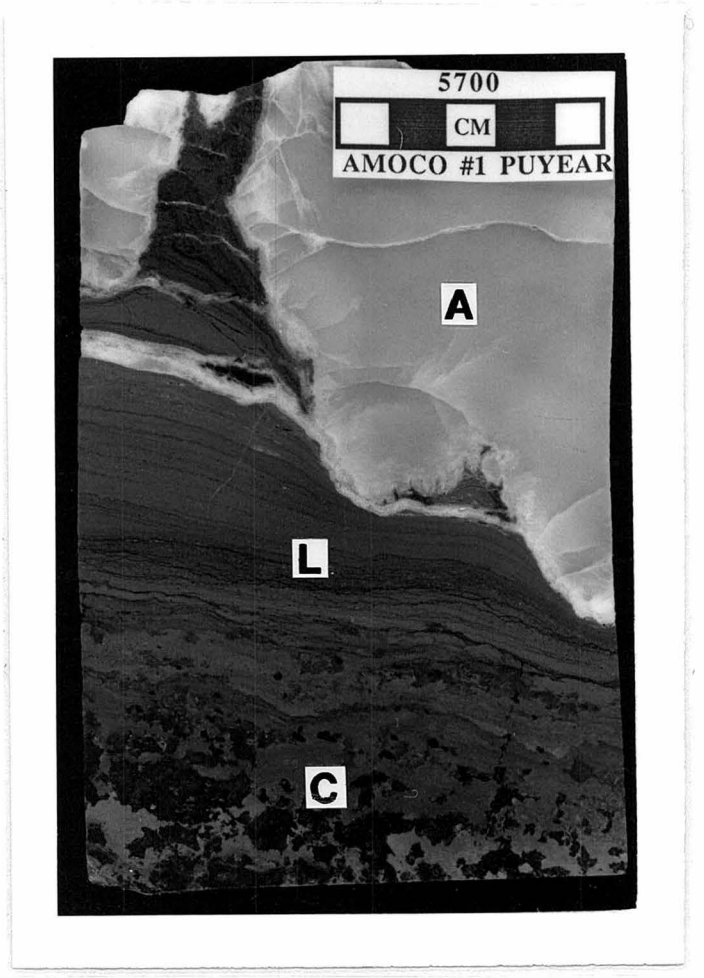


Figure 2.18 Spirorbid-encrusted colloform algal boundstone (C) overlain by laminar algal boundstone (L) and anhydrite (A). Amoco #1 Puyear, 5700 ft core depth.

Skeletal Packstone/Wackestone

Skeletal packstone/wackestone is the most extensive facies in the Stevens Member of the St. Louis Limestone. Echinoderms and bryozoans are abundant to rare. Common to rare allochems include brachiopods and ooids. Rugose and tabulate corals, bivalve? and gastropod casts, trilobite fragments, foraminifera (mainly endothyrids), ostracodes, siliceous sponge spicules, and worm tubes are rare (Fig. 2.19). Detrital quartz is generally absent to very rare, but makes up to 20 percent of the rock locally. Locally this facies contains enough clay to be considered a calcareous shale (e.g., basal 5.4 ft of Amoco #1 Breeding F core). Horizontal burrows are common in some intervals, whereas vertical burrows are rare. Truncated allochems, commonly capped by a vaguely laminated peloidal micritic crust, occur along subhorizontal surfaces locally in mud-poor packstones (Fig. 2.20).

Skeletal packstone/wackestone is commonly gray to tan. Chert is generally rare and typically bluish-gray in color. Sponge spicules, now molds filled by sparry calcite and silica cement, provided a biogenic source for much of the silica. Absence of significant grain interpenetration within chert nodules and deflection of stylolites around chert nodules indicate that chert is precompactional. Dolomite is a minor constituent and is best developed proximal to Hugoton Member anhydrite. Microstylolites, and less commonly sutured stylolites, are present throughout much of this facies (Fig. 2.19). Sutured and concavo-convex interpenetrating grain contacts indicate significant pressure solution. Porosity was originally restricted to mud-poor packstones. No porosity remains, however, because primary intergranular pores were totally occluded by sparry calcite cement and compaction.

Although the skeletal packstone/wackestone facies is most abundant in the Stevens Member, it does occur locally in the Hugoton Member. Many skeletal packstone/wackestone intervals are overlain by oolitic grainstone/packstone. The

Reproduced with permission of the copyright owner. Further reproduction prohibited without permission.

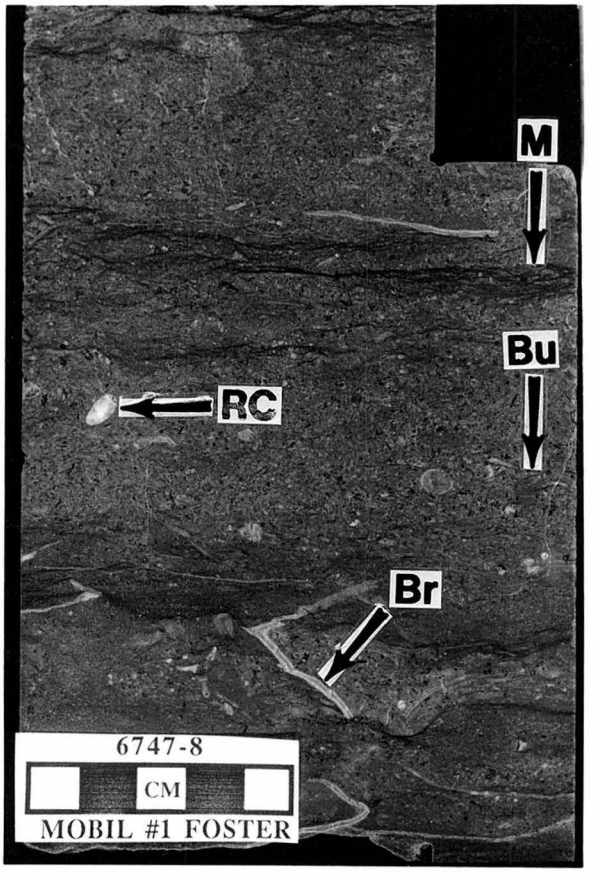


Figure 2.19 Skeletal packstone/wackestone from the Stevens Member of the St. Louis Limestone. Microstylolites (M), burrows (Bu), bryozoans (Br), solitary rugose coral (RC), and crinoids (C) are indicated by arrows. Mobil #1 Foster, 6747-6748 ft core depth.

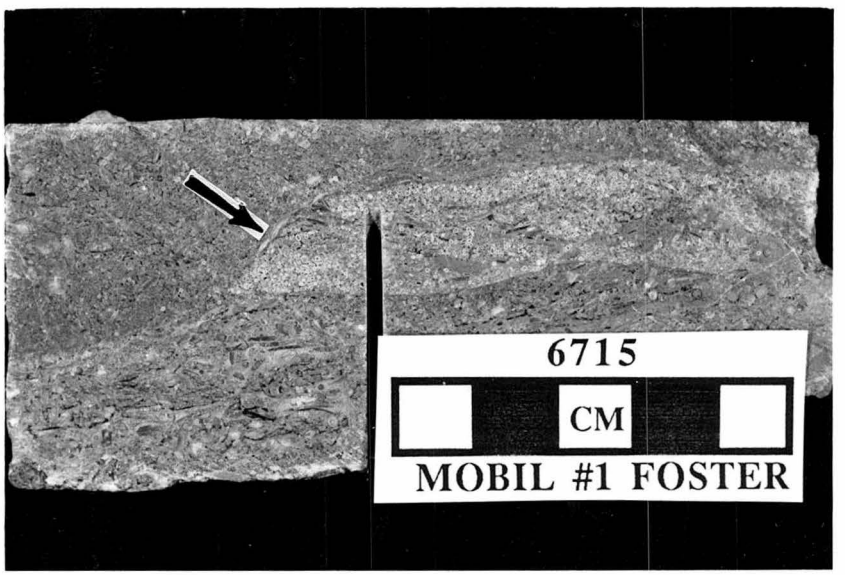


Figure 2.20 Two hardgrounds in skeletal and oolitic, mud-poor packstones from the Stevens Member of the St. Louis Limestone. Note the relief on the upper hardground surface. The upper hardground is overlain by a vaguely laminated peloidal crust (arrow) that is possibly algal in origin. Mobil #1 Foster, 6715 ft core depth.

skeletal packstone/wackestone facies is also intercalated with the dolomite, anhydrite, peloid dolomitic grainstone/packstone facies of the St. Louis, and the quartzose grainstone of the Ste. Genevieve (Appendix 1).

Oolitic Grainstone/Packstone

Well-sorted, very fine- to coarse-grained ooids dominate this facies (Fig. 2.21). Ooid cortices have a radial-concentric microstructure and are generally unbroken and relatively unabraded. Other allochems are rare and include echinoderms, brachiopods, bryozoans, gastropods, foraminifera, ostracodes, and lithoclasts. Detrital quartz is present only as nuclei of a few ooids.

Sedimentary structures are uncommon in many of the oolites. Unidirectional very low-angle cross stratification to parallel lamination are present locally. Truncated ooids and bioclasts, commonly capped by a vaguely laminated peloidal micritic crust, occur along subhorizontal surfaces locally (Fig. 2.20). Isopachous bladed cements are commonly well developed below the truncation surface, but are absent above.

This facies is the reservoir facies for most St. Louis production. Extant porosity is generally slightly solution-enlarged, cement-reduced interparticle (cf. Choquette and Pray, 1970). Syntaxial and equant cements penetrate into adjacent grains indicating that some of the calcite cement is precompactional. Dissolution, albeit minor, appears to have occurred in two stages. The first dissolutional event predates equant cements. A second dissolution event truncates all previous diagenetic phases.

The lower contact of the ooid grainstones and packstones is typically gradational. Many oolites are underlain by skeletal packstone or wackestone. The upper contact of the ooid grainstone/packstone facies is either abrupt or somewhat gradational. Many oolites are overlain by marine skeletal packstone or wackestone, peloid grainstone to packstone, or quartzose grainstone.

Reproduced with permission of the copyright owner. Further reproduction prohibited without permission.

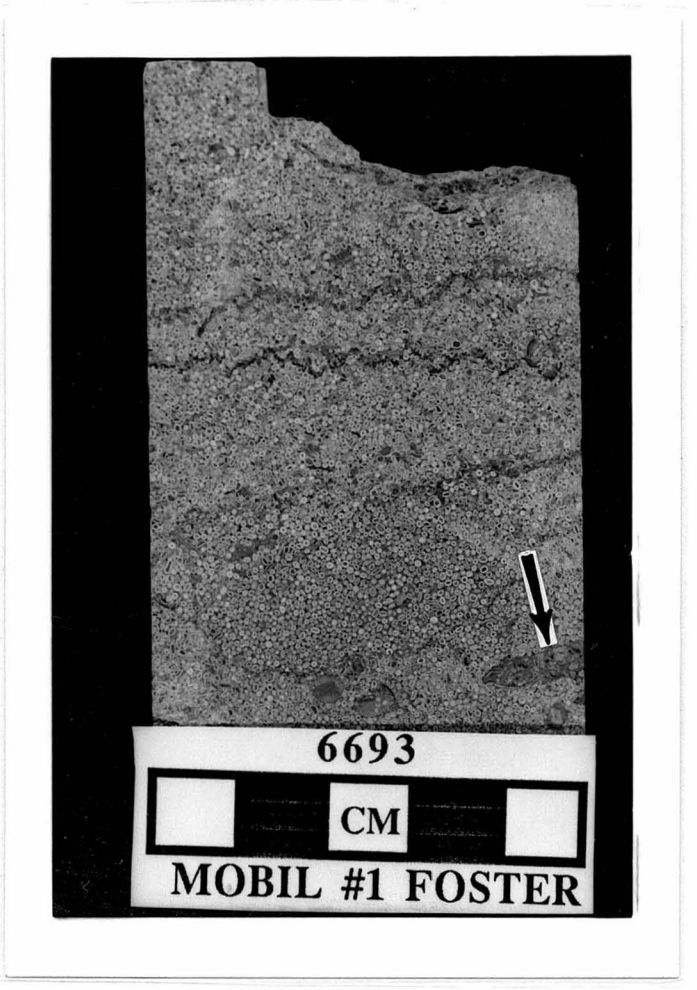


Figure 2.21 Ooid grainstone from the Stevens Member of the St. Louis Limestone. Note scattered lithoclasts (arrow). Crinoids and, to a lesser degree, brachiopods nucleate cements more readily than ooids. Rare uncoated crinoids nucleate syntaxial cements that occlude much of the interparticle porosity. Mobil #1 Foster, 6693 ft core depth.

Oolitic grainstone or packstone is most abundant in the upper Stevens Member. Oolites are also interbedded with quartzose grainstone in the Ste. Genevieve and in carbonate strata between the E1 and E2 anhydrites. The abundance of oolites does not appear to increase to the north toward the Transcontinental arch or to the east toward the Central Kansas uplift. However, additional work is needed to determine the controls on the lateral distribution of oolites in the Stevens Member of the St. Louis Limestone.

Fenestral Packstone/Wackestone

Limestone with fenestral pores is rare. Examples of well-developed fenestrae are limited to the St. Genevieve Limestone in Amoco #1 Puyear (5509.8 ft core depth), Amoco #1 Breeding F (5367.8 ft core depth), and Pan Am #1 Moser (4988.2 and 4988.9 ft core depth). Handford (1988) and Handford and Francka (1991) also recognized this facies from the Damme Field in Finney County and the Big Bow Field in Stanton and Grant Counties.

Peloids are rare to common in fenestral limestones. Calcified sponge spicules are common in this facies only in the Breeding core. Ostracodes, echinoderms, coated grains, and gastropods are rare. Detrital quartz silt and very fine sand comprise up to 10 percent of this facies. Muscovite is very rare.

The fenestral pores are commonly horizontally elongated and are locally connected by horizontal fractures. In the Moser core, pendant crusts of bladed calcite cement are well developed in fenestrae. Terminations of these cements are typically somewhat irregular.

Quartzose Grainstone

Quartzose grainstone is the most abundant facies in the Ste. Genevieve Limestone. Common grains include peloids, echinoderms, bryozoans, and ooids. Brachiopods,

Reproduced with permission of the copyright owner. Further reproduction prohibited without permission.

foraminifera, and lithoclasts are rare. Glauconitic grains are scattered throughout. Grain size ranges from very coarse silt to medium sand and varies with stratification type. Detrital quartz sand typically varies between 5 and 30 percent, but is up to 75 percent locally. Other detrital grains are rare, including feldspar, zircon and amphibole. Percentage of detrital quartz typically increases upward in quartzose grainstone intervals (Appendix 1).

Allochems are typically broken and well rounded, regardless of their original shape. Detrital quartz is not as well rounded as carbonate grains. In contrast to the ooid grainstone/packstone facies, ooid cortices are commonly noticeably abraded. This abrasion was originally reported by Clair (1948, p. 4, 1949, p. 61) as "elliptical rather than round" ooids. Syntaxial cement overgrowths of some echinoderm fragments are extremely well-rounded. Quartzose grainstones are well to moderately sorted, but individual laminae are typically well sorted.

Petrography of acid etched and polished of slabs, as well as thin-sections, indicate grain types are grain-size dependent. The fine- to medium-sand fraction consists of common bioclasts and ooids with a relatively minor peloid and quartz abundance. The very coarse-silt to very fine-sand fraction consists primarily of detrital quartz and peloids with a relatively minor bioclastic fraction.

Three types of fine structure, the smallest discernible structural components of a deposit (Hunter, 1977, 1981, 1985, 1989), are recognized from quartzose grainstones: 1) climbing translatent stratification, 2) indistinct stratification, and 3) structureless or fining-upward units.

Climbing Translatent Stratification.– The most common fine structure in the quartzose grainstone facies is marked by climbing translatent stratification. Individual strata coarsen upward internally. They are typically 2 to 5 mm thick, but some are as thick as 9 mm (Figs. 2.22 and 2.23). Ripple foreset lamination is typically rare.

Reproduced with permission of the copyright owner. Further reproduction prohibited without permission.

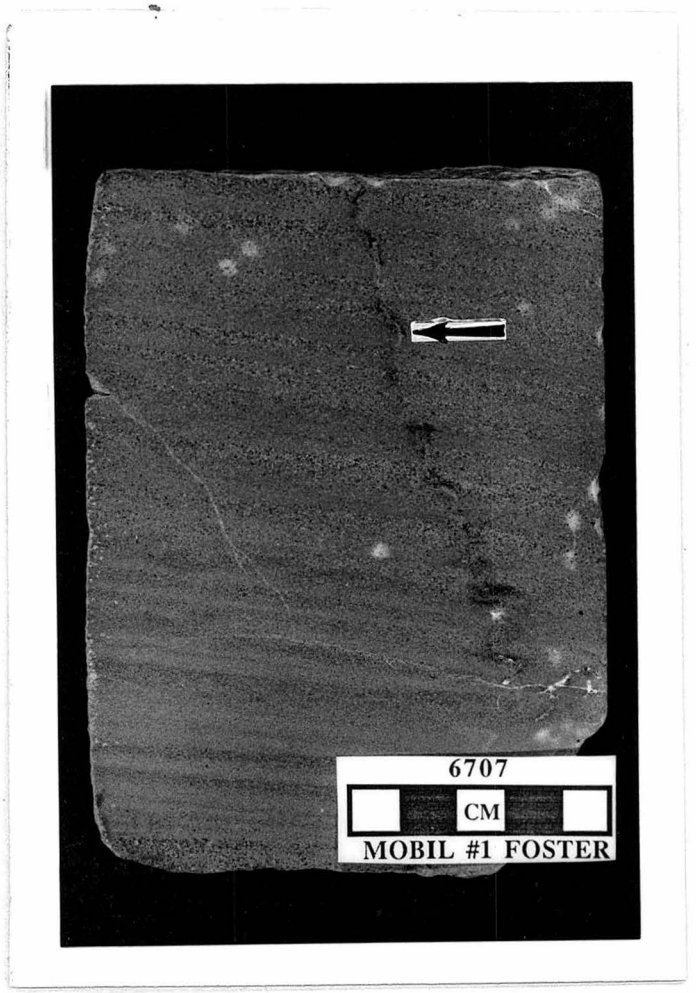


Figure 2.22 Quartzose grainstone in the Stevens Member of the St. Louis Limestone. Climbing translatent stratification, interpreted as eolian, dip at approximately 6°. The strata are unusually thick (up to 9 millimeters), coarsen upward, and contain well-developed ripple-foreset lamination. Direction of ripple migration is down the slope or to the right. Note the vertical rhizolith (arrow). Mobil #1 Foster, 6707 ft core depth.



Figure 2.23 Photomicrograph of climbing translatent stratification interpreted as eolian in origin. Mobil #1 Foster, 6707.3 ft core depth. Plane-polarized light. Scale bar is 1 mm.

Polishing or acid-etching surfaces enhances recognition of the translatent strata. Ripple foreset lamination and upward coarsening are best observed in the thickest strata. The basal 1 mm of each stratum contains minor very coarse silt and abundant very fine sand grains of detrital quartz and peloids with rare scattered bioclasts. Fine to medium sand grains are rare. The coarser grained top portion consists of very fine to medium sand grains composed primarily of bioclasts and ooids admixed with quartz and peloids. Climbing translatent stratification commonly dips at angles less than 10° where it is the dominant type of stratification, but locally dips are as steep as 24°. Climbing translatent stratification also dominates at the base of tangential cross-stratified sets, up to 2.5 ft (0.8 m) thick, where dip angles are low. In the more steeply dipping upper portions of cross-bed sets, climbing translatent stratification is intercalated with other types of fine structure.

Indistinct Stratification.– The second most abundant type of fine structure is indistinct stratification (Fig. 2.24), that typically dips 10° to 24°. Stratification, commonly highlighted by microstylolites, is poorly developed because most of these deposits are very-well-sorted, very-fine sand, but grains up to medium sand are present. Indistinctly stratified units are most abundant in the more steeply dipping, upper portions of cross-strata sets.

Structureless or Fining-upward Units.– Units that lack stratification or that fine upward are rare (Fig. 2.24). The bottom and top of an individual stratum are commonly sharp. The base is typically slightly irregular; underlying strata are locally truncated at a low angle. Thickness ranges from 2 to 16 mm, and individual units thin by as much as 4 mm across a 3.5 inch (8.9 cm) core. Sorting in these units is not as good as in the types described above. Internal primary sedimentary structures are typically absent. Fining-upward units were noted only in Mobil #1 Foster (Abegg, 1991, in press (b)) (Fig. 2.24). Dips rarely exceed 25°. Structureless or fining-

Reproduced with permission of the copyright owner. Further reproduction prohibited without permission.

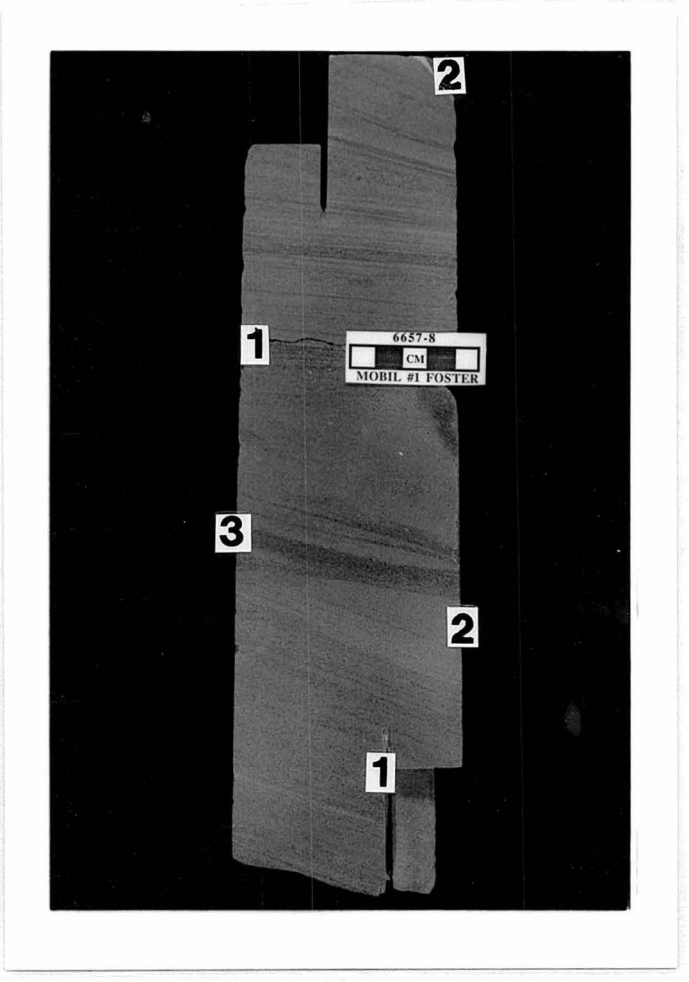


Figure 2.24 Ste. Genevieve quartzose grainstone displaying three types of fine structure. Climbing translatent strata (1) are 2-5 millimeter thick and distinctly coarsen upward. Ripple-foreset lamination is developed only in the thicker strata. Grainfall units (2) consist of very fine to fine sand that is only vaguely stratified due to the excellent sorting. Grainflow (3) toes are fining upward to structureless, not as well sorted, and thin downward. The lower surface of the grainflows is concave-upward, possibly reflecting the preflow depositional surface. Dip of the grainflows is an apparent dip; true dip is slightly greater than 20°. Mobil #1 Foster, 6657-6658 ft core depth.

upward units are restricted to the uppermost parts of cross-strata sets and are interstratified with both climbing translatent and indistinctly stratified units.

Quartzose grainstone have either low-angle-stratified or cross-stratified deposits, or both. These types of accumulations can occur together in the same quartzose-grainstone interval (e.g., Amoco #1 Nordling).

Low-angle Deposits.– Low-angle deposits are dominated by climbing translatent stratification (Fig. 2.25). Other fine structure is rare. Intervals dominated by low-angle stratification commonly contain calcite-cemented tubes coated by indistinctly laminated, brown to dark-brown micrite (Fig. 2.25). The majority of the tubes are oriented subhorizontally. A few, typically somewhat larger tubes, are vertical. Some of these tubes bifurcate downward into smaller branches, although this is rare. Tubes with their micritic coatings are commonly less than 1 mm in diameter and many extend across the width of the core. Some of the calcite-filled tubes are divided by thin micritic walls (Fig. 2.26). Brownish, bladed, sparry-calcite cement also occurs within some intervals containing calcite-filled tubes. This cement is most commonly oriented downward from pore tops (pendant), but locally it is upward oriented (astropetal) (Fig. 2.27). Upward-oriented cement nucleates from the base of horizontal sheet cracks as thin semicontinuous layers extending laterally for up to 31 mm (1.25 in). Crystals grew upward into open pore space. Crystal terminations are commonly euhedral and rarely rounded. Compaction of crystal terminations against other grains, however, makes the rounded nature difficult to observe. Pendant cement hangs from the bottom of grains or from the tops of vuggy or fracture porosity; these cements are fibrous to bladed (Fig. 2.28). Cryptocrystalline cement coats many of these cements and occurs as thin bands within brownish fibrous cements. Terminations of fibrous cements are rounded whereas bladed cement terminations are

Reproduced with permission of the copyright owner. Further reproduction prohibited without permission.

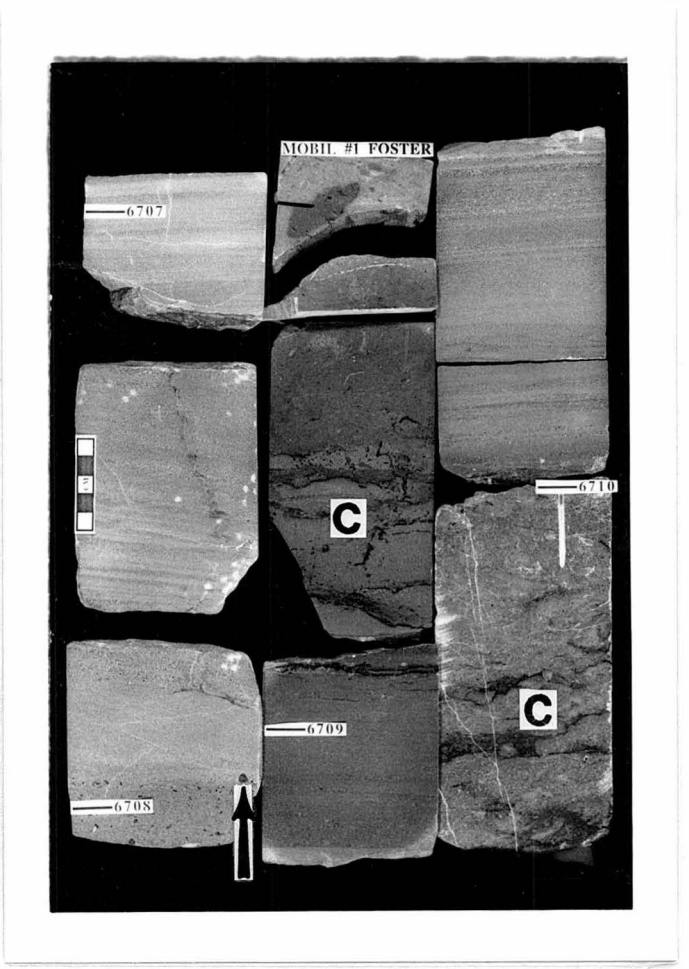


Figure 2.25 Quartzose grainstone from the Stevens Member was deposited as a vegetated eolian sand sheet. Note the dark brown rhizoliths in the two separate calcretes (C). Calcretes are overlain by lithoclast conglomerates containing reworked calcrete clasts (arrows). The strata are almost exclusively climbing translatent strata dipping at angles of less than 7°. Mobil #1 Foster , 6706-6710 ft core depth.

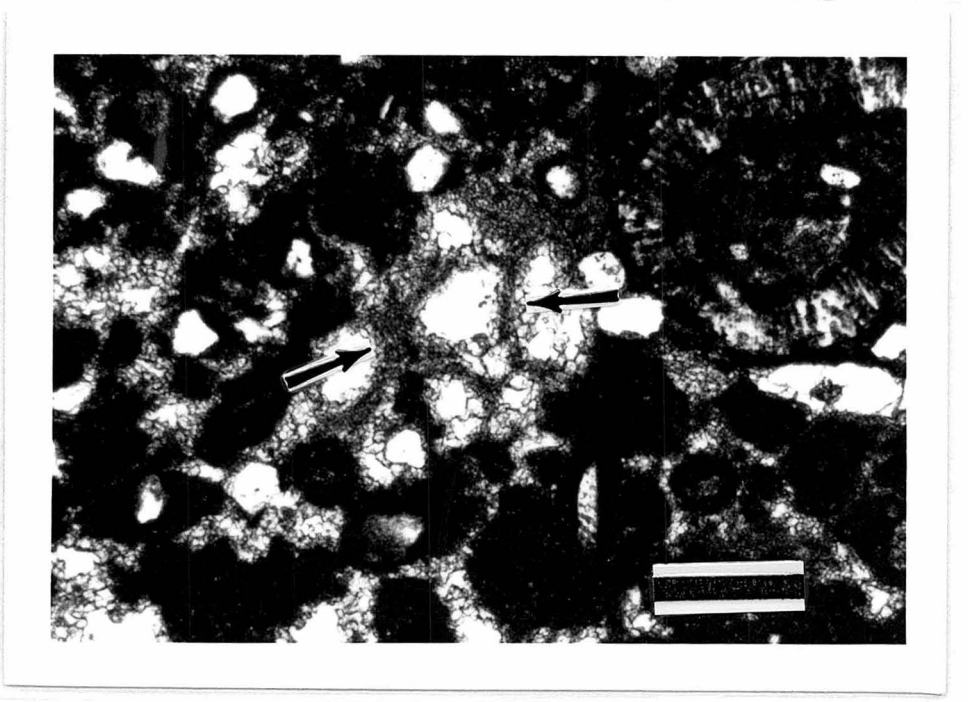


Figure 2.26 Thin micritic walls (arrows) that divide pores are interpreted as alveolar texture in a calcrete in the thin St. Louis eolianite. Mobil #1 Foster, 6709.0 ft core depth. Plane-polarized light. Scale bar is 0.25 mm.

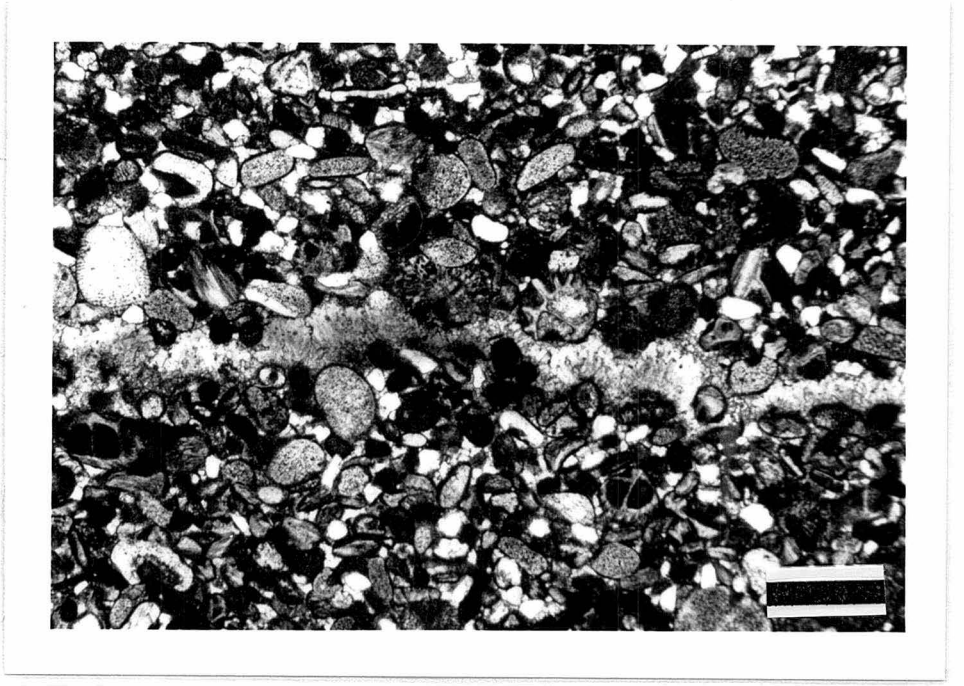


Figure 2.27 Upward-oriented brownish calcite cement formed along sheet cracks beneath a calcrete in the St. Louis eolianite. Possible rounded terminations, upward-orientation, and proximity to a calcrete suggest these cements may have formed in the capillary fringe. Mobil #1 Foster, 6709.0 ft core depth. Plane-polarized light. Scale bar is 0.5 mm.

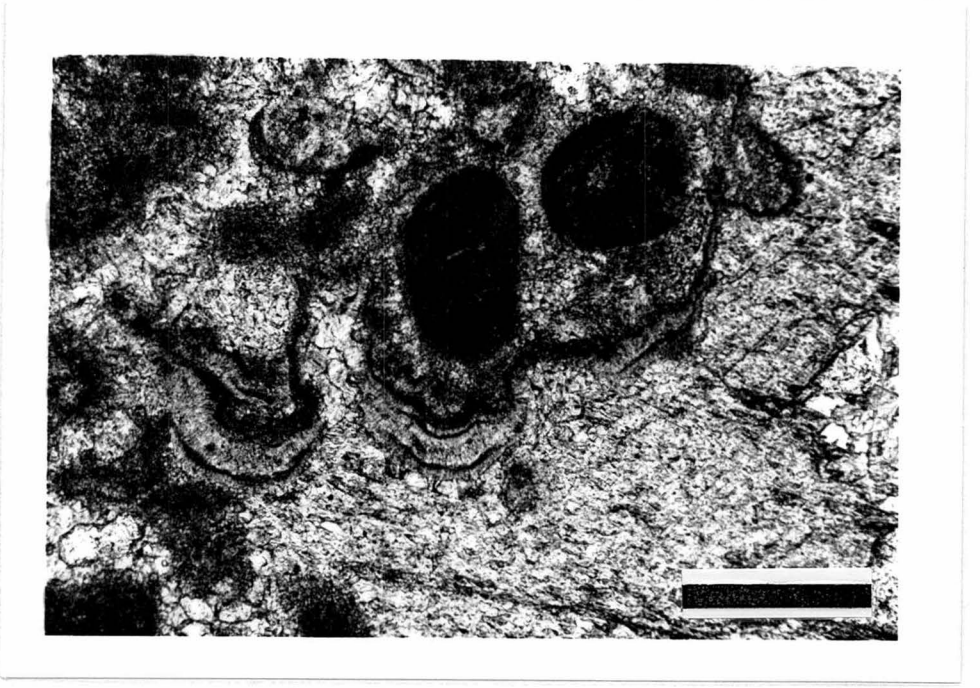


Figure 2.28 Photomicrograph of pendant sparry-calcite and micritic cements with rounded terminations. These cements are commonly associated with rhizoliths, a further indication of origin in the meteoric vadose zone. Amoco #3 Cohen C, 5285.9 ft core depth. Plane-polarized light. Scale bar is 0.25 mm.

euhedral.

Cross-stratified Deposits.– Cross-stratification is typically tangential. Cross-stratified sets are up to 2.5 ft (0.8 m) thick (Fig. 2.29). The base of tangential sets are typically dominated by low-angle foresets (<10°) with climbing translatent stratification. The upper, more steeply dipping portions of each cross-stratified set contain varying proportions of all three types of fine structure. Micrite-coated tubes, described above, occur toward the tops of such deposits but are rare. Brownish pendant cements nucleated from the tops of some pores.

The base of many quartzose grainstone intervals is marked by a lithoclastic conglomerate. Basal contacts of conglomerates are typically sharp. The thickness of these conglomerates typically range from 0.04 to 0.7 ft (0.01-0.2 m). Lithoclasts are up to 0.4 inches (1 cm) in size. Many conglomerates contain lithoclasts with dark-brown micrite and calcite-filled tubes described above. Locally conglomerates contain these brown lithoclasts although the parent lithology is absent in the immediately underlying strata (Fig. 2.29). One clast from the base of the Ste. Genevieve contains dark-brown, bladed and micritic cements (Fig. 2.30); geopetal internal sediment in a brachiopod in the clast indicates these are pendant cements.

SUMMARY

Ten lithofacies are recognized in the St. Louis and Ste. Genevieve core examined in this study (Appendix 1): 1) peloid dolomitic grainstone/packstone, 2) anhydrite, 3) breccia, 4) dolomite, 5) dolomitic lime mudstone, 6) algal boundstone, 7) skeletal packstone/wackestone, 8) ooid grainstone/packstone, 9) fenestral packstone/wackestone, and 10) quartzose grainstone.

Reproduced with permission of the copyright owner. Further reproduction prohibited without permission.

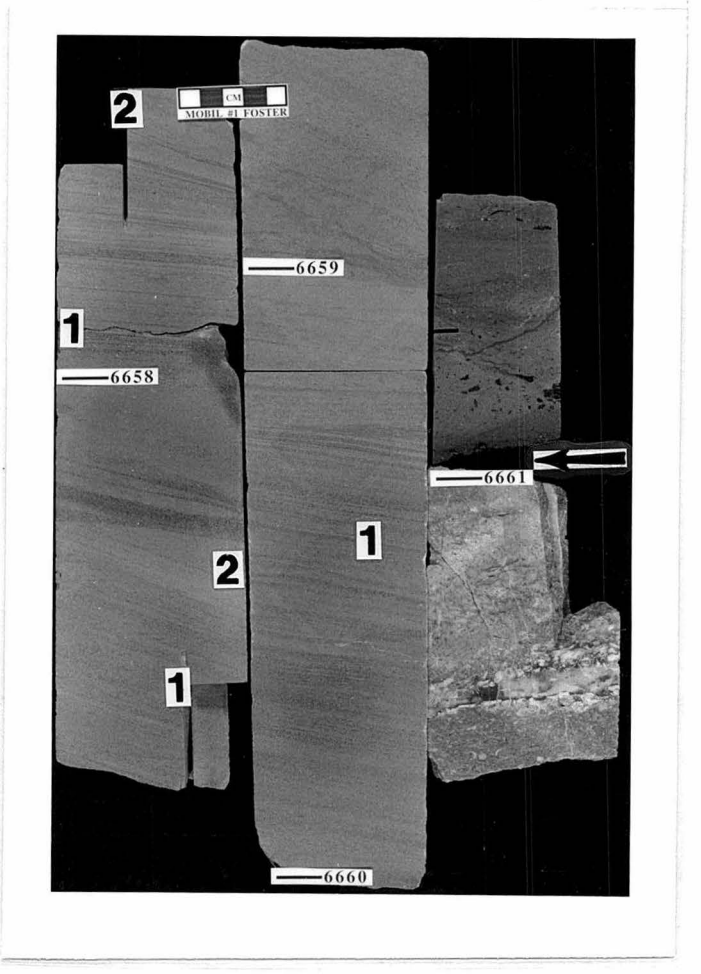


Figure 2.29 Quartzose grainstone from the base of the Ste. Genevieve Limestone. The base of the lithoclast conglomerate (arrow) at 6661 ft core depth is the St. Louis-Ste. Genevieve boundary. Abundance of cross-stratification sets and absence of rhizoliths indicates deposition took place in an active dune field. The majority of stratification is climbing translatent (1), but grainfall (2) and rare grainflow strata (3) also occur. Mobil #1 Foster, 6657-6661 ft core depth.



Figure 2.30 Brownish micritic and sparry-calcite cement (arrow) in a lithoclast at the base of the Ste. Genevieve. Rounded crystal terminations and geopetal sediment inside the brachiopod indicates the cement is a pendant cement (i.e. not upward oriented). Mobil #1 Foster, 6660.25 ft core depth. Plane-polarized light. Scale bar is 0.5 mm.

CHAPTER 3
Depositional Environments

INTRODUCTION

Despite important hydrocarbon reservoirs in ooid grainstones, little has been published concerning the facies, depositional environments, and sedimentology of the St. Louis and Ste. Genevieve Limestones (e.g., Goebel, 1968; Handford 1988, 1990; Handford and Francka, 1991). Recent advances in carbonate petrology and additional subsurface data warrant an update of the sedimentology of these carbonates. Interpretations of depositional environments of St. Louis and Ste. Genevieve strata should increase our understanding of Late Mississippian regional shelf sedimentation, paleogeography, and sea-level changes as well as improve hydrocarbon exploration and production.

DEPOSITIONAL ENVIRONMENTS

Ten lithofacies are recognized in the St. Louis and Ste. Genevieve cores examined in this study (Chapter 2, Appendix 1). Depositional environments are interpreted for each facies: 1) peloid dolomitic grainstone/packstone—restricted shelf; 2) anhydrite—saltern (shallow-subaqueous evaporite); 3) breccia—evaporite solution-collapse; 4) dolomite dolomitized mud-rich limestone, generally restricted shelf; 5) lime mudstone—restricted shelf; 6) algal boundstone—subtidal to lower intertidal restricted shelf; 7) skeletal packstone/wackestone—open-marine shelf; 8) ooid grainstone/packstone—oolite shoal 9) fenestral packstone/wackestone—tidal flat; and 10) quartzose grainstone—eolian.

Reproduced with permission of the copyright owner. Further reproduction prohibited without permission.

Dolomitic Peloid Grainstone/Packstone - Restricted Shelf

The abundance of peloids, paucity of stenohaline marine organisms, and association with anhydrite suggest peloid grainstone and packstone were deposited in a restricted-shelf setting. Parallel lamination of packstones indicates low energy. Periods of increased agitation are indicated by ripple cross laminae. Skeletal and oolitic grainstones are interpreted to have formed a barrier restricting connections with open-marine waters and dampening wave energy.

Anhydrite - Saltern (Shallow-Subaqueous Evaporite)

Most of the anhydrite in the Hugoton Member of the St. Louis Limestone is interpreted to have been deposited in a widespread, shallow-subaqueous setting or saltern. Warren (1989) coined the term saltern to describe regions of evaporite deposition that are laterally more extensive than salinas or evaporating pans. Salterns have no known modern analog. A sabkha origin cannot be discounted in all cases, but evidence indicates that most St. Louis evaporites were deposited as shallow-subaqueous gypsum (Table 3.1). Mosaic, nodular-mosaic, and massive textures are abundant in the St. Louis evaporites. These textures indicate a lack of significant carbonate matrix, and along with great lateral extent of the anhydrite (Fig. 2.6 and 2.7) and interbedded shallow-water carbonate, indicate that most of the Hugoton Member anhydrite was deposited in a shallow-subaqueous environment. Diagnostic supratidal and intertidal features (cf. Shinn, 1983) are typically absent. Upward-oriented anhydrite nodules, however, are rare (Fig. 2.5). Mosaic to nodular anhydrite structures are commonly attributed to sabkha environments (Kerr and Thomson, 1963). Other authors have shown that such textures can be produced in subaqueous evaporites (Dean et al., 1975; Warren and Kendall, 1985; Warren, 1989, 1991). The Ferry Lake

Reproduced with permission of the copyright owner. Further reproduction prohibited without permission.

Table 3.1 Distinguishing features of sabkha and saltern (extensive shallow-subaqueous) evaporites (modified from Warren, 1989, his Table 3.1)

SABKHA	SALTERN
Evaporite units are supratidal, matrix dominated, usually <60% sulfate	Evaporite units are subaqueous, relatively pure, often >70% sulfate
Each evaporite (supratidal) depositional unit is thin, usually 1-2 m	Each evaporite (subaqueous) unit is thick, 1-20 m
Displacive and replacive nodular and enterolithic textures	Bottom-nucleated evaporite crystal textures; often laminated, laminae can be laterally continuous, but do not extend across the whole basin
Evaporite crystals are diagenetic	Deposition can be mechanical; evaporites contain clastic textures; wave and current ripples, cross-beds, rip-up breccias, reverse and normal graded beds
Associated with tepees, flat-laminated and mudcracked algal mats	Associated with tepees, laminar algal mats and domal subaqueous stromatolites
Facies units tend to be laterally extensive, parallel to shoreline; deposition marked by subtidal, intertidal, and supratidal strata ("peritidal" trilogy of Warren and Kendall, 1985)	Facies often symmetric or asymmetric bull's eye-facies
Carbonate matrix washed in from lagoon during storms; quartz sands can be blown in from adjacent sand seas (ergs)	Carbonate facies outline areas of less saline water in basin
Dolomitization by storm recharge and shallow brine reflux	Dolomitization by evaporite drawndown and deeper brine reflux

Reproduced with permission of the copyright owner. Further reproduction prohibited without permission.

Anhydrite (Lower Cretaceous) in the Fairway field, east Texas, is interpreted as a saltern marked by mosaic, nodular-mosaic, and massive textures. Well-developed vertically-elongate anhydrite nodules were interpreted as relict vertical gypsum crystals (Loucks and Longman, 1982). Additionally, thickness and lateral correlation of the St. Louis anhydrite and interbedded carbonate lithologies are similar to those of the Ferry Lake Anhydrite (cf. Loucks and Longman, 1982; Pittman, 1985).

The common Salem-St. Louis vertical succession (in ascending order) of skeletal packstone/wackestone, ooid and skeletal grainstone, peloid grainstone/packstone, overlain by anhydrite suggests progradation of shallow-water facies. The oolites are interpreted to have formed shoals that became exposed following a relative fall in sea level, thus forming a sill. Evaporite deposition would begin shortly after the fall in relative sea level isolated the back-barrier lagoon. A relative fall in sea level is required to initiate evaporite deposition as autogenic aggradation of carbonates above sea level probably would not be continuous enough to restrict circulation to the point of gypsum precipitation. Moreover, subaerial carbonates facies, such as eolianites and tidalites, have not been identified in this position. Alternatively, restriction could be due in part to poor circulation across a very wide shallow shelf (cf. King, 1948). Lucia (1972) shows from modern settings, however, that sufficient restriction to produce evaporites requires a virtually continuous barrier. Absence of halite in the Hugoton Member suggests either a minor but continuous influx of marine waters refluxing through the barrier, reflux through underlying sediment, or a periodically breached barrier due to small-scale fluctuations in sea level. Interbedded carbonates probably developed during periods when the barriers to restriction were not as effective. Pinch out of anhydrite and carbonate beds (Figs. 2.6 and 2.7) may indicate variable salinities in the lagoon, and that carbonate and gypsum were precipitating simultaneously in different parts of the lagoon. The absence or thinning of the E2 anhydrite in southern Morton and

Reproduced with permission of the copyright owner. Further reproduction prohibited without permission.

Stevens County (Fig. 2.1 and 2.7) is interpreted to be the result of increasing marine influence to the south. Porous carbonate between E1 and E2 is interpreted as a flooding of the shelf by marine waters, temporarily ending evaporite deposition.

Warren (1989, 1991) reasoned that many saltern evaporites may have been precipitated from waters only tens of centimeters deep. Evaporitic drawdown initially reduced water depth. Complete evaporation of the lagoon was prevented by gypsum precipitation, forming an aquitard that prevented reflux through the underlying sediments. Evaporation of the saltern increased humidity in the immediately overlying air mass; this may have contributed to the absence of halite.

The thickest known individual St. Louis anhydrite interval is 66 ft (20 m) thick, based on a neutron-density log from the Barrett #1 Warner (sec. 28, T26S, R42W, Fig. 2.7). The log indicates the E2 anhydrite interval contains seven thin carbonate beds that are less than 2 ft (0.6 m) thick, less than the resolution of the density tool. Given a 38 percent volume loss from conversion of gypsum to anhydrite, the corresponding original gypsum thickness was approximately 106 ft (32 m). A continuous or periodic influx of marine waters is needed to provide such a thick evaporite bed, as complete evaporation of a 1,000 m column of seawater will yield only 0.75 m (2.5 ft) of gypsum (Blatt et al., 1980). Based on such estimates, the evaporation of an equivalent of a 43,000 m (140,000 ft) seawater column would be required to produce a 20 m (66 ft) anhydrite interval.

Such thick evaporites are inconsistent with a sabkha model (Warren and Kendall, 1985; Warren, 1989, 1991) (Table 3.1). Evaporite nodules and crystals grow displacively in the capillary zone of a sabkha (e.g., Kinsman, 1965; Evans et al., 1969; Warren, 1989, 1991). The thickness of supratidal nodular anhydrite is limited by the thickness of the capillary zone. Any evaporites above the capillary zone are subject to deflation or dissolution. Therefore, supratidal sabkha evaporites in a nonaggrading

Reproduced with permission of the copyright owner. Further reproduction prohibited without permission.

sabkha cycle can be no more than 1 to 2 m thick (Warren, 1989, 1991). Thus in order to accumulate 32 m (105 ft) of sabkha gypsum, an extremely static shoreline and subsidence are required (Schreiber, 1986). Given an average subsidence rate of 3 cm/1,000 yr for passive margin crust (Pittman, 1978), it would take approximately 1,000,000 yr to produce 32 m of sabkha gypsum. The widespread St. Louis evaporites are not consistent with a static shoreline.

Thick anhydrite indicates an arid to semi-arid climate during the late Meramecian. This is consistent with Cecil's (1990) interpretations of Late Mississippian climates in the eastern United States based on multiple lines of geologic evidence and on plate reconstructions. During the Visean (342 Ma), southwestern Kansas was situated at about 5°-10° south latitude (Scotese, 1986). Cecil suggests arid climates persisted throughout the Meramecian and into the early Chesterian. A more humid climate toward the end of the Mississippian (Cecil, 1990) probably reflects the northward migration of North America across the equator (Scotese, 1986).

Upon burial, the transformation of gypsum to anhydrite occurs at depths as shallow as 300 m (1000 ft) and is typically complete at depths of 1300 m (4300 feet) (Murray, 1964; Warren, 1989). The exact depth depends on the geothermal gradient and the salinity of the enclosed brine (Blatt et al., 1980).

Many shallow-subaqueous gypsum units have reported crude vertically-aligned, nodular anhydrite pseudomorphs after gypsum (Loucks and Longman, 1982; Schreiber et al., 1982; Shearman, 1985; Warren and Kendall, 1985; Warren, 1989, 1991). Matrix impurities outline the original crystal forms. Warren (1991) suggests that such "gypsum ghosts" are preserved when the conversion of gypsum to anhydrite takes place slowly and at relatively shallow depths. However, if dewatering is too slow, overpressure and rheologic flow destroy relict gypsum structures. The rarity of such features in most St. Louis anhydrites (Fig. 2.3 and 2.5) may be attributable to

Reproduced with permission of the copyright owner. Further reproduction prohibited without permission.

unfavorable dewatering rates or to an absence of significant matrix.

Breccia - Evaporite Solution-Collapse

The breccias of the Hugoton Member of the St. Louis Limestone in southwestern Kansas are interpreted as solution-collapse breccias formed by the dissolution of anhydrite. Goebel (1968) and Thompson and Goebel (1968), in contrast, interpreted the breccias to have formed by "intraformational erosion." Blocky anhydrite, gypsum casts, megaquartz with anhydrite inclusions, and length-slow spherulitic chalcedony (cf. Folk and Pittman, 1971) preserved within and between breccia clasts indicate an intimate association with evaporites. The breccias are stratigraphically equivalent to anhydrite of the Hugoton Member (Fig. 2.6; Pocket enclosure I-I'). Lucia (1972) states that stratigraphic equivalence to evaporites is the most reliable criteria in the recognition of solution-collapse breccias. In Amoco #1 Nordling, most of the anhydrite is preserved; a solution-collapse breccia occurs near the top of the E1 anhydrite (Fig. 2.6). Amoco #1 Nordling is situated near the boundary between preserved anhydrite and solution-collapse breccia (Figs. 2.1, 2.6, and 2.7). The breccia in the Nordling core apparently represents an incipient solution-collapse breccia that is "caught in the act" of evaporite dissolution. This further illustrates the relationship of evaporites and breccia. The absence of E1 anhydrite in Amoco #1 McPherson & Citizen State Bank, Oxy #3 Hoffman, and Barrett #1 Wilkerson is inferred to result from evaporite dissolution (Fig. 2.6 and 2.7). These wells lie near the northern limit of preserved evaporites where the E1 evaporite was dissolved in shallower groundwaters that were undersaturated with respect to gypsum. Meanwhile, E2 evaporite was preserved in deeper saline groundwaters or brines.

The vertical succession of polymictic, monomictic, and fractured carbonate is similar to the generalized facies of solution-collapse breccias as proposed by Laznicka (1988). Similar solution-collapse successions have been described from the Madison Limestone

Reproduced with permission of the copyright owner. Further reproduction prohibited without permission.

(Kinderhookian-lower Meramecian, Mississippian) of north-central and western Wyoming (Sando, 1974, 1988; Sieverding and Harris, 1991).

Evaporites are preserved in parts of Morton, Stanton, Hamilton, Stevens, Grant, Seward, Haskell, and possibly Meade Counties (Fig. 2.1). Solution-collapse breccias demonstrate that evaporites had a much wider distribution than previously known. Solution-collapse breccias from Gove, Logan, and Scott Counties indicate that evaporites once covered most of the Hugoton embayment (Fig. 2.1).

The timing of the dissolution of the evaporite is difficult to establish. The collapse of basal Stevens Member strata indicates dissolution was not penecontemporaneous with deposition. Fractured carbonates in the Ste. Genevieve suggest that evaporite dissolution postdates Ste. Genevieve deposition. Evaporites were probably dissolved by groundwaters recharged during subaerial exposure associated with the sub-Pennsylvanian unconformity (cf. Jorgensen, 1989). The postulated conditions—extended exposure, estimated at a few million years (Sloss, 1984; Saunders and Ramsbottom, 1986), humid climate (Cecil, 1990), and large fall of relative sea level (Vail et al., 1977)—are ideal for large-scale evaporite dissolution. Evaporites are only preserved in the deepest part of the Hugoton embayment (Fig. 2.1), far from potential groundwater recharge areas flanking the Central Kansas uplift (Fig. 1.2). Breccias could also have resulted from meteoric dissolution during subaerial exposure associated with calcrete paleosols or eolian strata in the Stevens Member of the St. Louis or Ste. Genevieve. However, the short duration and probable semi-arid climates (Cecil, 1990) make these unconformities unlikely candidates for large-scale evaporite dissolution. In addition, dissolution probably was post-Ste. Genevieve. The evaporites were probably buried too deeply to be affected by groundwaters associated with shorter intervals of subaerial exposure during deposition of the Shore Airport Formation (cf. Abegg, in press (a)). Subaerial erosion associated with the sub-Pennsylvanian unconformity

Reproduced with permission of the copyright owner. Further reproduction prohibited without permission.

brought the evaporites closer to the surface where they were vulnerable to undersaturated groundwater.

Dolomite - Dolomitized Mud-rich Limestone (generally restricted shelf)

Rare stenohaline marine crinoids, brachiopods, and fenestrate bryozoans preserved in dolomite indicate local marine deposition of the precursor. Common laminations and detrital quartz suggest some dolomitized beds are altered peloid packstone. Because dolomitization is selective for matrix, however, packstone and grainstone are less likely to be dolomitized. Therefore, extensively dolomitized facies most likely were rich in lime mud. The fine-grained nature of much of the dolomite supports such an interpretation. Only planar-e dolomite crystals are present in chert; this indicates that chertification postdates planar-e dolomite crystallization and predates planar-s and nonplanar dolomite.

Dolomitic carbonate is intercalated or laterally correlative to anhydrite and solution-collapse breccia in the Hugoton Member. Most strata in the overlying Stevens Member contain little or no dolomite, even though muddy facies are present. This relationship suggests evaporitic brines were responsible for much of the dolomitization, possibly due to refluxing lagoonal brines or connate brines expressed during compaction. Minor baroque dolomite indicates some deeper burial dolomitization. Additional investigation is needed to determine the genesis of dolomite in the Hugoton Member.

Dolomitic Lime Mudstone - Restricted Shelf

Lime mudstone are interstratified with anhydrite and solution-collapse breccias, contain calcite pseudomorphs after gypsum, and lack stenohaline marine fossils. These features indicate deposition on a low-energy, severely restricted shelf.

Reproduced with permission of the copyright owner. Further reproduction prohibited without permission.

Algal Boundstone - Subtidal to Lower Intertidal Restricted Shelf

Colloform and domal stromatolites in the algal boundstone facies are interpreted to have formed in a subtidal restricted-shelf environment. However, the rejection of an intertidal or supratidal origin for laminar stromatolites is based largely on negative evidence and is therefore tenuous. Subtidal stromatolites form today where invertebrate grazers and burrowers are excluded, for example by hypersalinity (Garrett, 1970; Gebelein, 1969, 1976). The Hugoton restricted backshoal lagoon would have been such an environment. However, Holocene subtidal stromatolites are also reported from waters of near normal salinity (Dill et al., 1986). Many workers associate stromatolites with intertidal and supratidal environments (Playford and Cockbain, 1976). Modern subtidal stromatolites in Hamelin Pool of Shark Bay, Western Australia (Hoffman, 1976; Playford and Cockbain, 1976), and in the Bahamas (Gebelein, 1969, 1976; Dill et al., 1986), and ancient subtidal stromatolites interbedded with many subaqueous evaporites (Schreiber, 1986) and in the Devonian of the Canning basin (Playford et al., 1976) show that ancillary evidence is needed to determine if stromatolites are subtidal, intertidal, or supratidal.

Spirorbid-encrusted Colloform.– Encrusting spirorbid worm tubes suggest that the colloform algal boundstone was deposited subtidally. According to Hoffman (1976), encrusting organisms disrupt mat growth and contribute to the irregular margins and internal cavities of these stromatolites. The interruption of algal growth by encrusters permits the internal pores to be lined by crusts of brownish fibrous calcite cement (Fig. 2.17) that are irregularly distributed to locally isopachous. However, rare alveolar texture within these stromatolites possibly suggest brief subaerial exposure (cf. Esteban and Klappa, 1983). Additional features indicative of subaerial exposure (e.g., mudcracks, fenestral porosity) are apparently absent.

Laminar.– Laminar stromatolites are commonly interbedded with anhydrite, which

Reproduced with permission of the copyright owner. Further reproduction prohibited without permission.

is interpreted as subtidal in origin (Figs. 2.15 and 3.1). This suggests that algae were able to colonize the seafloor as salinities elevated to the point that grazing and burrowing invertebrates were significantly reduced in number. In Amoco #1 Puyear (5700 ft core depth) (Fig. 2.18) and the Amoco #3 Cohen C (5702-5703 ft core depth), colloform stromatolites that are encrusted by spirorbid worms are overlain by laminar stromatolites and then anhydrite or solution-collapse breccia. This sequence is interpreted to result from deposition under increasing salinity (Fig. 3.1). Colloform algal mats formed while salinities were low enough to permit encrustation by spirorbid worm tubes. The lower colloform mats have more numerous encrustations compared to uppermost colloform mats consistent with an upward increase in salinity. Colloform stromatolites were succeeded by laminar stromatolites when salinities became high enough to exclude invertebrates (cf. Hoffman, 1976). The lack of encrustation allowed the subtidal algal mats to spread extensively (cf. Hoffman, 1976). Eventually, salinity reached 130 to 160 ‰ (cf. Warren, 1989) and gypsum precipitation commenced. Absence of halite suggests salinities did not exceed approximately 340 ‰ (cf. Warren, 1989).

Following a more uniformitarian approach, some of the laminar stromatolites may have formed in a lower intertidal environment. Fenestrae and mudcracks would be rare in such environments (Shinn, 1983). In the Ferry Lake Anhydrite, a widely accepted subtidal evaporite deposit (Loucks and Longman, 1982), interbedded carbonates contain algal boundstones that typically occur above anhydrite beds, but are rare below anhydrite, unlike the St. Louis stromatolites. Based on very rare mudcracks, Loucks and Longman (1982) interpret these stromatolites to have formed in a lower intertidal setting. Ferry Lake stromatolites were not described, so a comparison to St. Louis stromatolites is not possible. Warren (1989; 1991, p. 151) reasoned that evaporites deposited in the Ferry Lake saltern may have been precipitated from waters

Reproduced with permission of the copyright owner. Further reproduction prohibited without permission.

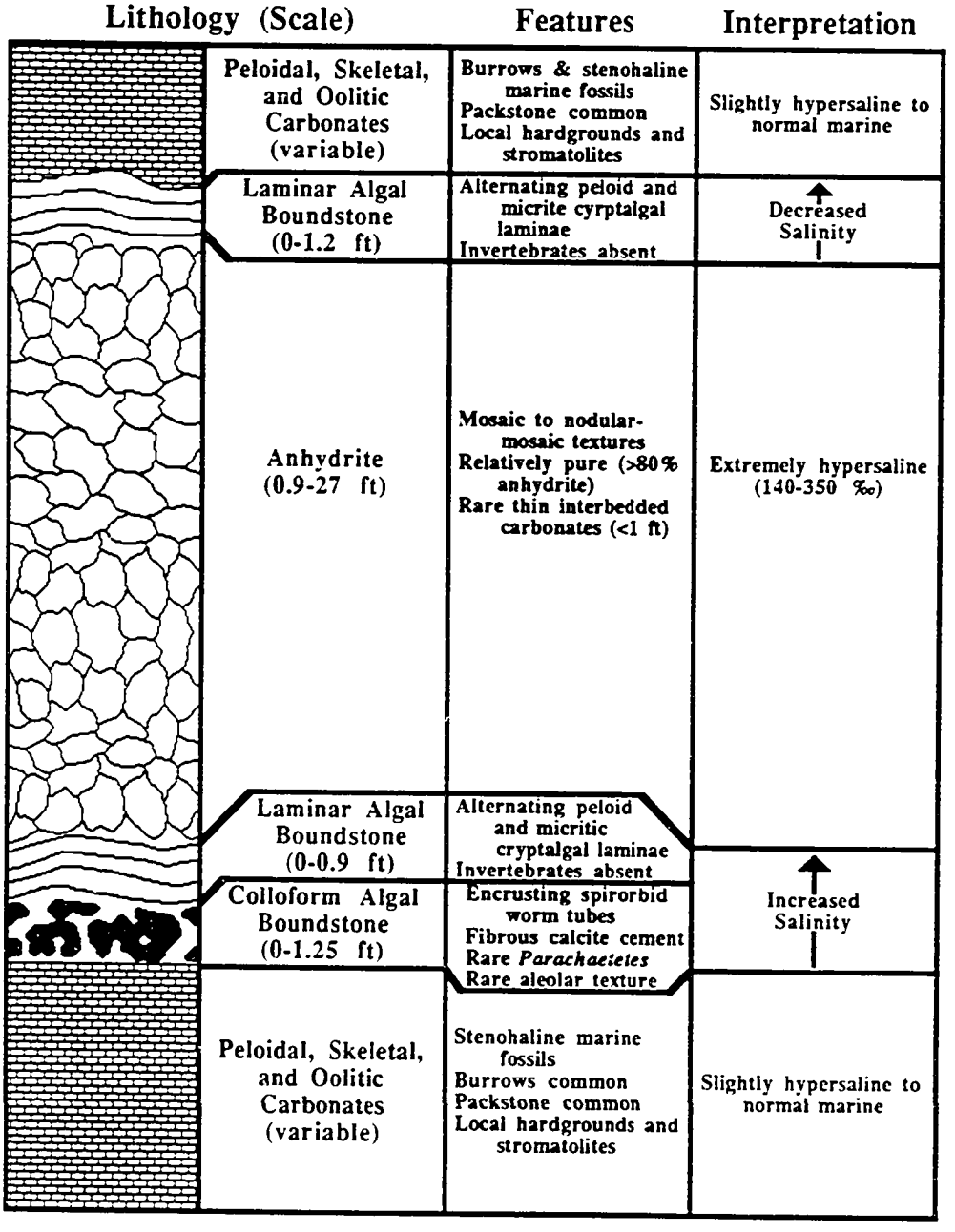


Figure 3.1 Features typical of interbedded algal boundstone and anhydrite from the Hugoton Member of the St. Louis Limestone.

Reproduced with permission of the copyright owner. Further reproduction prohibited without permission.

only tens of centimeters deep. If this were true for St. Louis evaporites, laminar stromatolites could easily represent very shallow subtidal to intertidal deposition.

Domal.– Domal stromatolites are interbedded with ooid grainstone and packstone, indicating that they formed in high-energy settings. Shifting substrates in these high-energy settings do not permit algal mats to spread laterally (Gebelein, 1969, 1976).

Skeletal Packstone/Wackestone - Open-marine Shelf

The diverse and abundant assemblage of stenohaline echinoderms, brachiopods, and bryozoans found in the skeletal packstone/wackestone indicate deposition in a normal-marine environment. Periodic winnowing and intercalated oolites suggest deposition at or above fair-weather wave base. An abundance of horizontal trace fossils, characteristic of the *Cruziana* ichnofacies, is also consistent with shallow-marine deposition. Marine allochems and absence of subaerial exposure features indicate the truncation surfaces are probably marine hardgrounds.

Oolitic Grainstone/Packstone - Oolite Shoal

The dominance of ooids and grainstone texture, minor cross stratification, and scattered stenohaline marine fossils indicate that oolitic grainstone/packstone accumulated in a highly agitated, marine environment. Modern ooids generally form at depths less than 6 ft (2 m), with the majority of ooid-rich facies being deposited in depths less than 15 ft (5 m) (Newell et al., 1960). Near absence of cross stratification may indicate bioturbation. Vaguely laminated, peloidal, micritic crusts with fenestral porosity on oolitic truncation surfaces (Fig. 2.20) may be algal in origin, suggesting they formed with the aid of substrate-stabilizing algal mats (Gebelein, 1969). Absence of subaerial exposure features (cf. Esteban and Klappa, 1983) indicates the micritic crusts are not laminated calcretes. Dravis (1979) reports that algae were important in

Reproduced with permission of the copyright owner. Further reproduction prohibited without permission.

the formation of oolitic hardgrounds in the Bahamas. St. Louis stromatolites cap truncation surfaces, so they may not have been involved in formation of these surfaces. Algae may simply have encrusted a lithified substrate. Isopachous bladed cements that are present only below the hardground may be marine in origin.

Grainstones where nearly all grains are coated by thick ooid cortices formed on an ooid shoal. Percentage of oolitically coated grains on Bahamian oolite shoals drops off sharply on both the seaward and bankward shoal margins (Newell et al., 1960). By analogy to Bahamian oolite shoals, grainstone and packstone with mixtures of ooids and skeletal grains in the Stevens Member are interpreted as forming in an environment transitional between the shoal crest ooid grainstone and deeper water skeletal packstone/wackestone. Hydrocarbon reservoirs are typically best developed in the ooid grainstone where nearly all grains have superficial or thicker cortices. Ball (1969), on the other hand, suggests that porosity is best developed in skeletal-ooid grainstone. The occurrence of skeletal grains, especially crinoids, was typically accompanied by increased cementation that occludes primary porosity. Youle (1990) noted this relationship from the Wendell Pool in Gray County. However, skeletal-ooid grainstones are reservoirs locally (e.g., Handford and Francka, 1991).

Fenestral Packstone/Wackestone - Tidal Flat

Fenestral limestones were deposited on tidal flats. The near absence of stenohaline marine organisms in fenestral limestone suggests formation in hypersaline or brackish conditions. In Pan American #1 Moser (4988.2 ft core depth), bladed pendant cements are tentatively interpreted as vadose cements precipitated in the meteoric or possibly marine vadose realm. Minor dissolution is suggested by irregular terminations of these cements. The vadose cements and fenestral porosity suggests deposition in the upper intertidal, supratidal, or subaerial zones (Shinn, 1983). This facies is associated with

Reproduced with permission of the copyright owner. Further reproduction prohibited without permission.

nearshore strata in the Ste. Genevieve Limestone.

Quartzose Grainstone - Eolian

Based on multiple lines of evidence (Table 3.2), quartzose grainstones are interpreted as largely eolian in origin. Climbing translatent strata are generally considered diagnostic of eolian sedimentation (Hunter, 1977, 1981; Kocurek and Dott, 1981; Kocurek, 1991). Most other criteria indicative of an eolian interpretation are equivocal in isolation. Therefore, multiple lines of evidence are commonly required to affirm a wind-blown origin for carbonate grainstones.

Hunter (1989) ascribed a similar facies from the Illinois basin in southern Indiana to eolian origin. Handford (1990) and Handford and Francka (1991) interpreted the quartzose grainstone in the Damme Field (Finney County) and the Big Bow Field (Stanton and Grant Counties), Kansas as eolian in origin. Handford and Francka (1991) recognized climbing translatent, grainfall, and grainflow stratification from cores in the Big Bow Field in Stanton and Grant Counties, Kansas. Handford (1988) had previously interpreted quartzose grainstone from the Damme Field as subaqueous tidal channels, illustrating that differences between eolian and subtidal strata are subtle.

Climbing Translatent Stratification.– Climbing translatent stratification is considered the product of migration of wind ripples. Climbing wind ripples are distinct in form and appearance from climbing subaqueous ripples (Fig. 3.2). Each millimeter-scale, coarsening-upward stratum forms from the migration of a single, climbing wind ripple. The coarsest grains are concentrated along ripple crests while finer grains are protected in the ripple troughs (Hunter, 1977; Fryberger and Schenk, 1988). In the ripple troughs, very fine sand and very coarse silt are protected from incoming saltating grains and from direct airflow across the ripple crests (Fryberger and Schenk, 1988). The thin layers of very fine sand and very coarse silt that are deposited in ripple troughs

Reproduced with permission of the copyright owner. Further reproduction prohibited without permission.

Table 3.2. Contrasting features of eolian and subaqueous grainstones (based largely on Hunter, 1981 and 1989). Boldface indicates features present in quartzose grainstones in the Upper Mississippian of southwestern Kansas. Features are illustrated in Figures 2.22, 2.23, 2.24, 2.25, 2.26, 2.27, 2.28, 2.29, 2.30, and 3.2.

EOLIAN	SUBAQUEOUS
Climbing translatent stratification	Subaqueous climbing ripples
Grainfall	**Grainfall**
Grainflow	**Grainflow**
Well to very well sorted	Moderate sorting
Typically very fine to medium sand, grains >4 mm extremely rare	Grains >4 mm common
Well-rounded and abraded allochems	Rounding variable
Frosted quartz grains[1]	Frosted grains absent[1]
Absence of shale/micrite, and mica (except in interdunes)[2]	Mud or clay/micrite, and mica present
Large-scale (>1 meter) cross strata	**Large-scale cross strata rare**
Planar to wedge-planar cross strata	Wedge-planar less common
Tangential foresets	Tangential foresets less common
Straight-crested, low-amplitude ripples (high ripple indices) (cf. Fig. 4.2)	Sinuous, high-amplitude ripples (low ripple indices) (cf. Fig. 4.2)
Trace fossils absent to very rare	Trace fossils present
Adhesion ripples	Adhesion ripples absent
Calcrete (scattered rhizoliths, alveolar texture, etc.)	**Calcrete** present only at exposure surfaces
Vadose cements (scattered pendant, upward-oriented, and meniscus)	**Vadose cements** present only at exposure surfaces

[1]Not examined.

[2]Interdune deposits not recognized.

Reproduced with permission of the copyright owner. Further reproduction prohibited without permission.

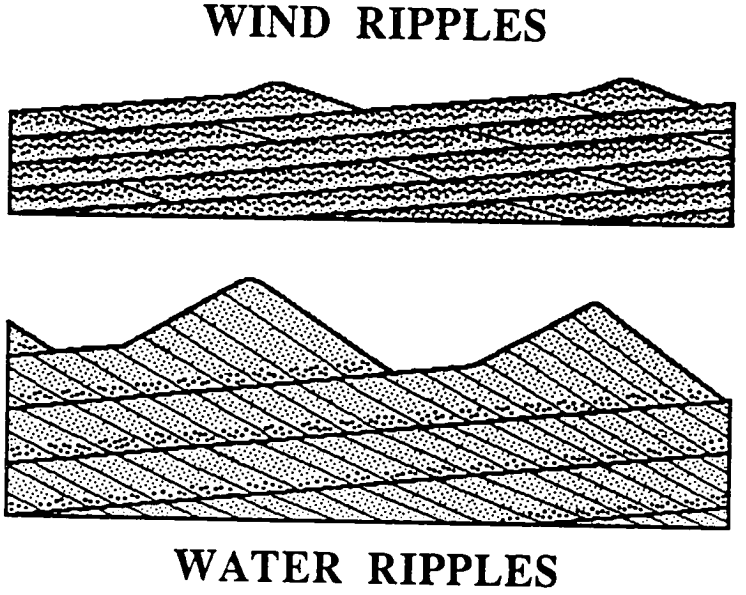


Figure 3.2 Features of eolian and subaqueous climbing ripples. Wind ripples have low amplitudes and relatively long wavelengths with the coarser grains concentrated at the ripple crest. Low-angle foresets retard avalanching on lee sides of ripples. These features produce climbing translatent strata that are characteristically thin, uniform thickness, commonly inversely graded, and contain few visible ripple-foreset laminae. In contrast, subaqueous ripples have higher amplitudes with the coarser grains relegated to the ripple troughs. Avalanching is common on the steep lee sides of the ripples. These features produce climbing translatent strata that are typically thicker, normally graded, and contain well-developed ripple-foreset laminae (Modified from Kocurek and Dott, 1981, their Fig. 3)

Reproduced with permission of the copyright owner. Further reproduction prohibited without permission.

are typically less than 1 mm thick and produce a feature termed pin stripe lamination (Fryberger and Schenk, 1988). Ripple-foreset laminae are not well developed in eolian climbing translatent strata due to an absence of avalanching on the gently sloping lee sides of wind ripples. Distinctly coarsening-upward strata that is characteristic of eolian climbing translatent strata is poorly developed locally due to coarser grain sizes (lack of fines) or very low angles of ripple climb (Hunter, 1977). Fryberger and Schenk (1981) report experimental data suggesting climbing translatent strata may show no grading at all.

In Mobil #1 Foster, climbing translatent strata are as thick as 9 mm (Fig. 2.23). The unusual thickness might reflect damp conditions that would have made the grains more cohesive, thus reducing the amount of the ripple crest that was destroyed prior to burial by the succeeding ripple train. According to Fryberger and Schenk (1981), high rates of deposition and low rates of ripple migration also can account for unusually thick climbing translatent strata.

Grainfall Strata.– Indistinctly stratified units in quartzose grainstones are interpreted to have formed by grainfall in the flow separation on the lee side of dunes. Fine to very fine sand grains overrun the crest and are deposited on the lower slipface or apron as grainfall strata. The lack of distinct stratification is the result of excellent sorting of grains.

Grainfall strata are distinguished from climbing translatent strata because wind-ripple stratification exhibits coarsening-upward grain distribution, ripple-foreset laminae, and generally has lower dips, although some overlap exists. However, Collinson (1986) recognizes that some grainfall strata may be difficult to distinguish from climbing translatent strata. Grainfall laminae also may coarsen upward in response to increases in wind velocity (Fryberger and Schenk, 1981). In many of the quartzose grainstones, therefore, the origin of millimeter-scale alternating medium and

Reproduced with permission of the copyright owner. Further reproduction prohibited without permission.

very fine sand laminae is equivocal. Deposition by either climbing wind ripples or by grainfall under fluctuating wind regimes is possible. Only where ripple-foreset laminae are present can wind-ripple origin be recognized unequivocally. The majority of alternating medium- and very fine-sand layers in the quartzose grainstone facies are very likely climbing translatent strata based on recognition of ripple-foreset laminae in many of the coarsening-upward strata.

Grainflow Strata.– Fining-upward and structureless units are interpreted as grainflow deposits. Medium-sand grains that concentrate at the slipface crest subsequently avalanche, pick up finer grains by eroding underlying strata, and are deposited as grainflows. Fining-upward and structureless strata are extremely rare in the quartzose grainstone facies. As other evidence suggests that dunes were present, either the upper parts of dunes were truncated by interdune erosion or avalanching on slipfaces was rare. Fining-upward and structureless deposits are intercalated with indistinctly stratified grainfall deposits and climbing translatent strata, as is common in small eolian dunes (Kocurek and Dott, 1981). Slipfaces in modern dunes commonly dip 33° to 34°, grainflows dips rarely exceed 24°. Dips angles of approximately 20° to 24° are consistent with grainflow deposition at the angle-of-repose and subsequent flattening through 35 percent compaction (cf. Rittenhouse, 1972). Compactional features are common and include stylolites and interpenetrating grain contacts. Erosion of steeper upper parts of slipfaces could also explain low dips, as well as the scarcity of grainflow deposits (cf. McKee, 1979).

Basal contacts of grainflow deposits locally truncate underlying strata indicating scour. Thinning of as much as 4 mm across a 8.9 cm (3.5 in) core is interpreted as wedging at the toe of a grainflow. Grainflow deposits commonly coarsen upward because of dispersive pressure during flow (Bagnold, 1954; Hunter, 1977; Kocurek and Dott, 1981). Grain-size distribution, however, depends on the location in a

Reproduced with permission of the copyright owner. Further reproduction prohibited without permission.

grainflow. Upward coarsening is common in proximal parts of grainflows (Fryberger and Schenk, 1981; Ahlbrandt and Fryberger, 1982). The mantle of coarser grains outrun the finer grains to the distal part of the grainflow and are later buried by finer grainflow material, creating a fining-upward unit (Ahlbrandt and Fryberger, 1982).

The paucity of grainfall and grainflow stratification in cross-strata sets seen in this study may be attributed to 1) incomplete dune preservation, 2) large dune size, 3) barchan dune morphology, or 4) variations in wind directions (Kocurek and Dott, 1981; Kocurek, 1991). If the slipface of the dune is not preserved, grainflow and grainfall stratification may be nearly absent (Kocurek and Dott, 1981). Distribution of stratification types varies with dune size. According to Kocurek and Dott (1981), small dunes typically have varying combinations of climbing translatent, grainfall, and grainflow stratification. In larger dunes, grainfall occurs only on the upper slipface, so deposits are less likely to be preserved. Dune morphology can also affect the distribution of stratification types. In barchan dunes, only the central part of the lee side of the dune will have grainfall and grainflow deposits (cf. Hunter, 1977). The horns of the barchan do not have flow separation and grains will be reworked into wind ripples. Climbing translatent stratification intercalated with grainfall and grainflow deposits (Figs. 2.24 and 2.29) can also form from well-developed lee-side eddies or reversing to oblique winds that rework slipfaces (Hunter, 1981; Clemmensen and Abrahamsen, 1983; Kocurek, 1991). The proportions of varieties of fine structure also differ with eolian environment.

Eolian Sub-environments.– Cross-stratified and low-angle stratified deposits represent different environments of eolian accumulation. Low-angle-stratified deposits are formed as vegetated sand sheets and cross-stratified deposits indicate dune fields.

Vegetated Sand Sheet.– The relative abundance of climbing translatent stratification indicates that the many Mississippian eolianites in southwestern Kansas

Reproduced with permission of the copyright owner. Further reproduction prohibited without permission.

were vegetated sand sheets (Figs. 2.22 and 3.3). The numerous calcite-filled tubes coated by indistinctly laminated, dark-brown micrite are interpreted as rhizoliths with calcite-filled root casts and dark-brown rhizocretions (Figs. 2.22) (cf. Klappa, 1980). The dark-brown color may indicate organic matter, probably incorporated under waterlogged, conditions (cf. Goldstein, 1988). This indicates a hydromorphic calcrete paleosol. The thin micritic bridges associated with the rhizoliths (Fig. 2.26) are excellent examples of alveolar texture (cf. Esteban and Klappa, 1983). Pendant cements are interpreted as microstalactitic cements precipitated in the meteoric vadose zone. Upward-oriented (astropetal), bladed, brownish, sparry-calcite cement (Fig. 2.27) is very similar to ribbon spar described from the Pennsylvanian Holder Formation in New Mexico (Goldstein, 1988). Goldstein reasoned that these cements precipitated in the capillary fringe at the base of the vadose zone. A similar origin for the brownish cements in the eolianites is likely, based on the preferred upward orientation. Possible rounded terminations of some crystals may reflect a meniscus air-water contact.

Sand sheets are regions of predominantly eolian sedimentation where dunes with slipfaces are lacking (Kocurek, 1986; Kocurek and Nielson, 1986). Sand sheets commonly occur along the margins of dune fields (Kocurek, 1986). Conditions inhibiting the formation of dunes and favoring sand-sheet development include the following: 1) high water table, 2) surface cementation or binding, 3) periodic flooding, 4) significant coarse-grained sediment population, and 5) vegetation (Kocurek and Nielson, 1986). Many of these conditions appear to have been present during deposition of Upper Mississippian carbonate eolianites. The dark-brown color of paleosol features, indicative of organic material that was probably incorporated under waterlogged and conditions, and upward oriented capillary-fringe cements provide evidence for a high water table. Early cementation is indicated by calcrete and quartzose grainstone lithoclasts. Although coarse-grained sands are absent in wind-

Reproduced with permission of the copyright owner. Further reproduction prohibited without permission.

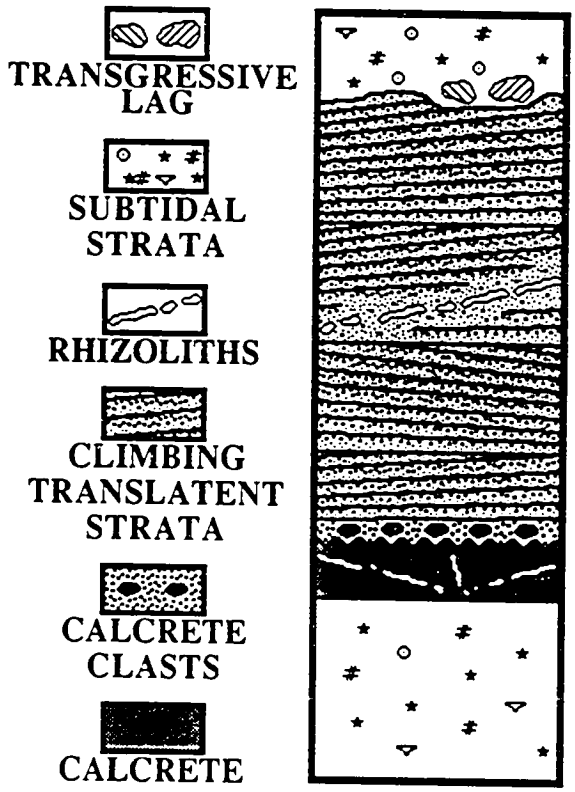


Figure 3.3 Features of eolian sand-sheets deposits. Stratification is almost exclusively climbing translatent with dips commonly less than 15°. Tangential cross-strata sets with grainfall (and grainflow?) deposits are rare. Rhizoliths are scattered throughout the unit and locally disrupt stratification. An entire eolian interval may form from sand sheets or contain interbedded cross-stratified units deposited by migrating dunes. Most Upper Mississippian eolianites in southwestern Kansas contain sand-sheet deposits, but not all (e.g., Abegg, 1991).

Reproduced with permission of the copyright owner. Further reproduction prohibited without permission.

ripple deposits, lithoclasts in conglomerates are as large as 9 mm. Abundant rhizoliths indicate that the sand surface was partially stabilized by vegetation. Another factor in development of a sand sheet is time (Kocurek, 1991). Thousands to tens of thousands of years are required to build a dune several hundred feet high (Ahlbrandt and Fryberger, 1982). The thinness of some sand sheets (e.g., Abegg, 1991) is consistent with short-lived eolian sedimentation, so dunes may not have had time to develop. Although it is difficult to isolate the contribution of each variable to the formation of Upper Mississippian sand sheets, the abundance of rhizoliths suggests vegetation was an important factor. Handford and Francka (1991) recognized sand-sheet deposits from the Big Bow Field in Stanton and Grant Counties, but did not describe them.

Dune Fields.– Cross-stratified deposits contain cross stratification at higher angles (up to 32°) in sets as thick as 2.5 ft (0.8 meters) (Figs. 2.24, 2.29, and 3.4). Rhizoliths are rare. This indicates deposition in a sparsely vegetated, active dune field. Cross-strata sets are typically dominated by climbing translatent stratification, but the upper parts of the thickest sets contain grainfall and, rarely, grainflow stratification. The majority of cross-strata dip less than 20°, suggesting that only dune aprons are commonly preserved. Compactional flattening could also help explain the low dip angles (cf. Rittenhouse, 1972). Thickness of eolian grainflows is proportional to slipface height (Hunter, 1977). Based on a plot of maximum thickness of eolian grainflow versus slipface height (Kocurek and Dott, 1981), the thickest eolian grainflow observed, 1.6 cm, corresponds to a slipface 0.9 m high. This is consistent with the maximum observed cross-strata thickness, 0.8 m, from cores in southwestern Kansas.

The base of many quartzose grainstone intervals is marked by a lithoclast conglomerate (Figs. 2.25 and 2.29). Sharp basal contacts are interpreted as erosional. Dark-brown lithoclasts are reworked from the underlying paleosol. These

Reproduced with permission of the copyright owner. Further reproduction prohibited without permission.

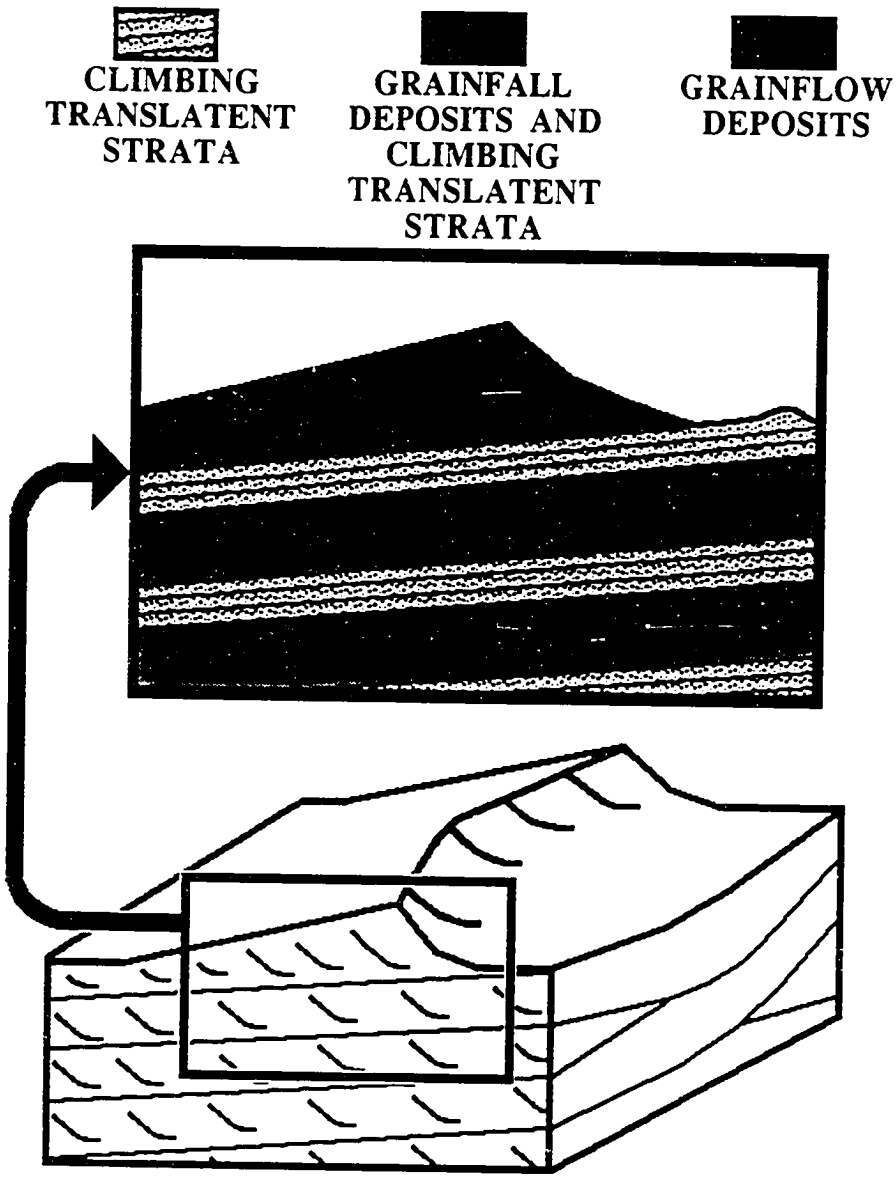


Figure 3.4 Distribution of stratification types in deposits of active dune fields in Upper Mississippian eolianites of southwestern Kansas. Preserved strata are composed of abundant climbing translatent strata, common grainfall deposits, and rare grainflow units. Rhizoliths are rare to absent. Dips typically increase upward, reflecting preferential preservation of dune aprons and lower slipfaces and tangential foresets. Cross-strata sets are up to 2.5 ft (0.8 m) thick.

Reproduced with permission of the copyright owner. Further reproduction prohibited without permission.

conglomerates were probably formed in part by erosion of the underlying skeletal limestones and calcretes. Lithoclasts and well-rounded, syntaxial-cement overgrowths in the overlying climbing translatent strata are evidence of the reworking of lithified limestones. Some conglomerates are not underlain by a calcrete, yet the basal lag contains calcrete lithoclasts (Abegg, 1991). Either the calcrete was removed by erosion or the calcrete clasts were transported from nearby. Because armoring by wind deflation produces deposits that are typically only one grain thick (Bagnold, 1954), conglomerates cannot be attributed to wind deflation alone. Hunter (1989) described a similar lithoclast conglomerate at the base of Ste. Genevieve carbonate eolianites in southeastern Indiana, and interpreted it as alluvium. Handford (1990) and Handford and Francka (1991) interpreted calcareous sandstones from the Ste. Genevieve in southwestern Kansas as interdune and wadi deposits.

Upward increase in quartz content in many Upper Mississippian carbonate eolianites may result from sediment bypassing or abrasion of carbonate grains associated with increased distance from the shoreline. Sedimentary bypassing occurs because smaller quartz grains outrun larger carbonate grains downwind (Folk, 1980; Rice and Loope, 1991). Additionally, carbonate grains are less resistent to abrasion than quartz (Kuenen, 1960; Glennie, 1970; Rice and Loope, 1991). Carbonate grains would, therefore, become less abundant downwind. Thus the upward increase in quartz content may reflect increased distance from shoreline and subsequent rapid transgression.

The regional correlation of quartzose grainstone units is difficult. Changes in unit thickness and in quartz content are the main factors that make correlation problematical. Many eolianites have minor amounts of detrital quartz (cf. Handford and Francka, 1991) making log recognition difficult. Quartz-rich eolian limestone may grade laterally over several miles into quartz-poor eolianite or possibly subtidal limestones; the result

Reproduced with permission of the copyright owner. Further reproduction prohibited without permission.

would appear the same on logs. Changes in thickness of eolian strata is attributable to several possible factors including paleotopography, sand supply, or wind-transport capacity (Kocurek and Halvholm, in review). It is difficult to isolate the contributions of each of these to changes in thicknesses of eolianites. Sand supply may change with proximity to source, likely a beach in carbonate eolianites. Vegetation may reduce transport capacity as well as sand supply. Deposition is favored in paleotopographic lows because of flow deceleration as flow expands vertically in a setting with accumulation space (Wilson, 1973; Kocurek, 1988, 1991; Kocurek and Halvholm, in review). Paleotopography may result from differential deposition, as in oolite shoal development, or from erosion associated with subaerial exposure surfaces. If paleotopography is the main factor controlling the thickness of eolian units, it might be useful in explaining the distribution of ooid-grainstone reservoirs in underlying strata. Oolite thickness appears inversely proportional to quartzose grainstone thickness in the Big Bow Field in Stanton and Grant Counties, Kansas (cf. Handford and Francka, 1991, their Fig. 9).

Quartz content of quartzose grainstone units varies laterally. This may reflect a transition from carbonate-rich coastal dunes to more quartz-rich continental deposits. Semeniuk and Glassford (1988) report such a transition from the Quaternary of the Perth basin, southwestern Australia, where carbonate-rich detached parabolic dunes were deposited as isolated limestone lenses in siliciclastic-rich continental deposits. This would account for the apparent isolated nature of many quartz-poor carbonates observed on log cross sections.

A thin quartzose grainstone that is apparently laterally discontinuous occurs in the middle Stevens Member in Shallow Water #4 Maune (sec. 31, T21S, R33W, Finney County, Appendix 1, Pocket Enclosure I-I'). The lower contact of this unit was not cored. This deposit contains approximately three percent detrital quartz. Coarsening-

Reproduced with permission of the copyright owner. Further reproduction prohibited without permission.

upward climbing translatent stratification indicate an eolian origin.

SUMMARY

Ten lithofacies are recognized in the St. Louis and Ste. Genevieve cores examined in this study. Depositional environments for each facies include: 1) restricted-shelf peloid grainstone/packstone; 2) shallow-subaqueous anhydrite; 3) evaporite solution-collapse breccia; 4) dolomite from dolomitization of limestone, generally restricted shelf; 5) restricted-shelf lime mudstone; 6) subtidal to lower intertidal, restricted-shelf algal boundstone; 7) marine-shelf skeletal packstone/wackestone; 8) oolite shoal deposits of ooid grainstone/packstone; 9) tidal-flat fenestral packstone/wackestone; and 10) eolian quartzose grainstone.

Reproduced with permission of the copyright owner. Further reproduction prohibited without permission.

CHAPTER 4
Stratigraphy

INTRODUCTION

Ooid grainstones in the St. Louis and Ste. Genevieve Limestones are important hydrocarbon reservoirs. Despite the economic importance, the lithostratigraphy of these units in southwestern Kansas has not been updated since the work of Goebel (1968), Thompson and Goebel (1968), and Maples (1992). Ste. Genevieve and St. Louis strata of the Illinois basin and southwestern Kansas share many similarities; however, differences between the two areas exist. Lithologic similarities and entrenched usage in the literature and in the petroleum industry warrant continued use of these formational names in Kansas. Updated facies descriptions and standardized stratigraphic terminology are needed to increase our understanding of the depositional history for the St. Louis and Ste. Genevieve Limestones.

The St. Louis is subdivided into the Hugoton and Stevens Members. These members are being proposed as new lithostratigraphic units (Abegg, in press (b)). A reference section for the Ste. Genevieve Limestone in southwestern Kansas is also being proposed (Abegg, in press (b)). The Hugoton Member is the lower member and is dominantly composed of restricted-shelf facies. The overlying Stevens Member is predominantly normal-marine facies. In the Illinois basin, informal members are lithologically somewhat similar (Jorgenson and Carr, 1973).

The core from Mobil #1 Foster (sec. 5, T34S, R36W, Stevens County, 6 mi southeast of Hugoton, Kansas) is proposed as the type section for the Hugoton and Stevens Members of the St. Louis Limestone and as a reference section for the Ste. Genevieve Limestone. The core is designated as the type and reference section because neither the Ste. Genevieve nor the St. Louis crop out anywhere in the state. The Foster

Reproduced with permission of the copyright owner. Further reproduction prohibited without permission.

core facies are representative of these lithostratigraphic units over most of the Hugoton embayment of southwestern Kansas.

The Mobil #1 Foster core contains 285 ft (87 m) of the Hugoton and Stevens Members of the St. Louis as well as the Ste. Genevieve (6625 to 6910 ft). The core is currently housed at the Kansas Geological Survey core facility in Lawrence, Kansas. The base of this core was incorrectly identified as Salem on the scout card and by Abegg (1991). Stratigraphic cross sections indicate the basal 56 ft of the core is the carbonate unit between the E1 and E2 evaporite of the Hugoton Member. Log depths and core depths are approximately coincident (Fig. 4.1). Neither the Salem-St. Louis nor the Ste. Genevieve-Shore Airport Formation boundaries were cored. In addition to stratigraphic completeness, this core was selected because it is available to the general public and contains facies representative of these lithostratigraphic units over much of the Hugoton embayment.

The type section of the Hugoton Member does not contain the Salem-St. Louis boundary. Principle reference cores, therefore, are needed to facilitate recognition of this boundary. The lower boundary of the Hugoton Member is cored in the Atlantic #1 Mark A, sec. 28, T20S, R33W, Scott County, Kansas (Thompson and Goebel, 1968), and is currently housed at the Kansas Geological Core Facility in Lawrence, Kansas. Amoco #1 Nordling and Amoco #3 Wilson A (Appendix 1) cores also contain the Salem-St. Louis boundary and are currently housed at Amoco's core facility in Denver, Colorado.

LITHOSTRATIGRAPHIC UNITS

Salem Limestone

The Salem Limestone is not present in the Mobil #1 Foster core and has only been examined in two cores. The upper Salem strata in cores of the Amoco #1 Nordling and Amoco #3 Wilson A consists of cyclic, shoaling-upward marine limestones.

Reproduced with permission of the copyright owner. Further reproduction prohibited without permission.

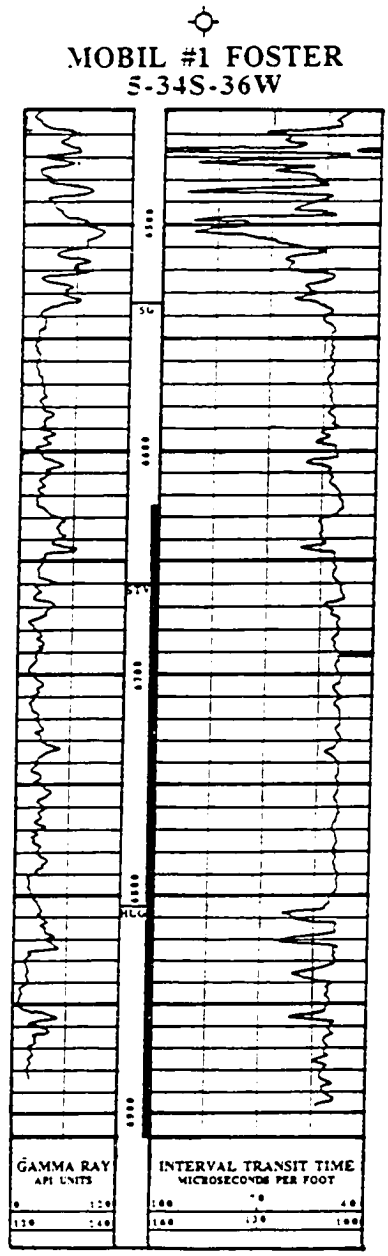


Figure 4.1 Gamma ray-sonic log from the Mobil #1 Foster (sec. 5, T34S, R36W), Stevens County, Kansas. Lithostratigraphic boundaries are picked from a combination of core studies and cross-section correlations (SG, Ste. Genevieve; STV, Stevens Member of the St. Louis Limestone; HUG, Hugoton Member of the St. Louis Limestone). Shore Airport (Chesterian) overlies the Ste. Genevieve. Note the extremely clean gamma ray response of the E1 anhydrite (6854-6842 ft). Cored interval is indicated in depth track. Core and log depths are approximately equal. Depths in feet.

Reproduced with permission of the copyright owner. Further reproduction prohibited without permission.

Lithologically it is similar to the Salem in the western part of the Illinois basin (cf. Cluff, 1984). The uppermost part of the Salem in the Hugoton embayment is commonly a high-energy oolitic or skeletal grainstone that has up to 15 percent intergranular porosity. Salem carbonates are commonly partially to completely dolomitized. Locally the Salem contains nodular chert. The uppermost Salem is recognized on gamma-ray/porosity logs as a clean, porous, slightly dolomitic grainstone, representing the uppermost shoal facies (Figs. 2.2 and 2.14). This grainstone is not extensively dolomitized because dolomite preferentially replaces micrite.

St. Louis Limestone

Hugoton Member of the St. Louis Limestone.– Strata of the Hugoton Member consist primarily of six lithologies: 1) peloid grainstone/packstone, 2) dolomite, and 3) anhydrite, 4) breccia, 5) lime mudstone, and 6) algal boundstone. Oolitic grainstone/packstone and skeletal packstone/wackestone occur locally and are best developed in the carbonate unit between the E1 and E2 evaporites. In the eastern and northern parts of the Hugoton embayment, typical lithologies of the Hugoton Member are brecciated (Fig. 2.1) and member designation is more difficult on wireline logs alone. Hugoton strata yield moderately low gamma-ray values with minor shale kicks. Crossover of the neutron-density curves with lower porosity on the density log than on the neutron log, a reflection of dolomitization, is characteristic (Figs. 2.2 and 2.14). Anhydrite produces very low gamma ray values and negative porosity on the density log (Fig. 2.2).

Stevens Member of the St. Louis Limestone.– The Stevens Member of the St. Louis is composed primarily of skeletal packstone and wackestone that contain shoaling-upward cycles capped by thin oolitic and skeletal grainstone and packstone.

Reproduced with permission of the copyright owner. Further reproduction prohibited without permission.

Oolitic caps are typically thicker in the uppermost Stevens Member. A thin quartzose grainstone unit, typically 2-5 ft (0.6-1.5 m) thick, in the Stevens Member is laterally traceable in core over much of southwestern Kansas and is commonly interbedded with porous oolitic grainstones. However, this unit is commonly too thin to be easily resolved on neutron-density logs. This quartzose grainstone is 46 to 56 ft (14.0 to 17.1 m) below the St. Louis-Ste. Genevieve boundary in Stevens County. To the north of Stevens County, this thin quartzose grainstone unit is 1 to 27 ft (0.3-8.2 m) below the St. Louis-Ste. Genevieve boundary. It is placed in the St. Louis, however, because it is very thin and is not easily recognizable on logs. On gamma ray logs, the upper St. Louis is a relatively clean limestone. Neutron and density log traces are nearly coincident (Figs. 2.2 and 2.14), indicating the Stevens Member is a relatively pure limestone with only minor chert, dolomite, and detrital quartz.

Ste. Genevieve Limestone

Intercalated quartzose grainstone, ooid grainstone and packstone, peloid grainstone and packstone, and skeletal packstone and wackestone characterize the Ste. Genevieve Limestone. Quartzose grainstone is typically tight and has low gamma-ray values and slightly lower neutron porosity than density porosity (Figs. 2.2 and 2.14). Ooid grainstones are typically porous (porosity locally exceeding 10 percent) and have low gamma-ray values. Skeletal packstone and wackestone and peloid grainstone and packstone are typically tight and have moderately low gamma-ray values and slightly higher neutron porosity than density porosity (Pocket Enclosure I-I'), characteristic of argillaceous limestone.

Shore Airport Formation

The overlying Shore Airport Formation (Abegg, in press (a)) consists primarily of

Reproduced with permission of the copyright owner. Further reproduction prohibited without permission.

argillaceous peloidal packstone and thin interbedded calcareous shales. In the Amoco #1 Breeding F, these shale beds are paleosol horizons, with clay concentrated in the B soil horizon (Abegg, in press (a)). Shales are variegated red, green, and purple and contain rhizoliths. The Shore Airport includes a local basal sandstone and conglomerate (Clair, 1948, 1949; Veroda, 1959; Fugitt and Wilkinson, 1959). Fossiliferous marine oolite (Clair, 1948, 1949) and argillaceous, fossiliferous marine limestone are also found in the Shore Airport (e.g., Anadarko #2 Etzold B, sec. 22, T33S, R34W). Logs of Shore Airport strata typically have moderate gamma-ray values and relatively higher neutron porosity than density porosity (Figs. 2.2 and 2.14), characteristic of argillaceous limestones.

LATERAL VARIABILITY

Vertical successions of lithologies are similar within the St. Louis and Ste. Genevieve Limestones occur over much of the Hugoton embayment. Log cross sections, calibrated by cores, permit characterization of lateral variability in facies and composition across southwestern Kansas.

Anhydrite, characteristic of the Hugoton Member of the St. Louis Limestone, is preserved in portions of Morton, Stanton, Stevens, Grant, Seward, Haskell, Hamilton, Kearny, and possibly Meade Counties, southwestern Kansas (Figs. 2.1, 2.6, and 2.7). Many anhydrite units are laterally correlative over several counties, but some are discontinuous (Figs. 2.6 and 2.7). Anhydrite is thin in southern Stevens County and is absent in southern Morton, southwestern Stevens, and southern Seward Counties (Fig. 2.1). To the north and east recognition of characteristic anhydrite and slightly argillaceous dolomitic carbonate on wireline logs is difficult because of brecciation (Fig. 2.1 and 2.14).

The Stevens Member of the St. Louis Limestone consists largely of normal-marine

Reproduced with permission of the copyright owner. Further reproduction prohibited without permission.

skeletal packstone and wackestone in southwestern Kansas. Ooid grainstones are thickest near the top of the Stevens Member. A thin quartzose grainstone is interstratified with oolitic grainstone and packstone in the Stevens Member (Appendix 1). This unit is very close to the base of the Ste. Genevieve in most cores, but in Stevens County it is separated by a thicker section of subtidal strata.

Porous oolitic grainstones occur in many areas, but no regional trend has been recognized. Based on the location of oolite reservoirs, Handford (1988) concluded that oolite bodies are oriented northwest-southeast. Because these fields roughly parallel the Central Kansas uplift, Handford reasoned oolites developed parallel to depositional strike and are similar to Bahamian marine sand belts (Ball, 1967). However, local structure and diagenesis may also contribute to oolite reservoir distribution. Moreover, Youle (1990, his Fig. 1) indicates a northeast-southwest orientation of Stevens Member oolites in the Wendel Pool in Gray County, Kansas. Additional work is needed to determine the controls on distribution of porous ooid grainstones in the Stevens Member of the St. Louis.

Quartzose grainstones interbedded with peloidal, oolitic, or skeletal carbonates comprise the Ste. Genevieve Limestone. As many as four quartzose grainstone units are recognized in the Ste. Genevieve in core. In some wells, quartzose grainstone is either poorly developed, absent, or simply not recognizable in the logs. This suggests that quartzose grainstone units are discontinuous or that quartz content is variable. Handford and Francka (1991, their Fig. 11) illustrate quartz-poor and quartzose grainstones. Minor detrital quartz occurs in many interbedded peloidal and skeletal carbonates; some contain as much as 40 percent quartz. The presence of quartz in other facies, combined with the absence of significant quartz in some Ste. Genevieve sections, make tracing of individual quartzose grainstones extremely difficult. This emphasizes the need for core to facilitate correlation. No consistent regional trends in quartz concentration have been recognized.

Reproduced with permission of the copyright owner. Further reproduction prohibited without permission.

LITHOSTRATIGRAPHIC BOUNDARIES

In order to facilitate consistent identification of Upper Mississippian lithostratigraphic boundaries, criteria for such picks need to be standardized. Facies changes make identification of Upper Mississippian units difficult locally. Facies changes are difficult to recognize unless core or cuttings are utilized. In this report, 13 cores covering much of the southern Hugoton embayment are used to calibrate log response to facies (Pocket Enclosure I-I'). This section discusses lithostratigraphic boundaries between the: 1) Salem Limestone, 2) Hugoton Member of the St. Louis Limestone, 3) Stevens Member of the St. Louis Limestone, 4) Ste. Genevieve Limestone, and 5) Shore Airport Formation (Fig. 1.4).

Salem-St. Louis Boundary

In core, the Salem-St. Louis boundary is marked by a change from ooid-skeletal grainstones of the Salem to algal boundstone (Amoco #1 Nordling) and breccia (Amoco #1 Wilson) of the Hugoton Member of the St. Louis. On wireline logs, the exact placement of the boundary is difficult as both units are typically dolomitic. It is commonly possible to recognize a change from clean, porous dolomitic limestone of the upper Salem to slightly more argillaceous, dolomitic carbonate intercalated with anhydrite in the Hugoton (Figs. 2.2 and 2.14). Cored breccias in the Hugoton Member consist of dolomitic carbonates that are typically less porous than the underlying Salem. Breccias can also be differentiated from the Salem using the gamma-ray log; cross-stratified upper Salem grainstones are typically clean, whereas low-energy, dolomitic carbonates and breccias of the Hugoton Member are typically somewhat shaly.

Reproduced with permission of the copyright owner. Further reproduction prohibited without permission.

Hugoton Member-Stevens Member Boundary

The boundary of the Hugoton and Stevens Members of the St. Louis is commonly placed at the change from dolomitic carbonate and anhydrite to skeletal packstone/wackestone (Figs. 2.2 and 2.14, Appendix 1). This facies transition is commonly marked by a thin (≤ 3 ft) skeletal-ooid grainstone to packstone. Typical logs of the Hugoton Member indicate lower neutron porosity than density porosity, indicating dolomitic carbonates (Figs. 2.2 and 2.14). Interbedded anhydrites have very low gamma-ray values and negative density porosities (Fig. 2.2). In the Stevens Member the density and neutron curves are nearly coincident, indicating relatively pure limestones (Figs. 2.2 and 2.14).

St. Louis-Ste. Genevieve Boundary

In southwestern Kansas, previous authors place oolitic limestones in the St. Louis Limestone (e.g., Clair, 1948, 1949; Thompson and Goebel, 1963, 1968). In the Illinois basin, however, the base of the Ste. Genevieve is generally placed at the stratigraphically lowest prominent oolitic limestone (Atherton et al., 1975). In order to be consistent with the original definition in the type area, a similar boundary could be adopted in the Hugoton embayment. However, several considerations argue against such a boundary.

The base of the stratigraphically lowest prominent oolite is difficult to pick without core or cuttings. Although many of the ooid grainstones are porous, intergranular porosity is occluded in many others by a combination of compaction and cementation, as in the Mobil #1 Foster. In wells without porous carbonates, this formation boundary would not be easily determined from wireline logs. Additionally, including oolites in the St. Louis in the Hugoton embayment is so entrenched by usage in industry and the literature that it is best not to change unless a more practical boundary

Reproduced with permission of the copyright owner. Further reproduction prohibited without permission.

can be determined.

The base of the Ste. Genevieve is herein placed at the stratigraphically lowest prominent quartzose grainstone. In order of decreasing reliability, the four most dependable ways to pick the St. Louis-Ste. Genevieve boundary in wireline logs include: 1) at the change from coincident neutron and density logs to a log crossover with lower neutron than density porosity, 2) at an uphole negative shift in the photoelectric (Pe) curve, 3) at an uphole positive shift in the interval transit time on sonic logs, and 4) at the top of the highest porous ooid grainstone. In many areas, the quartzose Ste. Genevieve is marked by a prominent crossover of the neutron and density log patterns, both calibrated for limestone (Figs. 2.2 and 2.14) and also by shifts in the Pe and sonic logs. Where quartzose facies are absent or poorly developed, the Ste. Genevieve-St. Louis boundary can be placed at the base of a small positive gamma-ray shift immediately above the uppermost porous, presumably oolitic, limestone.

Ste. Genevieve-Shore Airport Boundary

The boundary between the Ste. Genevieve and the Shore Airport is one of the most consistent picks in the Mississippian section because of the increased argillaceous component in the Shore Airport. This boundary should be placed where neutron porosity lower than density porosity in the quartzose Ste. Genevieve changes to neutron porosity greater than lower density porosity in the argillaceous carbonates of the Shore Airport (Fig. 2.2, 2.14, and 4.1). This boundary typically corresponds to the base of a shale observable on the gamma ray log. Locally, however, the basal Shore Airport is sandstone. In this case, the Shore Airport neutron-density logs are similar to those of the Ste. Genevieve, but the sandstone typically has higher porosity than the tight quartzose grainstone (e.g., Southland #1-19 Hampton, sec. 19, T34S,

Reproduced with permission of the copyright owner. Further reproduction prohibited without permission.

R34W, Pocket Enclosure A-A'). In sonic logs, the top of the Ste. Genevieve is marked by low velocity of the first prominent shale bed.

Mississippian-Pennsylvanian Boundary

The Mississippian-Pennsylvanian boundary in southwestern Kansas is a highly erosional disconformity (e.g., Thompson and Goebel, 1968). Upper Mississippian strata in southwestern Kansas are overlain by the Kearny Formation (Morrowan). To the north and east, however, the Upper Mississippian is overlain by the "Gray group" (cf. Youle, 1991) and the Cherokee Group (Desmoinesian) (Goebel and Stewart, 1979).

The Kearny Formation consists of interbedded shales, sandstones, and carbonates (McManus, 1959; Swanson, 1978). The lower Kearny consists of shales interbedded with dolomitic calcareous sandstones and dolomitic arenaceous carbonates (McManus, 1959). Reworked Mississippian lithoclasts are common at the base of the Pennsylvanian. These conglomerates are interpreted as a transgressive lag that formed as the seas flooded the previously subaerially exposed shelf (cf. Youle, 1991). Log signatures of dolomitic sandstones and carbonates typically have low gamma-ray values and higher density porosity than neutron porosity.

The contact of the Kearny and Shore Airport Formations is locally difficult to place. Character of this boundary is variable because of the highly erosional unconformity that separates Mississippian and Pennsylvanian strata. Additionally, lower Kearny sandstones and carbonates are locally difficult to resolve from argillaceous limestones of the Shore Airport (McManus, 1959). The Kearny commonly contains significantly more shale and sandstone than the underlying Shore Airport.

In the eastern and northern Hugoton embayment, the Shore Airport is directly overlain by carbonates and thin shales of the Atokan? "Gray group"(Youle, 1991) (e.g., Pendleton #1 Schauf, sec. 16, T27S, R29W, Gray County) or siliciclastics of

Reproduced with permission of the copyright owner. Further reproduction prohibited without permission.

the Desmoinesian Cherokee Group (e.g., Alma #1 Watchorn, sec. 13, T15S, 33W, Logan County). "Gray group" carbonates are commonly less argillaceous and the shales are more radioactive than are the limestones and shales of the underlying Shore Airport. This produces more contrast in "Gray group" gamma-ray log signatures relative to the Shore Airport. In cases where the Shore Airport has been eroded (Fig. 1.1), the Ste. Genevieve or the St. Louis are directly overlain by Morrowan, Atokan, or Desmoinesian strata. The increased siliciclastic component of Pennsylvanian strata makes this an reliable log pick in many areas because Pennsylvanian strata typically have higher gamma-ray log values (Figs. 2.2 and 2.14).

CONODONT BIOSTRATIGRAPHY

Conodont biostratigraphy has been extensively used in conjunction with lithostratigraphic studies of Mississippian strata in Kansas (e.g., Thompson and Goebel, 1963, 1968). Definition of lithostratigraphic boundaries should be independent of biostratigraphic zones. Formations are rock-stratigraphic units defined by lithofacies. Conodont data, however, are useful in several ways. Comparison of conodont fauna from a correlative lithofacies on different parts of the shelf can indicate diachroneity, if resolution is sufficient. Conodont data are useful in comparison of lithofacies from different basins, for example to test whether St. Louis and Ste. Genevieve strata are roughly coeval in the Hugoton embayment and the Illinois basin. Thompson and Goebel (1968, p. 19) report that St. Louis and Ste. Genevieve strata in Kansas are "synchronous with the equivalent formations in the Mississippi River Valley" region based on conodonts. In addition, conodont biostratigraphy can help constrain lithostratigraphic correlations. Biostratigraphy combined with regional correlations indicates that the base of Mobil #1 Foster was not in the Salem as reported on the scout card (Abegg, 1991), but is instead the porous carbonate between the

Reproduced with permission of the copyright owner. Further reproduction prohibited without permission.

Hugoton Member E1 and E2 anhydrite.

The influence of environmental factors on conodont distribution is a concern in biostratigraphy. This concern is minimized in correlating between similar depositional settings. The general coincidence of Mississippian biostratigraphic and lithostratigraphic boundaries in Kansas (Thompson and Goebel, 1968) suggests that facies dependency is a strong possibility or that diachroneity of facies boundaries is lacking.

Samples from the base of the Mobil #1 Foster core contain both *Taphrognathus* and *Cavusgnathus* (Table 4.1). In the type area, the lower St. Louis corresponds to the upper part of the *Taphrognathus varians-Apatognathus*? (Warsaw Formation to lower St. Louis Limestone) zone (Collinson et al., 1971). The upper St. Louis corresponds to the *Apatognathus scalenus-Cavusgnathus* (upper St. Louis) zone (Collinson et al., 1971). The boundary between these zones is distinguished by the earliest occurrence of common *Cavusgnathus* and *Apatognathus*, and the last occurrence of *Taphrognathus* (Collinson et al., 1971). The exact location of this biostratigraphic boundary in the Foster core is uncertain. Judging by more reliable first occurrences, the lower-upper St. Louis biostratigraphic boundary in the Mobil #1 Foster core is somewhere in the upper part of the Hugoton Member. In the type area, the St. Louis-Ste. Genevieve lithostratigraphic boundary corresponds to the base of the *Gnathodus bilineatus-Cavusgnathus charactus* zone (Ste. Genevieve Limestone to Cypress Sandstone) (Collinson et al., 1971). The lower boundary of this zone is marked by the last common occurrences of *Apatognathus* and *Spathognathodus scitulus* (Collinson et al., 1971). Above the quartzose grainstone at the base of the Stevens Member, these conodonts are absent, suggesting the quartzose grainstone (6710 ft core depth) approximates the base of the *Gnathodus bilineatus-Cavusgnathus charactus* zone. No conodonts were recovered from the Ste. Genevieve of the Foster core because most

Reproduced with permission of the copyright owner. Further reproduction prohibited without permission.

Table 4.1. Conodonts recovered from the Mobil #1 Foster (sec. 5, T34S, R36W) in Stevens County, Kansas. Formation and member boundaries determined by facies, independently of biostratigraphy. Conodont identification by Richard Lane of Amoco.

DEPTH (FT)/IDENTIFICATION	NO.
6909-6910.0	
Cavusgnathus altus	1
Taphragnathus 23360	3
Spathognathodus eoscitulus	1
Indeterminant conodonts	17
6906-6907	
Apatognathus n. sp. A.	5
Cavusgnathus altus	1
Taphrognathus 23360	2
Taphrognathus varians	2
Spathognathodus penescitulus	1
Spathognathodus eoscitulus	1
Indeterminant conodonts	21
6902-6903	
Taphragnathus 23360	5
Cavusgnathus unicornis	2
Apatognathus n. sp. a	2
Spathognathodus penescitulus	1
Indeterminant conodonts	12
6888-6889	
Taphragnathus 23360	1
Apatognathus n. sp. a	1
Indeterminant conodonts	10
6878	
Indeterminant conodonts	2
6825	
Indeterminant conodonts	3
6815	
Apatognathus geminus	3
Apathognathus porcatus	1
Cavusgnathus unicornis	1
Taphragnathus 23360	2
Spathognathodus penescitulus	1
Indeterminant conodonts	26
6811.5-6812.5	
Barren of conodonts	
6806.5-6807.5	
Taphrognathus 23360	1
Indeterminant conodonts	7
Top of the Hugoton Member (6804 ft)	
6803-6804	
Apatognathus geminus	3
Cavusgnathus unicornis	4
Cavusgnathus altus	3
Spathognathodus scitulus	4
Spathognathodus cristulus	2
Indeterminant conodonts	14
6790-6791	
Spathognathodus scitulus	4
Apatognathus geminus	4
Apathognathus porcatus	1
Indeterminant conodonts	11
6783-6784.5	
Spathognathodus penescitulus	1
Taphrognathus 23360	1
Cavusgnathus sp.	1
Indeterminant conodonts	5
6772	
Indeterminant conodonts	5
6761-6762.5	
Barren of conodonts	
6752.5-6753.5	
Spathognathodus penescitulus	2
Indeterminant conodonts	7

DEPTH/IDENTIFICATION	NO.
6743.5-6744.5	
Barren of conodonts	
6740-6741	
Cavusgnathus altus	1
Cavusgnathus sp.	1
Spathognathodus cristulus	2
Indeterminant conodonts	18
6737.0	
Barren of conodonts	
6732-6733	
Magnilateralla robusta	1
6729.0-6730	
Ligonodina levis	1
6722.5-6723.5	
Spathognathodus scitulus	1
Gnathoduscommutatus commutatus	1
Cavusgnathus altus	1
Magnilateralla robusta	2
Apathognathus porcatus	1
Indeterminant conodonts	19
6713-6714	
Cavusgnathus altus	2
Indeterminant conodonts	6
6710-6711	
Cavusgnathus unicornis	1
Indeterminant conodonts	10
6699-6700	
Cavusgnathus unicornis	1
Indeterminant conodonts	3
6690	
Barren of conodonts	
6686.0	
Barren of conodonts	
6662.5-6663.5	
Cavusgnathus unicornis	1
Cavusgnathus offset	1
Inderterminant conodonts	4
6661-6662	
Cavusgnathus unicornis	2
Cavusgnathus sp.	2
Neopriontiodus sp.	1
Ligonodina sp.	2
Inderterminant conodonts	18
Top of the Stevens Member (6660 ft)	
6649-6650	
Barren of conodonts	
6643	
Barren of conodonts	
6640-6641	
Barren of conodonts	
6632-6633	
Barren of conodonts	

Reproduced with permission of the copyright owner. Further reproduction prohibited without permission.

samples were taken from restricted shelf facies that are generally barren of fossils. Conodonts from Mobil #1 Foster indicate that lithostratigraphic boundaries in southwestern Kansas are roughly synchronous with equivalent formations in the Illinois basin.

SUMMARY

1. The Hugoton Member of the St. Louis is dominated by peloid grainstone/packstone, anhydrite, breccia, lime mudstone, dolomite, and algal boundstone facies. Strata of the Hugoton Member are distinct from the ooid-skeletal grainstones of the upper Salem Limestone.

2. The Stevens Member of the St. Louis is typically skeletal packstone/wackestone with shoaling-upward cycles capped by oolitic grainstones and packstones. A thin quartzose grainstone commonly occurs near the top of the St. Louis Member in many areas. Stevens Member strata are distinct from dolomitized carbonate and anhydrite of the Hugoton Member.

3. Ste. Genevieve strata are typified by quartzose grainstone interbedded with oolitic and peloid grainstone and packstones, and skeletal packstone and wackestone. The base of the Ste. Genevieve is placed at the base of the stratigraphically lowest quartzose grainstone. Ste. Genevieve strata are distinct from interbedded argillaceous limestones and shales of the overlying Shore Airport Formation.

Reproduced with permission of the copyright owner. Further reproduction prohibited without permission.

CHAPTER 5

Sequence Stratigraphy

INTRODUCTION

Regional characterization of St. Louis and Ste. Genevieve depositional sequences will increase understanding of Late Mississippian shelf sedimentology and paleogeography, Late Mississippian sea-level history, and sequence stratigraphy in carbonates. Division of the St. Louis and Ste. Genevieve into sequences is useful in hydrocarbon exploration to help predict the relationships of roughly coeval facies. The sequence stratigraphic framework proposed for southwest Kansas can be extended to adjacent areas and allows comparison to more distant regions.

Sequence stratigraphy methodology (e.g., Vail et al., 1977; Sarg, 1988; Van Wagoner et al., 1990) is useful in determining time and rock relationships. Sequence boundary unconformities elucidate chronostratigraphy because they separate younger from older strata. Sequence boundaries subdivide these strata into depositional sequences composed of genetically related strata. Sequence stratigraphic frameworks provide more predictability of facies distributions than traditional lithostratigraphic or biostratigraphic approaches. Lithostratigraphy stresses subdivision by facies that may or may not have chronostratigraphic significance. Biostratigraphy may lack the resolution of sequence stratigraphy, as in the Upper Mississippian (cf. Sando, 1985). Sequence stratigraphy has evolved an extensive set of definitions (Table 5.1).

St. Louis and Ste. Genevieve strata are subdivided into seven depositional sequences (S1 through S7); the upper sequence boundaries are designated SB1 through SB7 (Pocket Enclosure J). Sequences S1 through S3 are within the St. Louis, and S4 through S7 are within the Ste. Genevieve. These sequences are readily recognized in cores, but are locally difficult to identify in well logs, making detailed correlation of

Reproduced with permission of the copyright owner. Further reproduction prohibited without permission.

Table 5.1. Definitions of sequence stratigraphic terms used in this report.

Sequence - "A relatively conformable succession of genetically related strata bounded by unconformities and their correlative conformities" (Van Wagoner et al., 1988, p. 39).

Sequence boundary - "An unconformity and its correlative conformity; it is a laterally continuous, widespread surface covering at least an entire basin..." (Van Wagoner et al., 1990, p. 30).

Type 1 sequence boundary - "Characterized by subaerial exposure and concurrent subaerial erosion associated with stream rejuvenation, a basinward shift in facies, a downward shift in coastal onlap, and onlap of overlying strata" (Van Wagoner et al., 1988. p. 41).

Type 2 sequence boundary - "Marked by subaerial exposure and a downward shift in coastal onlap landward of the depositional-shoreline break; however, it lacks both subaerial erosion associated with stream rejuvenation and a basinward shift in facies" (Van Wagoner et al., 1988, p. 42).

Sequence set - "A set of sequences arranged in a distinctive progradational, aggradational, or retrogradational stacking pattern" (Mitchum and Van Wagoner, 1991, p. 142).

Parasequence - "A relatively conformable succession of genetically related beds or bedsets bounded by marine-flooding surfaces and their correlative surfaces" (Van Wagoner et al., 1988, p. 39).

Transgressive surface - "The first significant marine-flooding surface across the shelf within the sequence" (Van Wagoner et al., 1988, p. 44).

Reproduced with permission of the copyright owner. Further reproduction prohibited without permission.

sequences problematical in some areas.

The following sections describe and interpret St. Louis and Ste. Genevieve depositional sequences and sequence boundaries. Identification of systems tracts (cf. Van Wagoner et al., 1988) is not feasible as many parts of these strata do not easily fit into currently defined system tracts.

EVIDENCE FOR SEQUENCE BOUNDARIES

In the basal Stevens Member in southwestern Kansas, evaporites are interpreted to have formed as a result of a relative sea level fall that exposed a shoal to the south, creating extremely restricted conditions in a back-barrier lagoon. Autocylcic shoaling of carbonates probably would not produce a barrier laterally extensive enough to allow for gypsum precipitation. Oolites and stromatolites in the Hugoton Member also indicate very shallow-water conditions. Therefore, evaporite deposition probably correlates to an unconformity toward the Transcontinental arch. The exact location of SB1, however, is problematical as strata are relatively conformable on this part of the shelf (i.e. type 2 sequence boundary). The base of the oolite records the incursion of marine water as sea level rose and is tentatively identified as SB1. However, SB1 could also be reasonably located lower in the Hugoton Member or at the top of the E1 anhydrite.

SB2 through SB6 are recognized by evidence of subaerial exposure and by basinward shifts in facies (cf. Van Wagoner et al., 1988). SB7 was not observed in core. Subaerial exposure in SB2 through SB6 is indicated by calcretes with rhizoliths (paleosols), vadose cements, negative shifts in whole-rock $\delta^{13}C$ (Chapter 6), and lithoclast conglomerates with reworked calcrete clasts that are overlain by eolianites. Eolianites rest directly on subtidal strata, such as skeletal packstones and wackestones, without intervening beach or tidal-flat deposits; these relationships indicate subaerial

Reproduced with permission of the copyright owner. Further reproduction prohibited without permission.

exposure was a result of a fall in relative sea level. Lithoclasts at the base of some eolianites indicate at least minor erosion, but it is unlikely that erosion completely removed beach or tidal-flat deposits beneath each eolian unit. Eolian deposits overlying subtidal strata reflects a basinward shift in facies, a characteristic of sequence boundaries. Subaerial exposure, therefore, was not the result of a localized highstand aggradation of carbonates above sea level.

ST. LOUIS SEQUENCES

Sequence 1

The first depositional sequence in the St. Louis (S1) consists of at least part of the Salem Limestone and most of the Hugoton Member; only the upper part has been observed in core. This sequence is up to 213 ft (64.9 m) thick. The top of the Salem in many cores is a relatively thick, porous, ooid to skeletal grainstone that is cross stratified locally (e.g., Amoco #3 Wilson A). Deposition of anhydrite, dolomitic peloidal carbonate, dolomitic lime mudstone, and algal boundstone of the Hugoton Member record the onset of restricted conditions. Basinward progradation of high-energy grainstone shoals of the upper Salem combined with a relative sea-level fall severely restricted circulation over much of western Kansas (Figs. 2.1 and 5.1). E1 and E2 evaporites are separated by porous dolomitic carbonate that contains ooid or skeletal grainstones and packstones (Figs. 2.2, 2.6 and 2.7). These strata are interpreted as a minor flooding of the shelf by marine waters that temporarily ended evaporite deposition. Most S1 strata, upper Salem and Hugoton Member, are interpreted as deposition in southward prograding shoal and back-barrier lagoon environments.

The exact location of SB1 is problematical as strata are relatively conformable on this part of the shelf. SB1 is tentatively placed at the top of Hugoton Member in

Reproduced with permission of the copyright owner. Further reproduction prohibited without permission.

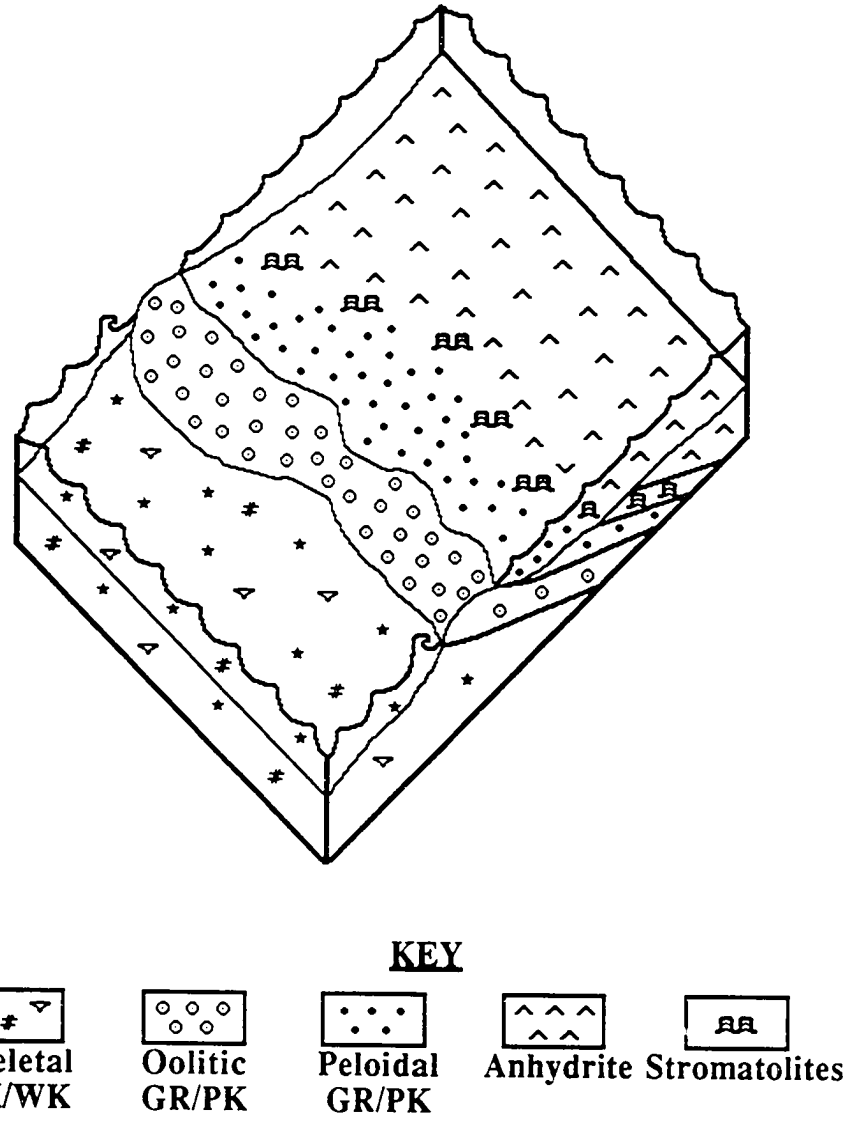


Figure 5.1 Block diagram of depositional environments of the upper Salem and Hugoton Member of the St. Louis. Oolitic shoals combined with a fall in relative sea level restricted marine circulation enough to precipitate gypsum but not halite. Most evaporites are interpreted as extensive deposits of shallow lagoons (salterns). Diagnostic intertidal and supratidal features are rare. Stromatolites, interpreted to be largely subtidal in origin, occur in many Upper Mississippian cores and are interbedded with both anhydrite and subtidal strata. GR-grainstone; PK-packstone; WK-wackestone.

Reproduced with permission of the copyright owner. Further reproduction prohibited without permission.

southwestern Kansas (Fig. 5.2a). In solution-collapse breccias further north and east, SB1 is placed at the highest occurrence of restricted-shelf clasts. In Stanton County SB1 is located at or near the top of the E1 anhydrite. In Amoco #1 Puyear in Stanton County, E1 anhydrite is almost directly overlain by oolites that mark the flooding of the shelf by marine waters resulting in deposition of the overlying Stevens Member (Fig. 5.2a). To the south in Stevens County, the E1 anhydrite in Mobil #1 Foster is overlain by 22 ft (6.7 m) of restricted-shelf dolomite and minor skeletal packstone and grainstone (Fig. 5.2a). These restricted-shelf strata in Stevens County are probably lateral facies of the evaporite in Stanton County.

Alternatively, these restricted-shelf facies may correspond to nondeposition to the north (Fig. 5.2b). In this case, SB1 might be placed at the top of the E1 anhydrite, the initial working hypothesis for this sequence boundary (Abegg, 1991). The top of the E1 anhydrite is probably diachronous and, therefore, lacks chronostratigraphic significance.

The base of the E1 anhydrite is an additional alternative location for SB1. This would require that evaporites were deposited during a relative rise in sea level. Evidence supporting this location for SB1 includes a minor upward increase in carbonate bed thickness and a minor decrease in evaporite bed thickness (Figs. 2.6 and 2.7). Evaporite deposition would begin shortly after a fall in relative sea level that isolated the back-barrier lagoon. If a relative rise in sea level began after initiation of evaporite deposition, evaporite deposition could only continue by subaerial aggradation of carbonates. Aggradation of carbonates above sea level probably would not be continuous enough to permit restriction to continue. Moreover, subaerial carbonates facies, such as eolianites and tidalites, have not been identified in this position.

Additional work is needed to more accurately define the location of SB1.

The top of the E2 anhydrite might be considered as an additional sequence

Reproduced with permission of the copyright owner. Further reproduction prohibited without permission.

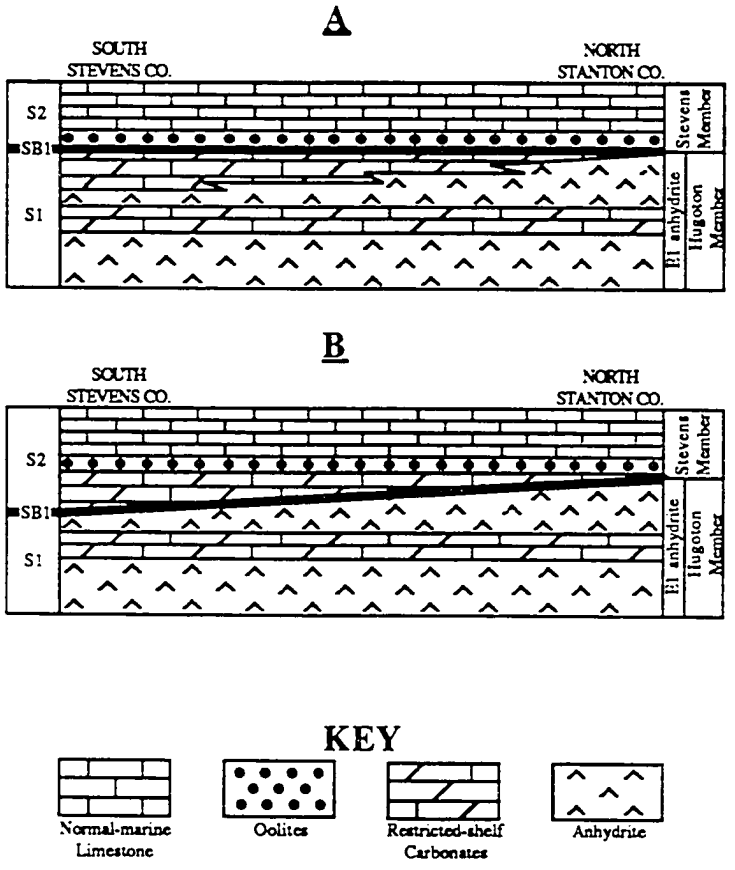


Figure 5.2 North-south schematic cross section of upper Hugoton and lower Stevens strata from Stanton to Stevens Counties. (A) The tentative location of SB1 is at the top of the Hugoton Member. (B) An alternative location of SB1 is at the top of the E1 anhydrite.

Reproduced with permission of the copyright owner. Further reproduction prohibited without permission.

boundary. Carbonates that divide the E1 and E2 anhydrites into two separate genetic units may represent a minor relative sea-level rise. These carbonates are similar to those between individual anhydrite beds, but are thicker (Figs. 2.6 and 2.7). The top of the E2 anhydrite and the overlying carbonates lack evidence of subaerial exposure. Until additional regional stratigraphic information is available, the top of the E2 anhydrite is interpreted as a parasequence boundary.

Sequence 2

The second sequence consists of most of the Stevens Member of the St. Louis. This sequence is thickest in southernmost Kansas where it is 116 ft (35.4 m) thick in Mobil #1 Foster (Appendix 1). S2 thins to the north possibly due to decreased accommodation space further up on the shelf, resulting from a lower tectonic subsidence rate or regional shelf slope. S2 is approximately 71 ft (21.6 m) thick in Alma #1 Watchorn (Appendix 1) based on an incomplete core and nearby log. A thin (≤ 3 ft) ooid-skeletal grainstone and packstone marking the base of the Stevens Member is interpreted as a transgressive deposit, representing the initial incursion of marine waters across the shelf during a relative sea-level rise. Most of the Stevens Member consists of normal-marine skeletal packstone and wackestone with minor shoaling-upward successions. Shoaling-upward cycles, parasequences, are typically capped by thin ooid-skeletal grainstone and packstone. Even where cores are closely spaced, parasequences are not easily correlated, suggesting possible autocyclicity. Caps of ooid-skeletal grainstone and packstone are thicker in the upper part of S2 where they are local reservoirs. The change from interbedded restricted shelf and normal-marine carbonate of S1 to a thin grainstone overlain by normal-marine limestone with mud-rich parasequences indicates that the lower part of S2 is a deepening-upward succession. The thicker grainstone caps on parasequences indicate that the upper part of S2 is a

Reproduced with permission of the copyright owner. Further reproduction prohibited without permission.

shoaling-upward succession. The maximum flooding surface that separates the upper and lower parts is not precisely located.

A thin eolian deposit occurs in the middle of the Stevens Member in Shallow Water #4 Maune (Appendix 1, Pocket Enclosure I-I'). The lower contact of this eolianite was not cored. This eolianite is interpreted as a local highstand accumulation of carbonates above sea level. Evidence for this includes apparent laterally discontinuity of the unit, paucity of detrital quartz (3 percent), and absence of evidence for subaerial exposure elsewhere within S2.

Calcrete with rhizoliths, vadose cements (upward-oriented and pendant), negative shifts in whole-rock $\delta^{13}C$ (Chapter 6), and lithoclast conglomerates with reworked calcrete clasts subadjacent to SB2 indicate this surface was subaerially exposed. This exposure surface can be recognized from southern Stevens County north possibly as far as Logan County (Pocket Enclosure J). Because this surface has not been traced south of Kansas, it is uncertain whether it is a type 2 sequence boundary or a type 1 with subaerial erosion and stream rejuvenation.

Sequence 3

Sequence 3 consists of the uppermost Stevens Member of the St. Louis Limestone. Typical thicknesses of S3 range from only 10 to 24 ft (3.0 to 7.3 m). In southernmost Stevens County, Kansas, however, S3 is 50 ft (15.2 m) thick in Mobil #1 Foster and 79 ft (24.1 m) in Mobil #1 Headrick. The increased thickness of S3 suggests greater accommodation in the southern Hugoton embayment, probably owing to greater tectonic subsidence rates or a regional shelf slope. Increased thickness of S3 to the south could also result from erosion of S2 strata beneath the unconformity. This is unlikely as small lithoclasts above SB2, comprised of the underlying lithology, suggest only minor erosion.

Reproduced with permission of the copyright owner. Further reproduction prohibited without permission.

The base of S3 is an eolian quartzose grainstone, typically deposited as a vegetated sand sheet (Abegg, 1991). This eolianite is only 2 to 5 ft (0.6 to 1.5 m) thick over much of the shelf. In most cases the thinness of this quartzose grainstone precludes recognition of this sequence boundary from wireline logs alone (cf. Pocket Enclosure I-I'). This lowermost eolianite is interpreted as a lowstand deposit because it overlies subtidal strata without transitions, demonstrating a fall in relative sea level. Deposition of eolianites during initial transgression is also possible. Encroachment of the shoreline would provide an abundant source of carbonate sediment and the concomitant water table rise would increase preservation potential. Eolianites are typically overlain by shallow subtidal oolitic or peloidal limestone. These oolites are extremely porous locally. The oolitic and peloidal subtidal strata thicken to the south in Stevens County where they are interbedded with normal-marine limestones containing up to three parasequences. S3 subtidal strata formed as a result of a relative sea-level rise and are interpreted as deepening-upward deposits.

Subaerial exposure of SB3 is indicated by subadjacent calcretes with rhizoliths, pendant cement, negative shifts in whole-rock $\delta^{13}C$ (Chapter 6), and lithoclast conglomerates with reworked calcrete clasts.

STE. GENEVIEVE SEQUENCES

Sequences 4-7

The Ste. Genevieve Limestone can be subdivided into four sequences (S4-S7). These sequences are very similar because they consist of a basal eolian unit overlain by subtidal strata (Fig. 5.3). Most Ste. Genevieve cores contain only the lower part of the formation, hence understanding of S6 and S7 is poor. Of the cores studied, only Amoco #1 Breeding F, Morton County, Kansas contains the contact of the Ste. Genevieve and Shore Airport (Abegg, in press (a)). Ste. Genevieve sequences S5 to

Reproduced with permission of the copyright owner. Further reproduction prohibited without permission.

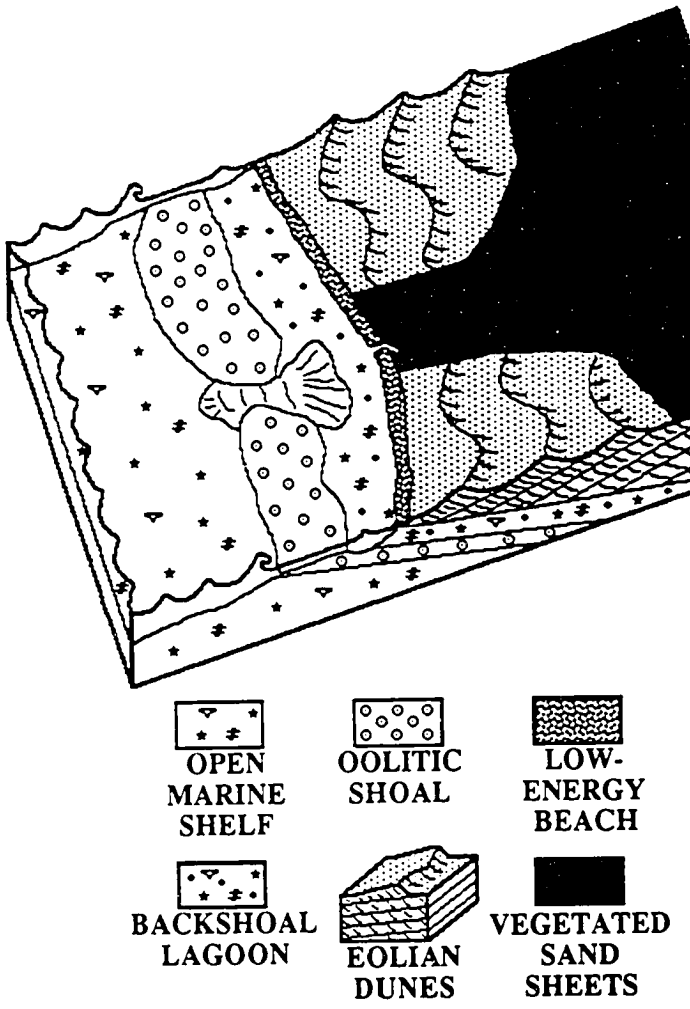


Figure 5.3 Block diagram showing the lateral distribution of facies that deposited strata of the Stevens Member of the St. Louis and Ste. Genevieve. Angle of dune climb is exaggerated for illustrative purposes. Dunes are shown as crescentic, but their morphology is uncertain. Because most subtidal strata lack detrital quartz, such grains in eolianites may have been transported by wadis. Detrital carbonate grains are interpreted to have been derived from beach sediments or, based on lithoclasts and reworked crinoids with rounded overgrowths, erosion of previously lithified limestones. The shoreline is interpreted to be a low-energy beach, energy having been dissipated on oolitic shoals. Beach strata have not been recognized, perhaps owing to subsequent erosion. Modified from Handford and Francka (1991, their Fig. 15).

Reproduced with permission of the copyright owner. Further reproduction prohibited without permission.

S7 are thin (average 31 ft or 9.4 m) compared to S1 and S2. S4 is quite variable in thickness (16 to 94 ft or 4.9 to 28.7 m), but its maximum thickness is comparable to S1 and S2 at many localities (Pocket Enclosure J-J').

Numerous mechanisms can account for the variable thickness of S4. A likely explanation is that it is filling paleotopographic lows. Eolian deposition is favored in paleotopographic lows because of flow deceleration as flow expands vertically in a setting with accumulation space (Wilson, 1973; Kocurek, 1988, 1991; Kocurek and Halvholm, in review). Subsequent transgression ends eolian deposition, but increases the preservation potential of the eolianite (Kocurek and Halvholm, in review). S4 is the first significant eolian accumulation and would fill depositional or erosional topography. Deposition of S4 apparently filled nearly all accumulation space because subsequent eolian accumulations are more uniform in thickness. A consistent thickness relationship of sand sheets versus dune fields was not recognized. Alternative explanations for variations in thickness of S4 is differences in sand supply due to proximity to the shoreline, convergence of airflow, or vegetation. Thick eolian accumulations are favored near shorelines where shelf carbonates are exposed to eolian processes (cf. Ball, 1967). Deposition of eolianites during initial transgression is possible. Encroachment of the shoreline would provide an abundant source of carbonate sediment where shelf carbonates are exposed to eolian processes (cf. Ball, 1967). The relative rise in sea level and concomitant water-table rise would increase preservation potential (Kocurek and Halvholm, in review). Thick eolian accumulations may also represent shoreline stability and aggradation. Convergence of flow can produce thick eolian accumulations (Wilson, 1971; Kocurek, 1988). Subsequent transgression would bevel but not remove these deposits. Vegetation can trap sediments and produce eolian deposits locally. Vegetation is unlikely to have produced these thick eolian deposits because rhizoliths are scattered or localized in occurrence.

Reproduced with permission of the copyright owner. Further reproduction prohibited without permission.

The bases of Ste. Genevieve sequences (S4-S7) consist of eolian quartzose grainstones that are interpreted as lowstand or early transgressive deposits because they rest directly on subtidal strata, demonstrating falls in relative sea level. The top of the eolianites is commonly an erosional transgressive surface locally marked by lithoclasts of quartzose grainstone. Lithoclasts, along with meteoric vadose cements within eolianites, indicate early cementation of the eolianites.

The upper parts of Ste. Genevieve sequences consist of subtidal oolitic and peloidal grainstone or packstone and normal-marine skeletal packstone and wackestone. These subtidal strata formed as a result of a relative sea-level rise and are interpreted as deepening-upward deposits. The succession of facies is variable, reflecting a facies mosaic, but oolitic and peloidal limestones typically are the first subtidal deposits on the eolianites. Locally, however, the transition from eolianite to subtidal deposits is marked by fenestral limestones (e.g., Amoco #1 Breeding F). In some subtidal intervals, oolitic and peloidal strata are overlain by normal-marine skeletal packstone to wackestone up to 24 ft (7.3 m) thick. This indicates relative rise of sea-level great enough to allow marine limestones to be deposited near fair-weather wave base.

S7, the uppermost sequence in the Ste. Genevieve, is inferred from quartz-rich carbonates observed on neutron-density logs; it has not been examined in core. It is apparently not present in all localities (Pocket Enclosure I-I', J-J'). Possible explanations for this local absence include removal by pre-Shore Airport erosion, original lenticularity, or southward facies change to peloid packstone. As conditions became less favorable for eolian sedimentation leading to deposition of the Shore Airport, it is reasonable that the last eolianite would be reduced in size. The end of carbonate eolianite deposition may reflect a change to more humid climates evidenced by a change from calcretes to reddish, clay-rich paleosols (Abegg, in press (a)) and an increase in detrital quartz.

Reproduced with permission of the copyright owner. Further reproduction prohibited without permission.

Subaerial exposure at SB4 to SB6 is indicated by calcretes with rhizoliths, pendant cements, negative shifts in whole-rock $\delta^{13}C$, and lithoclast conglomerates with reworked calcrete clasts that are overlain by eolianites. In Amoco #1 Nordling and Amoco #1 Puyear (Appendix 1), SB4 rests directly on argillaceous normal-marine skeletal packstone to wackestone of S4 that were deposited at or near fair-weather wave base.

Shore Airport Formation

The sequence stratigraphy of the Shore Airport Formation is uncertain because cores are few. Shore Airport strata in Amoco #1 Breeding F in Morton County consist of peloid packstone intercalated with variegated green and maroon calcareous shale. Shales represent paleosols that formed during repeated subaerial exposure (Abegg, in press (a)). Eight paleosols have been recognized from Morton County (Abegg, in press (a)). These exposure surfaces directly overlie subtidal peloidal packstones that do not appear to shoal upward, suggesting the paleosols formed as a result of a relative drop in sea level. According to Harland et al. (1982) and Sando (1985), the Chesterian Stage (not including the Ste. Genevieve) lasted approximately 10 to 15 m.y.; this also includes part of the sub-Pennsylvanian unconformity. Therefore, the eight exposure surfaces have average time spans that would be short for typical third-order cycles (1-10 m.y.). Additional work is needed to better understand Shore Airport deposition and sequences.

Sub-Pennsylvanian Unconformity

The top of the Shore Airport is part of the subaerial exposure surface that separates the Mississippian and Pennsylvanian Systems over much of North America. This surface corresponds to the first-order sequence boundary between the Kaskaskia and

Reproduced with permission of the copyright owner. Further reproduction prohibited without permission.

Absaroka sequences of Sloss (1963). The unconformity involves an extended period of erosion, probably extending several million years (Sloss, 1984; Saunders and Ramsbottom, 1986). Coeval unconformities are also well developed in Scotland, north Africa, Turkey, southern Urals, Fergana (south-central USSR), southeast China, Japan, and Spain (Saunders and Ramsbottom, 1986), although the Mississippian-Pennsylvanian unconformity is not everywhere recognizable.

Erosion beveled progressively older units toward the north and east, culminating in removal of Mississippian strata on the axis of the Central Kansas uplift (Fig. 1.1). In extreme southwestern Seward County, Kansas (Pocket Enclosure A-A'), erosion over a structural high changes the thickness of the Shore Airport by as much as 247 ft (75 m) between two wells approximately 7 mi (11 km) apart (Abegg, 1991). The sub-Pennsylvanian unconformity is preserved in Amoco #3 Wilson A (5324 ft core depth), Amoco #1 Breeding F (5282 ft core depth), and Pendleton #1 Schauf (4959 ft core depth). Reworked Mississippian clasts in the basal Pennsylvanian are best developed in Pendleton #1 Schauf (cf. Youle, 1991). The Wilson, Breeding (Abegg, in press (a)), and Schauf cores contain mm-scale solution-enlarged fractures and vugs filled with Morrowan sediment, indicating that the pores were open during deposition of the overlying Kearny Formation. This suggests that the pores formed as microkarst. Karst-related porosity filled by Pennsylvanian sediment is a common feature in Mississippian strata from many localities across North America (e.g., Nodine-Zeller, 1981; DeVoto, 1988; Kaufman et al., 1988; Goldstein, 1990).

CORRELATION OF SEQUENCE BOUNDARIES

Sequence boundaries are most reliably correlated using a combination of core and wireline logs (Pocket Enclosures I-I', J-J'). SB1 corresponds to the upper boundary of the Hugoton Member at the top of restricted-shelf dolomitic carbonates or at the top of the E1 anhydrite, where restricted facies are absent above the anhydrite.

Reproduced with permission of the copyright owner. Further reproduction prohibited without permission.

SB2 through SB6 are subaerial exposure surfaces overlain by eolian strata. Commonly these sequence boundaries are easily identified in core. In wireline logs sequence boundaries are typically located at the base of quartz-rich carbonates (mostly eolian) that are identified by higher neutron porosities than density porosities (Figs. 2.2 and 2.14). However, SB2 is not easily recognized on porosity logs because the basal eolianite of S3 is typically too thin to be resolved on neutron-density logs. Eolian quartzose facies either grade laterally into quartz-poor subtidal facies or quartz content is variable. Therefore, correlation of sequence boundaries using wireline logs alone is extremely difficult in some areas. Correlation is even more difficult in the absence of neutron-density logs.

Sequence boundaries apparently extend across much of the Hugoton embayment. Additional data may prove some sequence boundary correlations to be more complicated than shown. Thin subtidal units might have been eroded locally producing amalgamated sequences. The difficulty in correlation of quartz-rich carbonates may indicate local discontinuity of eolianites. The current data set indicates similar numbers of both eolianites and sequence boundaries in many cores and wireline logs, suggesting that these sequence boundaries are laterally correlative in the Hugoton embayment.

SEQUENCE DURATION

Estimation of sequence duration is important in the interpretation of mechanisms of sea-level change. Second-order cycles span 10 to 100 m.y., third-order cycles span 1 to 10 m.y., and fourth-order cycles span 0.1 to 1 m. y. (e.g., Vail et al., 1977; Miall, 1984; Van Wagoner et al., 1990). Two orders of relative sea-level changes are recognized in St. Louis and Ste. Genevieve strata. Depositional sequences S1 through S7 are approximately fourth-order sequences and are superposed on a longer term fall in relative sea level that is part of a Late Mississippian second-order cycle (cf. Vail et

Reproduced with permission of the copyright owner. Further reproduction prohibited without permission.

al., 1977).

Fourth-order Cycles

According to Sando (1985), the St. Louis and Ste. Genevieve Limestones in the Illinois basin may have been deposited over a time span of four to seven m.y. If these numbers are valid for the Hugoton embayment, the seven sequences in the St. Louis and Ste. Genevieve correspond to an average periodicity of approximately 0.6 to 1.0 m.y. S1 includes some Salem strata, therefore this estimate is conservatively low.

Second-order Cycles

Evidence of widespread subaerial exposure was not observed in S1 and S2. In contrast, S3 through S7 are generally thinner and are bounded by subaerial exposure surfaces. These features are attributed to a decrease in the rate of addition of accommodation space due to a long-term fall in relative sea level superimposed on fourth-order cycles. This long-term sea-level change can occur by eustacy, tectonic uplift, or a long-term change in subsidence rate.

According to Vail et al. (1977, p. 93), a global highstand of sea level occurred during the late Osagean to earliest Meramecian, approximately 350 to 340 Ma (cf. Harland et al., 1982; Sando, 1985). The mid-Carboniferous global lowstand of sea level has been placed at 330 to 320 Ma (Vail et al., 1977; Harland et al., 1982; Miall, 1984; Sando, 1985; Saunders and Ramsbottom, 1986). Therefore this drop in sea level (i.e. part of a cycle) occurred over approximately 10 to 30 m.y., in the lower range of durations expected for second-order sea-level changes.

UPPER MISSISSIPPIAN SEQUENCE SET

The sequences in the St. Louis and Ste. Genevieve Limestone (S1 through S7) are

Reproduced with permission of the copyright owner. Further reproduction prohibited without permission.

interpreted as a progradational to aggradational sequence set (cf. Mitchum and Van Wagoner, 1991). S1 and S2 are subtidally-dominated sequences that lack evidence of widespread subaerial exposure on this part of the shelf (Fig. 5.4). Conversely, S3 through S6 contain evidence of widespread subaerial exposure (Fig. 5.5). The relative decrease in thickness and extensive subaerial exposure in S3 through S7 are attributed to decrease in the rate of addition of accommodation space on the shelf relative to S1 and S2. This change in accommodation is interpreted as a result of a second-order fall in relative sea level during the Late Mississippian (cf. Vail et al., 1977). S3 through S7 probably have a basinward (roughly southward) increase in marine influence and overall thickness. S3, for example, attains maximum thickness and is dominantly open marine in Stevens County in Mobil #1 Foster and Mobil #1 Headrick (Appendix 1).

MECHANISMS FOR SEA-LEVEL CHANGES

According to Sarg (1988), four variables account for most of the variation in stratal patterns and facies distributions in carbonate rocks: 1) eustatic sea-level change, 2) tectonic subsidence or uplift, 3) volume of sediment, and 4) climate. The following section evaluates the possible contributions of each of these factors to the deposition of St. Louis and Ste. Genevieve strata. Unfortunately, it is not possible to evaluate all mechanisms of eustatic sea-level change (cf. Miall, 1984; Kendall and Lerche, 1988).

Changes in Ice Volume

Evidence for Early Carboniferous glaciation has been reported by Crowell (1978), Caputo and Crowell (1985), and Veevers and Powell (1987). The presence of Visean (Osagean to Meramecian) and Namurian (Chesterian to Morrowan) glacial deposits in Gondwanaland supports glacioeustatic sea-level changes as a possible mechanism for St. Louis and Ste. Genevieve sequences. The aerial distribution of glacial deposits during the Visean suggests ice volumes on Gondwanaland were small (Veevers and

Reproduced with permission of the copyright owner. Further reproduction prohibited without permission.

SUBTIDALLY-DOMINATED SEQUENCES

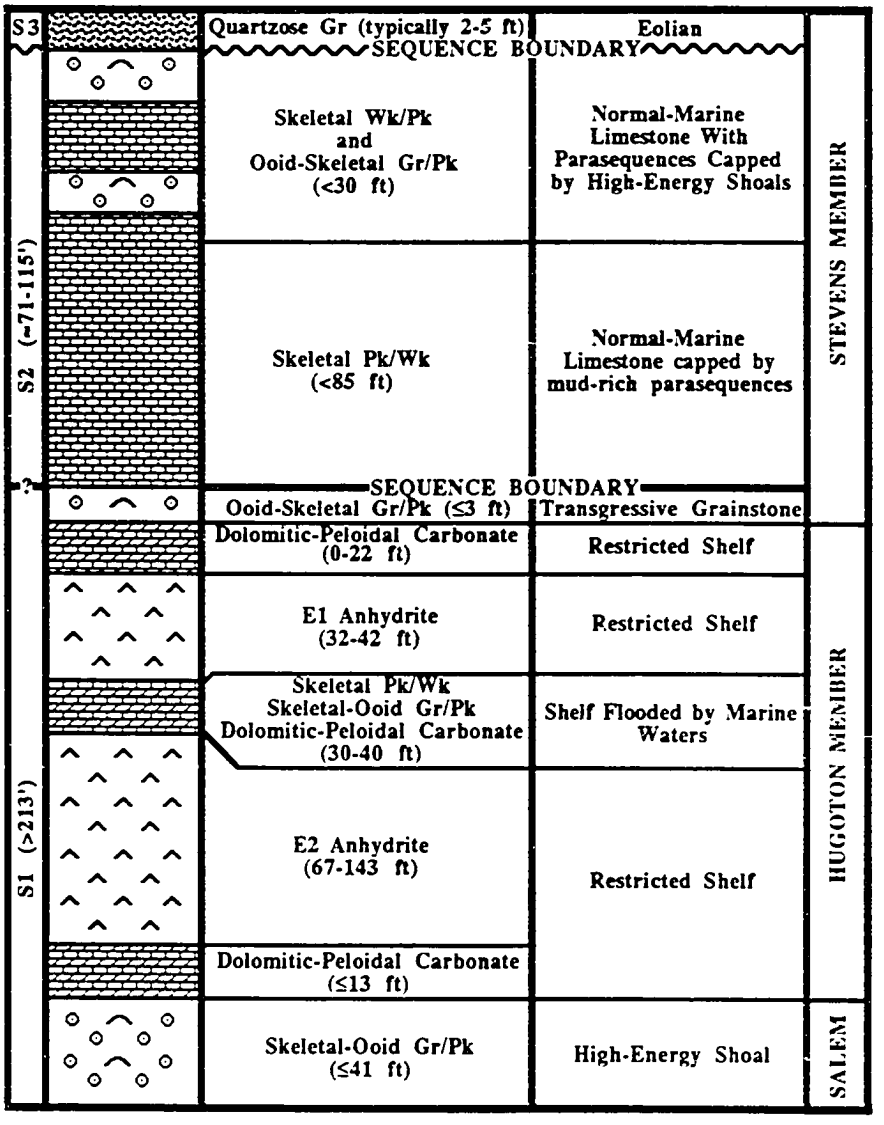


Figure 5.4 S1 and S2 in the St. Louis Limestone are subtidally-dominated sequences. S2 is a thick type-2 sequence that contains little evidence of subaerial exposure. Wavy line indicates a sequence boundary marked by subaerial exposure, whereas a bold, straight line indicates a relatively conformable sequence boundary.

Reproduced with permission of the copyright owner. Further reproduction prohibited without permission.

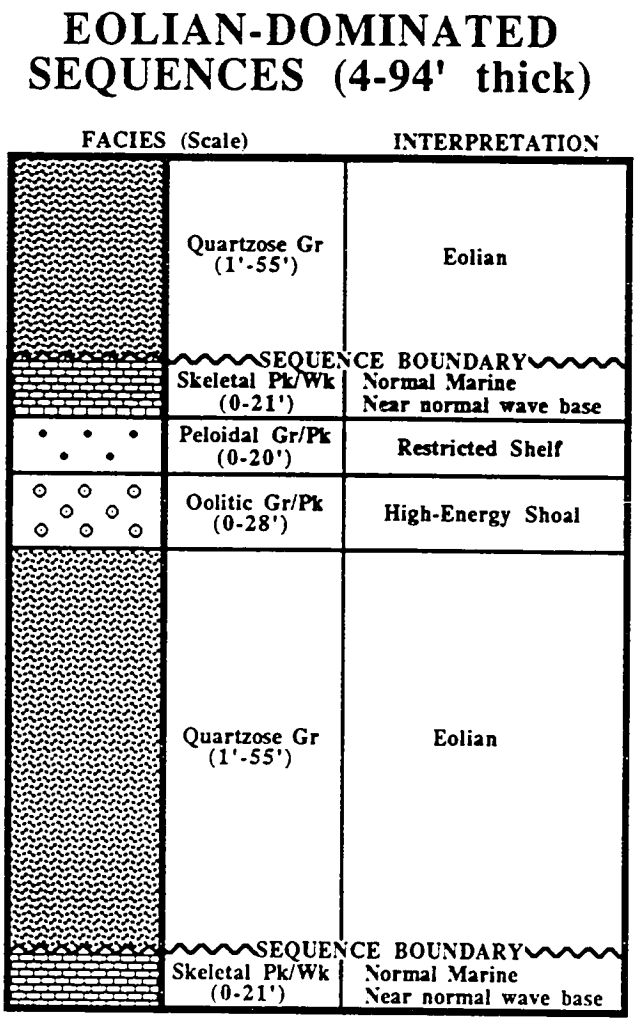


Figure 5.5 Eolian-dominated sequences are characteristic of S3 through S7 in the uppermost St. Louis and Ste. Genevieve Limestones. These are type-1 or type-2 sequences that are typically thinner than marine-dominated sequences and contain abundant evidence of subaerial exposure. Wavy line indicates a sequence boundary marked by subaerial exposure.

Reproduced with permission of the copyright owner. Further reproduction prohibited without permission.

Powell, 1987). Combined with position on the shelf, this may explain the absence of condensed sections in St. Louis and Ste. Genevieve sequences in southwestern Kansas.

The rough estimate of 0.6 to 1.0 m.y. for the average duration of seven sequences in the St. Louis and Ste. Genevieve is similar to durations suggested for other interstratified eolian and subtidal strata. Blakey and Middleton (1983) estimated 500,000 yr per cycle for the Schnebly Hill Formation and Coconino Sandstone (Permian) in central Arizona. Driese and Dott (1984) estimated 470,000 to 880,000 yr per cycle for the Morgan Formation (Pennsylvanian) in Utah and Colorado. Loope (1985) estimated 400,000 to 800,000 yr per cycle for the Rico and Hermosa Formations (Upper Pennsylvanian) in southeastern Utah. These authors also attributed interbedded eolian-subtidal successions to glacioeustatic sea-level changes. Note that these durations are all somewhat greater than the 413,000 yr periodicity for eccentricity (Hays et al., 1976; Imbrie and Imbrie, 1980; Berger et al., 1989a, 1989b). Many parasequences in the St. Louis and Ste. Genevieve may also result from glacioeustatic sea-level changes.

If glacioeustacy is the primary mechanism controlling St. Louis and Ste. Genevieve sequences, similar sequences should be observable globally. In the Illinois basin, the lower St. Louis evaporites and the less restricted upper St. Louis (Martorana, 1987) compare to a roughly coeval succession in southwestern Kansas (Thompson and Goebel, 1968) composed of restricted-shelf strata of the Hugoton Member and normal-marine strata of the Stevens Member in southwestern Kansas. At least three depositional sequences of interbedded eolian and subtidal strata occur in the Ste. Genevieve in southern Indiana (Hunter, 1989; personal observation). Lithofacies, calcretes with rhizoliths, lithoclast conglomerates, and scale of sequences in the Ste. Genevieve in Indiana are also similar to those from cores in southwestern Kansas.

Reproduced with permission of the copyright owner. Further reproduction prohibited without permission.

However, the exact number and lateral extent of Illinois-basin sequences has not been investigated. On a more global scale, Ross and Ross (1985, 1988) suggest Late Mississippian depositional sequences are synchronous and worldwide. Additional data seems necessary to prove a eustatic mechanism for the the St. Louis and Ste. Genevieve sequences.

Changes in Mid-Oceanic Ridge Volume

Changes in mid-oceanic ridge length and spreading rates can drastically affect sea level (Pittman, 1978). A decrease in seafloor spreading rates or ridge length would cause a drop in sea level. Such sea-level changes have typical periodicities of 10 to 100 m. y. (Vail et al., 1977; Miall, 1984).

The St. Louis-Ste. Genevieve aggradational to progradational sequence set is interpreted to be part of a second-order drop in relative sea level during the last 10 to 30 m.y. of Mississippian time that culminated in development of the sub-Pennsylvanian unconformity. Based on Pittman (1978), a change in spreading rates from 6 cm/yr to 2 cm/yr would result in a sea-level drop of approximately 37 m (121 ft) over 10 m.y. This magnitude of sea-level change is consistent with a major global unconformity. Increased Namurian (Chesterian-Morrowan) ice volume (Veevers and Powell, 1987) may also have enhanced development of the sub-Pennsylvanian unconformity.

Changes in the rate of second-order drop in eustatic sea level can produce fourth-order changes in relative sea level (cf. Posamentier et al., 1988, p. 123). A slow rate of fall, less than that of subsidence, can produce a relative sea-level rise without a eustatic rise.

Tectonism

The role of tectonism in formation of St. Louis and Ste. Genevieve depositional

Reproduced with permission of the copyright owner. Further reproduction prohibited without permission.

sequences is difficult to evaluate. Local tectonism is unlikely as similar sequences occur in the Illinois basin (Hunter, 1989; personal observation). Regional tectonism, however, cannot be discounted.

Tectonically-controlled subsidence may have affected sedimentation of the St. Louis and Ste. Genevieve sequences in the Hugoton embayment. S2 is at least 33 ft (10.1 m) thicker in southern Stevens County than in Logan County. This suggests slightly greater subsidence on more basinward portions of the shelf. Increased thickness of S3 in southernmost Kansas may also be attributable to increased subsidence. Alternatively, the southward thickness increase may be a result of a regional depositional slope.

The sub-Pennsylvanian unconformity in North America may also have been affected by tectonic uplift (Sloss, 1984). The local erosion of Shore Airport strata over structural highs and increased preservation in structural lows (e.g., southwestern Seward County, Pocket Enclosure A-A') indicates much of the deformation in the Hugoton embayment predates deposition of the Morrowan Kearny Formation (Abegg, 1991). No consistent relation of ooid grainstone distribution and structural highs has been observed. Major changes in facies or thickness have not been observed in St. Louis and Ste. Genevieve strata toward the Central Kansas uplift, although such observations are precluded as these strata have been removed from the crest of the structure. Additional work is needed to evaluate the effect of tectonic uplift on Late Mississippian sedimentation in southwestern Kansas.

Autocyclicity

The absence of shoaling-upward cycles indicates subaerial exposure did not result from sediment building up to sea level (i.e. autocyclicity), but rather from a drop in relative sea level. Evidence for a drop in relative sea level includes eolianites developed

Reproduced with permission of the copyright owner. Further reproduction prohibited without permission.

directly on subtidal strata without intervening intertidal beach or tidal-flat deposits, and calcretes and eolianites along sequence boundaries that commonly overlie normal-marine skeletal packstone/wackestone, probably deposited at or near fair-weather wave base. Subaerial exposure on the scale of at least 3600 mi^2 (9200 km^2) along sequence boundaries also strongly suggests an allocyclic control on sequences. Additionally, the fact that St. Louis and Ste. Genevieve strata contain similar depositional sequences in the Hugoton embayment and the Illinois basin is not consistent with autocyclicity, but more work is required to determine the degree of similarity.

Climate

Climate does not directly affect sea level, with the exception of desiccation of ocean basins (cf. Miall, 1984). Climate may, however, drive glacioeustatic sea-level changes (e.g., Hays et al., 1976; Imbrie and Imbrie, 1980; Berger et. al., 1989a, 1989b). Climate is also important because it helps controls the type of sediment deposited (Sarg, 1988). Evaporites in the Hugoton Member of the St. Louis indicate an arid climate. Carbonate eolianites and calcretes in the Ste. Genevieve suggest an arid to semi-arid climate. However, Marzolf (1988) reasoned that ancient climatic conditions for eolianites may have been different than they are today due to differences in vegetation. Increased percentages of siliciclastics and change from calcretes to reddish, clay-rich paleosols in the Shore Airport Formation (Abegg, in press (a)) suggest increasingly humid climates during the Chesterian. Increasingly humid climates might also be responsible for the end of eolianite deposition. Such climatic interpretations are consistent with paleoclimatic interpretations by Cecil (1990) and the northward migration of the North American continent. However, plate reconstructions estimate that from 342 Ma (late Meramecian) to 324 Ma (uppermost Chesterian) southwestern Kansas moved from approximately 9° to 6° south latitude (cf. Scotese, 1986), perhaps suggesting that latitude may not have been the major factor affecting climate.

Reproduced with permission of the copyright owner. Further reproduction prohibited without permission.

SUMMARY

1. St. Louis and Ste. Genevieve Limestones can be subdivided into seven sequences, S1 to S7, with upper sequence boundaries SB1 to SB7. S1 and S2 are relatively thick, subtidally-dominated sequences separated by a type 2 sequence boundary without widespread evidence of subaerial exposure (SB1). S3 through S7 are relatively thin, eolian-dominated sequences bounded by subaerial exposure surfaces. Eolian carbonates were deposited at the base of S3 through S7 and are overlain by subtidal carbonates. SB2 through SB6 are recognized by evidence of subaerial exposure and by basinward shifts in facies (cf. Van Wagoner et al., 1988). Relative falls in sea level can be demonstrated for SB2 through SB6 by paleosols or eolianites developed directly on subtidal strata. Autocyclicity can be discounted unless subaerial erosion has removed shoaling-upward strata, which is unlikely as erosion cannot proceed past baselevel.

2. Approximate average durations of St. Louis and Ste. Genevieve sequences are 0.6 to 1.0 m.y. The presence of Mississippian glaciation in Gondwanaland suggests the St. Louis and Ste. Genevieve sequences may have formed as a result of glacioeustatic sea-level changes. Alternatively, these fourth-order sequences can result from changes in the rate of second-order drop in eustatic sea level. A slow rate of fall, less than that of subsidence, can produce a relative sea-level rise without a eustatic rise.

3. St. Louis and Ste.Genevieve sequences S1 to S7 are interpreted as a progradational to aggradational sequence set based on an upward decrease in thickness and on the numerous exposure surfaces and eolianites in S3 to S7. The inferred progradational or aggradational nature of these sequences reflects the overall lowering of relative sea level during the Late Mississippian. This drop of relative sea level probably took place over a 10 to 30 m.y. period, a duration consistent with a decrease

Reproduced with permission of the copyright owner. Further reproduction prohibited without permission.

in seafloor spreading rates or in mid-oceanic ridge length. Greater Visean and Namurian ice volumes and Late Mississippian-Early Pennsylvanian tectonism may also have contributed.

Reproduced with permission of the copyright owner. Further reproduction prohibited without permission.

CHAPTER 6
Whole-Rock Isotopic Profiles

INTRODUCTION

Shifts in whole-rock values of $\delta^{13}C$ and $\delta^{18}O$ aid in the recognition of subaerial-exposure surfaces. The pattern was first recognized in cores of Pleistocene limestones from Barbados (Allan and Matthews, 1977). Similar isotopic signatures were subsequently found associated with subaerial-exposure surfaces in ancient carbonates (Videtich and Matthews, 1980; Allan and Matthews, 1982; Wagner and Matthews, 1982; Major and Matthews, 1983; Beeunas and Knauth, 1985; Humphrey et al., 1986; Beier, 1987; Abegg and Grover, 1990; Rush and Chafetz, 1990; Goldstein, 1991).

Allan and Matthews (1982) attributed the isotopic signatures associated with whole-rock analyses to meteoric recrystallization and cementation of limestone in the vadose zone directly beneath a subaerial exposure surface. Goldstein (1991) demonstrated through microsampling that pedogenic features such as rhizoliths, laminated crusts, and pedogenic cements preserve ^{12}C that results in the negative carbon shifts proximal to many subaerial-exposure surfaces. However, Rush and Chafetz (1990) noted negative carbon shifts in whole-rock samples, as well as in microsampled brachiopods, echinoderms, and cements, beneath an exposure surface that apparently lacks pedogenic features.

The majority of whole-rock isotopic studies have been tested on subtidal carbonate successions punctuated by calcretes. Calcretes are readily definable by numerous petrographic criteria (cf. Esteban and Klappa, 1983). In the identification of exposure surfaces, whole-rock isotopic analyses generally confirm what is already known petrographically. The whole-rock method, combined with detailed petrography, is a quick and useful first step in understanding the sedimentology and diagenesis of a

Reproduced with permission of the copyright owner. Further reproduction prohibited without permission.

succession of carbonates (Allan and Matthews, 1982; Goldstein, 1991). Deviations from expected trends indicate intervals requiring reinterpretation or microsampling.

The objective of this study was to test the utility of the whole-rock isotope method in the recognition of carbonate eolianites that are intercalated with subtidal limestones. Additionally, whole-rock isotopic analyses are useful in the recognition of subaerial-exposure surfaces that are used to subdivide strata into depositional sequences (Chapter 5). The original hypothesis was that eolian carbonates might yield more negative $\delta^{13}C$ values than subtidal strata. The whole-rock method apparently has not been previously tested on interbedded eolian and subtidal carbonate successions. Beier (1987) reported whole-rock isotope data from Pleistocene carbonate eolianites punctuated by paleosols on San Salvador Island, Bahamas, but her analyses did not include any subtidal strata.

The Stevens Member of the St. Louis Limestone in southwestern Kansas typically consists of normal-marine fossiliferous and oolitic limestones with a thin carbonate eolianite near the top (Abegg, 1991, in press (b)). The overlying Ste. Genevieve consists largely of eolian quartzose grainstones punctuated by several subtidal units (Handford, 1990; Abegg, 1991, in press (b); Handford and Francka, 1991). Eolian deposits are identified by a number of criteria (Table 4.2), most notably by subcritically climbing translatent strata (cf. Hunter, 1977). Calcrete features such as rhizoliths and pendant cements are present in and immediately below some eolianites, but they are poorly developed or absent from many eolian intervals. The rarity of calcrete features and subtle differences between eolian and subaqueous grainstones introduces a need for additional recognition criteria. The presence of distinctive eolian and exposure features at some levels provides a controlled test.

Three isotopic patterns are useful in the identification of subaerial-exposure surfaces (Allan and Matthews, 1982): 1) negative $\delta^{13}C$ shift beneath an exposure surface; 2) positive $\delta^{18}O$ shift immediately below an exposure surface; and 3) a shift in $\delta^{18}O$ across an exposure surface (Fig. 6.1). The negative $\delta^{13}C$ shift below an exposure

Reproduced with permission of the copyright owner. Further reproduction prohibited without permission.

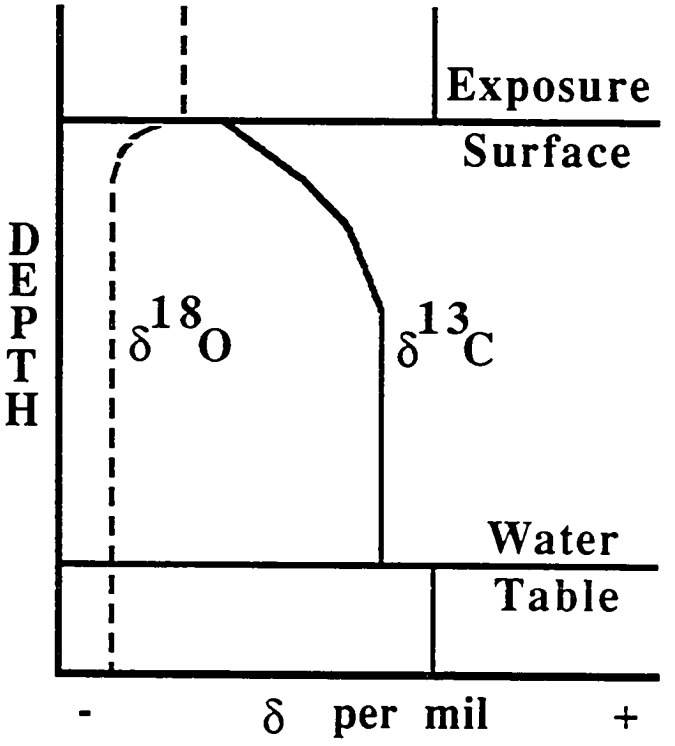


Figure 6.1 Potentially useful patterns in $\delta^{13}C$ and $\delta^{18}O$ in the recognition of ancient subaerial exposure surfaces. Modified from Allan and Matthews (1982, their Fig. 11) and from Goldstein (1991, his Fig. 2).

Reproduced with permission of the copyright owner. Further reproduction prohibited without permission.

surface results from precipitation or recrystallization of carbonates incorporating CO_2 enriched in ^{12}C through the activity of soil bacteria (e.g., Allan and Matthews, 1982). The heavier oxygen isotope, ^{18}O, is concentrated in residual waters by evaporation in the vadose zone resulting in carbonates enriched in ^{18}O. The shift in $\delta^{18}O$ across an exposure surface may result from differing diagenetic histories in carbonates above and below an exposure surface. Allan and Matthews (1982, p. 815) state that two out of three of these signatures indicate an ancient exposure surface.

Two patterns in carbon-oxygen isotopic crossplots are potentially useful in the recognition of diagenesis associated with subaerial exposure (Allan and Matthews, 1982). Meteoric diagenesis within a single groundwater system typically produces a wide range of $\delta^{13}C$ and a narrow range of $\delta^{18}O$ (Fig. 6.2). Carbon variation commonly results from concentration of ^{12}C in features such as rhizoliths and soil-precipitated cements proximal to exposure surfaces (Goldstein, 1991). Homogeneity of oxygen values reflects lack of compositional change in meteoric waters with repeated solution-reprecipitation (Allan and Matthews, 1982; Meyers and Lohmann, 1985). Covariance of $\delta^{13}C$ and $\delta^{18}O$ (Fig. 6.2) have been reported from alteration that occurs across salinity gradients in the marine-meteoric mixing zone (Allan and Matthews, 1982, their Fig. 8B) or from mixing of different diagenetic components (Allan and Matthews, 1982; Given and Lohmann, 1986).

Methods

Cores from Amoco #1 Nordling (Appendix 1) and Amoco #3 Cohen C (Appendix 1) were selected for isotopic analyses because they contain well-defined successions of interbedded eolian and subtidal limestones. Sample spacing was generally four to 20 ft (1.2 to 6.1 m) but was decreased to one to two ft (0.3 to 0.6 m) proximal to boundaries of subtidal and eolian strata to assist in the detection of isotopic shifts. Thin sections,

Reproduced with permission of the copyright owner. Further reproduction prohibited without permission.

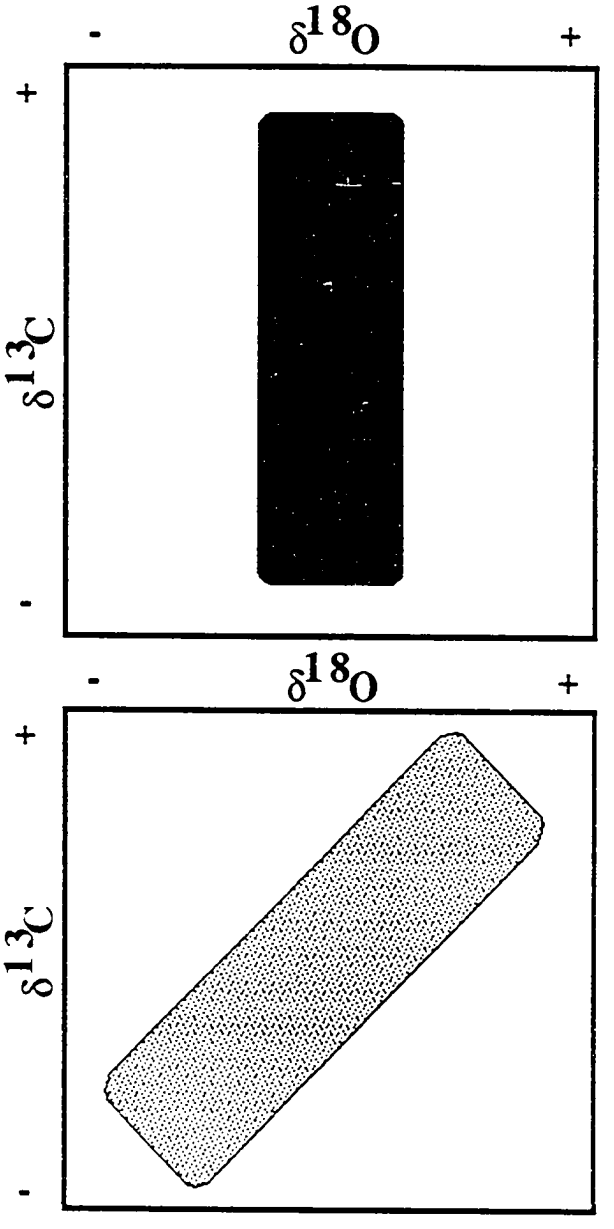


Figure 6.2 Carbon-oxygen crossplot patterns that are associated with subaerial exposure. Modified from Allan and Matthews (1982, their Fig. 11). The large variation in $\delta^{13}C$ and the small variation in $\delta^{18}O$ (dark stipple) results from meteoric diagenesis. Covariance of $\delta^{13}C$ and $\delta^{18}O$ (light stipple) may result from mixing-zone diagenesis or from marine sediments with cementation in several diagenetic environments (Allan and Matthews, 1982; Givens and Lohmann, 1985).

Reproduced with permission of the copyright owner. Further reproduction prohibited without permission.

stained with both Alizarin-Red S and potassium ferricyanide (Dickson, 1966), were examined for all horizons sampled for isotopes in order to petrographically characterize each sample and to understand the components contributing to the whole-rock signature. A dental drill was used to obtain whole-rock samples from thin section butts. In order to prevent sample bias from any particular interval, traverses perpendicular to bedding were drilled. Inhomogeneities such as a calcite-filled fractures or vugs were avoided because they might disproportionately affect individual values. Microsamples composed largely of rhizoliths (rhizocretion and root cast) and intervals containing pendant cements were analyzed to help determine $\delta^{13}C$ values of vadose components. However, single-phase microsampies of pendant or other cements were not analyzed.

Isotopic analyses were completed by Benedum Laboratory at Brown University where volatile organics were removed by vacuum roasting each sample for 1 hour at 300°C. The powder was then reacted with 100% H_3PO_4 at 90°C and the $\delta^{13}C$ and $\delta^{18}O$ for the evolved CO_2 determined by a mass spectrometer. All isotopic values (Table 6.1 and 6.2) are reported in per mil (‰) relative to the PDB standard (Craig, 1957). Random duplicates were run on approximately 10% of the samples. Precision for carbon and oxygen were ±0.07 and ±0.13 ‰, respectively.

LITHOFACIES AND DEPOSITIONAL ENVIRONMENTS

Three facies are recognized in the Ste. Genevieve Limestone and Stevens Member of the St. Louis Limestone of Amoco #1 Nordling and Amoco #3 Cohen C (Appendix 1) cores selected for isotopic analyses: subtidal skeletal packstone/wackestone, subtidal oolitic grainstone, and eolian quartzose grainstone. These facies are typical of these units over much of the Hugoton embayment in southwestern Kansas (Chapter 3).

Reproduced with permission of the copyright owner. Further reproduction prohibited without permission.

Table 6.1. Whole-rock analyses of samples from Amoco #1 Nordling, SW SE NE, 30-29S-39W, Stanton Co., Kansas

Depth	$\delta^{13}C$	$\delta^{18}O$	Description
5665.1A	2.07	-4.96	Porous subtidal ooid grainstone with lithoclasts
5665.1A	2.21	-4.67	Porous subtidal ooid grainstone with lithoclasts
5665.1B	2.12	-3.64	Detailed sample of several lithoclasts
5671.7	2.64	-4.46	Cross-stratified subtidal peloid grainstone
5680.9	2.81	-3.56	Subtidal ooid grainstone
5680.9	3.01	-3.06	Subtidal ooid grainstone
5682.0A	2.49	-3.74	Eolian lithoclast along transgressive surface
5682.0B	2.79	-3.51	Subtidal marine strata overlying eolian lithoclasts
5682.3	2.07	-4.76	Subtidal marine strata between lithoclasts
5686.8	1.97	-3.62	Climbing translatent strata in quartzose grainstone
5694.0	2.61	-3.31	Quartzose grainstone between calcrete lithoclasts
5696.1A	2.53	-3.61	Quartzose grainstone between calcrete lithoclasts
5696.1B	0.18	-5.46	Detailed sample of rhizocretions in lithoclasts
5711.8	2.52	-3.81	Quartzose grainstone
5713.5A	2.58	-3.07	Cross-stratified quartzose grainstone
5713.5B	2.06	-4.92	Detailed sample of thin light brown rhizocretions
5727.1	2.72	-3.31	Climbing translatent strata in quartzose grainstone
5730.5A	2.05	-4.64	Quartzose grainstone, pendent cements not sampled
5730.5B	2.53	-3.41	Detailed sample of interval with pendant cements
5737.8	1.87	-4.42	Quartzose grainstone at the base of eolian interval
5739.4	3.31	-2.17	Porous subtidal ooid grainstone
5742.3	3.12	-1.80	Subtidal ooid grainstone below hardground
5744.3	3.07	-2.08	Tight subtidal ooid grainstone (with calcrete clasts?)
5744.5	2.72	-2.93	Quartzose grainstone at the top of eolian interval
5746.3A	2.85	-2.72	Quartzose grainstone sampled away from rhizoliths
5746.3B	1.54	-4.44	Detailed sample of stylolitized brown rhizocretion
5748.3	1.40	-5.45	Climbing translatent strata at the base of eolian unit
5748.6	2.78	-3.80	Subtidal packstone below eolian lithoclast lag
5749.8	2.72	-3.62	Subtidal skeletal packstone
5752.0	2.62	-3.90	Subtidal skeletal packstone
5755.0	3.16	-3.43	Subtidal skeletal packstone
5769.2	3.17	-3.63	Subtidal skeletal packstone
5787.6	2.62	-4.08	Subtidal skeletal mud-poor packstone

Reproduced with permission of the copyright owner. Further reproduction prohibited without permission.

Table 6.2. Whole-rock analyses of samples from Amoco #3 Cohen C, C SE NE, 27-25S-38W, Stanton Co., Kansas

Depth	$\delta^{13}C$	$\delta^{18}O$	Description
5285.9A	1.53	-3.24	Quartzose grainstone in lithoclast with no rhizoliths
5285.9B	1.66	-4.15	Detailed sample of rhizolith-rich area
5286.1	2.29	-1.50	Quartzose grainstone with possible pendant cements
5286.8A	1.96	-2.67	Quartzose grainstone sampled away from rhizoliths
5286.8A	2.19	-2.84	Quartzose grainstone sampled away from rhizoliths
5286.8B	1.58	-4.71	Detailed sample of rhizolith-rich area
5295.4	2.39	-3.63	Climbing translatent strata in quartzose grainstone
5297.8	2.79	-4.08	Subtidal skeletal wackestone
5301.1	2.41	-3.13	Subtidal skeletal wackestone
5305.8	3.01	-1.52	Subtidal skeletal packstone
5311.3	2.79	-2.89	Porous subtidal ooid grainstone
5315.7	2.74	-3.89	Porous subtidal ooid grainstone
5319.0	2.71	-3.40	Porous subtidal ooid grainstone
5319.0	2.79	-3.45	Porous subtidal ooid grainstone
5321.6	2.84	-3.77	Quartzose grainstone at top of eolian? interval
5322.2A	2.87	-2.69	Subtidal ooid packstone, calcrete not sampled
5322.2A	2.80	-2.94	Subtidal ooid packstone, calcrete not sampled
5322.2B	1.92	-4.33	Calcrete lithoclast at top of subtidal interval
5323.0	3.16	-3.70	Subtidal skeletal packstone
5324.0	2.37	-3.44	Subtidal skeletal packstone
5328.0	2.00	-4.66	Subtidal skeletal packstone
5347.1	3.03	-3.30	Subtidal ooid grainstone
5364.7	3.44	-3.34	Subtidal peloid skeletal packstone

Reproduced with permission of the copyright owner. Further reproduction prohibited without permission.

DIAGENESIS

Diagenetic features of upper St. Louis (Stevens Member) and Ste. Genevieve rocks can be divided into eogenetic and mesogenetic (cf. Choquette and Pray, 1970). Eogenetic features include non-ferroan, isopachous bladed or pendant calcite cements; zoned non-ferroan and ferroan calcite cements; and minor dissolution (Fig. 6.3). Mesogenetic diagenesis consists of post-compactional, unzoned ferroan calcite cements and minor dissolution (Fig. 6.3).

Eogenesis

Isopachous, bladed calcite cements occur locally in oolitic grainstones. In Amoco #1 Nordling, these cements are best developed immediately below a truncation surface (5742.3 ft core depth) and are absent above the surface (Fig. 6.4). The truncation surface is interpreted as a marine hardground. Bladed to fibrous morphology and isopachous distribution suggest these cements precipitated in the marine diagenetic realm (Longman, 1980). Immediately beneath the truncation surface, the whole-rock $\delta^{18}O$ value of -1.80‰ is similar to Mississippian marine values (Brand, 1982; Meyers and Lohmann, 1985). This value is isotopically enriched (heavy) relative to surrounding values, consistent with isotopic shifts across hardgrounds reported by Marshall and Ashton (1980). Isotopic evidence for subaerial exposure is absent.

Brownish, bladed or fibrous, sparry-calcite cement occurs within some intervals containing rhizoliths (Fig. 3.16). Micritic cement coats, and locally occurs within, many of these fibrous cements. Fibrous and micritic cements nucleate from the underside of grains and from the top of fracture and vuggy pores. Terminations of fibrous cements are rounded; bladed cement terminations are euhedral. Fibrous crystals contain numerous solid inclusions. The microstalactitic distribution, rounded terminations, association with eolian strata and rhizoliths, and early paragenetic position

Reproduced with permission of the copyright owner. Further reproduction prohibited without permission.

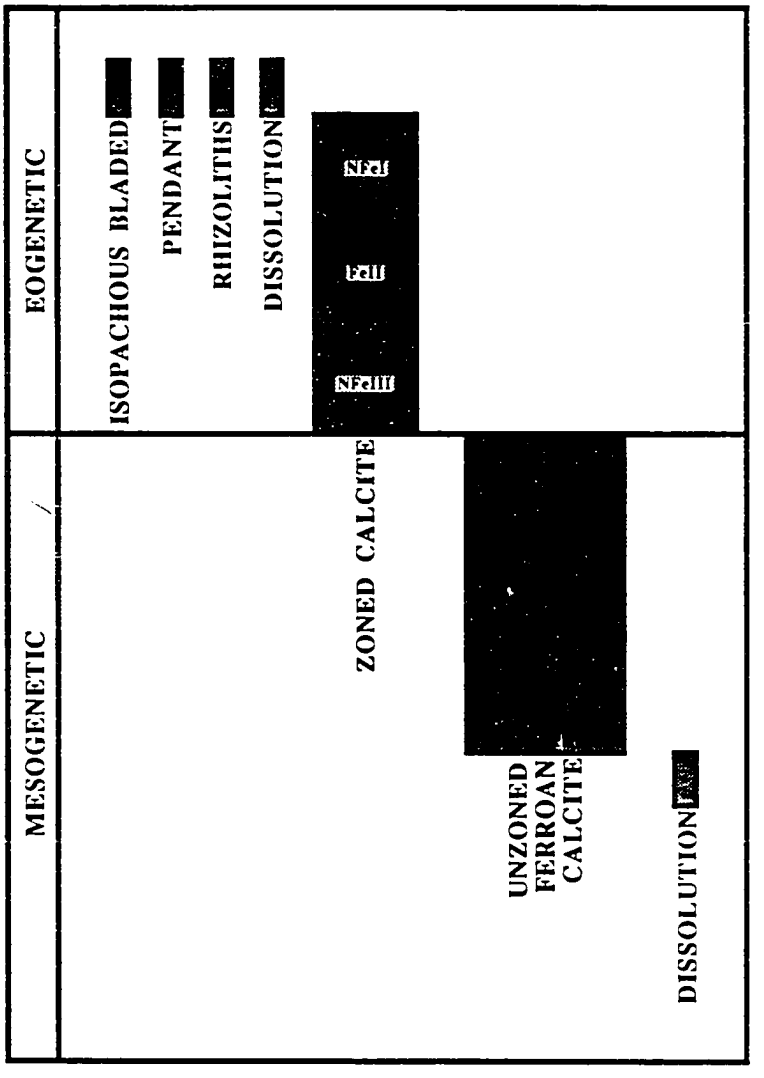


Figure 6.3 Paragenesis of most extensive diagenetic features (excluding evaporite diagenesis and dolomitization) from the Amoco #1 Nordling and Amoco #3 Cohen C. Width of features indicates relative abundance. Eogenetic refers to early diagenesis that took place in waters that are affected by near-surface conditions. Mesogenetic refers to later diagenesis in waters that are buried deeply enough to be unaffected by near-surface processes. No overlap of diagenetic features was observed in any individual sample. These diagenetic features are common in many St. Louis and Ste. Genevieve cores in southwestern Kansas.

Reproduced with permission of the copyright owner. Further reproduction prohibited without permission.

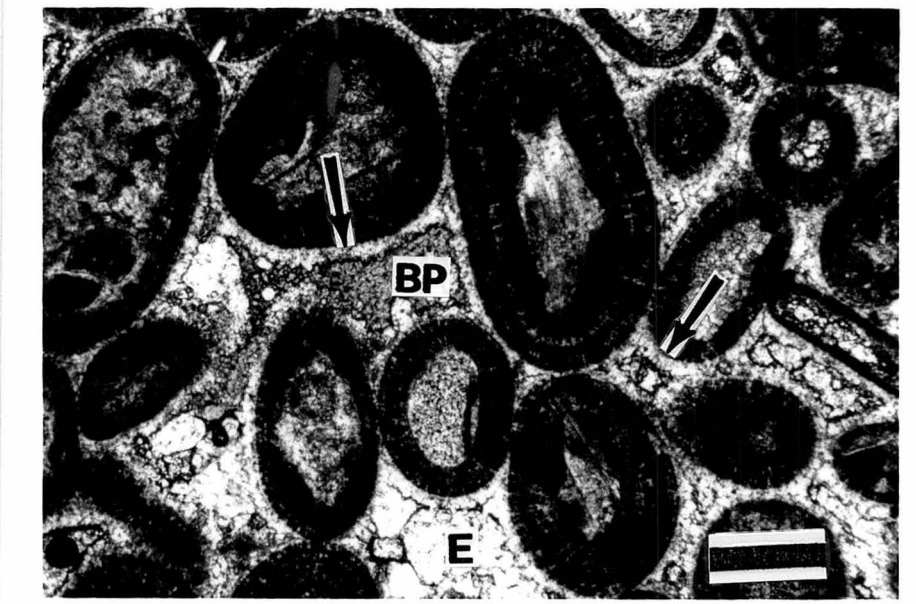


Figure 6.4 Photomicrograph of bladed isopachous calcite cement (arrows) below a truncation surface, most likely a hardground. FeIV cement (E) patchily occludes primary intergranular porosity (BP). The isopachous cement is absent above the truncation surface, suggesting it is a marine cement. Amoco #1 Nordling, 5742.3 ft core depth. Plane-polarized light. Scale bar is 0.25 mm.

indicate that this is a pendant cement formed in the meteoric vadose zone (cf. Longman, 1980). Brownish color in cements has been commonly attributed to trapped organic matter or high metal content (Goldstein, 1988).

Molds outlined by ooid cortices or micritic envelopes are cemented by minor amounts of non-ferroan calcite and more abundant unzoned ferroan calcite. Mineralogically metastable allochems were presumably dissolved by meteoric waters. The non-ferroan calcite in molds indicates dissolution was probably eogenetic (cf. Evamy, 1969).

Zoned calcite cements typically consist of alternating non-ferroan and ferroan calcite. Cement zones are best seen in syntaxial overgrowths on echinoderms where the zones are typically 10-40 μm thick. All cement zones may not be visible within an individual crystal. The most common cement zonation consists of two non-ferroan zones (NFeI and NFeIII) separated by a ferroan zone (FeII). Zoned cements locally penetrate adjacent grains, indicating they are precompactional (Fig. 6.5). These zones are commonly followed by an unzoned ferroan-calcite cement (Fig. 6.5). A tentative interpretation for the zoned cements is that NFeI was precipitated from oxidized near-surface ground waters during subaerial exposure events during St. Louis to Ste. Genevieve deposition. Upon further burial due to deposition of the Shore Airport, groundwaters became reduced resulting in precipitation of FeII. Subaerial erosion associated with the sub-Pennsylvanian unconformity removed significant amounts of Mississippian strata. The overlying Shore Airport Formation was completely removed in the Cohen and only 24 ft (7.3 m) remains in the Nordling. The erosion would promote the return of near-surface oxidized groundwaters resulting in the precipitation of NFeIII. A similar interpretation of zoned cements in Upper Mississippian strata from northeastern Kentucky was proposed by Niemann and Read (1988). It is possible, however, that zoned cements were precipitated prior to deposition of the

Reproduced with permission of the copyright owner. Further reproduction prohibited without permission.



Figure 6.5 Photomicrograph of a syntaxial overgrowth of calcite cement on an echinoderm. Zoned eogenetic NFeI, FeII, and NFeIII calcite cements (arrow) penetrate into a trilobite, indicating these cements are precompactional. NFeIV, unzoned ferroan calcite cement (F), does not penetrate into the trilobite and locally this cement heals fractured allochems, indicating it is a postcompactional burial cement. Amoco #1 Nordling, 5665.1 ft core depth. Plane-polarized light. Scale bar is 0.5 mm

Shore Airport Formation.

Mesogenesis

Unzoned ferroan-calcite cement postdates zoned cements (Fig. 6.5). Unzoned cement occurs as equant crystals and in the outer fringes of syntaxial overgrowths. Fractures and broken portions of allochems cemented by this ferroan cement indicate that it is postcompactional. These cements were not observed penetrating into adjacent grains. Unzoned ferroan cements probably precipitated away from near-surface oxidized waters following increased burial during the Pennsylvanian or later. Minor dissolution post-dates all other diagenetic events. Uncemented outer edges of cortices are slightly to moderately irregular, whereas edges of ooids protected by cement are relatively smooth. Dissolution may be related to hydrocarbon migration (Youle, 1990).

WHOLE-ROCK ISOTOPIC DATA

Carbon Isotopic Profiles

In the Nordling and Cohen cores, the mean values of whole-rock $\delta^{13}C$ in eolian strata, excluding microsamples containing rhizoliths and pendant cements, are 0.43 to 0.56 ‰ depleted (lighter) relative to interbedded subtidal strata (Table 6.1 and 6.2; Appendix 3). Standard deviations of eolian strata are slightly greater than for subtidal strata (Appendix 3). The means and standard deviations of samples from comparable environments are very similar between Nordling and Cohen cores (Appendix 3).

Some subtidal intervals display a minor shift to isotopically depleted carbon proximal to overlying eolian strata (Figs. 6.6, 6.7 and 6.8). Microsamples were taken from intervals containing such pedogenic features as rhizoliths and pendant cements. These vadose features are typically enriched in ^{12}C (cf. Goldstein, 1991) and commonly produce the most depleted $\delta^{13}C$ values. However, a sample of a thin

Reproduced with permission of the copyright owner. Further reproduction prohibited without permission.

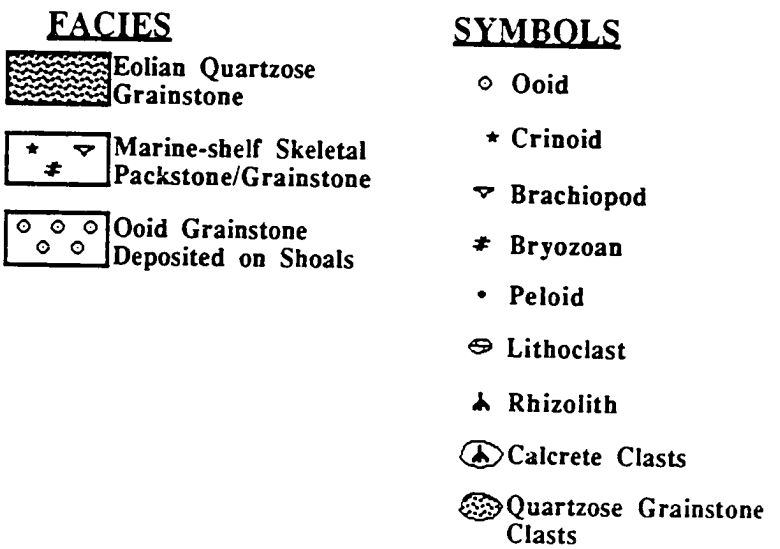


Figure 6.6 Key to grains and lithic symbols for Figures 6.7 to 6.10.

Reproduced with permission of the copyright owner. Further reproduction prohibited without permission.

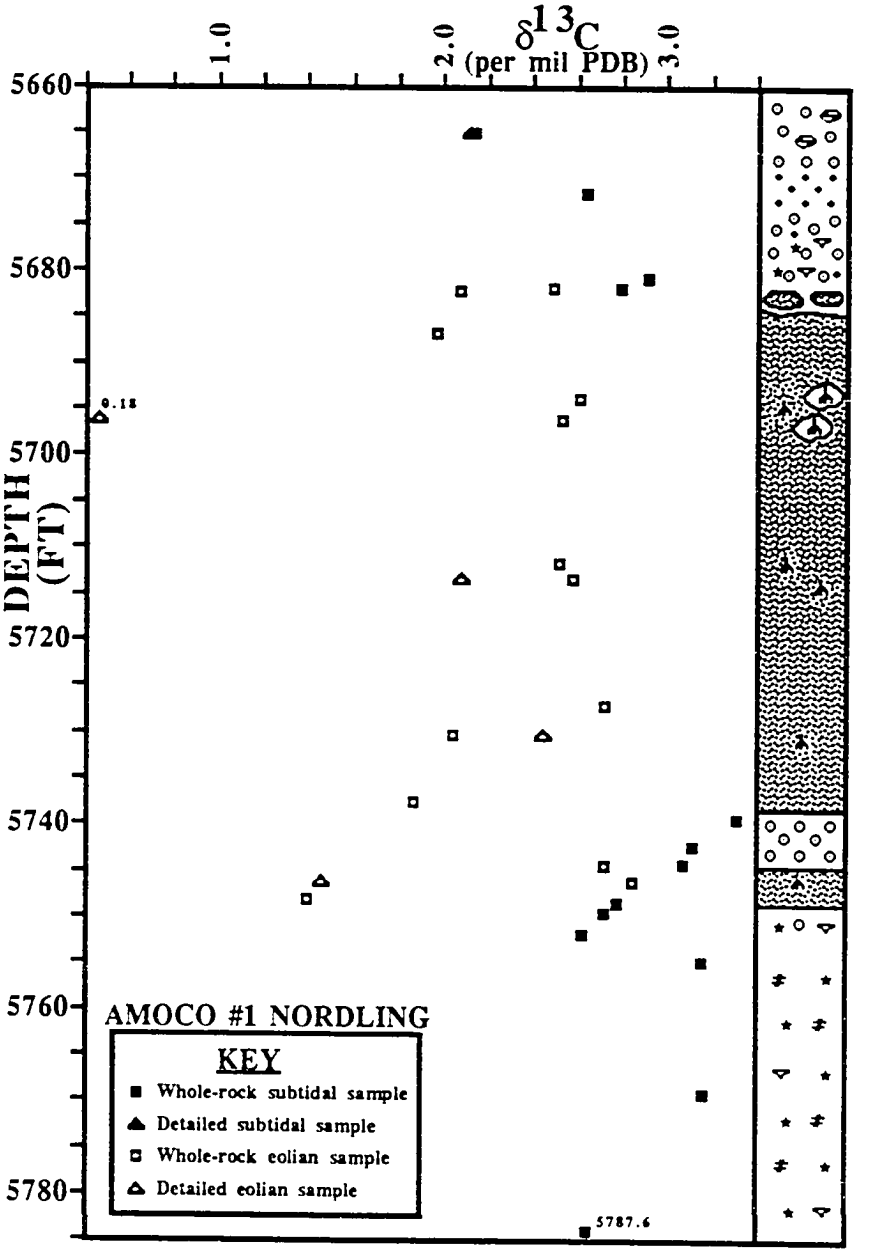


Figure 6.7 Carbon isotopic profile of the Hugoton Member of the St. Louis and Ste. Genevieve in the Amoco #1 Nordling. Note minor light carbon shift in subtidal strata below lower eolianite. Light carbon values at 5665.1 may correspond to a subaerial-exposure surface at the base of an eolianite at 5655.5 See Table 6.1 for $\delta^{13}C$ values. See Fig. 6.6 for key to grains and lithic symbols.

Reproduced with permission of the copyright owner. Further reproduction prohibited without permission.

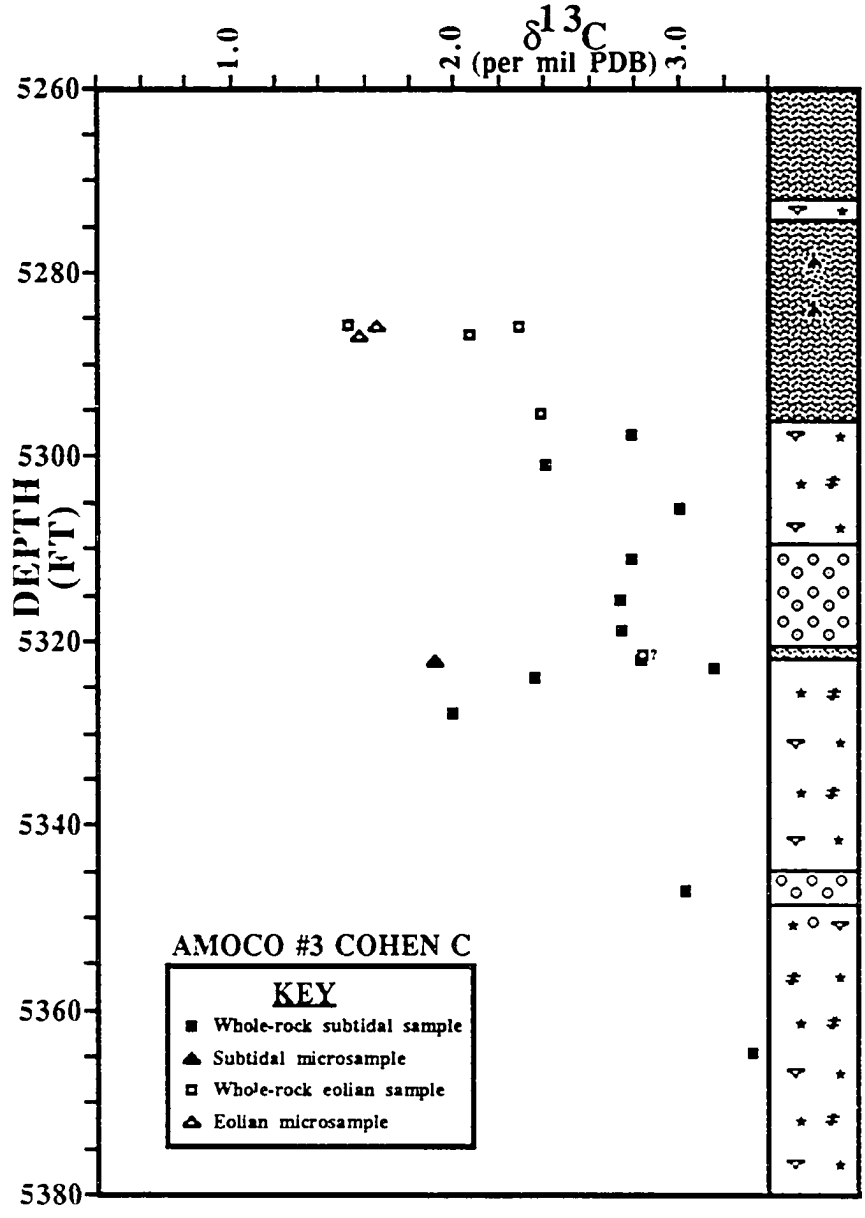


Figure 6.8 Carbon isotopic profile of the Hugoton Member of the St. Louis and Ste. Genevieve in the Amoco #3 Cohen C. A light carbon shift corresponds to an exposure surface (5322) marked by a calcrete. Eolian interpretation of sample at 5321.6 is questionable. See Table 6.2 for $\delta^{13}C$ values. See Fig. 6.6 for key to grains and lithic symbols.

Reproduced with permission of the copyright owner. Further reproduction prohibited without permission.

interval containing pendant cements, zoned cements (NFeI, FeII, NFeIII), and unzoned ferroan cements (FeIV, Amoco #1 Nordling, 5730.5B) was more positive than an adjacent stratum (5730.5A) that lacked significant cements (Fig. 6.7).

A t-test was used to test whether the means of eolian and subtidal isotopic values are different. Three assumptions need to be satisfied for the results of this test to be reliable: 1) independent random samples, 2) normal populations, and 3) a common variance for the two populations. Because detailed (purposeful) sampling has been excluded from the statistical analysis, the sampling is fairly random. Sampling at evenly spaced or random intervals was not attempted because it would require excessive number of samples and would be expensive. The t-test is fairly robust for the assumption of normality, providing the distributions are not too different from normal (Manly, 1986). Normality can be tested by examination of kurtosis and skewness of the populations (e.g., Remington and Schork, 1970). However, large samples are required to accurately estimate the parameters of strongly skewed or kurtotic populations (Sokal and Rohlf, 1981). Remington and Schork (1970, p. 221) suggest that skewness tests require sample sizes of at least 25. Therefore, normality in $\delta^{13}C$ with sample sizes of five to 14 (Table 6.1 and 6.2) cannot be reliably assessed. The assumption of common variance is not crucial, especially if the ratio of the true variances is within the limits of 0.4 to 2.5 (Manly, 1986). All ratios of sample variances are close to one (Appendix 3).

T-tests strongly suggest that means of eolian and subtidal strata are statistically separable (Appendix 3). The t-variable is -2.687 ($p = 0.011$) for Nordling samples, -2.545 ($p = 0.023$) for Cohen samples. However, these p-values (cf. Huntsberger and Billingsley, 1981) are tenuous because some t-test assumptions may have been violated. Based on samples from the Nordling and Cohen cores, mean $\delta^{13}C$ values of eolian and subtidal strata are separable at all α values less than 0.023. Inclusion of

Reproduced with permission of the copyright owner. Further reproduction prohibited without permission.

microsamples composed largely of rhizoliths in eolianites would make this difference even more significant.

Interpretation.– Eolian grainstones contain rhizoliths, pendant cements, and zoned meteoric phreatic cements in greater abundances than subtidal strata. The exclusion of microsamples composed largely of pedogenic components indicates the shift to isotopically depleted carbon is not due solely to visible vadose features. Even the eolian samples that lack vadose features are 0.43 to 0.56 ‰ depleted relative to subtidal strata. This suggests the shift is in part due to meteoric recrystallization or phreatic cements. Meteoric recrystallization may be either vadose or phreatic. The striking similarity of statistics for $\delta^{13}C$ between the two wells (Appendix 3) is attributed to similar styles of diagenesis and degrees of pedogenic alteration of coeval strata that are separated by approximately 40 miles (64 km).

The absence of pronounced shifts to isotopically depleted carbon in subtidal strata subadjacent to eolian strata may result from the lack of well-developed calcretes beneath exposure surfaces or their removal by erosion. More prominent negative carbon shifts are expected where paleosols are better developed. Microsamples composed largely of pedogenic components are typically more negative than surrounding whole-rock samples because rhizoliths concentrate ^{12}C derived from soil gas (Goldstein, 1991)

Oxygen Profiles

Mean values of $\delta^{18}O$ for eolian and subtidal strata are statistically similar in the Nordling (p-value = 0.592), but are less similar for Cohen samples (p-value = 0.072) (Fig. 6.9 and 6.10, Appendix 3). $\delta^{18}O$ values display greater standard deviation than $\delta^{13}C$ values (Appendix 3). Microsamples composed largely of rhizoliths are commonly more negative than whole-rock samples with respect to $\delta^{18}O$. Other samples with more negative values commonly contain greater amounts of unzoned

Reproduced with permission of the copyright owner. Further reproduction prohibited without permission.

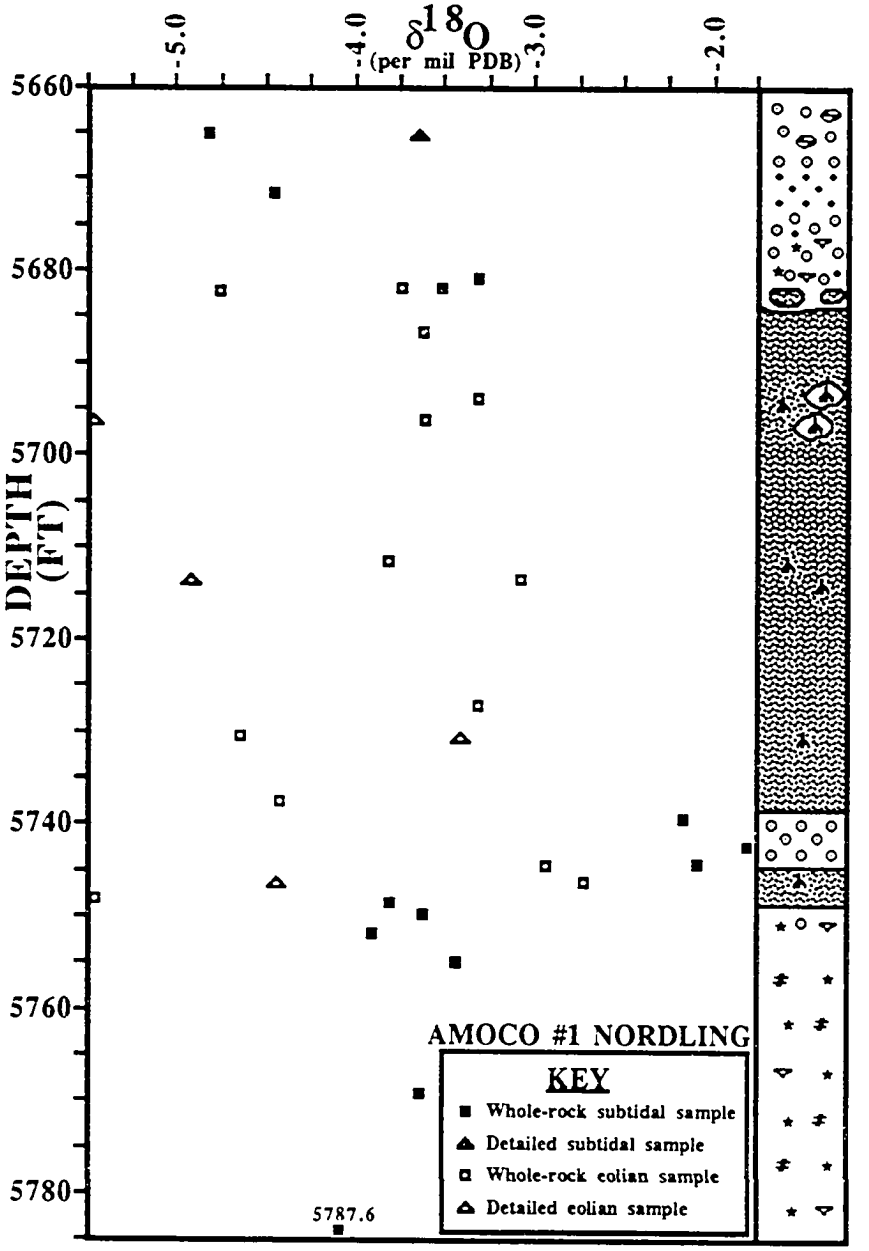


Figure 6.9 Oxygen isotopic profile of the Hugoton Member of the St. Louis and Ste. Genevieve in the Amoco #1 Nordling. See Table 6.1 for $\delta^{18}O$ values. See Fig. 6.6 for key to grains and lithic symbols.

Reproduced with permission of the copyright owner. Further reproduction prohibited without permission.

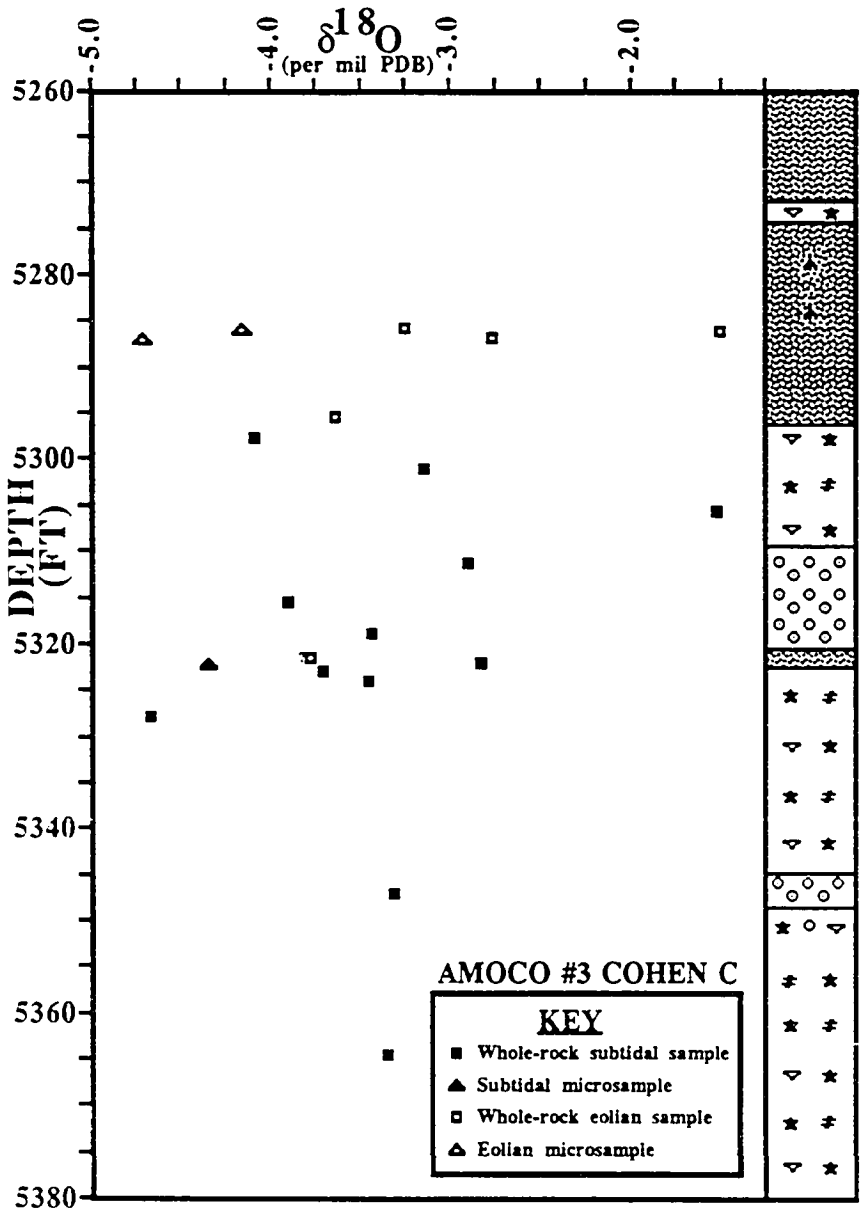


Figure 6.10 Oxygen isotopic profile of the Hugoton Member of the St. Louis and Ste. Genevieve in the Amoco #3 Cohen C. Eolian interpretation of sample at 5321.6 is questionable. See Table 6.2 for $\delta^{18}O$ values. See Fig. 6.6 for key to grains and lithic symbols.

Reproduced with permission of the copyright owner. Further reproduction prohibited without permission.

ferroan-calcite cement (FeIV).

Interpretation.– Microsamples composed largely of pedogenic components indicate that one source of more negative $\delta^{18}O$ values is rhizoliths. Additional sources of more negative $\delta^{18}O$ values are probably pendant cements and unzoned, ferroan burial cements. Rhizocretions and pendant cements precipitated from meteoric water that almost certainly had $\delta^{18}O$ values that were more negative than Mississippian seawater due to distillation and condensation fractionations in the atmosphere. Burial cements typically are more negative with respect to $\delta^{18}O$ than meteoric cements largely due to increased temperature with depth (e.g., Choquette and James, 1987).

The statistically similar mean values of $\delta^{18}O$ in eolian and subtidal strata probably result from similar diagenesis. The higher variation of $\delta^{18}O$ values compared to $\delta^{13}C$ values is probably the result of inhomogeneity of common unzoned ferroan (burial) cement, and volumetrically minor rhizoliths and pendant cements. Variation of subtidal $\delta^{18}O$ values is probably largely a function of amount of unzoned ferroan (burial) cements.

In the Nordling core, ooid grainstone samples between the two eolianites contain $\delta^{18}O$ values that are substantially enriched (heavier) relative to most other samples due to abundance of marine cements or a lack of abundant unzoned ferroan cements. The sample from the 5742.3 ft (core depth) was taken immediately below a hardground that contains abundant isopachous bladed cements that are probably marine in origin. The whole-rock $\delta^{18}O$ value for this sample is -1.80 ‰, consistent with Mississippian marine values estimated from brachiopods (-2.3 to -1.7 ‰) from the Lake Valley Formation (Osagean) in New Mexico (Brand, 1982). Meyers and Lohmann (1985) estimated Mississippian marine ($\delta^{13}C$ 4.0 ‰ PDB, $\delta^{18}O$ -1.5 ‰) values from analyses of Lake Valley micrite, marine cement, and crinoid skeletal fragments. In addition, $\delta^{18}O$ values at the Nordling hardground are more positive than surrounding

Reproduced with permission of the copyright owner. Further reproduction prohibited without permission.

values; this is consistent with whole-rock isotope trends across marine-cemented Jurassic hardgrounds (cf. Marshall and Ashton, 1980).

Carbon-Oxygen Crossplots

Plots of carbon versus oxygen stable isotopes indicate the range of $\delta^{13}C$ is smaller than the range in $\delta^{18}O$ (Figs. 6.11 and 6.12). The Nordling crossplot suggests some covariance of carbon and oxygen values (Fig. 6.11). Most eolian populations are distinctly separate from subtidal populations, with the exception of the thin eolian unit sampled from the Cohen well (Fig. 6.12).

Interpretation.– The small variation in $\delta^{13}C$ values is attributed to the lack of well-developed calcretes that concentrate ^{12}C in pedogenic features such as rhizoliths. The larger variation in $\delta^{18}O$ may be due to inhomogeneities in common unzoned ferroan (burial) calcite cements, and volumetrically minor rhizoliths and pendant cements. The small variation in carbon isotopes versus oxygen is opposite the trend observed by Allan and Matthews (1982). The covariance in the Nordling core (Fig. 6.11) could be the result of mixing of different diagenetic components (Allan and Matthews, 1982; Given and Lohmann, 1986). Some of this covariance is the result of depleted $\delta^{13}C$ and $\delta^{18}O$ values of microsamples composed largely of rhizoliths. The covariance could also result from alteration in the mixing zone, but this is not a unique solution for carbonates with cements from multiple diagenetic environments (Allan and Matthews, 1982; cf. Given and Lohmann, 1986).

Eolian samples are typically distinct from subtidal samples largely because of depleted $\delta^{13}C$ values in eolian strata. The difference in eolian and subtidal $\delta^{13}C$ values is obvious on a carbon-oxygen crossplot; it is less apparent on carbon profiles. Possible sources for the isotopically depleted carbon values include rhizoliths, pendant cements (volumetrically minor), zoned (meteoric) cements, or possibly

Reproduced with permission of the copyright owner. Further reproduction prohibited without permission.

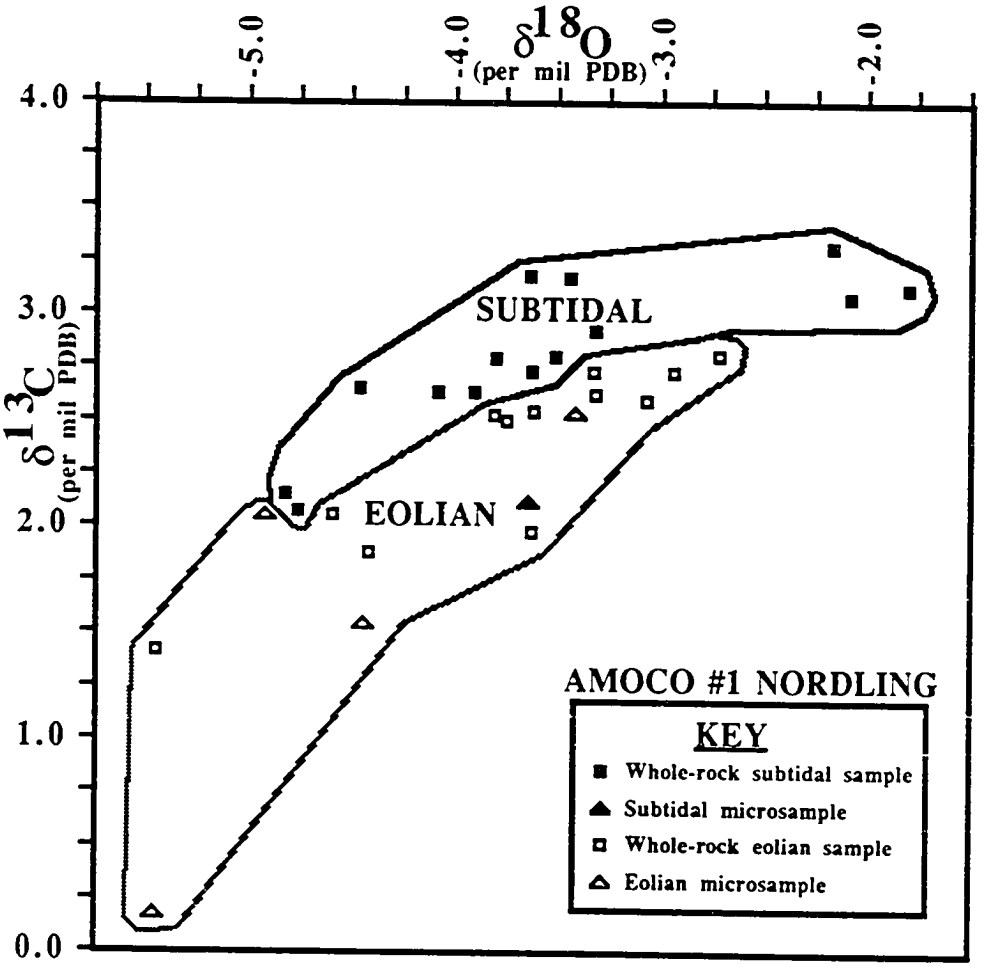


Figure 6.11 Carbon-oxygen crossplot from the Amoco #1 Nordling. Eolian and subtidal samples plot separately mainly due to lighter $\delta^{13}C$ values in eolian strata.

Reproduced with permission of the copyright owner. Further reproduction prohibited without permission.

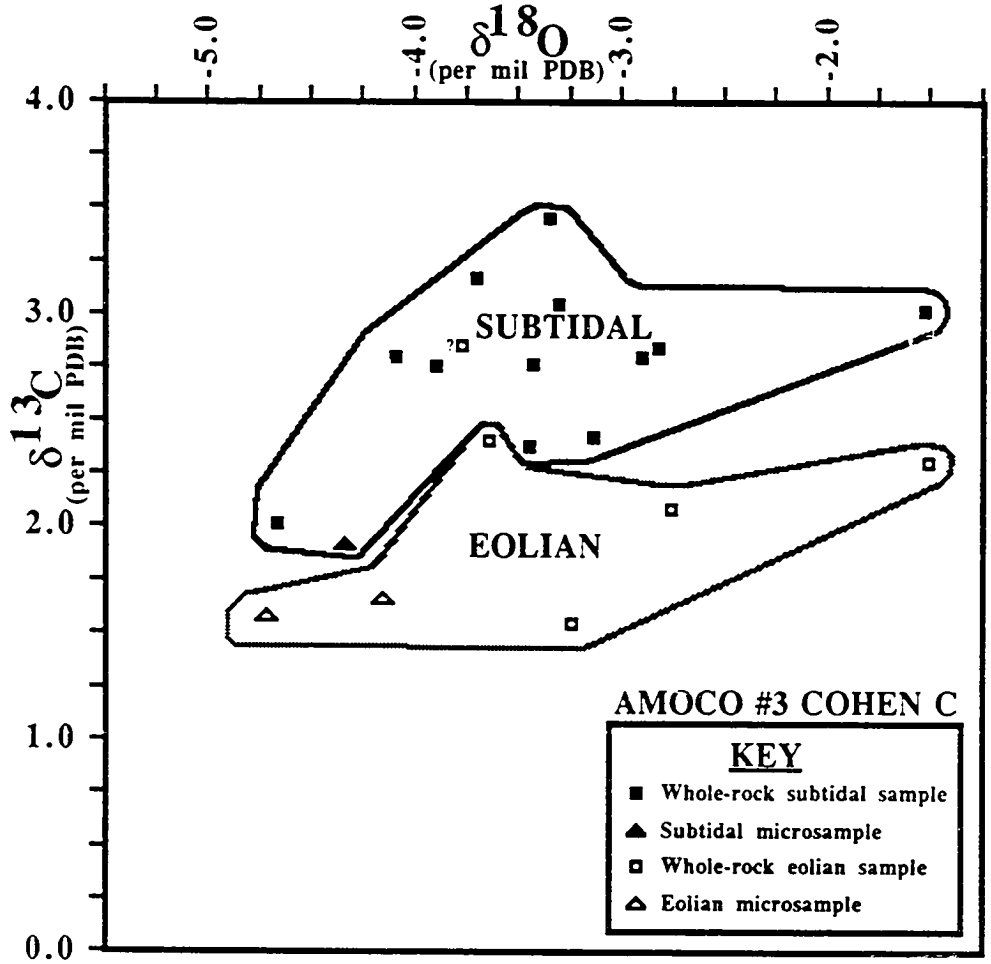


Figure 6.12 Carbon-oxygen crossplot from the Amoco #3 Cohen C. Eolian and subtidal samples plot separately except for the thin eolian? (5321.6 ft) unit in the Stevens Member.

Reproduced with permission of the copyright owner. Further reproduction prohibited without permission.

recrystallization. Whereas most eolian populations plot separately, values from the thin eolian unit in the Cohen plot within the subtidal population. One possible explanation is that the unit is not eolian. However, the presence of a calcrete paleosol overlain by vaguely coarsening-upward strata that are interpreted as possible climbing translatent stratification suggest an eolian origin. Evidence for eolian deposition, however, is not conclusive. If it is eolian, then it must have had a diagenetic history similar to subtidal strata. A short time of exposure or an arid climate would limit early diagenesis that is needed to produce isotopically depleted carbon values. Additionally, if vegetation was unable to stabilize the mobile substrate prior to transgression, then an abundant source of ^{12}C was unavailable.

A carbon-oxygen crossplot of samples from both the Amoco #1 Nordling and Amoco #3 Cohen C indicates that eolian and subtidal values overlap slightly (Fig. 6.13). This suggests that isotopically differentiable eolian and subtidal groupings are site specific and that absolute values of $\delta^{13}C$ and $\delta^{18}O$ cannot be used to plot unknowns from other sites.

SUMMARY

1. Carbon profiles are useful in distinguishing eolian from subtidal strata. Excluding microsamples composed largely of pedogenic components, mean values of $\delta^{13}C$ are 0.43-0.56 ‰ more negative than adjacent subtidal strata. A t-test of eolian and subtidal $\delta^{13}C$ values suggests the two populations are statistically separable (p-values <0.023). Including microsamples composed largely of rhizoliths in eolianites would make the difference in means even more significant. Sources of isotopically depleted $\delta^{13}C$ in eolian strata include rhizoliths, pendant cements, and possibly zoned (meteoric) cements and recrystallized allochems.

2. Oxygen profiles are not useful in distinguishing eolian and subtidal strata. Eolian

Reproduced with permission of the copyright owner. Further reproduction prohibited without permission.

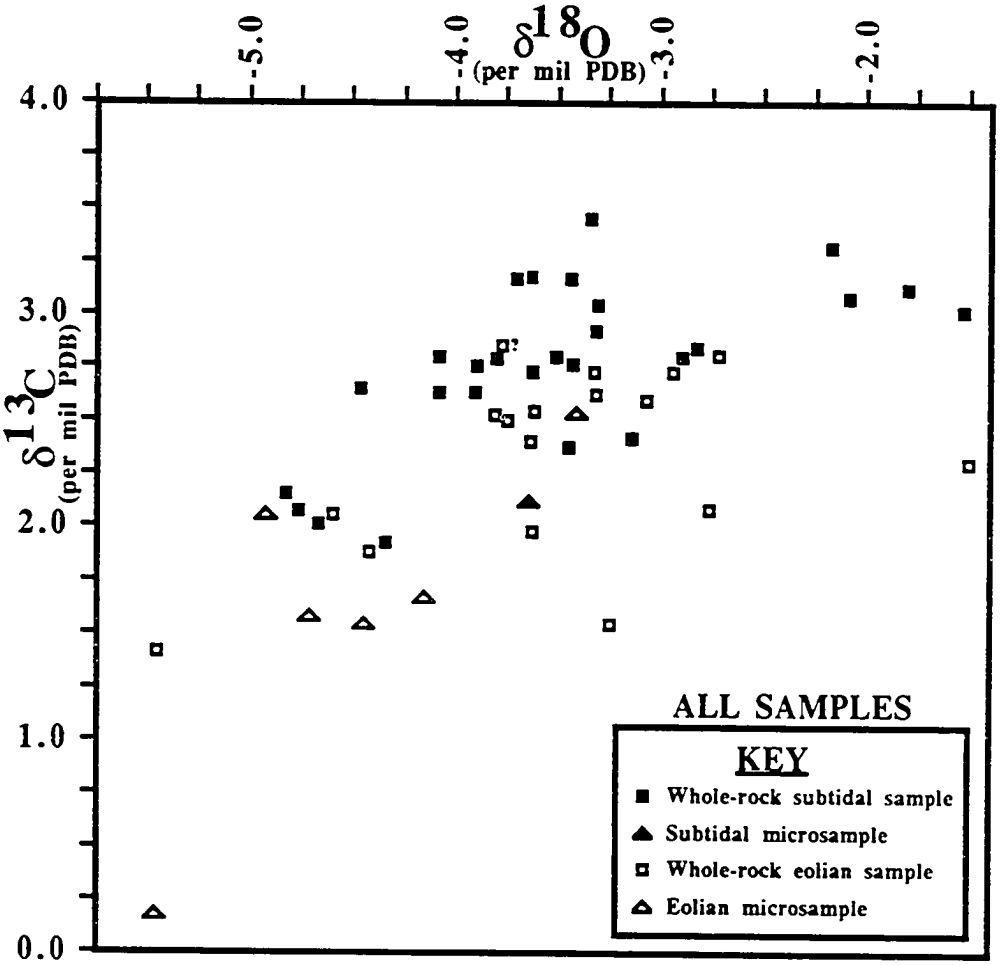


Figure 6.13 Carbon-oxygen crossplot from both the Amoco #1 Nordling and Amoco #3 Cohen C. Eolian and subtidal samples overlap slightly.

Reproduced with permission of the copyright owner. Further reproduction prohibited without permission.

and subtidal populations may have statistically similar means and relatively large standard deviations.

3. Carbon-oxygen crossplots typically show a separation of eolian and subtidal populations. Eolian strata have characteristically depleted $\delta^{13}C$ values. Samples display a relatively small range in $\delta^{13}C$ and a relatively wide range in $\delta^{18}O$ values, opposite trends reported by Allan and Matthews (1982). The small range in $\delta^{13}C$ results from widely scattered and poorly developed pedogenic features. The wide range in $\delta^{18}O$ is probably due to inhomogeneity of ferroan cements combined with erratic contributions from rhizoliths and pendant cements.

Reproduced with permission of the copyright owner. Further reproduction prohibited without permission.

CHAPTER 7
Conclusions and Suggestions for Further Research

CONCLUSIONS

1. Ten lithofacies are recognized in the St. Louis and Ste. Genevieve cores examined in this study. Depositional environments for each facies include: 1) restricted-shelf peloid grainstone/packstone; 2) shallow-subaqueous anhydrite; 3) evaporite solution-collapse breccia; 4) dolomite from dolomitization of limestone, generally restricted shelf; 5) restricted-shelf lime mudstone; 6) subtidal to lower intertidal, restricted-shelf algal boundstone; 7) marine-shelf skeletal packstone/wackestone; 8) oolite shoal deposits of ooid grainstone/packstone; 9) tidal-flat fenestral packstone/wackestone; and 10) eolian quartzose grainstone.

2. The Hugoton Member of the St. Louis is predominantly dolomitic peloid grainstone/packstone, anhydrite, breccia, dolomitic lime mudstone, dolomite, and algal boundstone facies. Facies of the Hugoton Member are distinct from the ooid-skeletal grainstones of the upper Salem Limestone.

3. The Stevens Member of the St. Louis is predominantly skeletal packstone/wackestone with shoaling-upward cycles capped by oolitic grainstones and packstones. A thin quartzose grainstone, not easily recognized on logs, occurs near the top of the St. Louis Member in many areas. Stevens facies are readily distinguished from dolomitized carbonate and anhydrite of the Hugoton Member.

4. The Ste. Genevieve is typified by quartzose grainstone interbedded with oolitic and peloid grainstone and packstones and with skeletal packstone and wackestone. The St. Louis-Ste. Genevieve boundary is placed at the base of the stratigraphically lowest prominent quartzose grainstone. Ste. Genevieve facies are distinct from interbedded argillaceous limestones and shales of the overlying Shore Airport Formation.

Reproduced with permission of the copyright owner. Further reproduction prohibited without permission.

5. St. Louis and Ste. Genevieve Limestones can be subdivided into seven depositional sequences (S1 to S7). S1 and S2 are relatively thick, subtidally-dominated sequences separated by a type 2 sequence boundary without widespread evidence of subaerial exposure. S3 through S7 are relatively thin, eolian-dominated sequences bounded by subaerial-exposure surfaces. Eolian carbonates form the base of S3 through S7 and are overlain by subtidal carbonates.

6. Calcretes and eolianites directly affecting subtidal deposits with no intervening beach or tidal flat strata indicate a drop in relative sea level. Approximate average durations of St. Louis and Ste. Genevieve sequences is 0.6 to 1.0 m.y. Cycle duration and the presence of Visean glaciation in Gondwanaland suggests the St. Louis and Ste. Genevieve sequences may have formed as a result of glacioeustatic sea-level changes.

7. St. Louis and Ste.Genevieve sequences S1 to S7 are interpreted as a progradational to aggradational sequence set based on an upward decrease in sequence thickness and numerous exposure surfaces and eolianites in S3 to S7. Progradation or aggradation of these sequences was facilitated by the overall lowering of relative sea level during the Late Mississippian. This drop of relative sea level probably took place over a 10 to 30 m.y. period, a duration consistent with a decrease in seafloor spreading rates or in mid-oceanic ridge length. Greater Visean and Namurian ice volumes and Late Mississippian-Early Pennsylvanian tectonism may also have contributed.

8. Whole-rock carbon isotopic profiles are useful in distinguishing eolian from subtidal strata. Excluding microsamples composed largely of rhizoliths and vadose cement, mean values of $\delta^{13}C$ are 0.43 to 0.56 ‰ more negative than adjacent subtidal strata. A t-test of eolian and subtidal $\delta^{13}C$ values indicates the two populations are statistically separable (p-values <0.023). Including light-carbon samples of rhizoliths in eolianites would make the difference in means even more significant. Sources of lighter $\delta^{13}C$ in eolian strata include rhizoliths, pendant cements, and possibly zoned

Reproduced with permission of the copyright owner. Further reproduction prohibited without permission.

(meteoric) cements and recrystallized allochems.

9. Whole-rock oxygen isotopic profiles are not useful in distinguishing eolian and subtidal strata. Eolian and subtidal populations may have statistically similar means and relatively large standard deviations.

10. Carbon-oxygen isotopic crossplots typically show a separation of eolian and subtidal populations. Eolian strata have characteristically lighter $\delta^{13}C$ values. Samples display a relatively small range in $\delta^{13}C$ and a relatively wide range in $\delta^{18}O$ values, opposite trends reported by Allan and Matthews (1982). The small range in $\delta^{13}C$ results from widely scattered and poorly developed pedogenic features. The wide range in $\delta^{18}O$ is probably due to inhomogeneity of ferroan cements with minor contributions from rhizoliths and pendant cements.

SUGGESTIONS FOR FUTURE RESEARCH

1. Correlation of sequences at a reservoir scale needs to be investigated. S2 through S6 are apparently recognizable and laterally continuous across the Big Bow Field in Stanton and Grant Counties (cf. Handford and Francka, 1991). Small-scale lateral variability of Stevens Member ooid grainstones as well as the eolianites and interbedded subtidal strata need to be better understood. The Damme Field (cf. Handford, 1988) might be a good candidate for such a study because of the availability of numerous cores at the Kansas Geological Society core facility in Lawrence, Kansas.

2. Correlation of parasequences in the St. Louis Limestone has not been attempted. This probably should be attempted first at the reservoir scale and then regionally.

3. Sedimentology of these units to the east in Colorado and to the south in the panhandles of Oklahoma and Texas is not well understood. Do the eolian-dominated sequences become more marine-dominated and thicken to the south toward the Anadarko basin?

4. A diagenetic study of the St. Louis and St. Genevieve Limestones will increase

Reproduced with permission of the copyright owner. Further reproduction prohibited without permission.

our understanding of diagenetic control of reservoirs. The abundance of grainstones and mud-poor packstones makes these carbonates ideal for diagenetic study. Diagenetic events could be tied into the sedimentological history proposed here. Cement stratigraphy, fluid inclusions, trace elements, and isotopic analyses should be utilized. Possible features useful in determining cross-cutting relationships in order to determine the paragenetic relationships of diagenetic events include: 1) solution-collapse breccia, 2) lithoclast conglomerates at the base of eolian units, 3) conglomerates on transgressive surfaces on top of eolian units, 4) Ste. Genevieve clasts in a conglomerate in the basal Shore Airport sandstone, and 5) reworked clasts above the sub-Pennsylvanian unconformity (cf. Youle, 1991).

5. A sequence stratigraphic framework for the Shore Airport Formation (Chesterian) needs to be established. Namurian Gondwanaland glaciation, cyclicity of Chesterian strata across much of North America, and abundant paleosols in the type section of the Shore Airport (Abegg, 1992a) indicates that numerous sequence or parasequence boundaries are present in the Shore Airport in southwestern Kansas.

6. The St. Louis and Ste. Genevieve Limestones in the Illinois basin need to be examined to determine if the depositional sequences of southwestern Kansas are recognizable.

7. Cross-stratified quartz-rich carbonates in the upper Beulah Limestone in the Front Range, Colorado (Ramirez, 1974), need to be examined to determine if they are eolianites. These strata are roughly coeval with eolian carbonates in the Hugoton embayment and the Illinois basin.

8. More detailed descriptions of Quaternary carbonate eolianites are needed (cf. MacKenzie, 1964; Ball, 1967; Land et al., 1967; Vacher, 1973; Semeniuk and Johnson, 1982; McKee and Ward, 1983; Semeniuk and Glassford, 1988), especially in the Bahamas. With the exception of White and Curran (1988), description of fine

Reproduced with permission of the copyright owner. Further reproduction prohibited without permission.

structure (cf. Hunter, 1977, 1981, 1985, 1989) in such carbonates is lacking. Quaternary carbonate eolian sand sheets apparently have not been recognized. If ancient carbonate eolianites are to be recognized, detailed characterization of modern analogs is needed.

9. Sulfates in the St. Louis of the Illinois basin have generally been interpreted as sabkha deposits (Jorgensen and Carr, 1973; Martorana, 1987). The thickness and purity of these deposits suggest a shallow-subaqueous origin.

10. Additional whole-rock isotope sampling of Upper Mississippian interbedded subtidal and eolian strata in southwestern Kansas. A larger sample would facilitate a t-test on pooled eolian and subtidal values to test if the method is site specific. The whole-rock method could also be tested on Ste. Genevieve carbonate eolianites in southern Indiana (cf. Hunter, 1989).

11. Influence of structure on sedimentation and stratigraphy. More closely spaced well and core data is needed to address this problem.

Reproduced with permission of the copyright owner. Further reproduction prohibited without permission.

REFERENCES CITED

Abegg, F. E., 1991, Sedimentology and lithostratigraphy of the Upper Mississippian Ste. Genevieve and St. Louis Limestones, southwestern Kansas, *in* Watney, W. L., Walton, A. W., Caldwell, C. D., Dubois, M. K., workshop organizers: Integrated studies of petroleum reservoirs in the Midcontinent: American Association of Petroleum Geologists Midcontinent Meeting Core Workshop, p. 1-33.

Abegg, F. E., in press (a), Lithostratigraphy of the Shore Airport Formation (Chesterian), southwestern Kansas, *in* Baars, D. L., ed., Revision of stratigraphic nomenclature in Kansas: Kansas Geological Survey Bulletin 230.

Abegg, F. E., in press (b), Lithostratigraphy of the Hugoton and Stevens Members of the St. Louis Limestone and the Ste. Genevieve Limestone (Upper Mississippian), southwestern Kansas, *in* Baars, D. L., ed., Revision of stratigraphic nomenclature in Kansas: Kansas Geological Survey Bulletin 230.

Abegg, F. E., and Grover, G. A., 1990, Calcrete profiles, porosity development, and cement stratigraphy of the Wagon Wheel (Pennsylvanian) Field, Ward County, Texas (abs.): American Association of Petroleum Geologists Bulletin, v. 74, p. 594-595.

Ahlbrandt, T. S., and Fryberger, S. G., 1982, Introduction to eolian deposits, *in* Scholle, P.A., and Spearing, D., eds., Sandstone depositional environments: American Association of Petroleum Geologists Memoir 31, p.11-47.

Allan, J. R., and Matthews, R. K., 1977, Carbon and oxygen isotopes as diagenetic and stratigraphic tools: surface and subsurface data, Barbados, West Indies: Geology, v. 5, p. 16-20.

Allan, J. R., and Matthews, R. K., 1982, Isotopic signatures associated with early meteoric diagenesis: Sedimentology, v. 29, p. 797-817.

Atherton, E., Collinson, C., and Lineback, J. A., 1975, Mississippian System, *in* Willman, H. B., Atherton, E., Buschbach, T. C., Collinson, C., Frye, J. C., Hopkins, M. E., Lineback, J. A., and Simon, J. A., eds., Handbook of Illinois stratigraphy: Illinois State Geological Survey Bulletin 95, p. 123-163.

Bagnold, R. A., 1954, The physics of blown sand and desert dunes: London, Methuen, 265p.

Ball, M. M., 1967, Carbonate sand bodies of Florida and the Bahamas: Journal of Sedimentary Petrology, v. 37, p. 556-591.

Ball, S. M., 1969, Predictions of effective porosity in some marine oolite deposits: Kansas Geological Survey Open-File Report 66-6, 6p.

Beebe, B. W., 1959a, Characteristics of Mississippian production in the northwestern Anadarko basin: Tulsa Geological Society Digest, v. 27, p. 190-205.

Reproduced with permission of the copyright owner. Further reproduction prohibited without permission.

Beebe, B. W., 1959b, Characteristics of Mississippian production in the northwestern Anadarko basin, *in* Moore, C. A., ed., Proceedings of the sixth biennial geological symposium: Norman, University of Oklahoma, p. 176-196.

Beeunas, M. A., and Knauth, L. P., 1985, Preserved stable isotopic signature of subaerial diagenesis in the 1.2-b.y. Mescal Limestone, central Arizona: implications for the timing and development of a terrestrial plant cover: Geological Society of America Bulletin: v. 96, p. 737-745.

Beier, J. A., 1987, Petrographic and geochemical analysis of caliche profiles in a Bahamian Pleistocene dune: Sedimentology, v. 34, p. 991-998.

Berger, A., Loutre, M. F., and Dehant, V., 1989a, Pre-Quaternary Milankovitchian frequencies: Nature, v. 342, p. 133.

Berger, A., Loutre, M. F., and Dehant, V., 1989b, Influence of the changing lunar orbit of the astronomical frequencies of pre-Quaternary insolation patterns: Paleoceanography, v. 4, p. 555-564.

Blakey, R. C., and Middleton, L. T., 1983, Permian shoreline eolian complex in central Arizona: dune changes in response to cyclic sea-level changes, *in* Brookfield, M. E., and Ahlbrandt, T. S., eds., Eolian sediments and processes: Elsevier, Amsterdam, p. 551-582.

Blatt, H., Middleton, G., and Murray, R., 1980, Origin of sedimentary rocks: 2nd edition, Englewood Cliffs, NJ, Prentice-Hall, 782p.

Brand, U., 1982, The oxygen and carbon isotope composition of Carboniferous fossil components: sea-water effects: Sedimentology, v. 29, p. 139-147.

Burchette, T. P., and Riding, R., 1977, Attached vermiform gastropods in Carboniferous marginal marine stromatolites and biostromes: Lethaia, v. 10, p. 17-28.

Caputo, M. V., and Crowell, J. C., 1985, Migration of glacial centers across Gondwanaland during Paleozoic Era: Geological Society of America Bulletin, v. 96, p. 1020-1036.

Cecil, C. B., 1990, Paleoclimate controls on stratigraphic repetition of chemical and siliciclastic rocks: Geology, v. 18, p. 533-536.

Choquette, P. W., and Pray, L. C., 1970, Geologic nomenclature and classification of porosity in sedimentary carbonates: American Association of Petroleum Geologists Bulletin, v. 54, p. 207-250.

Choquette, P. W., and James, N. P., 1987, Diagenesis #12. Diagenesis in limestones-3. The deep burial environment: Geoscience Canada, v. 14, p. 3-35.

Clair, J. R., 1948, Preliminary notes on lithologic criteria for identification and subdivision of the Mississippian rocks in western Kansas: Kansas Geological Society, 14 p.

Clair, J. R., 1949, Lithologic criteria of Mississippian rocks in western Kansas: World

Reproduced with permission of the copyright owner. Further reproduction prohibited without permission.

Oil, v. 129, no. 8, p. 61-66.
Clark, E. L., 1937, The St. Louis Formation of southwestern Missouri: Missouri Geol. Surv. and Water Resources, Biennial Report of State Geologist to the 59th General Assembly, Appendix 4, 13p.
Clemmensen, L. B., and Abrahamsen, K., 1983, Aeolian stratification and facies association in desert sediments, Arran basin (Permian), Scotland: Sedimentology, v. 30, p. 311-339.
Cluff, R. M., 1984, Carbonate sand shoals in the Middle Mississippian (Valmeyeran) Salem-St. Louis-Ste. Genevieve Limestones, Illinois basin, *in* Harris, P. M., ed., Carbonate sands-a core workshop: Society of Economic Paleontologists and Mineralogists Core Workshop No. 5, p. 94-135.
Collinson, C., Rexroad, C B., and Thompson, T. L., 1971, Conodont zonation of the North American Mississippian, *in* Sweet, W. C., and Bergstrom, S. M., eds., Symposium on conodont biostratigraphy: Geological Society of America Memoir 127, p. 353-394.
Collinson, J. D., 1986, Deserts, *in* Reading, H. G, ed., Sedimentary environments and facies: Oxford, Blackwell, p. 95-112.
Craig, H., 1957, Isotopic standards for carbon and oxygen and correction factors for mass spectrometric analysis of carbon dioxide: Geochemica et Cosmochimica Acta, v. 12, p. 133-149.
Crowell, J. C., 1978, Gondwanan glaciation, cyclothems, continental positioning, and climate change: American Journal of Science, v. 278, p. 1345-1372.
Dean W. E., Davies, G. R., and Anderson, R. Y., 1975, Sedimentological significance of nodular and laminated anhydrite: Geology, v. 3, p. 367-372.
DeVoto, R. H., 1980, Mississippian stratigraphy and history of Colorado, *in* Kent, H. C., and Porter, K. C., eds., Colorado geology: Rocky Mountain Association of Geologists, Denver, p. 57-70.
DeVoto, R. H., 1988, Late Mississippian paleokarst and related mineral deposits, Leadville Formation, central Colorado, *in* James, N. P., and Choquette, P. W., eds., Paleokarst: New York, Springer-Verlag, p. 278-305.
Dickson, J. A. D., 1966, Carbonate identification and genesis as revealed by staining: Journal of Sedimentary Geology, v. 36, p. 491-505.
Dill, R. F., Shinn, E. A., Jones, A. T., Kelly, K., Steinen, R. P., 1986, Giant subtidal stromatolites forming in normal salinity waters: Nature, v. 324, p. 55-58.
Dravis, J., 1978, Rapid and widespread generation of recent oolitic hardgrounds on a high energy Bahamian platform, Eleuthera bank, Bahamas: Journal of Sedimentary Petrology, v. 49, p. 195-208.
Driese, S. G., and Dott, R. H., Jr., 1984, Model for sandstone-carbonate "cyclothems" based on upper member of Morgan Formation (Middle Pennsylvanian) of northern Utah and Colorado: American Association of Petroleum

Reproduced with permission of the copyright owner. Further reproduction prohibited without permission.

Geologists Bulletin, v. 68, p. 574-597.
Dunham, R. J., 1962, Classification of carbonate rocks according to depositional texture, in Ham, W. E., ed., Classification of Carbonate Rocks-a Symposium: American Association of Petroleum Geologists Memoir 1, p. 108-121.
Ebanks, W. J., Brady, L. L., Heckel, P. H., O'Connor, H. G., Sanderson, G. A., West, R. R., Wilson, F. W., 1979, The Mississippian and Pennsylvanian (Carboniferous) Systems in the United States - Kansas: United States Geological Survey Professional Paper 1110Q, 30p.
Engleman, G., 1847, Remarks on the St. Louis Limestone: American Journal of Science, series 2, p. 119-120.
Esteban, M., and Klappa, C. F., 1983, Subaerial exposure environment, in Scholle, P. A., Bebout, D. G., and Moore, C. H., eds., Carbonate depositional environments: American Association of Petroleum Geologists Memoir 33, p. 1-54.
Evamy, D. B., 1969, The precipitational environment and correlation of some calcite cements deduced from artificial staining: Journal of Sedimentary Petrology, v. 39, p. 787-793.
Evans, G., Schmidt, V., Bush, P., Nelson, H., 1969, Stratigraphy and geologic history of the sabkha, Abu Dhabi, Persian Gulf: Sedimentology, v. 12, p. 145-159.
Folk, R. L., 1980, Petrology of sedimentary rocks: Austin, Texas, Hemphill Publishing Company, 184p.
Folk, R. L., and Pittman, J. S., 1971, Length-slow chalcedony: a new testament for vanished evaporites: Journal of Sedimentary Petrology, v. 41, p. 1045-1058.
Fryberger, S. G., and Schenk, C. J., 1981, Wind sedimentation tunnel experiments on the origins of aeolian strata: Sedimentology, v. 28, p. 805-821.
Fryberger, S. G., and Schenk, C. J., 1988, Pin stripe lamination: a distinctive feature of modern eolian and ancient sediments: Sedimentary Geology, v. 55, p. 1-15.
Fugitt, L. B., and Wilkinson, R. D., 1959, Eubank field, *in* Kansas oil and gas fields, vol. II, western Kansas: Kansas Geological Society, p. 13-20.
Garrett, P., 1970, Phanerozoic stromatolites: noncompetitive ecologic restriction by grazing and burrowing animals: Science, v. 169, p. 171-173.
Gebelein, C. D., 1969, Distribution, morphology, and accretion rate of Recent subtidal algal stromatolites: Journal of Sedimentary Petrology, v. 39, p. 49-69.
Gebelein, C. D., 1976, Open marine subtidal and intertidal stromatolites (Florida, the Bahamas and Bermuda), *in* Walter, M. R., ed., Stromatolites, Developments in Sedimentology 20: Amsterdam, Elsevier, p. 381-388.
Girty, G. H., 1940, Report on fossils of Mississippian age from well cores in western Kansas, *in* Lee, W., Subsurface Mississippian Rocks of Kansas: Kansas Geological Survey Bulletin 33, p. 97-114.

Reproduced with permission of the copyright owner. Further reproduction prohibited without permission.

Given, R. K., and Lohmann, K. C., 1986, Isotopic evidence for the early meteoric diagenesis of the reef facies, Permian reef complex of west Texas and New Mexico: Journal of Sedimentary Petrology, v. 56, p. 183-193.

Glennie, K. W., 1970, Desert sedimentary environments, developments in sedimentology 14: Amsterdam, Elsevier, 222p.

Goebel, E. D., 1968, Mississippian rocks of western Kansas: American Association of Petroleum Geologists Bulletin, v. 52, p. 1732-1778.

Goebel, E. D., and Stewart, G. F., 1979, Kansas, *in* Craig, L C., and Conner, C. W., eds., Paleotectonic investigations of the Mississippian System in the United States: United States Geological Survey Professional Paper 1010, p. 113-123.

Goldstein, R. H., 1988, Paleosols of Late Pennsylvanian cyclic strata, New Mexico: Sedimentology, v. 35, p. 777-803.

Goldstein, R. H., 1990, Petrographic and geochemical evidence for origin of paleospeleothems, New Mexico: implications for the application of fluid inclusions to studies of diagenesis: Journal of Sedimentology Petrology, v. 60, p. 282-292.

Goldstein, R. H., 1991, Stable isotope signatures associated with palaeosols, Pennsylvanian Holder Formation, New Mexico: Sedimentology, v. 38, p. 67-77.

Handford, C. R., 1988, Review of carbonate sand-belt deposition of ooid grainstones and application to Mississippian reservoir, Damme Field, southwestern Kansas: American Association of Petroleum Geologists Bulletin, v. 72, p. 1184-1199.

Handford, C. R., 1990, Mississippian carbonate eolianites in southwestern Kansas (abs.): American Association of Petroleum Geologists Bulletin, v. 74, p. 669.

Handford, C. R., and Francka, B. J., 1991, Mississippian carbonate-siliciclastic eolianites in southwestern Kansas, *in* Lomando, A. J., and Harris, P. M., eds., Mixed carbonate - siliciclastic sequences: Society of Economic Paleontologists and Mineralogists Core Workshop No. 15, p. 205-243.

Harland, W. B., Cox, A. V., Llewellyn, P. G., Pickton, C. A. G., Smith, A. G., and Walters, R., 1982, A geologic time scale: Cambridge, England, Cambridge University Press, 131p.

Hays, J. D., Imbrie, J., and Shackleton, N. J., 1976, Variations in the Earth's orbit: Pacemaker of the ice ages: Science, v. 194, p. 1121-1132.

Hoffman, P., 1976, Stromatolite morphogenesis in Shark Bay, western Australia, *in* Walter, M. R., ed., Stromatolites, developments in sedimentology 20: Elsevier, Amsterdam, p. 261-272.

Humphrey, J. D., Ransom, K. L., and Matthews, R. K., 1986, Early meteoric control of upper Smackover production, Oaks Field, Louisiana: American Association of Petroleum Geologists Bulletin, v. 70, p. 70-85.

Hunter, R. E., 1977, Basic types of stratification in small eolian dunes: Sedimentology, v. 24, p. 361-387.

Reproduced with permission of the copyright owner. Further reproduction prohibited without permission.

Hunter, R. E., 1981, Stratification styles in eolian sandstones: some Pennsylvanian to Jurassic examples from the western interior U.S.A., *in* Ethridge, F. G., and Flores, R. M., eds., Recent and ancient non-maine depositional environments: models for exploration: Society of Economic Paleontologists and Mineralogists Special Publication 31, p. 315-329.

Hunter, R. E., 1985, Subaqueous sand-flow cross-strata: Journal of Sedimentary Petrology, v. 55, p. 886-894.

Hunter, R. E., 1989, Eolianites in the Ste. Genevieve Limestone of southern Indiana: American Association of Petroleum Geologists Eastern Section Meeting Guidebook, 19p.

Huntsberger, D. V., and Billingsley, P., 1981, Elements of statistical inference: Boston, Allyn and Bacon, 505p.

Imbrie, J., and Imbrie, Z. L., 1980, Modeling the climatic response to orbital variations: Science, v. 207, p. 943-952.

Jorgensen, D. G., 1989, Paleohydrology of the Anadarko basin, central United States, *in* Johnson, K. S., ed., Anadarko basin symposium: Oklahoma Geological Survey Circular 90, p. 176-193.

Jorgensen, D., and Carr, D. D., 1973, Influence of cyclic deposition, structural features, and hydrologic controls on evaporite deposits in the St. Louis Limestone in southwestern Indiana, *in* Proceedings, eighth forum on geology of industrial minerals: Iowa Geological Survey Public Information Circular 5, p. 43-65.

Kammer, T. W., Brenckle, P. L., Carter, J. L., and Ausich, W. I., 1990, Redefinition of the Osagean-Meramecian boundary in the Mississippian stratotype region: Palaios, v. 5, p. 414-431.

Kaufman, J., Cander, H. S., Daniels, L. D., and Meyers, W. J., 1988, Cement stratigraphy and cementation history of the Burlington-Keokuk Formation (Mississippian), Illinois and Missouri: Journal of Sedimentary Petrology, v. 58, p. 312-326.

Kendall, C. G. St. C., Lerche, I., 1988, The rise and fall of eustasy, *in* Wilgus, C. K., Hastings, B. S., Kendall, C. G. St. C., Posamentier, H. W., Ross, C. A., and Van Wagoner, J. C., eds., Sea-level changes: an integrated approach: Society of Economic Paleontologists and Mineralogists Special Publication 42, p. 3-17.

Kerr, S. D., and Thomson, A., 1963, Origin of nodular and bedded anhydrite in Permian shelf sediments, Texas and New Mexico: American Association of Petroleum Geologists Bulletin, v. 47, p. 1726-1732.

King, P. B., 1948, Geology of the southern Guadalupe Mountains: United States Geological Survey Professional Paper 215, 183p.

Kinsman, D. J. J., 1965, Gypsum and anhydrite of recent age, Trucial Coast, Persian Gulf, *in* Rau, J. L., ed., Second Symposium on Salt: Northern Ohio Geological Society, v. 1, p. 302-326.

Reproduced with permission of the copyright owner. Further reproduction prohibited without permission.

Klappa, C. F., 1980, Rhizoliths in terrestrial carbonates; classification, recognition, genesis and significance: Sedimentology, v. 27, p. 613-629.
Kluth, C. F., and Coney, P. J., 1981, Plate tectonics of the Ancestral Rocky Mountains: Geology, v. 9, p. 10-15.
Kocurek, G., 1986, Origins of low-angle stratification in aeolian deposits, *in* Nickling, W. G., ed., Aeolian Geomorphology: Boston, Allen & Unwin, p.177-193.
Kocurek, G., 1988, First-order and super bounding surfaces in eolian sequences—bounding surfaces revisited: Sedimentary Geology, v. 56, p. 193-206.
Kocurek, G., 1988, First-order and super bounding surfaces in eolian sequences—bounding surfaces revisited: Sedimentary Geology, v. 56, p.193-206.
Kocurek, G., 1991, Interpretation of ancient eolian sand dunes: Annual Review of Earth and Planetary Sciences, v. 19, p. 43-75.
Kocurek, G., and Dott, R. H., 1981, Distinctions and uses of stratification types in the interpretation of eolian sand: Journal of Sedimentary Petrology, v. 51, p. 579-596.
Kocurek, G., and Nielson, J., 1986, Conditions favourable for the formation of warm-climate aeolian sand sheets: Sedimentology, v. 33, p. 795-816.
Kocurek, G., and Halvholm, in review, Eolian event stratigraphy--a conceptual framework: Geological Society of America Bulletin.
Kuenen, P. H., 1960, Experimental abrasion 4: eolian action: Journal of Geology, v. 68, p. 427-449.
Land, L. S., MacKenzie, F. T., and Gould, S. J., 1967, Pleistocene history of Bermuda: Geological Society of America Bulletin, v. 78, p. 993-1006.
Lane, H. R., and DeKeyser, T. L., 1980, Paleogeography of the late Early Mississippian (Tournaisian 3) in the central and southwestern United States, *in* Fouch, T. D., and Magathan, E. R., eds., Paleozoic paleogeography of the west-central United States: Rocky Mountain Society of Economic Paleontologists and Mineralogists, p. 149-162.
Laznicka, P., 1988, Breccias and coarse fragmentities: Amsterdam, Elsevier, 832p.
Lee, W., 1940, Subsurface Mississippian rocks of Kansas: Kansas Geological Survey Bulletin 33, 114 p.
Longman, M. W., 1980, Carbonate depositional textures from nearshore diagenetic environments: American Association of Petroleum Geologists Bulletin, v. 64, p. 461-487.
Loope, D. B., 1985, Episodic deposition and preservation of eolian sands: a late Paleozoic example from southeastern Utah: Geology, v. 13, p. 73-76.
Loucks, R. G., and Longman, M. W., 1982, Lower Cretaceous Ferry Lake Anhydrite, Fairway Field, east Texas: product of shallow-subtidal deposition, *in* Handford, C. R., Loucks, R. G., and Davies, G. R., eds., Depositional and diagenetic

Reproduced with permission of the copyright owner. Further reproduction prohibited without permission.

spectra of evaporites - a core workshop: Society of Economic Paleontologists and Mineralogists Core Workshop No. 3, p. 130-173.

Lucia, F. J., 1972, Recognition of evaporite–carbonate shoreline sedimentation, *in* Rigby, J. K., and Hamblin, W. K., eds., Recognition of ancient depositional environments: Society of Economic Paleontologists and Mineralogists Special Publication 16, p. 160-191.

MacKenzie, F. T., 1964, Bermuda Pleistocene eolianites and paleowinds: Sedimentology, v. 3, p. 52-64.

Maiklem, W. R., Bebout, D. G., and Glaister, R. P., 1969, Classification of anhydrite - a practical approach: Canadian Petroleum Geologists Bulletin, v. 17, p. 194-233.

Major, R. P., and Matthews, R. K., 1983, Isotopic composition of bank margins on Midway Atoll: amplitude constraint on post-early Miocene eustacy: Geology, v. 11, p. 335-338.

Manly, B. F. J., 1986, Multivariate statistical methods, a primer: London, Chapman and Hall, 159p.

Maples, C. G., 1992, Revision of Mississippian stratigraphic nomenclature in Kansas, *in* Baars, D. L., ed., Revision of stratigraphic nomeclature in Kansas: Kansas Geological Survey Bulletin 230.

Maples, C. G., and Waters, J. A., 1987, Redefinition of the Meramecian/Chesterian boundary (Mississippian): Geology, v. 15, p. 647-651.

Marshall, J. D., and Ashton, M., 1980, Isotopic and trace element evidence for submarine hardgrounds in the Jurassic of eastern England: Sedimentology, v. 27, p. 271-289.

Martorana, A., 1987, Lithology and depositional environment of the St. Louis Limestone, *in* Zupann, C. W., and Keith, B. D., eds., Geology and petroleum production of the Illinois basin v. 2, p. 125.

Marzolf, J. E., 1988, Controls on late Paleozoic and early Mesozoic eolian deposition of the western United States: Sedimentary Geology, v. 56, p. 167-191.

McKee, E. D., 1979, Ancient sandstones considered to be eolian, *in* McKee, E. D. ed., A study of global sand seas: United States Geological Survey Professional Paper 1052, p. 187-233.

McKee, E. D., and Ward, W. C., 1983, Eolian environment, *in* Scholle, P. A., Bebout, D. G., and Moore, C. H., eds., Carbonate depositional environments: American Association of Petroleum Geologists Memoir 33, p. 131-170.

McManus, D. A., 1959, Stratigraphy and depositional history of the Kearny Formation (Lower Pennsylvanian) in western Kansas [unpublished Ph.D. dissertation]: Lawrence, University of Kansas, 150p.

Merriam, D. F., 1963, The geological history of Kansas: Kansas Geological Survey Bulletin 162, 317p.

Meyers, W. J., and Lohmann, K. C., 1985, Isotopic geochemistry of regionally

Reproduced with permission of the copyright owner. Further reproduction prohibited without permission.

extensive calcite cement zones and marine components in Mississippian limestones, New Mexico, *in* Schneidermann, N., and Harris, P.M., eds., Carbonate cements: Society of Economic Paleontologists and Mineralogists Special Publication 36, p. 223-240.

Miall, A. D., 1984, Principles of sedimentary basin analysis: New York, Springer-Verlag, 490p.

Mitchum, R. M., and Van Wagoner, J. C., 1991, High-frequency sequences and their stacking patterns: sequence-stratigraphic evidence of high-frequency eustatic cycles: Sedimentary Geology, v. 70, p. 131-160.

Murray, R. C., 1964, Origin and diagenesis of gypsum and anhydrite: Journal of Sedimentary Petrology, v. 34, p. 512-523.

Newell , N. D., Purdy, E. G., and Imbrie, J., 1960, Bahamian oolitic sands: Journal of Geology, v. 68, p. 481-497.

Niemann, J. C., and Read, J. F., 1988, Regional cementation from unconformity-recharged aquifer and burial fluids, Mississippian Newman Limestone, Kentucky: Journal of Sedimentary Petrology, v. 58, p. 688-705.

Nodine-Zeller, D. E., 1981, Karst derived Early Pennsylvanian congomerate in Ness County, Kansas—subsurface Mississippian-Pennsylvanian boundary delineated in well core: Kansas Geological Survey Bulletin 222, 30p.

Pittman, J. G., 1985, Correlation of beds within the Ferry Lake Anhydrite of the Gulf Coastal Plain: Gulf Coast Association of Geological Societies Transactions, v. 35, p. 251-260.

Pittman, W. C., III, 1978, Relationship between eustacy and stratigraphic sequences of passive margins: Geological Society of America Bulletin, v. 89, p. 1389-1403.

Playford, P. E., and Cockbain, A. E., 1976, Modern algal stromatolites at Hamelin Pool, a hypersaline barred basin in Shark Bay, western Australia, *in* Walter, M. R., ed., Stromatolites, developments in sedimentology 20: Elsevier, Amsterdam, p. 389-412.

Playford, P. E., Cockbain, A. E., Druce E. C., and Wray J. L., 1976, Devonian stromatolites from the Canning basin, western Australia, *in* Walter, M. R., ed., Stromatolites, developments in sedimentology 20: Elsevier, Amsterdam, p. 543-564.

Posamentier, H. W., Jervey, M. T., and Vail, P. R., 1988, Eustatic controls on clastic deposition I—conceptual framework, *in* Wilgus, C. K., Hastings, B. S., Kendall, C. G. St. C., Posamentier, H. W., Ross, C. A., and Van Wagoner, J. C., eds., Sea-level changes: an integrated approach: Society of Economic Paleontologists and Mineralogists Special Publication 42, p.

Ramirez, M. L., 1974, Stratigraphy of the Mississippian System, Las Animas arch, Colorado: The Mountain Geologist: v. 11, p. 1-32.

Reproduced with permission of the copyright owner. Further reproduction prohibited without permission.

Remington, R. D., and Schork, M. A., 1971, Statistics with applications to the biological and health sciences: Englewood Cliffs, New Jersey, Prentice-Hall, 418p.

Rice, J. A., and Loope, D. B., 1991, Geological Society of America Bulletin, v. 103, p. 254-267.

Rittenhouse, G., 1972, Cross-bedding dip as a measure of sandstone compaction: Journal of Sedimentary Petrology, v. 42, p. 682-683.

Ross, C. A., and Ross, J. R. P., 1985, Late Paleozoic depositional sequences are synchronous and worldwide: Geology, v. 13, p. 194-197.

Ross, C. A., and Ross, J. R. P., 1988, Late Paleozoic transgressive-regressive deposition, *in* Wilgus, C. K., Hastings, B. S., Kendall, C. G. St. C., Posamentier, H. W., Ross, C. A., and Van Wagoner, J. C., eds., Sea-level changes: an integrated approach: Society of Economic Paleontologists and Mineralogists Special Publication 42, p. 227-248.

Rush, P. F., and Chafetz, H. S., 1990, Fabric-retentive, non-luminescent brachiopods as indicators of original $\delta^{13}C$ and $\delta^{18}O$ composition: Journal of Sedimentary Petrology, v. 60, p. 968-981.

Sando, W. J., 1974, Ancient solution phenomena in the Madison Limestone (Mississippian) of north-central Wyoming: United States Geological Survey, Journal of Research, v. 2, p. 133-141.

Sando, W. J., 1985, Revised Mississippian time scale, western interior region, conterminous United States: United States Geological Survey Bulletin, v. 1605-A, p. 15-26.

Sando, W. J., 1988, Madison Limestone (Mississippian) paleokarst: a geological synthesis, *in* James, N. P., and Choquette, P. W., eds., Paleokarst: New York, Springer-Verlag, p. 256-277.

Sarg, J. F., 1988, Carbonate sequence stratigraphy, *in* Wilgus, C. K., Hastings, B. S., Kendall, C. G. St. C., Posamentier, H. W., Ross, C. A., and Van Wagoner, J. C., eds., Sea-level changes: an integrated approach: Society of Economic Paleontologists and Mineralogists Special Publication 42, p. 155-182.

Saunders, W. B., and Ramsbottom, W. H. C., 1986, The mid-Carboniferous eustatic event: Geology, v. 14, p. 208-212.

Schreiber, B. C., Roth, M. S., and Helman, M. L., 1982, Recognition of primary facies characteristics of evaporites and the differentiation of these forms from diagenetic overprints, *in* Handford, C. R., Loucks, R. G., and Davies, G. R., eds., Depositional and diagenetic spectra of evaporites - a core workshop: Society of Economic Paleontologists and Mineralogists Core Workshop No. 3, p. 1-32.

Schreiber, B. C., 1985, Arid shorelines and evaporites, *in*, Reading, H. G., ed., Sedimentary Environments and Facies: Second Edition, Oxford, Blackwell Scientific Publications, p. 189-228.

Reproduced with permission of the copyright owner. Further reproduction prohibited without permission.

Scotese, C., 1986, Atlas of Paleozoic basemaps: Paleooceanographic mapping project: Austin, University of Texas Institute for Geophysics, Technical Report 66, p. 1-23.

Semeniuk, V., and Johnson, D. P., 1982, Recent and Pleistocene beach/dune sequences, western Australia: Sedimentary Geology, v. 32, p. 301-328.

Semeniuk, V., and Glassford, D. K., 1988, Significance of aeolian limestone lenses in quartz sand formations: interdigitation of coastal and continental facies, Perth basin, southwestern Australia: Sedimentary Geology, v. 57, p. 199-209.

Shearman, D. J., 1985, Syndepositional and late diagenetic alteration of primary gypsum to anhydrite, in Schreiber, B. C., and Harner, H. L., eds., Sixth international symposium on salt, volume 1: Alexandria, VA, The Salt Institute: p. 41-50.

Shinn, E. A., 1983, Tidal flat environment, *in* Scholle, P. A., Bebout, D. G., and Moore, C. H., eds., Carbonate depositional environments: American Association of Petroleum Geologists Memoir 33, p. 171-210.

Shumard, B. F., 1859, Observation on the geology of the county of Ste. Genevieve, Missouri: Transactions of the Academy of Science of St. Louis, v. 1, p. 404-405.

Sibley, D. F., and Gregg, J. M., 1987, Classification of dolomite rock textures: Journal of Sedimentary Petrology, v. 57, p. 967-975.

Sierverding, J. L., and Harris, P. M., 1991, Mixed carbonates and siliciclastics in a Mississippian paleokarst setting, southwestern Wyoming thrust belt, *in* Lamando, A. J., and Harris, P. M., 1991, Mixed carbonate-siliciclastic sequences: Society of Economic Paleontologists and Mineralogists Core Workshop, p. 541-568.

Sloss, L. L., 1963, Sequences in the cratonic interior of North America: Geological Society of America Bulletin, v. 74, p. 93-114.

Sloss, L. L., 1984, Comparative anatomy of cratonic unconformities, *in* Schlee, J. S., ed., Interregional unconformities and hydrocarbon accumulation: American Association of Petroleum Geologists Memoir 36, p. 1-6.

Sokal, R. R., and Rohlf, F. J., 1981, Biometry (second edition): New York, W. H. Freeman and Company, 859p.

Sporleder, J. C., 1991, Structural control of the distribution of subtidal to supratidal paleoenvironments of the Americus Limestone Member (lowermost bed) in eastern Kansas: Kansas Geological Survey Subsurface Geology Series 13, 58p.

Swanson, D. C., 1978, Deltaic deposits in the Pennsylvanian upper Morrow Formation of the Anadarko basin, *in* Hyne, N. J., ed., Pennsylvanian sandstones of the Mid-Continent: Tulsa Geological Society Special Publication 1, p. 155-168.

Thompson, T. L., 1986, Mississippian System, Paleozoic succession in Missouri, part 4: Missouri Geological and Land Survey Report of Investigations 70, 182p.

Thompson, T. L., and Goebel, E. D., 1963, Preliminary report on conodonts of the Meramecian Stage (Upper Mississippian) from the subsurface of western Kansas:

Reproduced with permission of the copyright owner. Further reproduction prohibited without permission.

Kansas Geological Survey Bulletin 165, 16 p.
Thompson, T. L., and Goebel, E. D., 1968, Conodonts and stratigraphy of the Meramecian Stage (Upper Mississippian) in Kansas: Kansas Geological Survey Bulletin 192, 56 p.
Vacher, H. L., 1973, Coastal dunes of younger Bermuda, *in*, Coates, D. R., ed., Coastal Geomorphology, Publications in Geomorphology: Binghamton, NY, SUNY Binghamton, p. 355-391.
Vail, P. R., Mitchum, R. M., Jr., Thompson, S., III, 1977, Global cycles of relative changes of sea level, *in* Payton, C. E., ed., Seismic stratigraphy - applications to hydrocarbon exploration: American Association of Petroleum Geologists Memoir 26, p. 83-98.
Vacher, H. L., 1973, Coastal dunes of younger Bermuda, *in* Coates, D. R., ed., Coastal geomorphology, publications in geomorphology: Binghamton, NY, SUNY Binghamton, p. 355-391.
Van Wagoner, J. C., Posamentier, H. W., Mitchum, R. M., Vail, P. R., Sarg. J. F., Louitt, T. S., Hardenbol, J., 1988, An overview of the fundamentals of sequence stratigraphy, *in* Wilgus, C. K., Hastings, B. S., Kendall, C. G. St. C., Posamentier, H. W., Ross, C. A., and Van Wagoner, J. C., eds., Sea-level changes: an integrated approach: Society of Economic Paleontologists and Mineralogists Special Publication 42, p. 39-45.
Van Wagoner, J. C., Mitchum, R. M., Campion, K.M., and Rahmanian, V. D., 1990, Siliciclastic sequence stratigraphy in well logs, cores, and outcrops: American Association of Petroleum Geologists, Methods in Exploration Series 7, 55p.
Veevers, J. J., and Powell, C. McA., 1987, Late Paleozoic glacial episodes in Gondwanaland reflected in transgressive-regressive depositional sequences in Euramerica: Geological Society of America Bulletin, v. 98, p. 475-487.
Veroda, V. J., 1959, Mississippian rocks of southwest Kansas, *in* Moore, C. A., ed., Proceedings of the sixth biennial geological symposium: Norman, University of Oklahoma, p. 143-175.
Videtich, P. E., and Matthews, R. K., 1982, Origin of discontinuity surfaces in limestones: isotopic and petrographic data, Pleistocene of Barbados, West Indies: Journal of Sedimentary Petrology: v. 52, p. 971-980.
Wagner, P. D., and Matthews, R. K., 1982, Porosity preservation in the upper Smackover (Jurassic) carbonate grainstone, Walker Creek Field, Arkansas; response of paleophreatic lenses to burial processes: Journal of Sedimentary Petrology, v. 52, p. 3-18.
Wanless, H. R., 1979, Limestone response to stress: pressure solution and dolomitization: Journal of Sedimentary Petrology, v. 49, p. 437-462.
Warren, J. K., 1989, Evaporite sedimentology, importance in hydrocarbon

Reproduced with permission of the copyright owner. Further reproduction prohibited without permission.

accumulation: Englewood Cliffs, New Jersey, Prentice-Hall, 285p.
Warren. J. K., 1991, Sulfate dominated sea-marginal and platform evaporitive settings: sabkhas and salinas, mudflats and salterns, *in* Melvin, J. L., Evaporites, petroleum and mineral resources, developments in sedimentology 50: Amsterdam, Elsevier, p. 69-188.
Warren, J. K., and Kendall, G C. St. C., 1985, Comparison of marine sabkhas (subaerial) and salina (subaqueous) evaporites: modern and ancient: American Association of Petroleum Geologists Bulletin, v. 69, p. 1013-1023.
White, B., and Curran, H. A., 1988, Mesoscale physical sedimentary structures and trace fossils in Holocene carbonate eolianites from San Salvador Island, Bahamas: Sedimentary Geology, v. 55, p. 163-184.
Wilson, I. G., 1971, Desert sandflow basins and a model for the development of ergs: Geographical Journal, v. 137, p. 180-199.
Wilson, I. G., 1973, Ergs: Sedimentary Geology, v. 10, p. 77-106.
Wray, J. L., 1977, Calcareous algae: Amsterdam, Elsevier, 185p.
Youle, J. C., 1990, Petrology and porosity distribution in the Upper Mississippian, Wendel pool, Gray County, Kansas: Compass, v. 67, p. 154-165.
Youle, J. C., 1991, Sequence stratigraphy of the lower Middle Pennsylvanian in the eastern Hugoton embayment of southwestern Kansas, *in* Watney, W. L., Walton, A. W., Caldwell, C. D., Dubois, M. K., workshop organizers: Integrated studies of petroleum reservoirs in the Midcontinent: American Association of Petroleum Geologists Midcontinent Meeting Core Workshop, p. 142-172.
Zeller, D. E., 1968, The stratigraphic succession in Kansas: Kansas Geological Survey Bulletin 189, 81p.

Reproduced with permission of the copyright owner. Further reproduction prohibited without permission.

APPENDIX 1

Core Descriptions

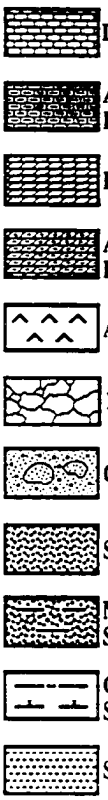
Thirteen cores were logged from southwestern Kansas. The lithology column indicates the either lithology (e.g. sandstone, silty shale) or or compositional percentages (e.g., 10 percent dolomite; 80 percent calcite; 10 percent siliciclastic sand). Included in the depth track are the lithostratigraphic units (FMS). Boundaries are based on core and log cross section correlations; scout cards are considered unreliable because of inconsistent criteria for boundary picks.

Right-hand track shows interpretations of shifts in depositional environments. Horizontal dashed lines represent shifts without accompanying deposition. Horizontal wavy lines are subaerial exposure surfaces or surfaces bracketing eolian strata. Abbreviations used include the following: SE - subaerial exposure, typically marked by calcretes or eolian strata; I - intertidal or tidally-influenced, fenestral porosity and possible tidal rhythmites occur locally; L - restricted lagoon/shelf, evidence of evaporites or absence of stenohaline marine fossils; SH - oolitic or skeletal shoal, grainstone to mud-poor packstone; SM - Shallow marine with evidence of at least intermittent agitation, above or near storm wave base (WB); M - Marine with little winnowing, typically wackestone deposited below storm wave base; AD - separates dysaerobic and anaerobic facies from overlying aerobic facies, only present in Kearny Formation (Morrowan). Depositional textures are also abbreviated: GR - Grainstone, PK - Packstone, WK - Wackestone, LM - Lime mudstone.

Reproduced with permission of the copyright owner. Further reproduction prohibited without permission.

APPENDIX 1. KEY TO CORE DESCRIPTIONS

LITHOLOGY



SYMBOLS

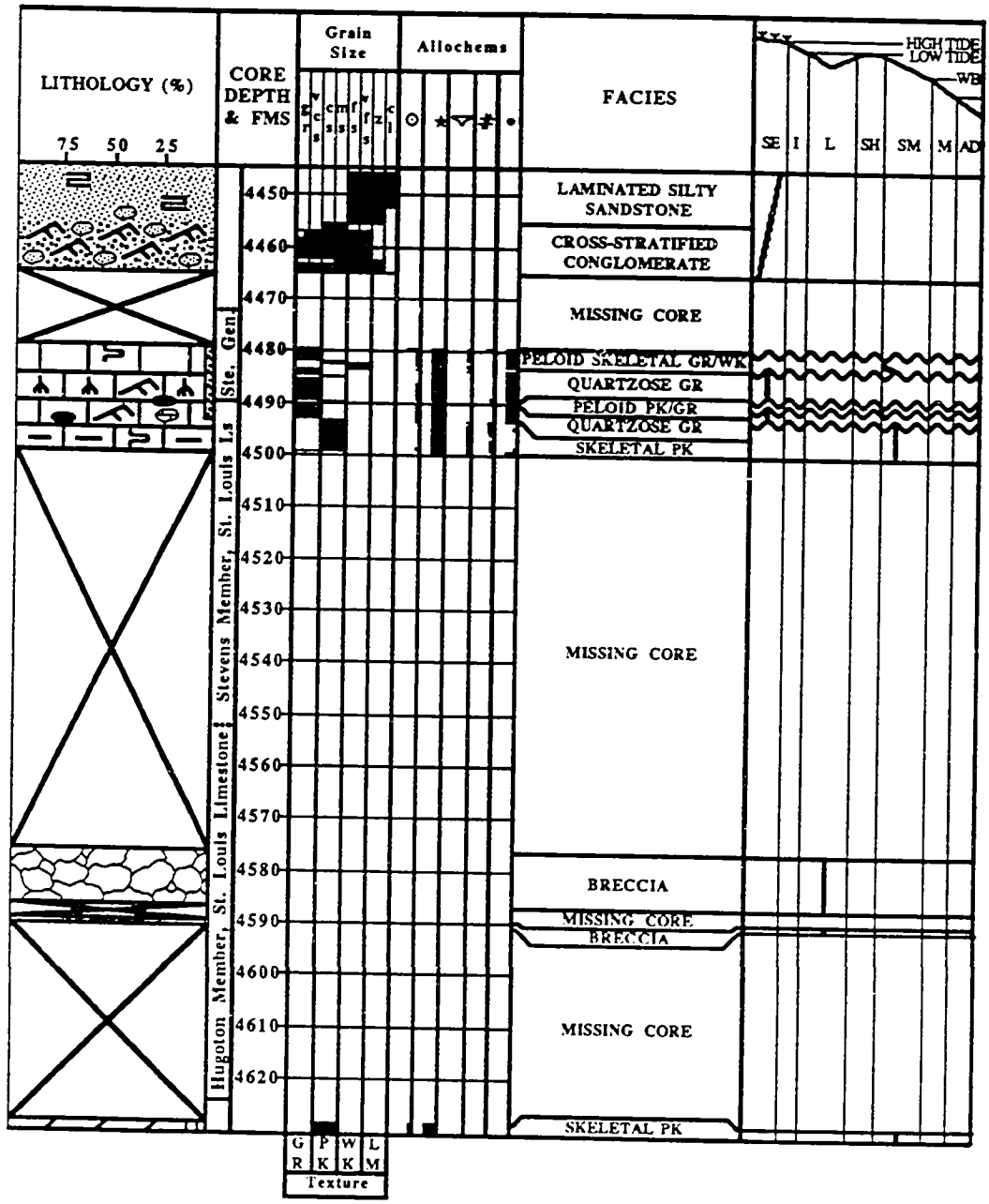
- Ooid
- Crinoid
- Brachiopod
- Bryozoan
- Peloid
- Nodular Chert
- Cross Stratification
- Lamination
- Fenestral Fabric
- Lithoclast
- Rhizolith
- Horizontal Burrow
- Vertical Burrow
- Stromatolites

ABUNDANCE



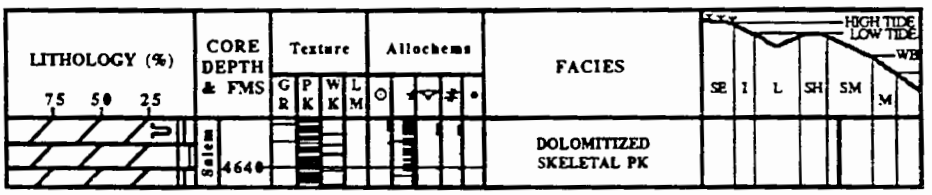
Reproduced with permission of the copyright owner. Further reproduction prohibited without permission.

ALMA #1 WATCHORN LOGAN CO. C SW NE 13-15S-33W



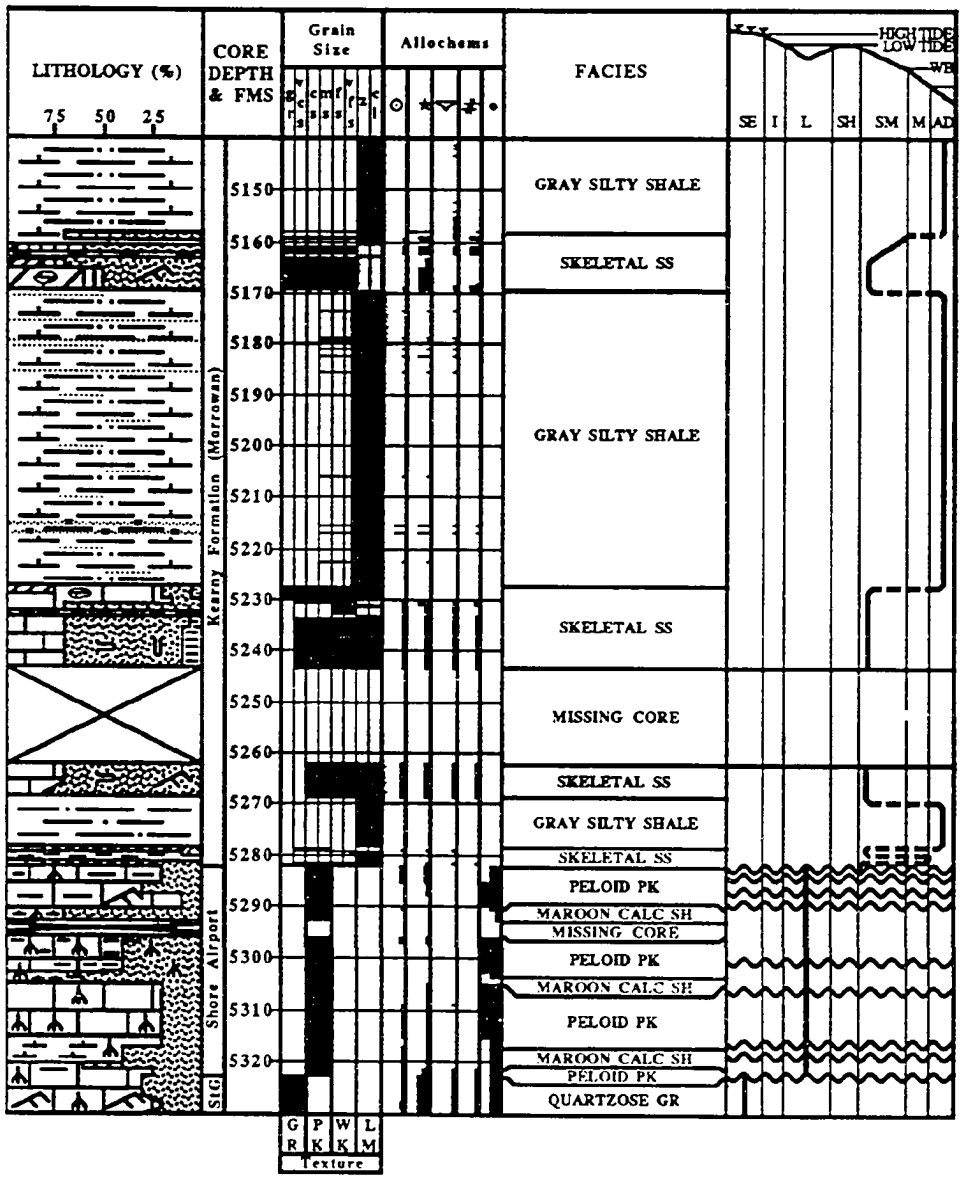
Reproduced with permission of the copyright owner. Further reproduction prohibited without permission.

ALMA #1 WATCHORN LOGAN CO. C SW NE 13-15S-33W



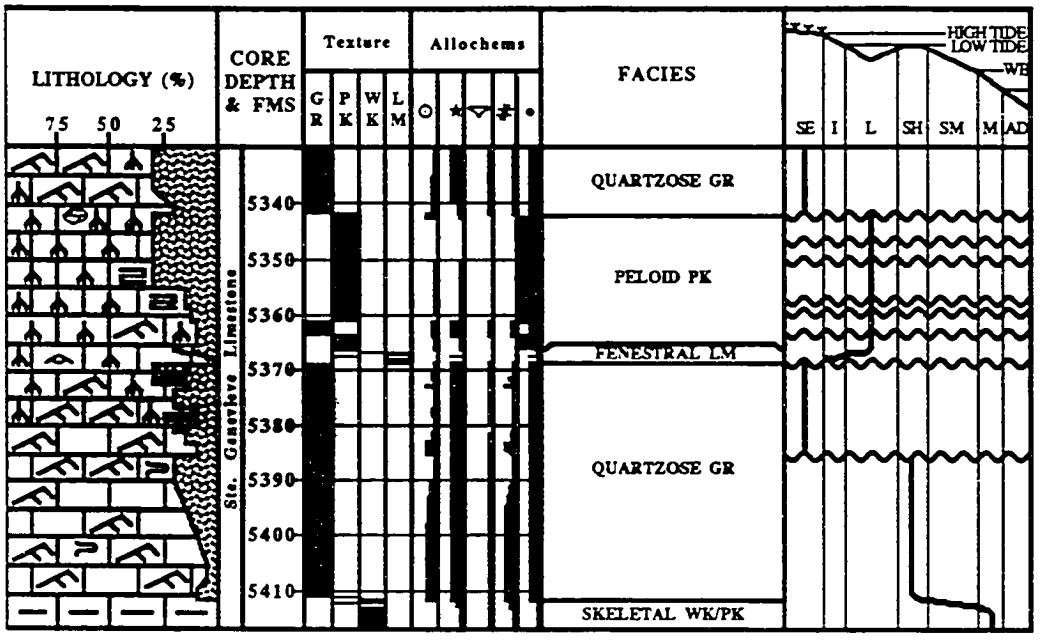
Reproduced with permission of the copyright owner. Further reproduction prohibited without permission.

AMOCO #1 BREEDING F MORTON CO. SW 34-31S-40W



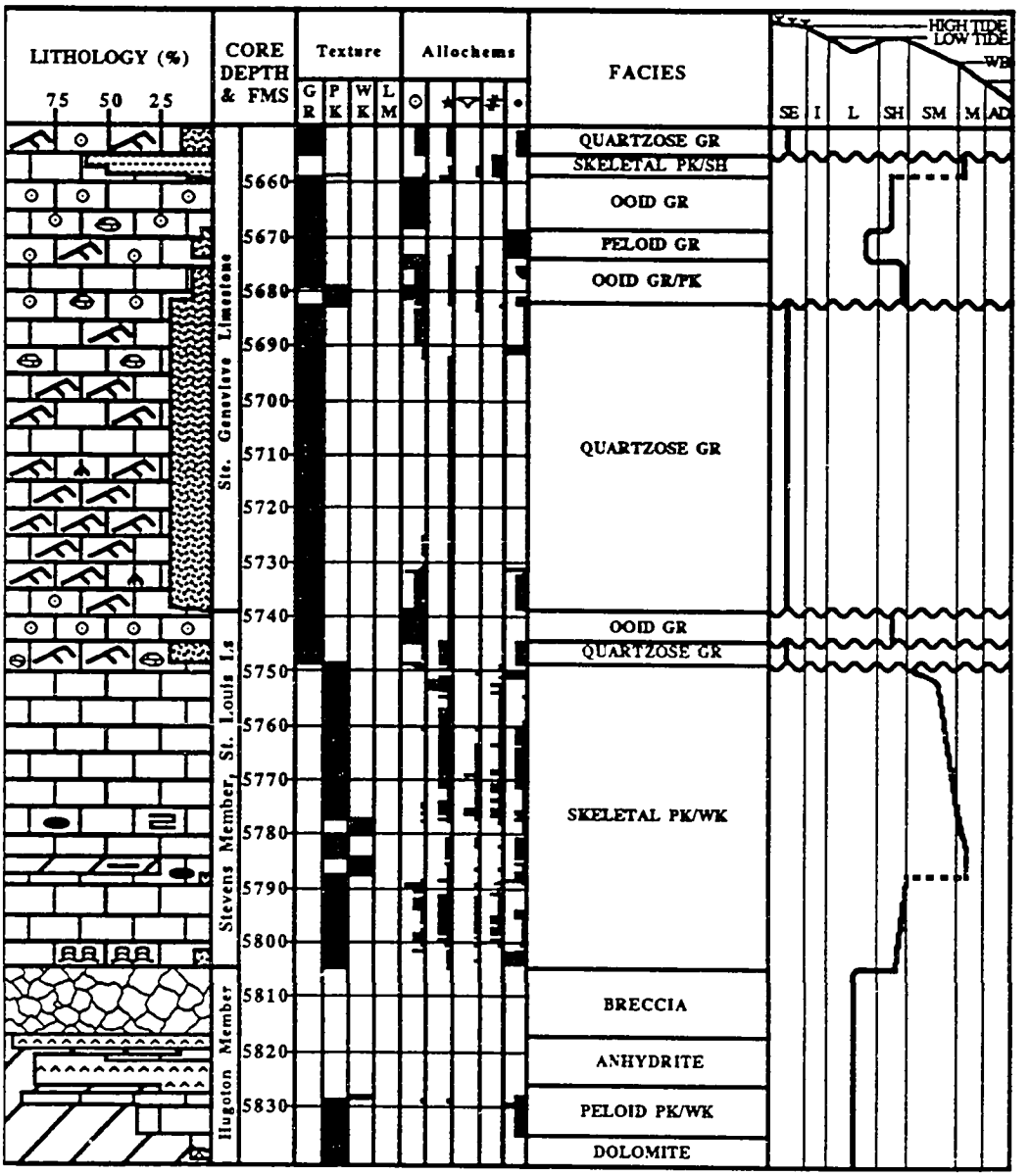
Reproduced with permission of the copyright owner. Further reproduction prohibited without permission.

AMOCO #1 BREEDING F MORTON CO. SW 34-31S-40W



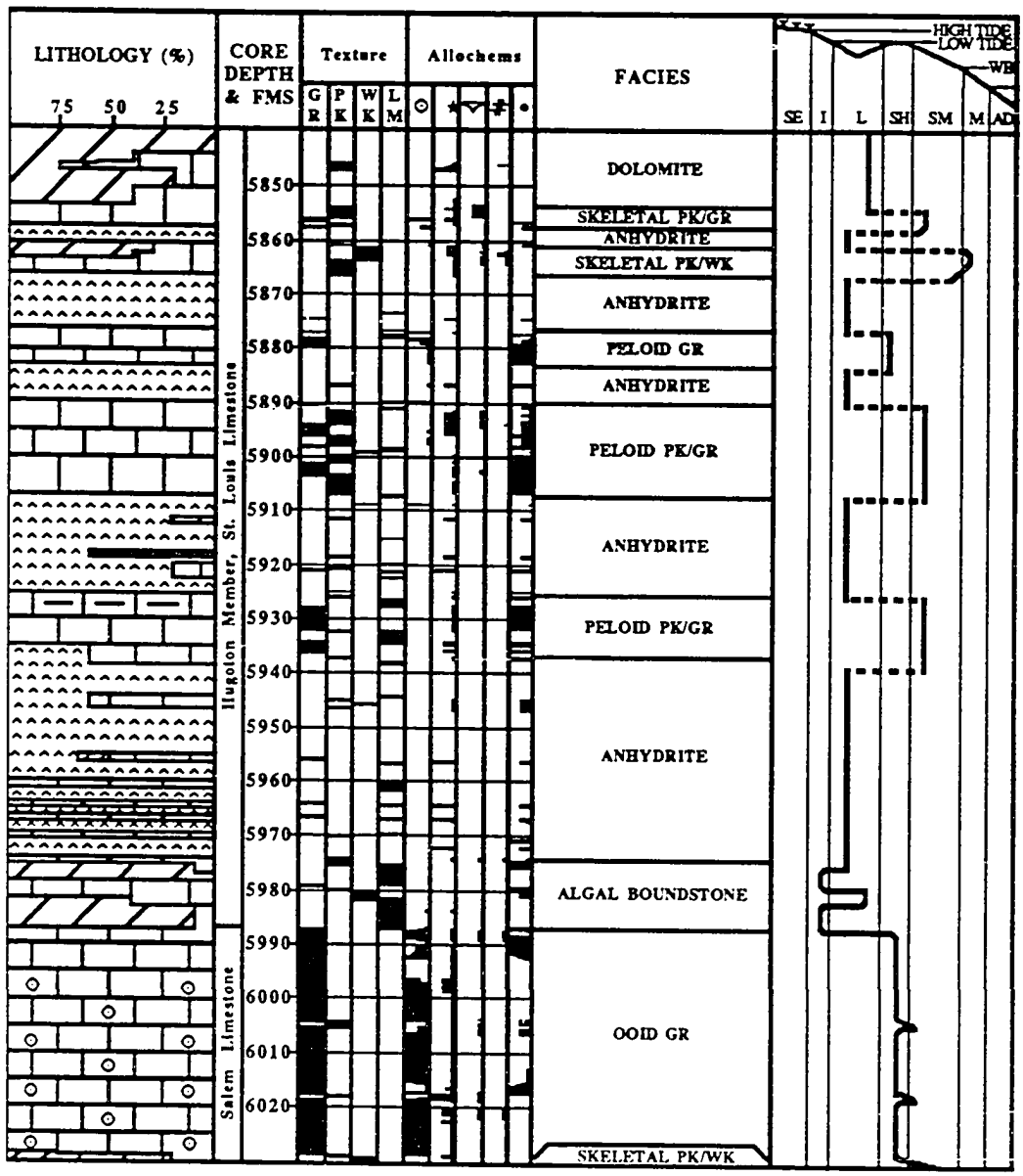
Reproduced with permission of the copyright owner. Further reproduction prohibited without permission.

AMOCO #1 NORDLING STANTON CO. SW SE NE 30-29S-39W



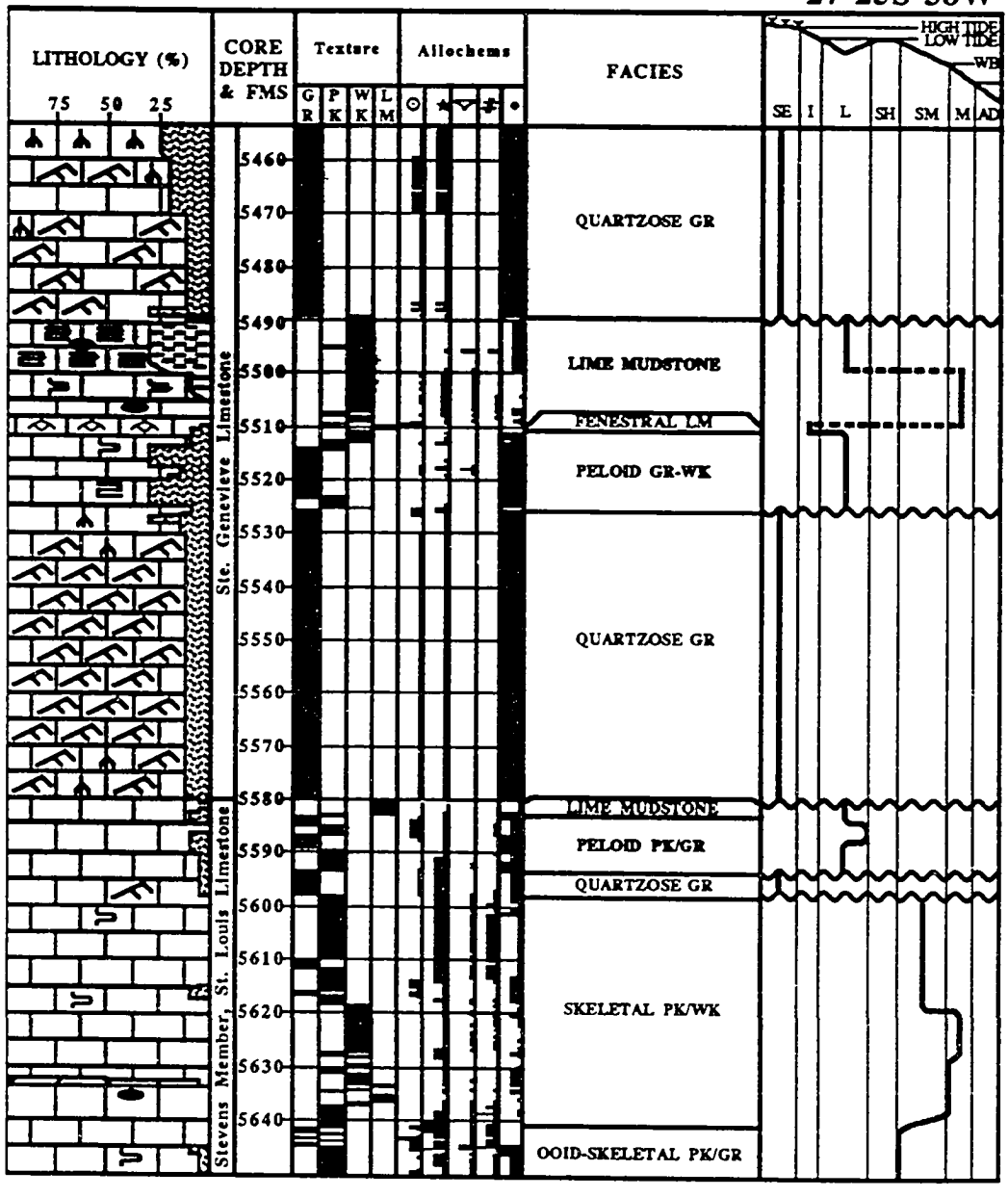
Reproduced with permission of the copyright owner. Further reproduction prohibited without permission.

AMOCO #1 NORDLING STANTON CO. SW SE NE 30-29S-39W



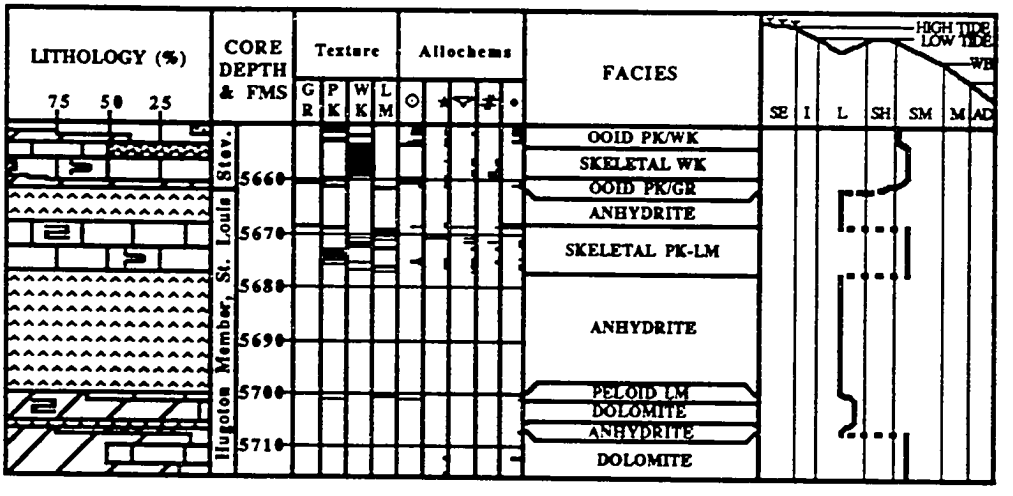
Reproduced with permission of the copyright owner. Further reproduction prohibited without permission.

AMOCO #1 PUYEAR **STANTON CO.** **660' FWL, 1980' FSL 27-25S-38W**



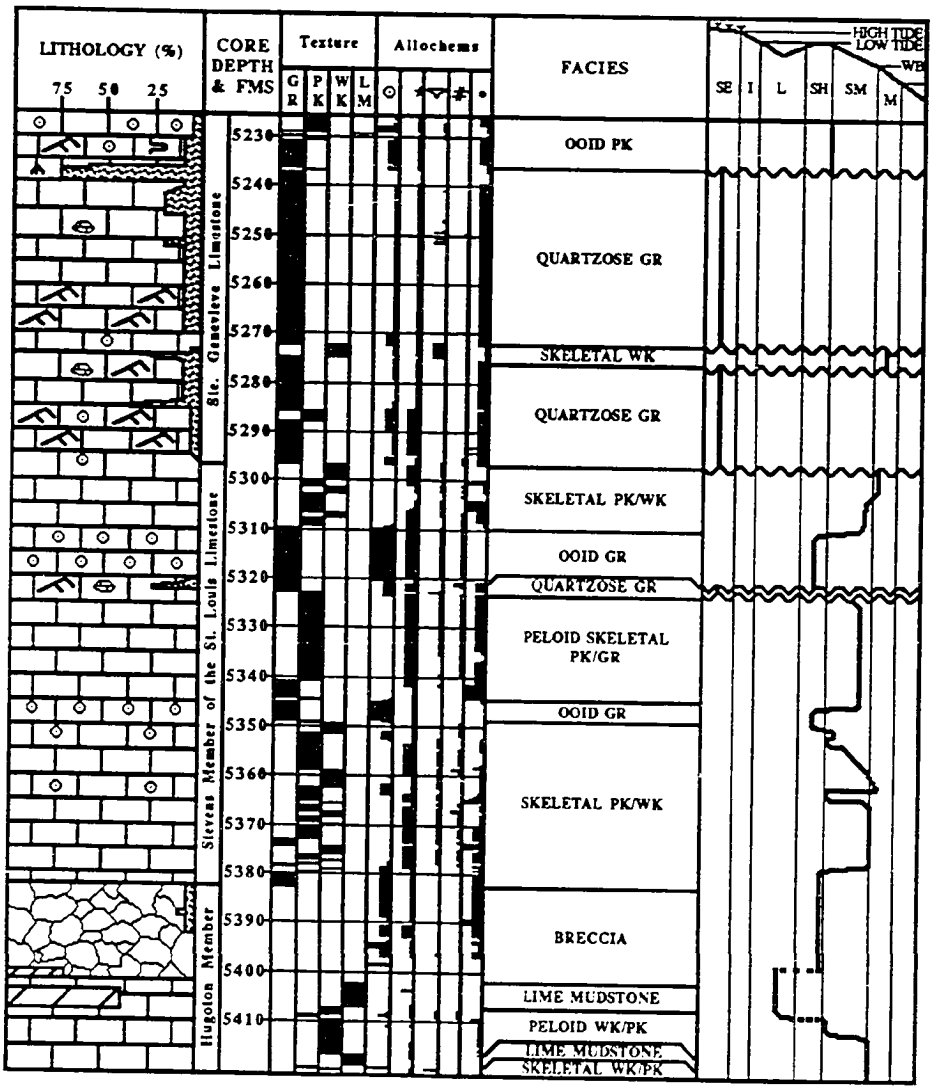
Reproduced with permission of the copyright owner. Further reproduction prohibited without permission.

AMOCO #1 PUYEAR **STANTON CO.** **660' FWL, 1980' FSL, 27-25S-38W**



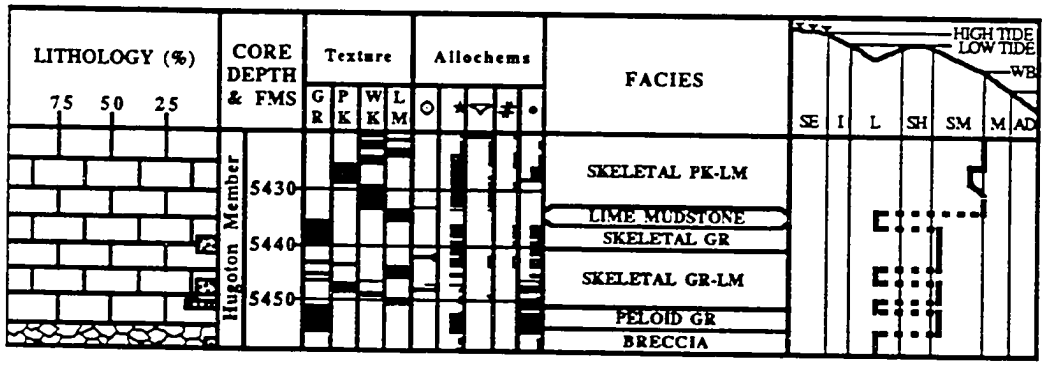
Reproduced with permission of the copyright owner. Further reproduction prohibited without permission.

AMOCO #3 COHEN C KEARNY CO. C SE NE 27-25S-38W



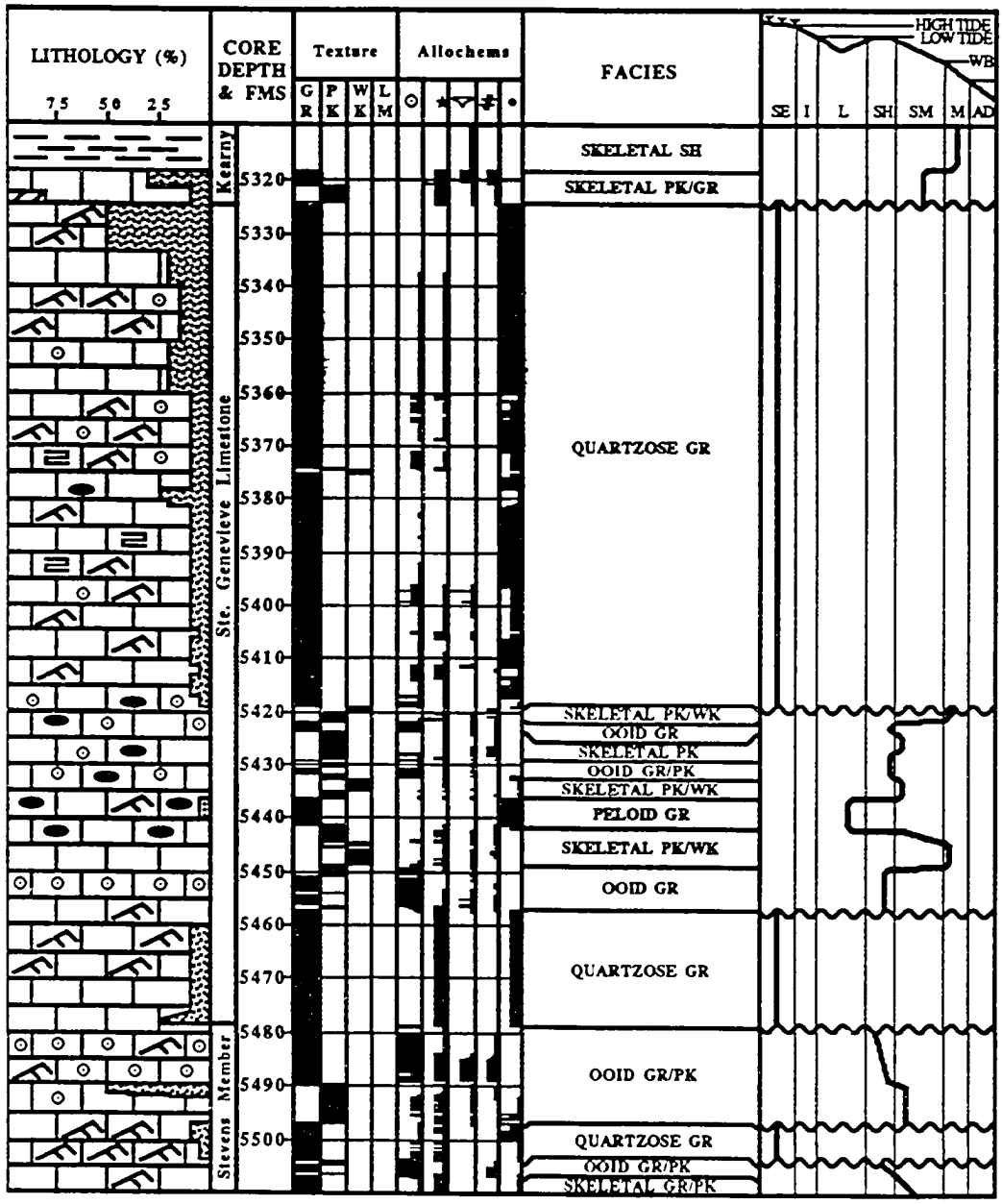
Reproduced with permission of the copyright owner. Further reproduction prohibited without permission.

AMOCO #3 COHEN C KEARNY CO. C SE NE 27-25S-38W



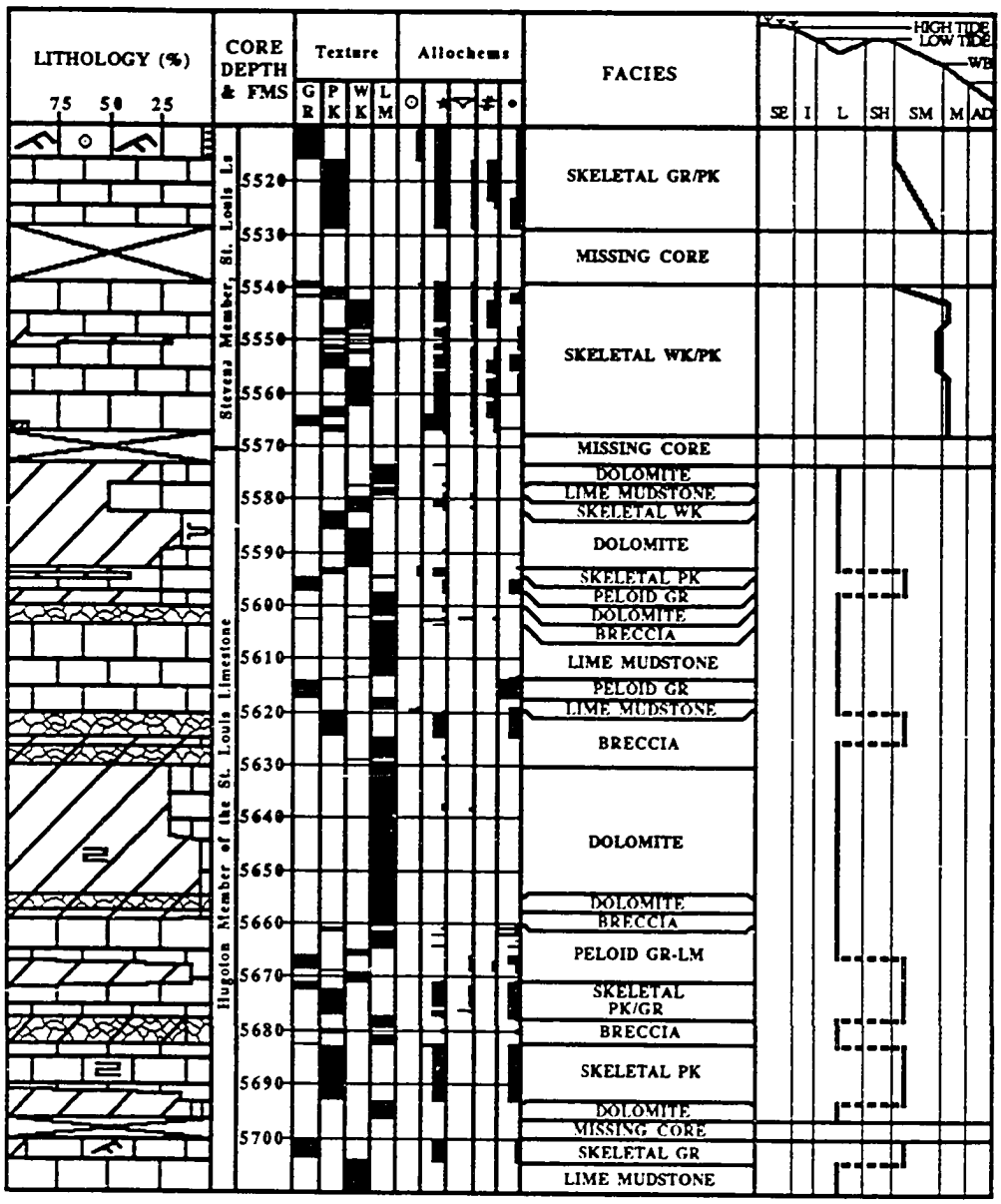
Reproduced with permission of the copyright owner. Further reproduction prohibited without permission.

AMOCO #3 WILSON A **HASKELL CO.** **SE SE NW 30-30S-33W**



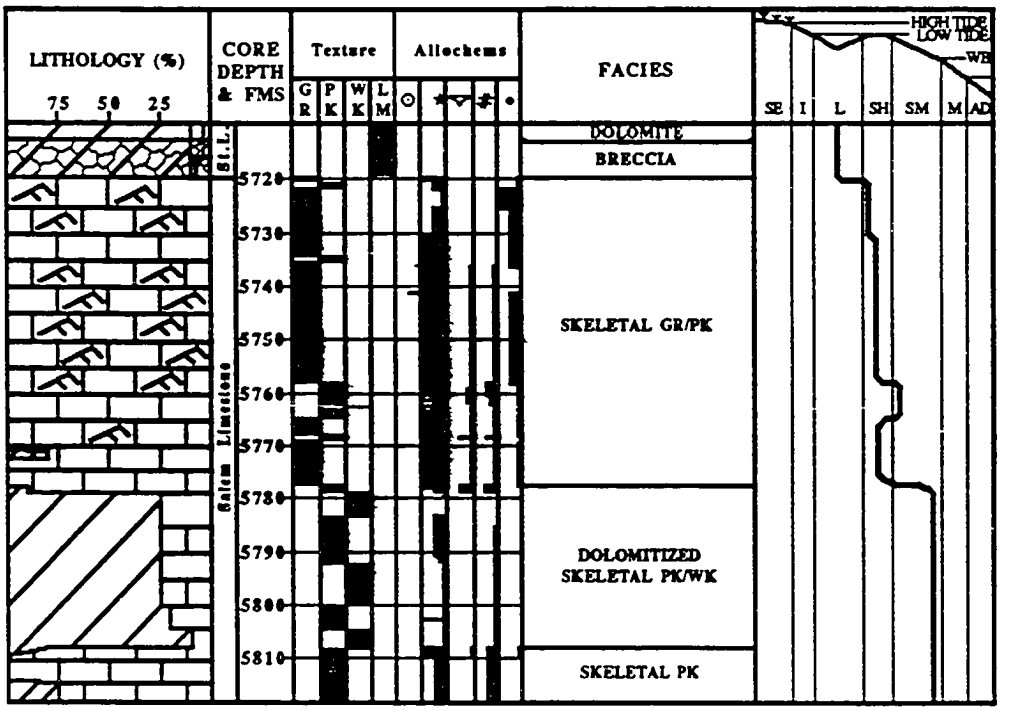
Reproduced with permission of the copyright owner. Further reproduction prohibited without permission.

AMOCO #3 WILSON A HASKELL CO. SE SE NW 30-30S-33W



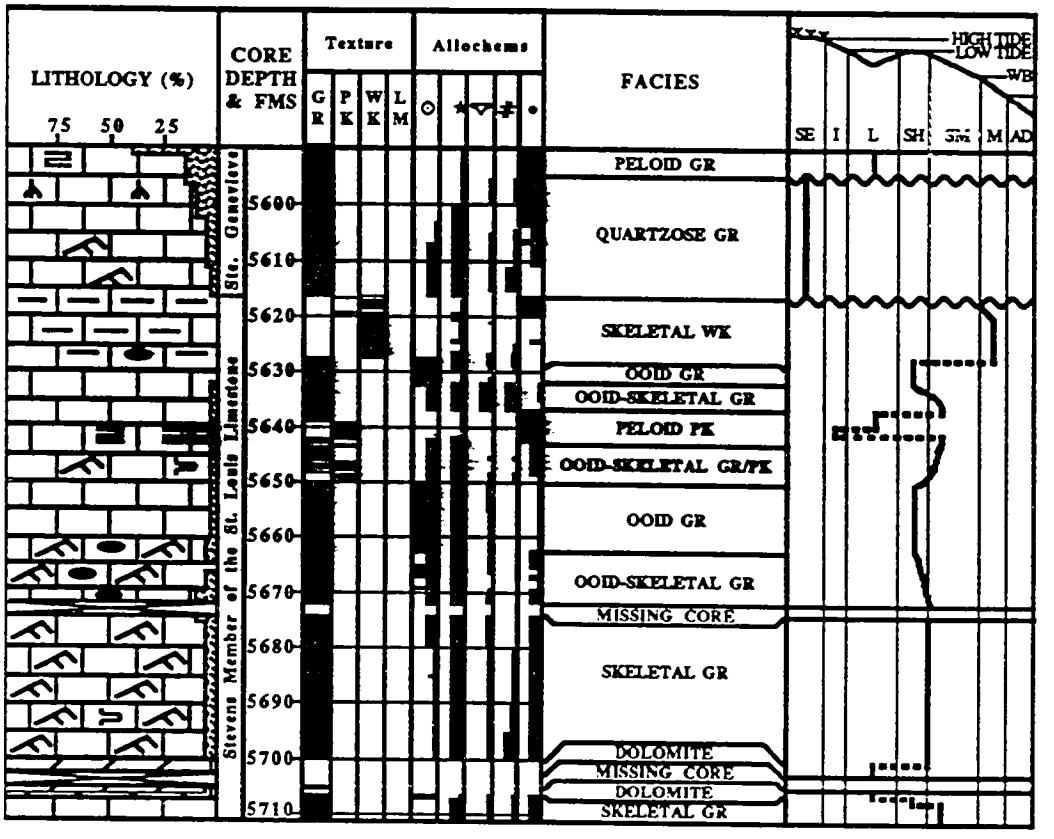
Reproduced with permission of the copyright owner. Further reproduction prohibited without permission.

AMOCO #3 WILSON A HASKELL CO. SE SE NW 30-30S-33W



Reproduced with permission of the copyright owner. Further reproduction prohibited without permission.

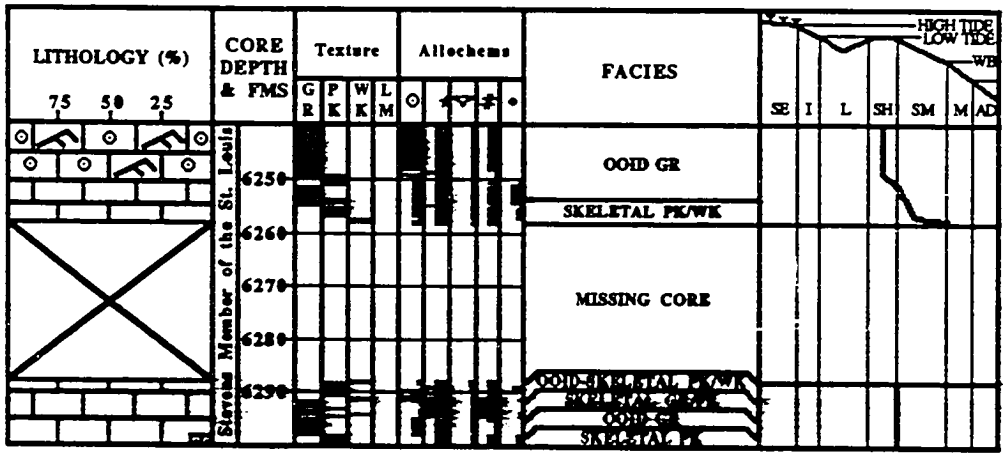
CITIES SERVICE #1 KELLS B HASKELL CO. C NW NW 5-28S-34W



This core contains numerous missing intervals. Most are less than one foot in thickness and are too thin to show on this scale.

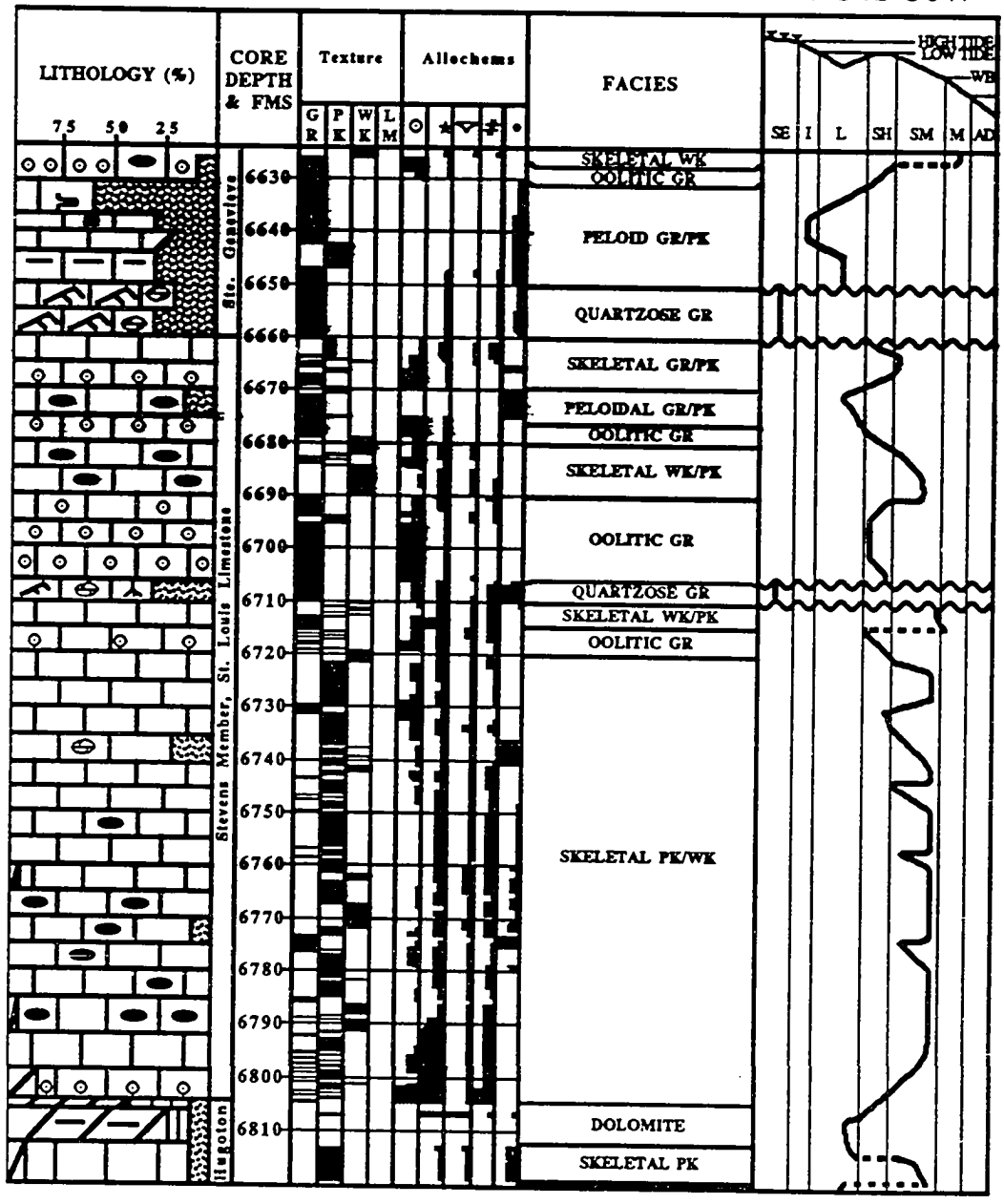
Reproduced with permission of the copyright owner. Further reproduction prohibited without permission.

COLORADO #2 FOX A MEADE CO. C NE SW 3-35S-30W



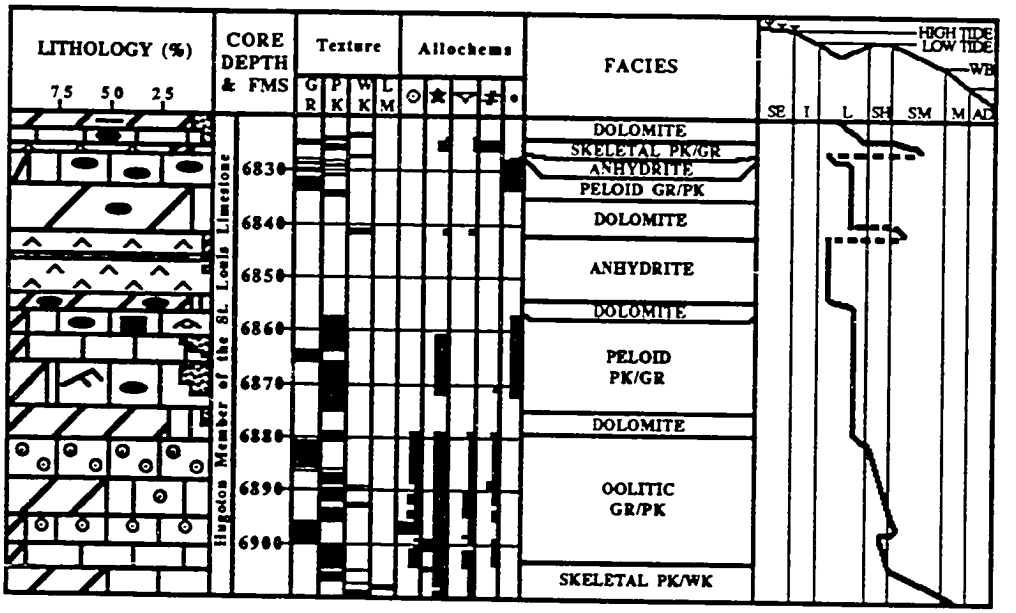
Reproduced with permission of the copyright owner. Further reproduction prohibited without permission.

MOBIL #1 FOSTER STEVENS CO. C NE SW 5-34S-36W



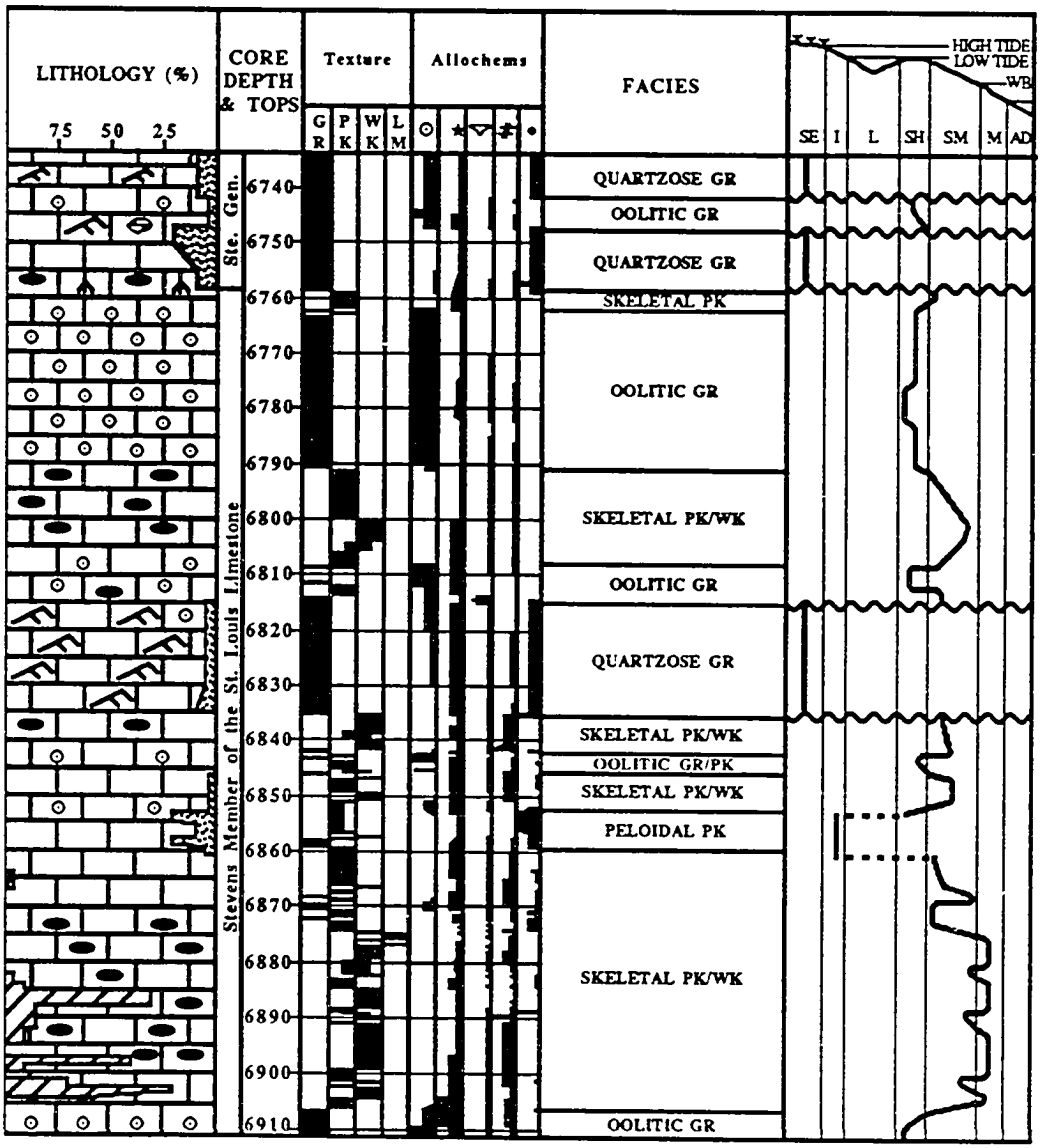
Reproduced with permission of the copyright owner. Further reproduction prohibited without permission.

MOBIL #1 FOSTER **STEVENS CO.** **C NE SW 5-34S-36W**



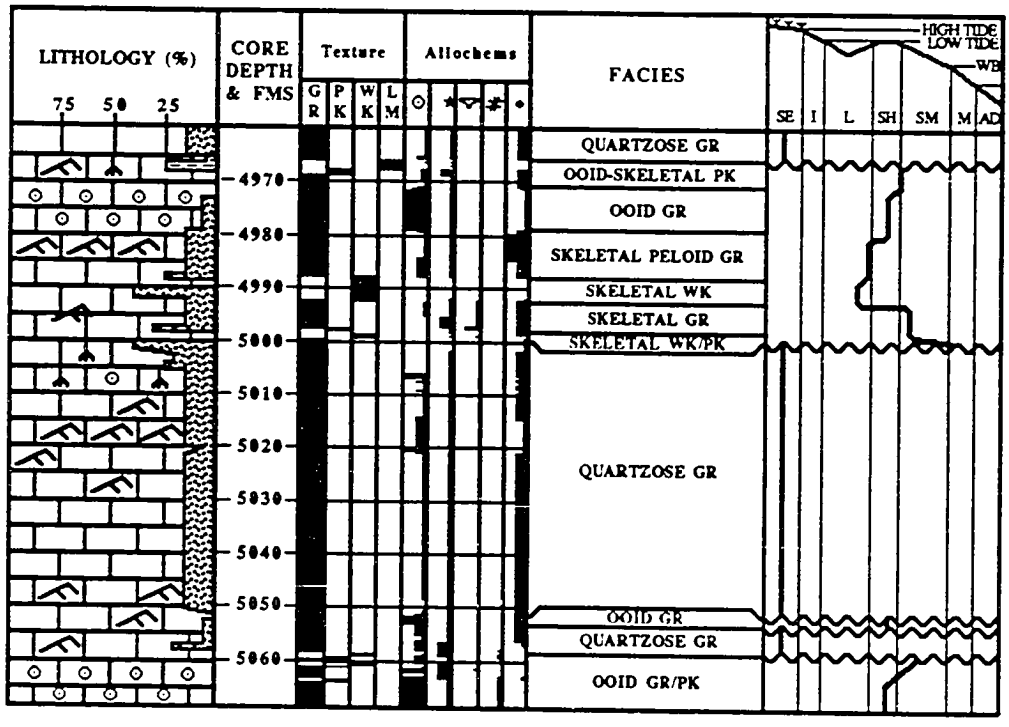
Reproduced with permission of the copyright owner. Further reproduction prohibited without permission.

MOBIL #1 HEADRICK STEVENS CO. SWNW 30-35S-37W



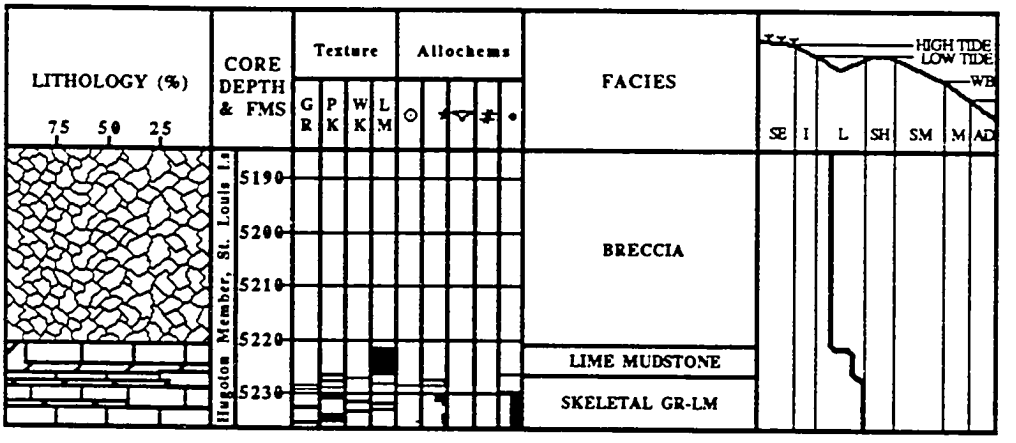
Reproduced with permission of the copyright owner. Further reproduction prohibited without permission.

PAN AM #1 MOSER KEARNY CO. C NW NW 31-24S-36W



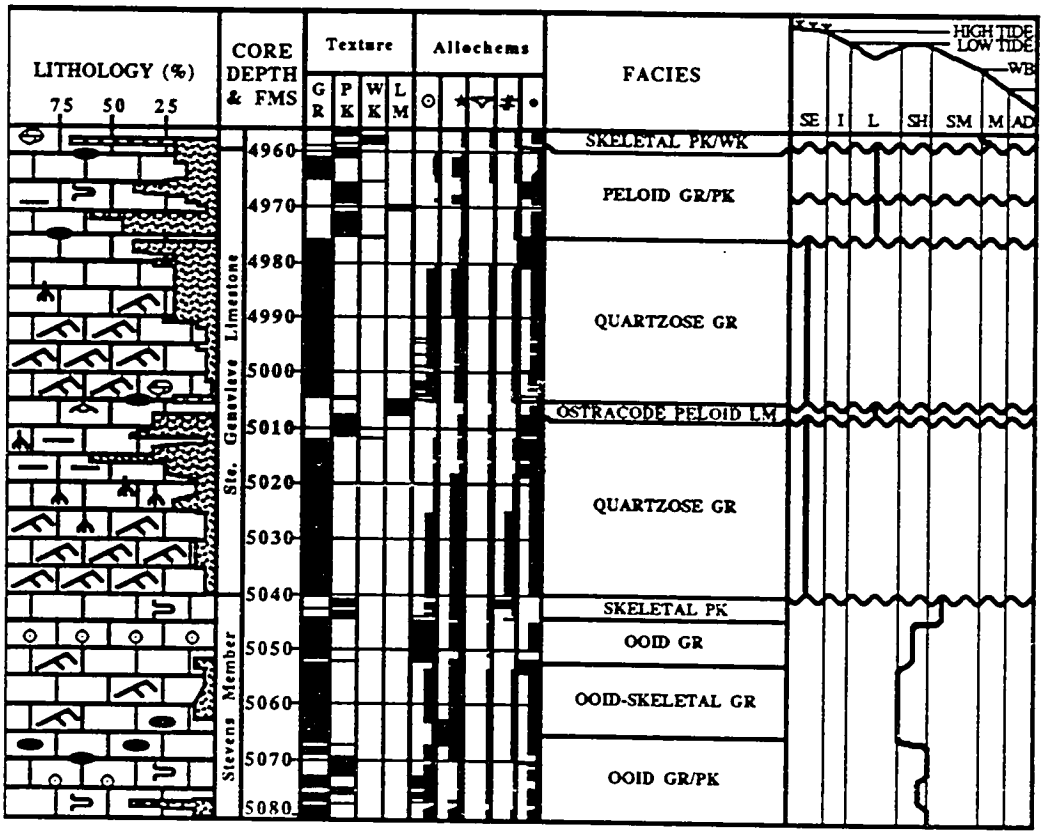
Reproduced with permission of the copyright owner. Further reproduction prohibited without permission.

PAN AM #1 MOSER KEARNY CO. C NW NW 31-24S-36W



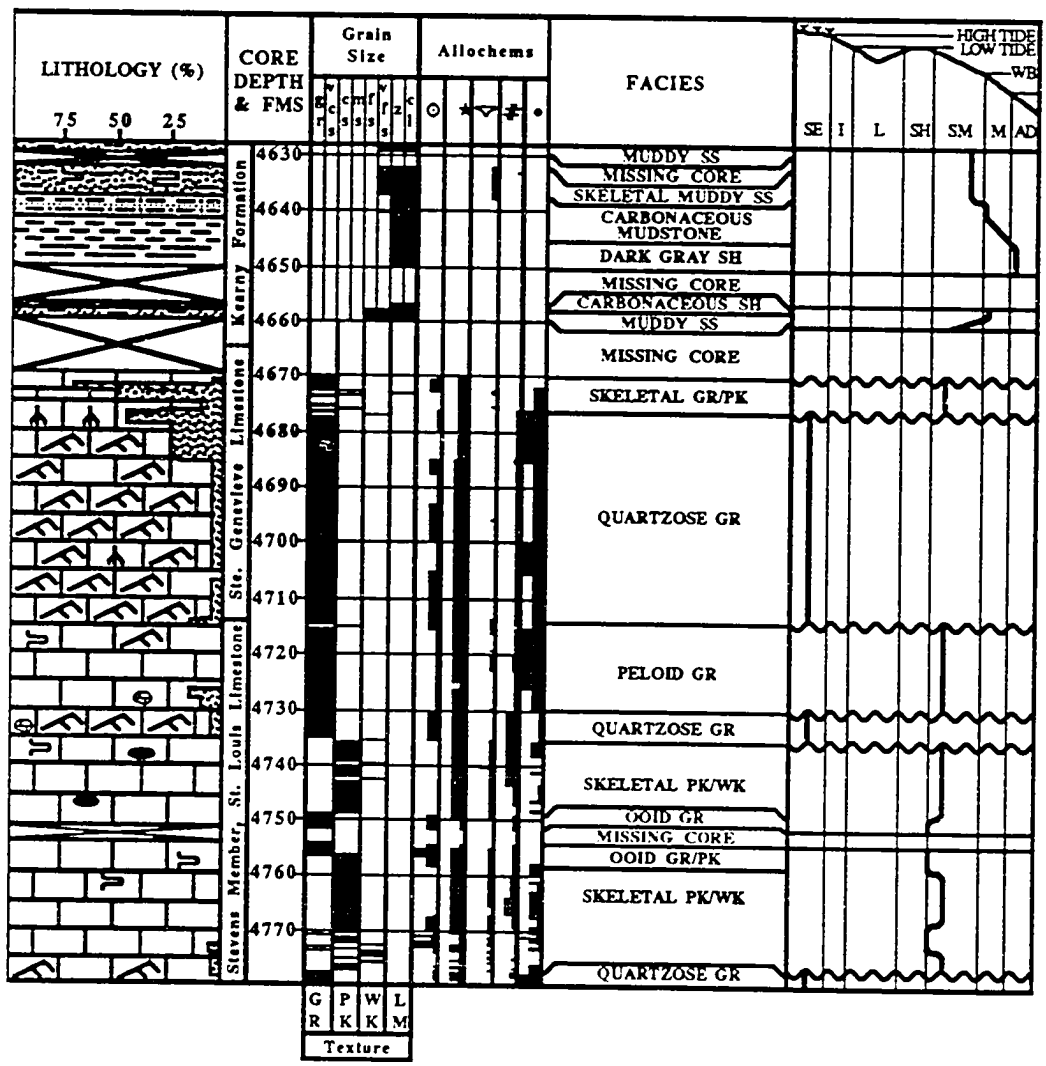
Reproduced with permission of the copyright owner. Further reproduction prohibited without permission.

PENDLETON #1 SCHAUF **GRAY CO.** **SW SW NE 16-27S-29W**



Reproduced with permission of the copyright owner. Further reproduction prohibited without permission.

SHALLOW WATER #4 MAUNE FINNEY CO. C NE NW 31-21S-33W



Reproduced with permission of the copyright owner. Further reproduction prohibited without permission.

Appendix 2. Tops of lithostratigraphic boundaries from logs used in stratigraphic cross sections (see Pocket Enclosures) in southwestern Kansas. Abbreviations used include: Sal., Salem Limestone; Hug., Hugoton Member of the St. Louis Limestone; Stev., Stevens Member of the St. Louis Limestone; Ste.G., Ste. Genevieve Limestone; S.A., Shore Airport Formation; NR, boundary not recognized; -----, well does not penetrate boundary; ?, uncertain boundary. Wells in boldface capital letters represent cores logged in this study. Lower case boldface represents wells with neutron-density logs that are in the same township as wells with examined cores that lacked neutron-density logs. Depths in ft.

A-A'	Sal.	Hug.	Stev.	Ste.G.	S.A.
1. Midwestern #1-17 Gear 17-35S-43W	------	------	4896	4760	4376
2. Coastal #1-3J Central Life 3-35S-42W	4980	NR	4804	4673	4403
3. Anadarko #1 Wacker "G" 8-34S-41W	------	------	5532	5414	5094
4. Cities Service #1 Fermaud "A" 15-34S-40W	------	6468	6340	6239	6092
5. Anadarko #1 Vickery "A" 1-35S-39W	7006	6873	6735	6630	6428
6. L.V.O. #1 Elliot 25-34S-38W	6818	6701	6582	6412	6255
7. MOBIL #1 HEADRICK 3-35S-37W	7089	6922	6766	6640	6358
8. MOBIL #1 FOSTER 5-34S-36W	------	6804	6660	6536	6250
9. Douglas #1-18 Thomas 18-34S-35W	6913?	6734	6612	6488	6150
10. Southland Royalty #1-19 Hampton 19-34S-34W	------	6753	6618	6508	6109
11. Cities Service #1 Salley "H" 16-34S-33W	------	6641	6517	6401	6067
12. Huber #1 Light "G" 3-35S-32W	6923	6800	6685	6522	6142
13. Kaiser-Francis #1 Black 11-34S-31W	------	------	5970	5818	5678
14. Quinque #3-4 Adams 4-35S-30W	------	6294	6140	6022	5776
15. Rosewood #1-23 Larabee 23-34S-29W	6502	6394	6278	6139	5776
16. Mesa #2-17 Baragree 17-35S-28W	6632	6491	6319	6225	5825
17. Apache #1 J-Barby 32-34S-27W	------	6760	6590	6486	6040
18. Hawkins #1-28 Walker 28-34S-25W	------	------	6268?	6139	5715

Reproduced with permission of the copyright owner. Further reproduction prohibited without permission.

B-B'	Sal.	Hug.	Stev.	Ste.G.	S.A.
19. Anadarko #1 Wagner 1-31S-43W	------	5618	5559	5405	5344
20. Huber #29-2 Heyen 29-30S-42W	5888	5634	5562	5384	5360
21. Anadarko #1 Johns "C" 26-31S-41W	------	5704	5610	5450	5444
22. AMOCO #1 BREEDING "F" 34-31S-40W	------	------	5487	5331	5290
23. Pan Am #1 Cooper "D" 21-31S-39W	6263	6162?	6094	5966	5945
24. Mesa #2-33 Lucas 33-30S-38W	------	------	5856	5758	5723
25. Anadarko #1 McCandless "A" 35-30S-37W	------	------	6041?	5910	5681
26. Mobil #1 Fairchild 36-30S-36W	------	------	6102	5962	5774
27. Mesa #1-6 Benney 6-30S-35W	------	------	5758	5616	5446
28. Flynn #31-1 Shaw 31-31S-34W	6079	5964	5914	5729	5568
29. AMOCO #3 WILSON "A" 30-30S-33W	5722	5567	5504	5325	E
30. Berexo #1-16 Hall 16-30S-32W	------	5754	5605?	5492	5345?
31. Arco #1 Ruby Dee 14-31S-31W	6040	5939	5760	5612	5464?
32. W.T.A. #1 Reiss 23-31S-29W	------	------	5688	5612	5440
33. Amarex #1 Hartshorn 1-31S-28W	------	------	5450	5350	5260?
34. Petroleum #1 Chance "C" 14-31S-27W	------	------	5528	5430	5292?
C-C'	**Sal.**	**Hug.**	**Stev.**	**Ste.G.**	**S.A.**
35. Sante Fe #1-36 Wilkerson 36-29S-42W	5824	5622	5535	5399	5362
36. Berexico #1 Cockerham 33-29S-41W	------	------	------	5462?	5410
37. AMOCO #1 PUYEAR 23-28S-40W	5874	5652	5580	5416	5391
38. Amoco #1 McPherson & Citizen 28-29S-39W	6018	5856	5789	5600	5576
39. Amoco #3 Johnson 30-29S-38W	6029	5848	5768	5580	5546
40. Mesa #2-21 Campbell 21-29S-37W	6130	6018	5918	5718	5508

Reproduced with permission of the copyright owner. Further reproduction prohibited without permission.

41. Oxy #3 Hoffman "Q" 29-28S-36W	6061	5905	5810	5652	5452
42. Cities Service #3 Fry Brothers 21-28S-35W	5963	5881	5745	5604	5481
43. Cities Service #3 Helmley "B" 3-29S-34W	------	------	5415	5336	5274
44. Berexco #2-13 Wright 13-29S-33W	------	5750	5636	5482	5412
45. Berexco #1-7 Demeritt 7-29S-32W	------	5762	5646	5457	5400
46. Petro-Lewis #1-16 Western Land 16-29S-31W	5796	5676	5504	5378	5361
47. Ladd #1 Reed 3-29S-30W	5590	5514	5345	5191	5147
48. PENDLETON #1 SCHAUF 16-27S-29W	------	------	5062	4972	E
49. Pendleton #1 Byer 31-27S-28W	5322	5322	5200	5089	E
50. Pendleton #1 Asher 31-28S-27W	5467	5417	5272	5172	E
D-D'	**Sal.**	**Hug.**	**Stev.**	**Ste.G.**	**S.A.**
51. Barrett #1 Warner 28-26S-42W	5727	5599	5530	5401	E
52. Amoco #1 Buhrle 13-26S-41W	------	------	5649	5503	E
53. L.V.O. # Coover 36-26S-39W	5774	5568	5479	5369	E
54. AMOCO #3 COHEN "C" 27-25S-38W	5532	5390	5284	5185	E
55. UPRC #3-6 Heintz 6-25S-37W	------	6375?	5251	5152	E
56. PAN AM #1 MOSER 31-24S-36W	5233	5150	5054	4905	E
57. L.V.O. #1 Nuss 26-24S-35W	5142	5055	4926	4841	E
58. UPRC #3-6 Esther 6-24S-34W	5125?	5058?	4971	4889	E
59. Northern Pump #11-1 Bass 11-24S-33W	------	------	4875	4804	E
60. Continental #1 Brookover 30-24S-32W	------	------	4920	4840	E
61. Continental #1 Skaggs 34-25S-31W	------	------	4896?	4850	E
62. Hadoon #1-15 Mooney 15-25S-30W	5140	5064?	4893	4848	E

Reproduced with permission of the copyright owner. Further reproduction prohibited without permission.

63. Falcon #1 Renick 31-25S-29W	------	NR	4898	4843	E
64. Patrick #1 Snowbarger 6-25S-28W	5044	NR	4864	E	E
65. Rine #1 Salem 22-25S-27W	5055	NR	4922	E	E
E-E'	**Sal.**	**Hug.**	**Stev.**	**Ste.G.**	**S.A.**
5. Anadarko #1 Vickery "A" 1-35S-39W	7006	6873	6735	6630	6467
4. Cities Service #1 Fermaud "A" 15-34S-40W	------	6468	6340	6239	6092
66. Anadarko Prod #8 Low "D" 18-33S-40W	------	------	5713	5611	5544
67. Anadarko #2 Younggren "B" 13-32S-39W	------	------	6122	6012	5940
22. AMOCO #1 BREEDING "F" 34-31S-40W	------	------	5487	5330	5290
68. Pan Am Petro. #1 Parks "C" 22-30S-40W	------	5552	5473	5312	5276
38. Amoco #1 McPherson & Citizen 28-29S-39W	6016	5856	5789	5600	5576
37. AMOCO #1 PUYEAR 23-28S-40W	5874	5652	5580	5416	5391
69. Pan Am #1 Helmle Gas Unit 21-27S-39W	------	------	5476	5363	E
53. L. V. O. #1 Coover 36-26S-39W	5774	5568	5479	5369	E
54. AMOCO #3 COHEN "C" 27-25S-38W	5532	5390	5284	5185	E
70. Woolsey #1 Spencer 2-23S-29W	5460	5398	5242	5213	E
71. Woolsey #1 Swisher 22-22S-39W	5493	5436	5222	E	E
72. Woolsey #1 Maune "E" 13-21S-39W	5418	5340	5237	5177	E
73. Shell #1 Shumi 8-20S-38W	------	------	5162	5112	E
74. Texaco Inc. #1 Roberts 26-19S-38W	5304	5220	5130	5003	E
75. Cities Service #1 Sell 9-18S-40W	------	5288	5188	5149	E
76. Mid-Am #1-31 Greeley Lnds 31-17S-41W	------	NR	5125	5067	E
77. BHP #13-5 Murphy 5-16S-41W	5222	NR	5204	E	E

Reproduced with permission of the copyright owner. Further reproduction prohibited without permission.

78. Chevron #1 Martin 26-15S-40W	5219	5163	5124	E	E
F-F'	**Sal.**	**Hug.**	**Stev.**	**Ste.G.**	**S.A.**
7. **MOBIL #1 HEADRICK** **3-35S-37W**	7089	6922	6766	6640	6358
8. **MOBIL #1 FOSTER** **5-34S-36W**	-----	6804	6660	6536	6250
79. Mobil #1 McCoy 35-33S-37W	------	6661	6520	6393	6144
80. Mobil #1 McGill 13-32S-36W	-----	6454	6306	6160	5892
81. Mobil #3 Gaskill 22-31S-36W	------	------	6212	6093	5785
26. Mobil #3 Fairchild 36-30S-36W	------	------	6102	5962	5774
40. Mesa #2-21 Campbell 21-29S-37W	6130	6018	5918	5796	5508
41. Oxy #3 Hoffman "Q" 29-28S-36W	6061	5905	5810	5652	5452
82. Mobil #1 Sentney 35-27S-37W	------	5574	5471	5338	5300
83. Kan/Neb #8-4 Masonic Home 4-26S-36W	5136	5050	4947	4842	4809
84. Union Pacific #3-2 Bahntge 2-25S-36W	5140	5058	4953	4802	E
56. **PAN AM #1 MOSER** **31-24S-36W**	5233	5150	5054	4905	E
85. Pan Am #1 Hoover 23-23S-36W	------	------	5015	4928	E
86. W. B. Osborn #1 Miller 18-22S-37W	------	------	4980	4912	E
87. L. V. O. #1 E. M. Smith 36-21S-38W	5153	5070	4970	4898	E
88. M. L. Brown #1 G.S. Smith "F" 4-20S-36W	5192	5114	5003	4944	E
89. Helmerich #1-27 Harris 27-19S-36W	5296	NR	5158	E	E
90. Helmerich & Pa. #1-1 Metheny 1-18S-36W	5168	5094	5010	4899	E
91. Bow Valley #1-30 Bauer 30-17S-37W	5241	5194	5080	5003	E
92. Sunburst #1 Linder "B" 19-15S-38W	5170	5130	5044	4995	E
G-G'	**Sal.**	**Hug.**	**Stev.**	**Ste.G.**	**S.A.**
93. Anadarko #3 Boles 3-35S-34W	------	6776?	6587	6460	6084

Reproduced with permission of the copyright owner. Further reproduction prohibited without permission.

10. Southland Royalty #2-19 Hampton 19-34S-34W	------	6740	6600	6475	6092
94. Cabot #2-35 Cook 35-33S-34W	------	6504	6422	6357	6006
95. Mobil #1 Brownell 1-32S-35W	6531	6342	6252	6091	5685
28. Flynn #31-1 Shaw 31-31S-34W	6079	5964	5914	5729	5568
29. AMOCO #3 WILSON "A" 30-30S-33W	5722	5567	5504	5325	E
44. Berexco #2-13 Wright 13-29S-33W	------	5750	5636	5482	5412
96. Cities Service #1 Kells "B" 5-28S-34W	------	------	5618	5495	5474
97. Berexco #2 Davis 1-27S-33W	------	5100?	5277	5103	E
98. Helmerich & Payne #16 USA "A" 31-26S-34W	5570	5417	?	5115	E
99. Mobil #1 Blocher 28-25S-34W	------	------	5126?	4974	E
58. UnionPacific #3-6 Esther 6-24S-34W	5125?	5058?	4971	4889	E
100. Union Pacific #2-16 Johnson 16-23S-33W	5078		4906	4858	E
101. Gulf #1-20 Burg 20-22S-34W	4932	4862	4700	4676	E
102. Brown #1 Wampler 17-21S-33W	4920	4839	4714	4678	E
103. Brown #1 Baker 34-20S-33W	4926	4852	4733	4708	E
104. Brown #2 Smith "A" 25-19S-33W	4758	4700	4575	4545	E
105. Woolsey #1 Hutchins 35-18S-33W	4942	4850	4720	4698	E
106. T-Bird #1 Weichman "C" 29-17S-32W	------	4817?	4710	E	E
107. Ladd #1-16 Koehn 16-16S-34W	4980	4912	4868	E	E
108. Cities Service #1 McDaniel "B" 28-15S-34W	4846	4773	4710	4692	E
H-H'	**Sal.**	**Hug.**	**Stev.**	**Ste.G.**	**S.A.**
14. Quinque #3-4 Adams 4-35S-30W	------	6294	6140	6022	5776
15. Rosewood #1-23 Larrabee 23-34S-29W	6502	6394	6278	6139	5776

Reproduced with permission of the copyright owner. Further reproduction prohibited without permission.

109. Elder & Vaughn #1 Felice 12-33S-29W	------	------	6097	5963	5570
110. Edwin Bradley #1 Easum 27-32S-29W	6351?	6328?	6143	6002	5690
32. WTA #1-23 Reiss 23-31S-29W	------	------	5688	5612	5440
47. Ladd #1 Reed 3-29S-30W	5590	5514	5345	5191	5147
111. Falcon #1 Frigon 10-28S-30W	------	------	5248	5163	E
48. PENDLETON #1 SCHAUF 16-27S-29W	------	------	5062	4972	E
112. Irex #1 Frack 36-26S-29W	------	------	5104	4996	E
62. Hadson #1-15 Mooney 15-25S-30W	5140	5064?	4893	4848	E
113. Beren #1 Werner 17-24S-30W	5164	5059	4950?	4883	E
114. Woolsey #3 Haag Farms 6-23S-30W	5002	NR	4805	4743	E
115. Woolsey #1 Samuelson 31-22S-30W	------	------	4823	4766	E
116. Ladd #1 Rissler "A" 32-21S-30W	4918	4837	4753	E?	E
117. Mobil #1 Hutchins 17-20S-31W	4865	4918	4697?	4637	E
118. Hinkle #1 Goering 30-19S-30W	4644	4608	E	E	E
119. Texas Energies #1-23 Sullivan 23-18S-29W	4826	4800	E	E	E
120. Griffin #1 Southern 4-17S-29W	?	4552	E	E	E
121. KRM #1-17 Huck 17-16S-30W	4509	4453	E	E	E
122. Anderson #1 Dowell "C" 34-15S-29W	4328	4288	E	E	E

I-I'	**Sal.**	**Hug.**	**Stev.**	**Ste.G.**	**S.A.**
7. MOBIL #1 HEADRICK 3-35S-37W	7089	6922	6766	6640	6358
8. MOBIL #1 FOSTER 5-34S-36W	------	6804	6660	6536	6250
79. Mobil #1 McCoy 35-33S-37W	------	6661	6520	6393	6144
123. Anadarko #2 Youngren B 13-32S-39W	------	------	6122	6011	5940

Reproduced with permission of the copyright owner. Further reproduction prohibited without permission.

22. AMOCO #1 BREEDING "F" **34-31S-40W**	------	------	5487	5331	5290
124. Rosewood #1-32 McGee 32-30S-41W	------	------	------	5436	5394
38. Amoco #1 McPherson & Citizen **28-29S-39W**	6018	5856	5789	5600	5576
37. AMOCO #1 PUYEAR **23-28S-40W**	5874	5652	5580	5416	5391
69. Pan Am #1 Helmle Gas Unit 21-27S-39W	------	------	5476	5363	E
53. L.V.O. # Coover 36-26S-39W	5774	5568	5479	5369	E
54. AMOCO #3 COHEN "C" **27-25S-38W**	5532	5390	5284	5185	E
56. PAN AM #1 MOSER **31-24S-36W**	5233	5150	5054	4905	E
125. Cities Service #3 Anderson "B" 11-23S-35W	------	------	4880	4852	E
101. Gulf #1-20 Burg 20-22S-34W	4932	4862	4700	4676	E
102. Brown #1 Wampler **17-21S-33W**	4920	4839	4714	4678	E
103. Brown #1 Baker 34-20S-33W	4926	4852	4733	4708	E
104. Brown #2 Smith "A" 25-19S-33W	4758	4700	4575	4545	E
105. Woolsey #1 Hutchins 35-18S-33W	4942	4850	4720	4698	E
106. T-Bird #1 Weichman "C" 29-17S-32W	------	4817	4710	E	E
107. Ladd #1-16 Koehn 16-16S-34W	4980	4912	4868	E	E
108. Cities Service #1 McDaniel "B" 28-15S-34W	4846	4773	4710	4692	E

Reproduced with permission of the copyright owner. Further reproduction prohibited without permission.

Appendix 3. T-tests of $\delta^{13}C$ and $\delta^{18}O$ values from eolian and subtidal strata. Average values for duplicate samples were used.

Amoco #1 Nordling
$\delta^{13}C$ DATA SUMMARY TABLE

	n	df	Mean	Std. Dev.	Variance
Eolian	12	11	2.36	0.44	0.19
Subtidal	14	13	2.79	0.37	0.14

H_0: $\mu_e = \mu_s$ Eolian and subtidal means are equal.
H_a: $\mu_e \neq \mu_s$ Eolian and subtidai means are not equal

t = -2.754
p-value = 0.011

Reject H_0 and conclude that that the means are not equal for all $\alpha > 0.011$.

Amoco #3 Cohen C
$\delta^{13}C$ DATA SUMMARY TABLE

	n	df	Mean	Std. Dev.	Variance
Eolian	5	4	2.22	0.48	0.23
Subtidal	12	11	2.78	0.38	0.15

H_0: $\mu_e = \mu_s$ Eolian and subtidal means are equal.
H_a: $\mu_e \neq \mu_s$ Eolian and subtidal means are not equal.

t = -2.523
p-value = 0.023

Reject H_0 and conclude that that the means are not equal for all $\alpha > 0.023$.

Reproduced with permission of the copyright owner. Further reproduction prohibited without permission.

Amoco #1 Nordling
$\delta^{18}O$ DATA SUMMARY TABLE

	n	df	Mean	Std. Dev.	Variance
Eolian	12	11	-3.72	0.78	0.61
Subtidal	14	13	-3.53	0.94	0.88

H_0: $\mu_e = \mu_s$ Eolian and subtidal means are equal.
H_a: $\mu_e \neq \mu_s$ Eolian and subtidal means are not equal

t = -0.543
p-value = 0.592

Reject H_0 and conclude that that the means are not equal for all $\alpha < 0.592$.

Amoco #3 Cohen C
$\delta^{18}O$ DATA SUMMARY TABLE

	n	df	Mean	Std. Dev.	Variance
Eolian	5	4	-2.98	0.92	0.84
Subtidal	12	11	-3.35	0.77	0.60

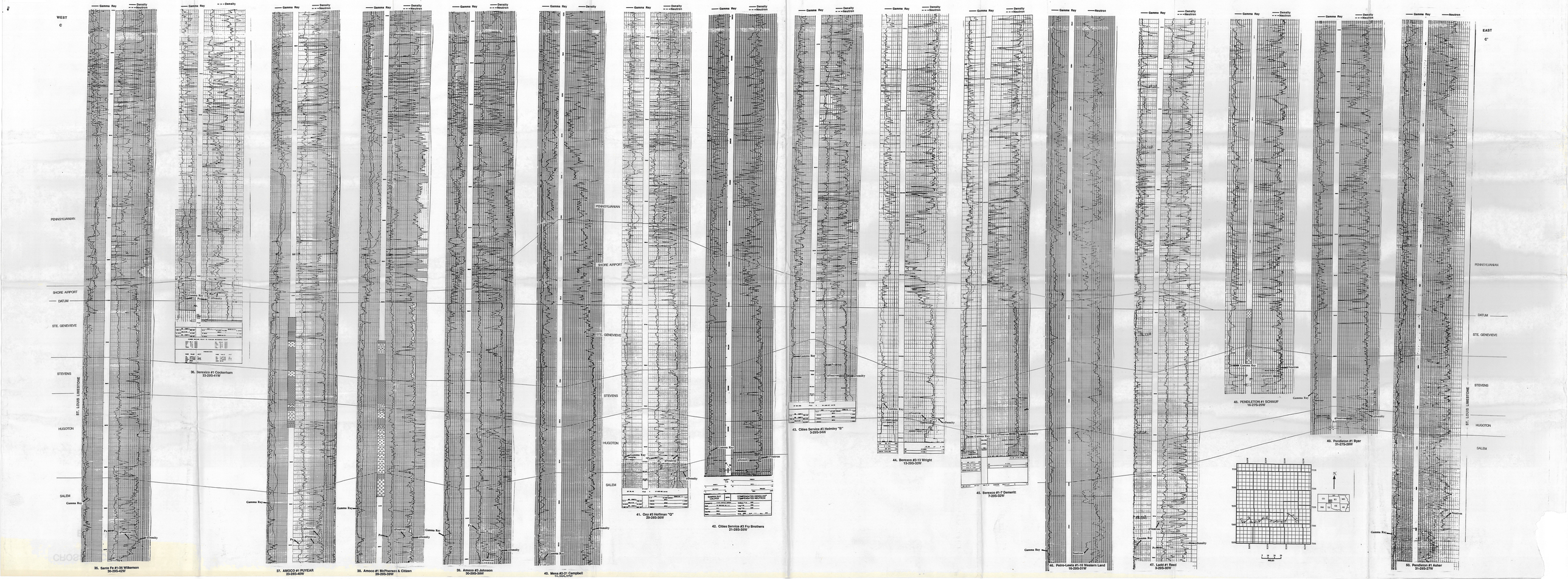
H_0: $\mu_e = \mu_s$ Eolian and subtidal means are equal.
H_a: $\mu_e \neq \mu_s$ Eolian and subtidal means are not equal.

t = -1.968
p-value = 0.072

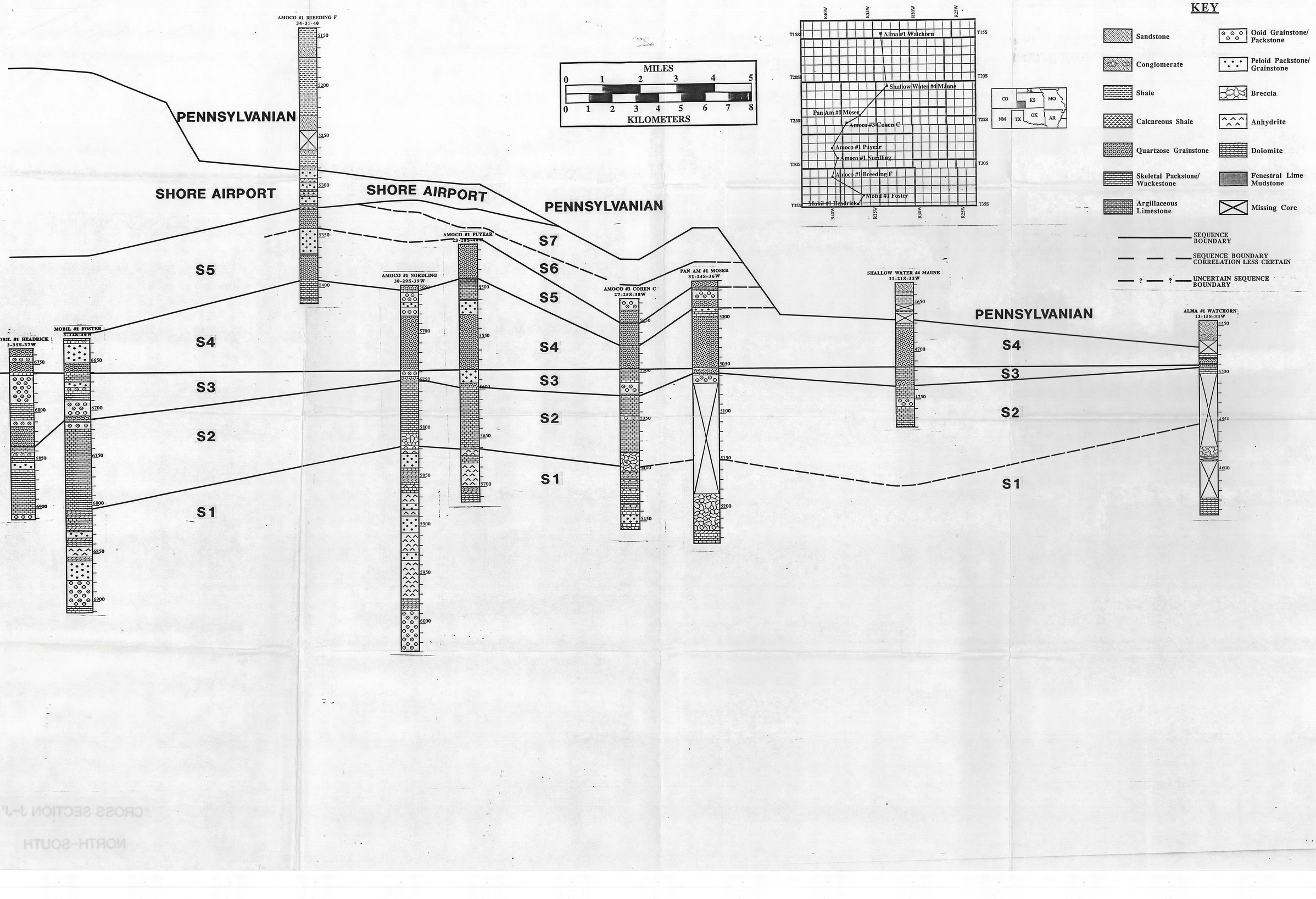
Reject H_0 and conclude that that the means are not equal for all $\alpha < 0.072$.

Reproduced with permission of the copyright owner. Further reproduction prohibited without permission.

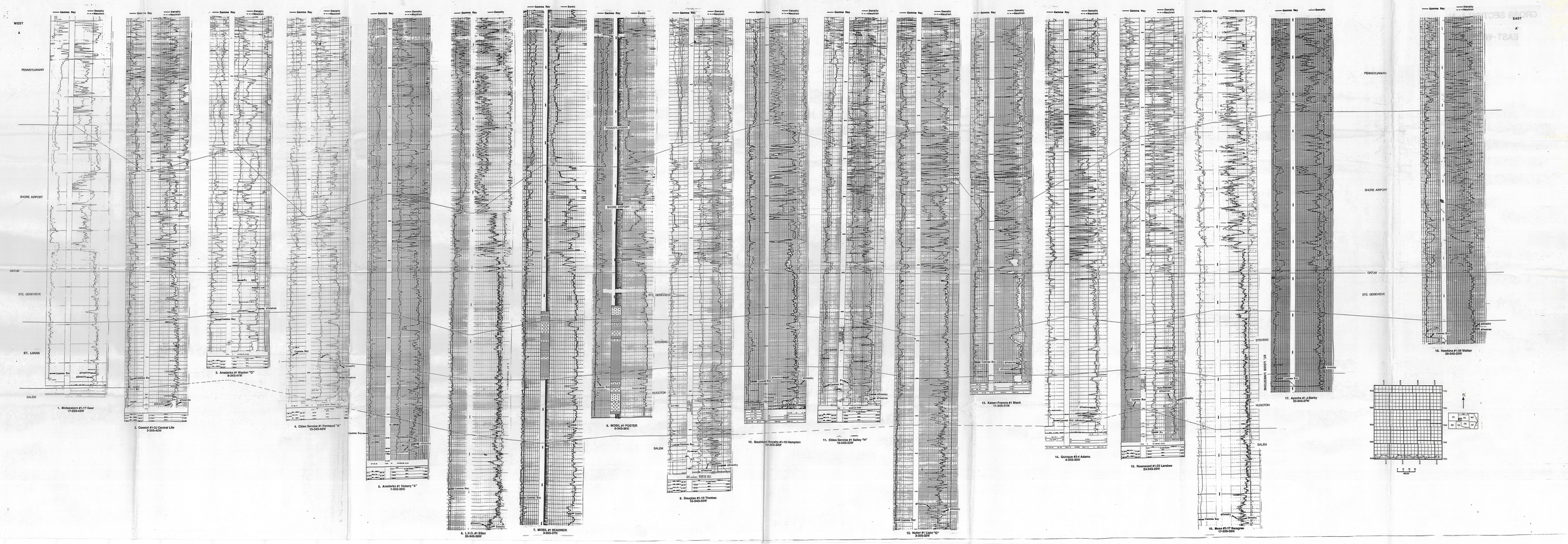
OF 92-42


WEST
C
EAST
C'
PENNSYLVANIAN
SHORE AIRPORT
DATUM
STE. GENEVIEVE
STEVENS
ST. LOUIS LIMESTONE
HUGOTON
SALEM
Gamma Ray
Density
Neutron
Resistivity
Sonic
35. Sante Fe #1-36 Wilkerson
36-29S-42W
36. Berexco #1 Cockerham
33-29S-41W
37. AMOCO #1 PUYEAR
23-28S-40W
38. Amoco #1 McPherson & Citizen
28-29S-39W
39. Amoco #3 Johnson
30-29S-38W
40. Mess #2-21 Campbell
41. Oxy #3 Hoffman "Q"
29-29S-34W
42. Cities Service #3 Fry Brothers
21-28S-33W
43. Cities Service #3 Helmley "B"
3-29S-34W
44. Berexco #0-13 Wright
13-29S-33W
45. Berexco #1-7 Demeritt
7-29S-32W
46. Petro-Lewis #1-15 Western Land
16-30S-31W
47. Ladd #1 Reed
3-29S-30W
48. PENDLETON #1 SCHAUF
16-27S-29W
49. Pendleton #1 Byer
21-27S-28W
50. Pendleton #1 Asher
31-26S-27W

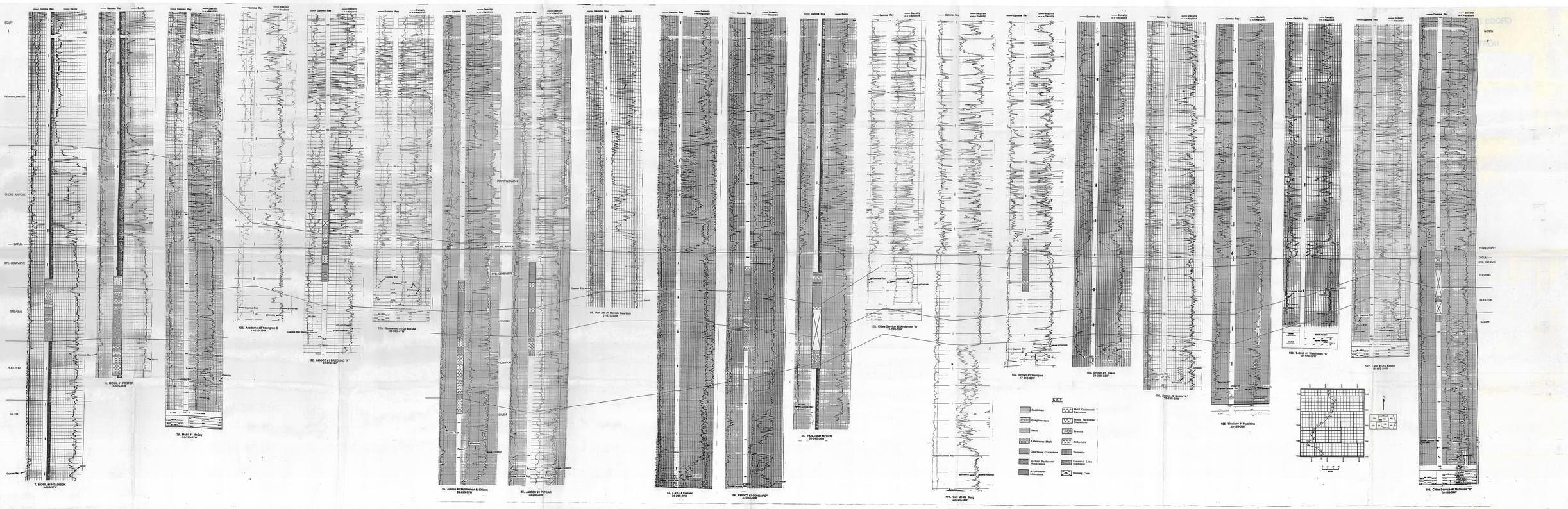
OF 92-42


AMOCO #1 BREEDING F
34-31-40
MOBIL #1 HEADRICK
3-35S-37W
MOBIL #1 FOSTER
5-34S-36W
AMOCO #1 NORDLING
30-29S-39W
AMOCO #1 PUYEAR
23-28S-40W
AMOCO #3 COHEN C
27-25S-38W
PAN AM #1 MOSER
31-24S-36W
SHALLOW WATER #4 MAUNE
31-21S-33W
ALMA #1 WATCHORN
13-15S-33W
PENNSYLVANIAN
SHORE AIRPORT
SHORE AIRPORT
PENNSYLVANIAN
PENNSYLVANIAN
S7
S6
S5
S5
S4
S4
S4
S3
S3
S3
S2
S2
S2
S1
S1
S1
MILES
0 1 2 3 4 5
0 1 2 3 4 5 6 7 8
KILOMETERS
R40W
R35W
R30W
R25W
T15S
T20S
T25S
T30S
T35S
Alma#1 Watchorn
Shallow Water #4 Maune
Pan Am #1 Moser
Amoco #3 Cohen C
Amoco #1 Puyear
Amoco #1 Nordling
Amoco #1 Breeding F
Mobil #1 Foster
Mobil #1 Headrick
NE
CO
KS
MO
NM
TX
OK
AR
KEY
Sandstone
Conglomerate
Shale
Calcareous Shale
Quartzose Grainstone
Skeletal Packstone/ Wackestone
Argillaceous Limestone
Ooid Grainstone/ Packstone
Peloid Packstone/ Grainstone
Breccia
Anhydrite
Dolomite
Fenestral Lime Mudstone
Missing Core
SEQUENCE BOUNDARY
SEQUENCE BOUNDARY CORRELATION LESS CERTAIN
UNCERTAIN SEQUENCE BOUNDARY

OF 92-42


WEST
A
EAST
A'
PENNSYLVANIAN
SHORE AIRPORT
DATUM
STE. GENEVIEVE
ST. LOUIS
SALEM
STEVENS
HUGOTON
Gamma Ray
Density
Neutron
Sonic
1. Midwestern #1-17 Gear
17-35S-42W
2. Cosorp #1-3J Central Life
3-35S-42W
3. Anadarko #1 Wacker "G"
8-34S-41W
4. Cities Service #1 Fermoid "A"
10-34S-40W
5. Anadarko #1 Vickery "A"
1-33S-39W
6. L.V.O. #1 Elliot
20-34S-38W
7. MOBIL #1 MEADRICK
3-35S-37W
6. MOBIL #1 FOSTER
9-34S-36W
9. Douglas #1-10 Thomas
10-34S-35W
10. Southland Royalty #1-19 Hampton
19-34S-34W
11. Cities Service #1 Salley "H"
16-34S-33W
13. Huber #1 Lyon "G"
3-35S-30W
13. Kaiser-Francis #1 Black
11-34S-31W
14. Quinque #3-4 Adams
4-35S-30W
15. Rosecrest #1-23 Larsbee
23-34S-29W
16. Mesa #3-17 Ramsprek
17-35S-28W
17. Apache #1 J-Barby
32-34S-27W
18. Hawkins #1-20 Walker
20-34S-26W
N
SCALE

OF 92-42


SOUTH
NORTH
PENNSYLVANIAN
SHORE AIRPORT
DATUM
STE. GENEVIEVE
STEVENS
HUGOTON
SALEM
KEY
Sandstone
Conglomerate
Shale
Calcareous Shale
Quartzose Grainstone
Skeletal Packstone/ Wackestone
Argillaceous Limestone
Oolid Grainstone/ Packstone
Fossil Packstone/ Grainstone
Breccia
Anhydrite
Dolomite
Fenestral Lime Mudstone
Missing Core
1. MOBIL #1 MEAKINOK 3-30S-37W
6. MOBIL #1 FOSTER 3-34S-30W
79. Mobil #1 McCoy 35-32S-37W
123. Amadarco #2 Youngren B 13-32S-33W
22. AMOCO #1 BREEDING "F" 34-31S-40W
124. Rosewood #1-32 McGee 32-30S-41W
38. Amoco #1 McPherson & Citizen 09-35S-39W
37. AMOCO #1 PITEAR 23-29S-40W
55. Pan Am #1 Hicinbothem Gas Unit 21-27S-39W
83. L.V.O. #1Conner 30-26S-39W
54. AMOCO #1 COHEN "C" 27-32S-39W
56. PAN AM #1 MOSER 31-34S-39W
125. Cities Service #3 Anderson "B" 17-33S-33W
101. Gul. #1-26 Burg 06-28S-34W
102. Brown #1 Wampler 17-31S-32W
103. Brown #1 Baker 04-30S-33W
104. Brown #2 Watts "A" 29-19S-32W
105. Woolsey #1 Yuschina 36-16S-33W
106. T-Bird #1 Weichmann "C" 09-17S-33W
107. Lebil #1-16 Koelzer 16-16S-34W
108. Cities Service #1 McDaniel "B" 28-12S-34W